CWPharma

CLEAR WATERS FROM PHARMACEUTICALS

Emissions and Environmental Levels of Pharmaceuticals – Upscaling to the Baltic Sea Region

SYKE

Interreg Baltic Sea Region

EUROPEAN UNION

EUROPEAN REGIONAL DEVELOPMENT FUND

EU STRATEGY FOR THE BALTIC SEA REGION FLAGSHIP

This report is an output of CWPharma project's work package 2, activity 2.3.

Authors:

Lauri Äystö[1)], Katri Siimes[1)], Ville Junttila[1)], Matti Joukola[1)], Ninni Liukko[1)]

Contributors:

Terhi Lehtinen[2)], Anete Kublina[3)], Helene Ek Henning[4)], Linda Fibiga[3)], Sara Lönnerud[4)], Aleksandra Bogusz[5)], Ülle Leisk[6)], Jukka Mehtonen[1)], Noora Perkola[1)]

1) Finnish Environment Institute (SYKE), Finland
2) Finnish medicines agency (Fimea), Finland
3) Latvian Environment, Geology and Meteorology Centre (LEGMC), Latvia
4) County administrative board of Östergötland (CAB), Sweden
5) Institute of Environmental Protection - National Research Institute (IOS), Poland
6) Estonian Environmental Research Centre (EERC), Estonia

Financier: European Union, Interreg Baltic Sea Region, European Regional Development Fund.

Year of issue: 2020

Citation example:

Äystö, L., Siimes, K., Junttila, V., Joukola, M., Liukko, N. 2020. Emissions and environmental levels of pharmaceuticals – Upscaling to the Baltic Sea Region. Project CWPharma activity 2.3 report. http://hdl.handle.net/10138/321722

Table of contents

Glossary

Abbreviation	Definition
API	Active pharmaceutical ingredient
BPL model	Baltic Pharma Load model
BS	Baltic Sea
BSE	Baltic Sea estuary
BSR	Baltic Sea region
CBZ	Carbamazepine
CLM	Clarithromycin
DCF	Diclofenac
GoF	Gulf of Finland
IBU	Ibuprofen
MTF	Metformin
OFL	Ofloxacin
PEC	Predicted environmental concentration
PNEC	Predicted no effect concentration
POC	Particulate organic carbon
TRD	Tramadol
VFX	Venlafaxine
WWTP	Wastewater treatment plant

Summary

This report describes the Baltic Pharma Load model (BPL) and the estimated environmental loads and concentrations of selected active pharmaceutical ingredients (APIs). The BPL model was developed as a part of the project Clear Waters from Pharmaceuticals (CWPharma) funded by the EU's Interreg Baltic Sea Region Programme. The calculation model uses national sales statistics as the driving parameter and takes into account selected differences in country-specific practices in e.g. waste management and sewer network coverage. The GIS-based model was compiled as a series of command scripts using the computing language and environment R (R Core Team 2020) and a calculation grid covering the entire Baltic Sea drainage basin. The calculation grid divides the Baltic Sea Region (BSR) into one square kilometer grid cells, with each grid cell containing the background information required for the calculations. Most of the country-specific input data used in the calculations was collected in parallel activities of the project CWPharma. These datasets included e.g. national sales statistics (Ek Henning et al. 2020) and waste management practices (Mehtonen et al. 2020).

The calculation method used in the BPL is based on the equations suggested in the guideline on the environmental risk assessment of medicinal products by the European Medicines Agency (EMA 2006). However, to produce more realistic estimates on the environmental occurrence of pharmaceuticals, the total residue approach advocated by EMA was supplemented with selected removal processes. These removal processes included elimination in waste management, metabolism, wastewater treatment plant processes and environmental processes during the transport from emission location to the Baltic Sea.

Using the BPL, we estimated the loads of eight APIs to the Baltic Sea as well as their concentrations at river mouths and in coastal waters. The loads of diclofenac, carbamazepine, tramadol, clarithromycin, ofloxacin and venlafaxine to the Baltic Sea were estimated to be the highest from Poland. Similarly, the highest metformin and ibuprofen emissions were estimated to occur from Russia. Despite these countries being estimated to emit the highest total loads to the Baltic Sea, there was a lot of variation in the estimated national per capita emissions for different APIs.

The highest API concentrations at river mouths were estimated to occur in southern parts of the BSR. Rivers with relatively high API concentrations were estimated to be located e.g. in Denmark, where the river flow rates are low, and population living in river basins is relatively high.

The predicted API concentrations in wastewaters and river mouths were compared to the measured concentrations in the same regions reported by Ek Henning et al. (2020). The predicted concentrations were generally within the observed range in wastewaters. However, ofloxacin concentrations were far below the measured range in influent and effluent wastewaters. This discrepancy was explained by the chemical analyses carried out by Ek Henning et al. (2020) covering the total concentration of the racemic mixture (ofloxacin), including also the enantiopure form (levofloxacin), while the sales statistics used in this calculation exercise covered only the racemic mixture.

The predicted concentrations in river mouths were generally higher than those measured by Ek Henning et al. (2020). However, there were also locations where the concentrations were lower than the measured ones. As the BPL model estimates the annual average concentration in river mouths based on long-term average flow rates, and the weather conditions were somewhat exceptional in many sampling sites during the CWPharma sampling campaign (Ek Henning et al. 2020), more data points would be required to properly calibrate the BPL model and to assess its performance.

The calculation approach used in the BPL model takes into account several real-life processes and estimates where potential hotspots may be located. This kind of visual and easy to use tool helps to target expensive and labor-intensive screening campaigns at areas of highest concern. Selected results of this calculation exercise can be viewed also in a web-based map application (SYKE 2020).

1. Introduction

Active pharmaceutical ingredients (APIs) have been detected in environmental samples in every inhabited continent (aus der Beek et al. 2016). Several APIs have also been detected in wastewaters and environmental samples in the Baltic Sea Region (BSR) (UNESCO & HELCOM 2017, Ek Henning et al. 2020). However, knowledge about the extent of contamination by pharmaceuticals entering the Baltic Sea is inadequate.

One of the aims in the project CWPharma was to estimate the overall loads of selected APIs to the Baltic Sea, and to identify potential hotspots for both emissions and occurrence. This would help to identify the APIs of highest concern, and the areas where monitoring should be carried out and emission reduction measures could have the highest overall impact.

The most straight forward way of increasing knowledge on the environmental levels of pharmaceuticals would be to carry out extensive monitoring campaigns. However, the Baltic Sea drainage basin is vast and has regionally varying environmental conditions. Achieving a comprehensive overview of API concentrations in a regional scale would require numerous samples, resulting in high costs.

Since pharmaceuticals are used in a very regulated manner, simulating their loads based on sales statistics could prove to be a more cost-efficient approach. The simplest way to achieve this would be to utilize the 'total residue approach' recommended in the European Medicines Agency's (EMA) guideline on pharmaceutical risk assessment (2006). However, for most APIs this approach will inherently result in overestimations of the load entering the environment, as it assumes that all sold mass is eventually emitted into the environment.

Therefore, the aim in this work was to produce more realistic estimates of the API load reaching the Baltic Sea (BS) by including several removal processes into the estimation. To do this, a calculation tool, Baltic Pharma Load model (BPL), was developed. This model takes into account the reductions in total API load due to metabolism, wastewater treatment plant (WWTP) processes and environmental processes.

BPL is a GIS-based calculation tool for estimating the API load entering the BS. Since the primary emission source of API emissions is estimated to be consumption and subsequent excretion (e.g. EC 2019), population and API sales information were selected as the driving parameters of the model. The uneven distribution of the population within the BSR (see Figure 1) was also taken into consideration. The approach chosen for the BPL model, some background information and selected results of this calculation exercise can be viewed in a web-based map application (SYKE 2020).

The aim of the work was to

A) estimate the loads of selected APIs to the BS,
B) estimate their concentrations in river mouths and in coastal areas, and
C) use these estimates to assess where the highest loads originate from, and which parts of the Baltic Sea receive highest API loading

Several scenarios were developed to estimate the natural variation in loads and concentrations, caused by variations in e.g. temperature and water flow volumes. The model was designed to give rough estimates of the current API concentrations along BS coasts for later risk estimations, and to be easily modifiable, allowing for estimates on the effects of proposed risk mitigation measures under CWPharma work package 5 (Äystö et al. 2020).

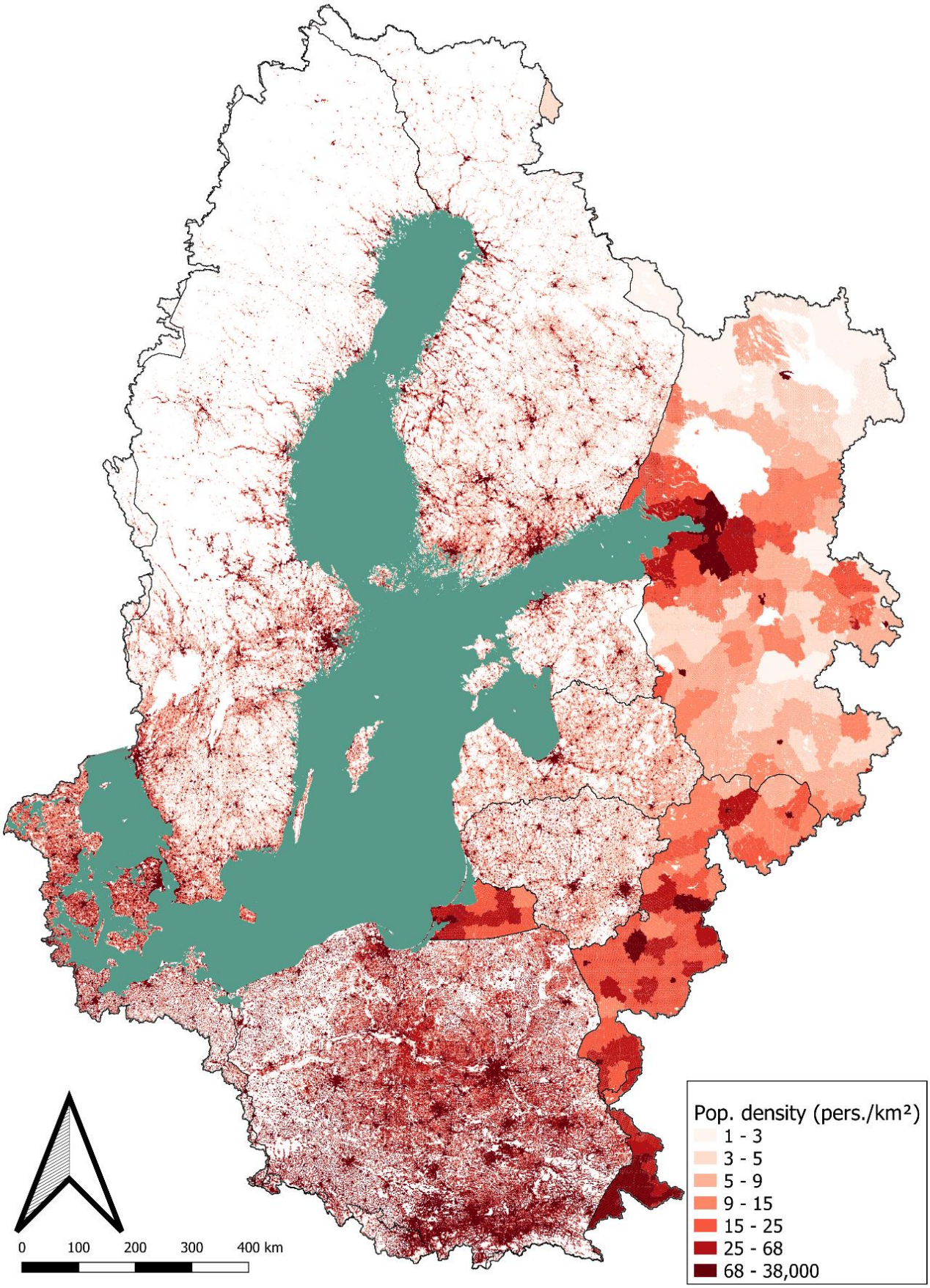

Figure 1. Population density in different parts of the Baltic Sea catchment area. Black lines represent country borders.

2. Methods

2.1. Model development & structure

The aim of the model development was to produce a calculation tool that would enable reliable estimation of pharmaceutical loads reaching the environment, and the API concentrations at various sites in the environment and in wastewaters. To do this, three removal processes were taken into consideration.

Counting from the ingestion of a pharmaceutical product to the eventual emission of its residues into the environment, the first removal process is metabolism in the human body. Metabolism of each API varies between individuals. Also, the route of administration may have a significant impact on how efficiently pharmaceuticals are transformed before their excretion. For instance, topically administered pharmaceuticals may be washed off before their absorption and metabolism. Therefore, the fraction of API excreted as the parent compound is not a natural constant. Additionally, while pharmaceuticals that are left unused never go through metabolic processes, some of them may be flushed into the sewer network. Emissions from unused pharmaceuticals were accounted for with the help of national statistics collected by Mehtonen et al. (2020).

The second dissipation process is removal during wastewater treatment. Current WWTPs are not designed to remove APIs, but several APIs are biodegradable and are therefore degraded or transformed in WWTP processes to a varying degree. For several APIs, binding to particles and eventually ending up in wastewater sludge may play a more important role in overall removal at WWTPs than biodegradation. However, not all sewage is treated at WWTPs. Thus, a country-specific fraction of wastewaters, as reported by UNICEF & WHO (2019), and the pharmaceutical residues they contain, was assumed to not go through the removal processes at WWTPs.

The third removal process is elimination due to degradation or sorption in the surface waters that receive the wastewaters. These removal processes are highly dependent on environmental conditions, such as temperature and light intensity. While these factors affect the degradation rate of APIs in the environment, the total load to the Baltic Sea depends on how long it takes for an API to travel from a discharge point to the sea. To account for this variability in removal rates, several scenarios aiming to present different seasons and annual variation were developed. Bio- and photodegradation were taken into consideration for the whole BSR catchment area. Sedimentation was only included in coastal regions.

The loads in wastewaters (influent and effluent) were calculated for all APIs screened in the CWPharma screening study (Ek Henning et al. 2020) and the predicted concentrations were compared to the ones measured by Ek Henning et al. (2020). The loads to the BS and their concentrations at river mouths and coastal waters were estimated for eight APIs: carbamazepine (CBZ), clarithromycin (CLM), diclofenac (DCF), ibuprofen (IBU), metformin (MTF), ofloxacin (OFL), tramadol (TRD) and venlafaxine (VFX).

The removal processes and assumptions on national practices contain high uncertainties. However, to implement them into the calculation tool, they were considered to behave as constants, and their values were selected based on data presented by Ek Henning et al. (2020) and Mehtonen et al. (2020), other data available in literature, and expert judgement. The processes included into the model are presented in Figure 2. Potential emissions from e.g. landfills, veterinary medication and utilization of sewage sludge were not included into the model. A comprehensive description of the structure of the BPL is presented in chapters 2.1.1 and 2.2, while the input data is presented in chapter 2.3.

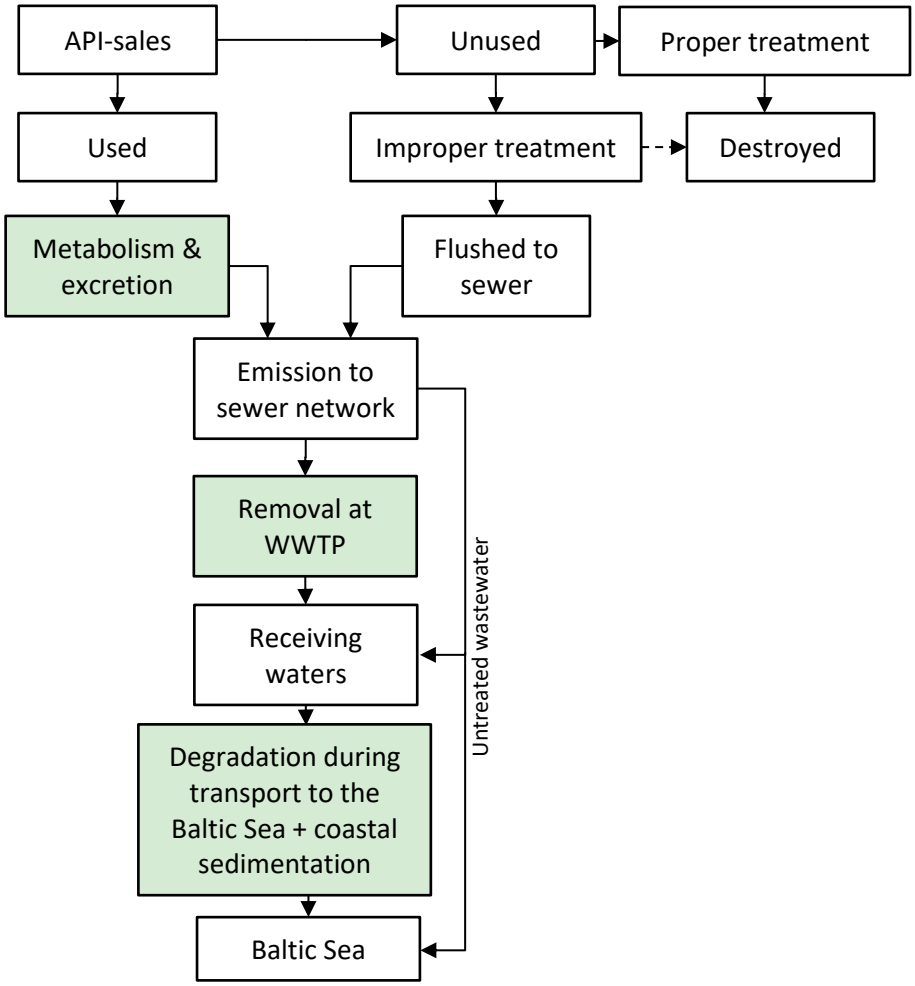

Figure 2. Calculation framework and removal processes included in the calculations (highlighted in green). The dotted line presents the situation, where unused pharmaceuticals are not treated properly, but where they are eliminated by e.g. incineration in municipal waste management or permanent encapsulation in landfills.

Some calculation exercises have previously been carried out to estimate API loads and concentrations in the environment. Bollmann et al. (2019) estimated the loads of selected micropollutants to the Baltic Sea using concentrations measured in treated and untreated wastewaters and stormwaters, and calculating the loads based on estimated water flows. Their approach was based on a model city with a wide range of input parameters. These input parameters were selected to represent the estimated situation in the Baltic Sea area. The calculation tool was then further expanded to cover the Baltic Sea area by modifying relevant input parameters. On the other hand, Oldenkamp et al. (2018) estimated the concentrations of a wide range of APIs in surface waters across Europe using national sales statistics and water flow networks. The removal processes they accounted for were degradation in the environment, sorption to particles and eventual sedimentation, and metabolism. Metabolism was also included as a process that may increase the API load, i.e. as the input from metabolism of prodrugs. Oldenkamp et al. (2018) included the WWTPs in the calculation region into the calculations by inserting them into the flow network and assigning WWTP-specific removal rates based on the processes in those WWTPs.

The approach selected in the BPL model contains parts of both approaches. Whereas Bollmann et al. (2019) used generic input parameters, and treated the BSR as one big block, and Oldenkamp et al. (2018) treated the area as a network, BPL-calculations are based on a grid-based approach, where every grid cell is an individual calculation unit containing all relevant processes, and a flow network used in estimating the distance of each individual grid cell from the BS coast.

2.1.1. GIS-materials & processing

To estimate the API load to the Baltic Sea, certain geographical and hydrographical parameters in different parts of Baltic Sea region had to be considered by using available data. To do this, several open data sources were accessed, and the data was further processed to accommodate the selected approach.

Both raster and vector analyses were utilized in the GIS-based modelling to process data to be applied in further calculations. The coordinate system used in the modelling was ETRS_1989_LAEA, which HELCOM mainly uses in its own spatial datasets. ESRI's mapping and analytics software were used to compile the GIS-materials for this model.

In the calculation model, the entire BS catchment area was divided into a 1 x 1 km² grid. Each grid cell contains vital information for the calculations, such as coordinates, estimated distance from the BS, population, elevation, lakes and rivers, country, and identifiers on several layers (grid cell-specific, catchment area-specific, etc.). With the help of the grid cell specific identifier, the source data and the data produced in further calculations could be e.g. rejoined to a specific coordinate, while other identifiers were used e.g. in aggregating the results. Each grid cell was assigned a virtual WWTP, in the sense that WWTP removal processes were assumed to take place in each cell, right after excretion. A comprehensive description of structure of the BPL calculation grid is presented in Annex 1.

The high-resolution grid (1 x 1 km²) used in the BPL model was selected after preliminary tests with a lower resolution (10 x 10 km²). The lower resolution would have resulted in the calculations requiring less computing power. However, this would have been achieved at the expense of the quality of the results. Using low resolution would have resulted in the input data, such as the distances from the BS and population, being of much lower quality, resulting in the results being of lower quality.

When selecting the input data for the model, the aim was to use open source data that are available to everyone free of charge. HELCOM map and data service (HELCOM 2020) was identified as a good source for regional information on the BSR. In many cases, however, more suitable open GIS datasets for modelling purposes were found elsewhere. The challenge was to find data that would cover the entire catchment area of the Baltic Sea and be of sufficient accuracy and quality. A particular challenge between the different data types and their sources and formats was to fit them to 1 x 1 km grid cells and a common GIS-based model, due to differences in location accuracy, unit accuracy, scale and quality of different data sets. This was achieved by processing the GIS-materials using different kinds of methods such as resampling and interpolating.

In general, EU countries usually had a common source of data of sufficient quality covering their regions, but certain data sets (e.g. population: Eurostat 2016b & CIESIN 2016, rivers and lakes: Eurographics 2018 and JRC 2007 & Vogt et al. 2007) had to be supplemented with data on non-EU-countries, from other sources. The quality of the data from non-EU-countries was not always as good as the data in other parts of the Baltic Sea catchment area.

The aim of the BPL model was to indicate areas with the highest API concentrations as well as possible emission hotspots. To do this the study area was classified into different region classes depending on the processes through which APIs reach the BS (presented in Table 1 and Figure 3). Within this regional division, the regions were divided further into smaller areal units (e.g. individual cities and river basins), which were given their own area IDs for further calculations.

Table 1. Emission and recipient areas, explanations on different region classes and processes included in each class.

Emission source areas							
Region class	**Area description**	**APIs sold & used**	**Removal at virtual WWTP**	**Unused & untreated**	**Sedimentation**	**Degradation in the environment**	**API load used to calculate concentration**
Inland area	Main river basins	Yes	Yes	Yes	No	During transport • Distance estimated based on elevation model (see p. 12) • Flow speed varies with scenario (see chapter 0)	At river mouth.
Inland urban cluster	Urban clusters located close to a large WWTP, a subset of inland areas	Yes	Yes	Yes	No		
Coastal land	Land areas between main river basins and on islands	Yes	Yes	Yes	No	No, wastewaters are assumed to be emitted into the Baltic Sea.	In coastal waters, both as background concentration and as the concentration at the urban coast.
Coastal urban cluster	Urban clusters located close to a large WWTP, with a high population density (see p. 11), a subset of coastal land	Yes	Yes	Yes	No		

Receiving areas					
Region class	**Area description**	**Load entering from**	**Sedimentation**	**Degradation in the environment, once recipient has been reached**	**Water volume where the API load is diluted**
River mouth	Mouths of the rivers included into the BPL	Inland areas	No	No	River flow
Urban coast	Coastal waters within a perimeter of 3 km from the closest coastal urban cluster	Inland and coastal areas	Yes	Yes, degradation rate varies with depth, season and region (see chapter 2.2.3)	Water volume in the coastal region
Coastal water	Coastal waters within a perimeter of 3 km of the closest grid cell flagged as land area	Inland and coastal areas	Yes		

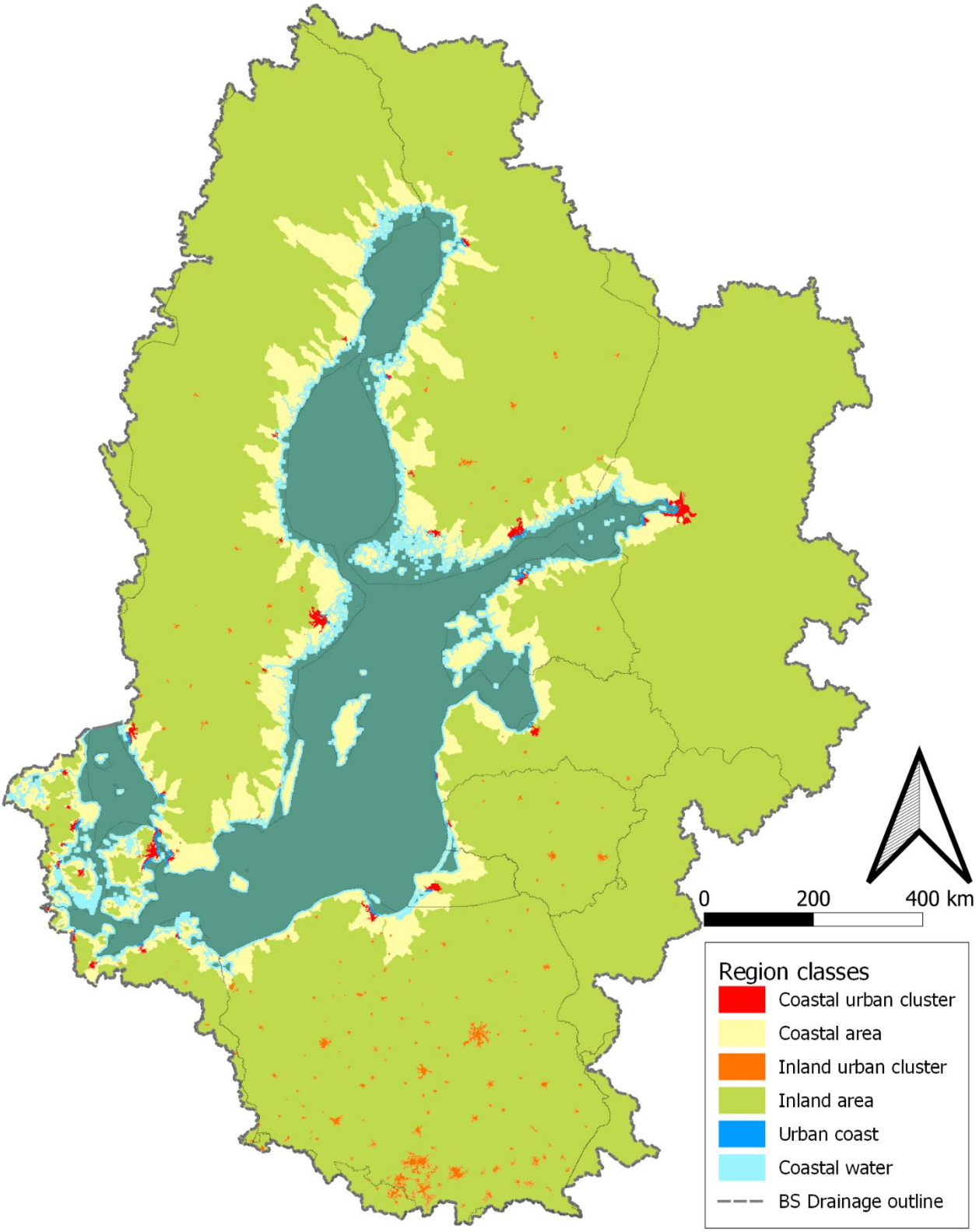

Figure 3. Regional classification used in the calculations.

The coastal urban clusters were defined as urban areas with more than 50,000 inhabitants within 5 km from the coast and with a WWTP (distance max 5.5 km from urban cluster) that treats over 3,650,000 m^3 wastewater per year (Eurostat 2016a, HELCOM 2011). Inland urban clusters were also determined based on the same data on urban clusters, but using the Urban Waste Water Directive (UWWTD) database v7 (EEA 2019), which contains the locations and PE-values of WWTPs located in EU member states. Different input data on WWTPs were used in identifying coastal and inland urban clusters, due to UWWTD not covering Russia. Using spatial data analyses, each WWTP with

a PE-value higher or equal to 50,000 was joined to the closest population cluster for further API load calculations.

As presented earlier in Figure 1, population is not distributed geographically uniformly within the BSR, and between different countries. Dividing the BSR into different region classes helps to highlight the differences also within countries. Within the whole BSR, 75% of the population is located in inland areas. However, there is high variation between countries. For instance, in Poland, 96% of the population is located in inland areas, while the same portion for Denmark is 27%. Population distribution by each region class is presented in Figure 4.

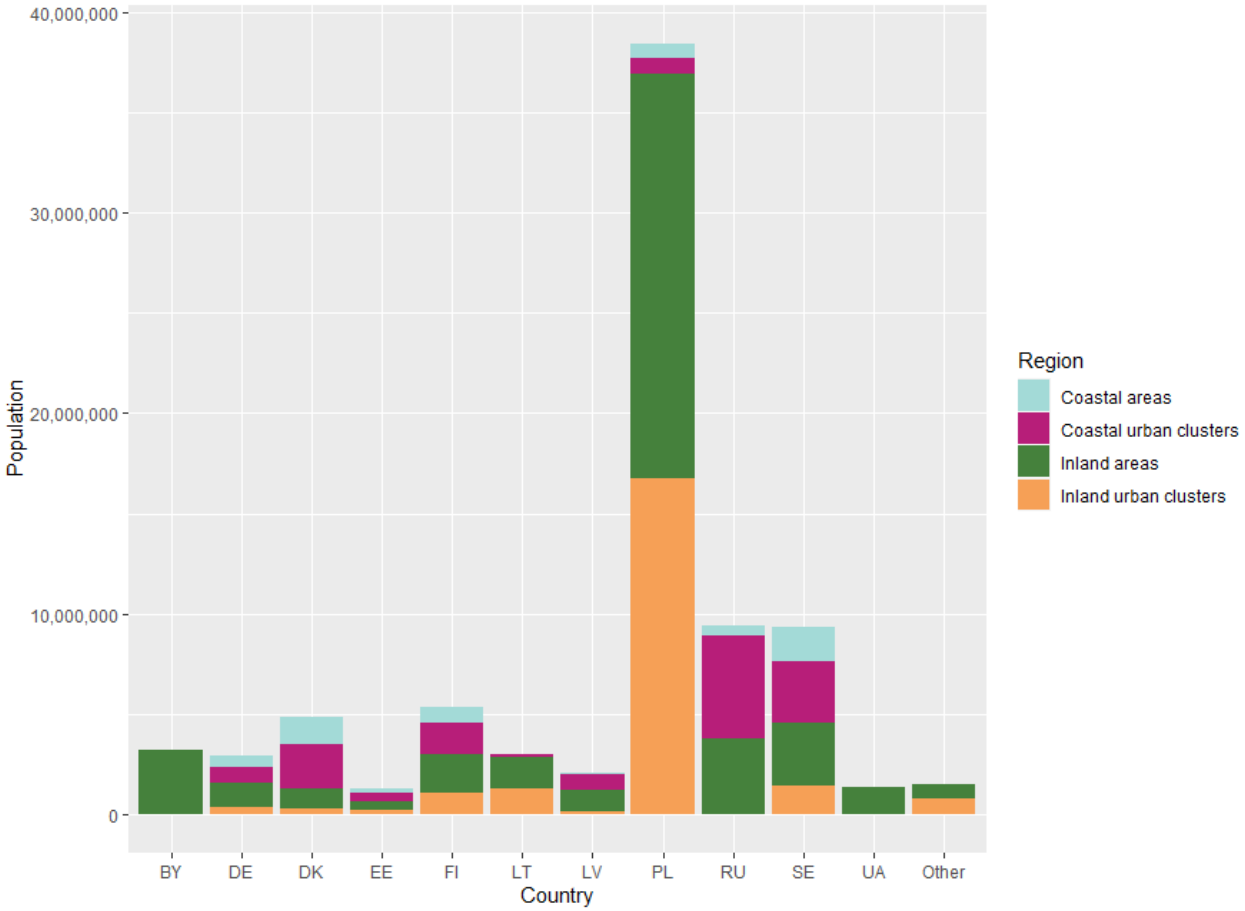

Figure 4. Population distribution by country and region class. Other countries include NO, SK and CZ, that have relatively small areas and little population within the BSR.

The regions classified as inland areas, include the main river basins of the Baltic Sea region. The source data was the Baltic Sea catchment area compilation which the HELCOM member countries have gathered from their own catchment area data (HELCOM 2018a). Coastal areas (emissions from WWTPs straight into the Baltic Sea) included areas between the main river basins on the coast and in the archipelago, as presented by HELCOM (HELCOM 2018a, HELCOM 2017).

The Global Multi-resolution Terrain Elevation Data 2010 (Danielson & Gesch 2011) model was used as the basis for modeling flow directions. To refine these estimates, known main flow paths were highlighted by burning in lakes and rivers into the digital elevation model. Stream burning is a flow enforcement technique used to correct surface drainage patterns derived from digital elevation models. The technique involves adjusting the elevation of grid cells that are coincident with the features of a vector hydrography layer. The watersheds in the Baltic Sea catchment area compiled by HELCOM (HELCOM 2018a) were also emphasized into the elevation model. A flow direction model, presenting the flow directions for each grid cell, was calculated by using the preprocessed elevation model. The flow direction modelling did not take into account bifurcations of streams.

A flow accumulation grid was produced and combined with the flow direction model to determine the flow paths for each grid cell. These datasets were further utilized to calculate the upper catchment areas and downstream distances to the sea for each grid cell. Identifying the upstream

grid cells is especially important for identifying which cells flow through which lakes and river mouths. Additionally, the average flow rate (m^3/s) of the annual flow data (HELCOM 2018b) for 1995–2006 was included to the grid cells of the main river basins. The calculated flow distances to the BS and main flow routes are presented in Figure 5.

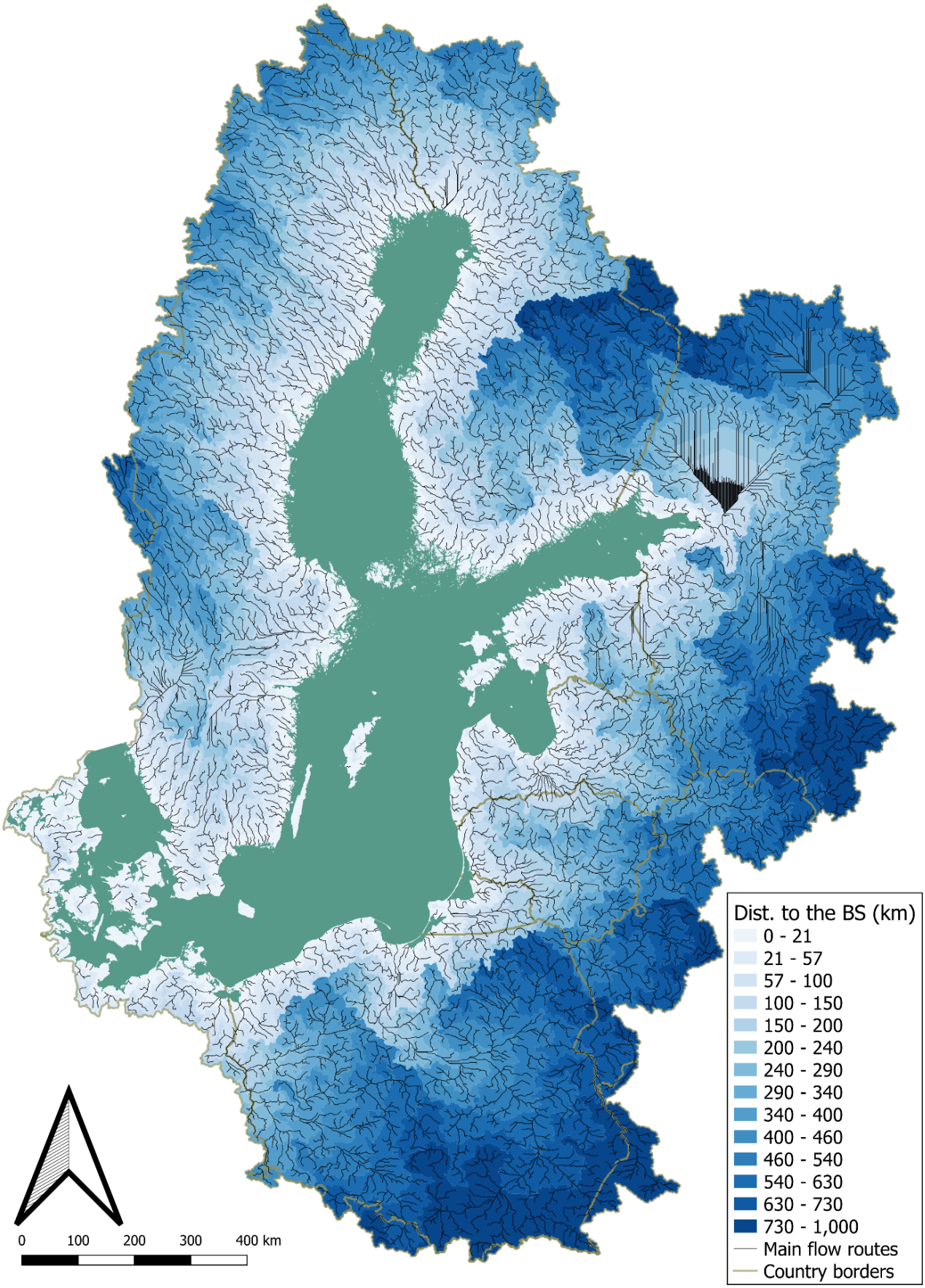

Figure 5. Calculated distances to the Baltic Sea along the calculated flow routes. Main flow routes area presented in turquoise line and country borders in black line.

The coastal areas into which each emission cell flows were also calculated based on the flow direction model. This information is vital for estimating the total load reaching different sections of the BS coastline. On the other hand, sea depth data were interpolated by using the raster grid of the Baltic Sea bathymetry computed from the original Digital Topography of the Baltic Sea (HELCOM 2005). Volume estimates (m^3) of each grid cell in the sea were derived from sea depth data. In addition, a three-km wide coastal zone was defined for the coastal areas and used in the concentration calculations. The sea depths within the calculation grid are presented in Figure 6.

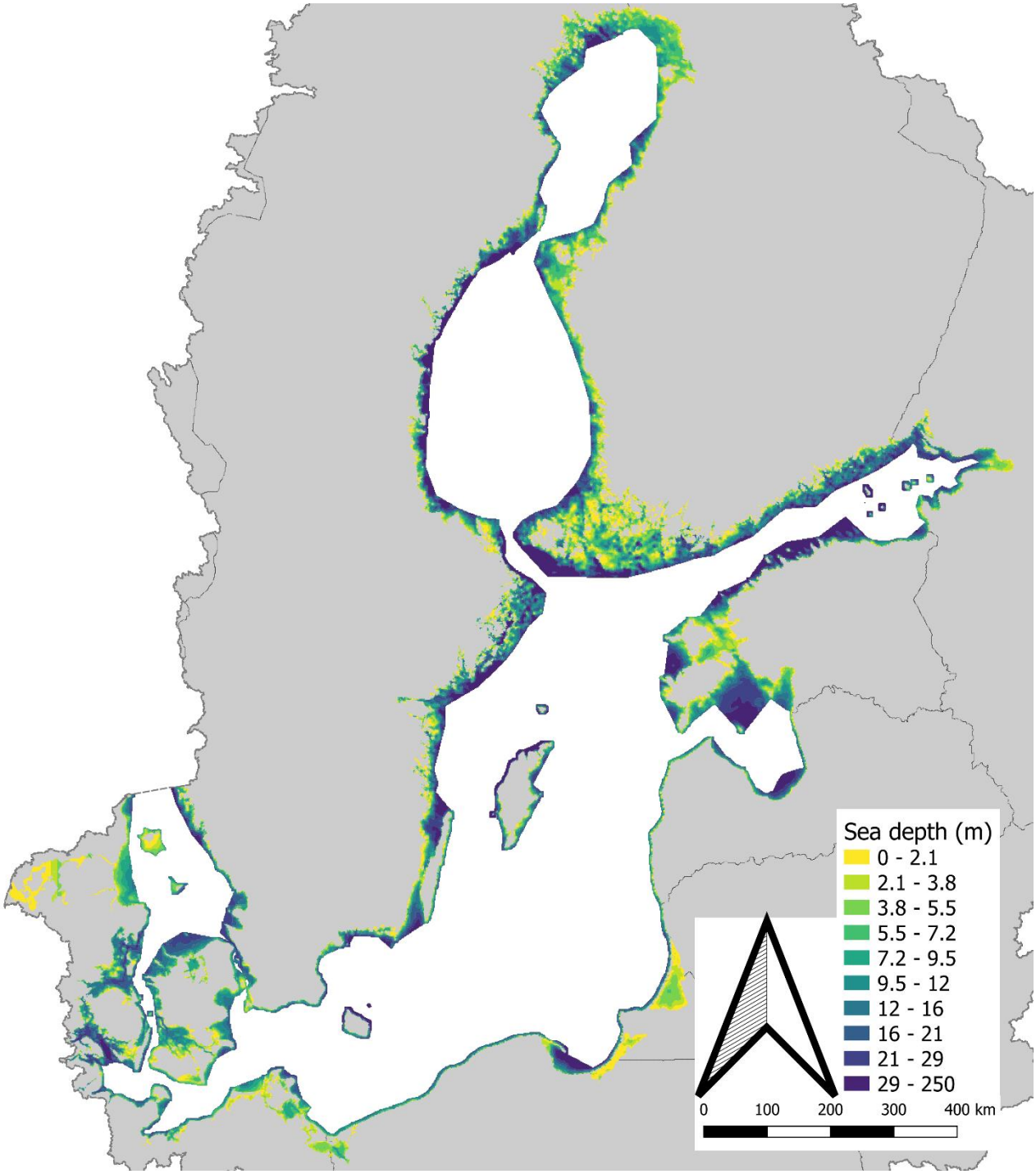

Figure 6. Sea depth in the calculation area.

2.2. Calculation approach & included processes

The calculation grid contains 1.9 million cells. To make the calculation process efficient, calculations were carried out using the computing language and environment R (R Core Team 2020). The calculation process presented in chapters 2.2.1 through 2.2.4 were compiled into R scripts. Compiling the calculation method into scripts allowed the calculation to be repeated efficiently, while minimizing human error. The scripts are available in the web (http://hdl.handle.net/10138/321722).

2.2.1. Load and concentration estimation in wastewaters

Sales of each API were calculated for each grid cell as the national per capita sales multiplied by the number of inhabitants in the cell. These values were further used in estimating the load entering the virtual WWTP, by multiplying the cell-specific consumption by the API-specific excretion rate. This value was modified according to national information on the fraction of pharmaceuticals that is eventually left unused, which fraction of this goes through appropriate pharmaceutical waste management, and assumptions on which fraction of the remainder is flushed into the sewer network. The API-specific input values on national sales and environmental properties are presented in Tables 2 and 6, respectively.

The resulting influent load to virtual WWTP, in turn, was used further in estimating the effluent load from the virtual WWTP, with the help of the API-specific WWTP removal rate. These removal rates were calculated based on concentration data presented by Ek Henning et al. (2020), and accounts only for removal from the water phase, disregarding potential emissions from e.g. sewage sludge utilization.

Loads in influent and effluent wastewaters were calculated using Eq. (1) and (2), respectively. The estimated loads were transformed into concentrations using an average per capita water consumption (V_{pc}) of 140 l/d/person (see Eq. (3) and (4)). Estimates on the total load eventually reaching the BS were calculated using the estimated loads in effluent wastewater, taking into account selected removal processes in the environment (see chapter 2.2.2).

(1) $$L_{inf} = C \times (1 - F_u) \times E + C \times \left(F_u \times (1 - F_p) \times F_{w2s}\right)$$

, where

L_{inf} = Load in influent wastewater [mg/a]

C = Total annual sales in grid cell [mg/a]

F_u = Fraction of sold medicines left unused [-]

E = API-specific excretion rate [-]

F_p = Fraction of unused medicines treated properly [-]

F_{w2s} = Fraction of improperly treated pharmaceutical waste flushed down the sewer [-]

(2) $$L_{eff} = F_s \times L_{inf} \times (1 - RR) + (1 - F_s) \times L_{inf}$$

L_{eff} = Load in effluent wastewater [mg/a]

F_s = Fraction of wastewater connected to sewer network [-]

RR = API-specific removal rate at WWTP [-]

(3) $$C_{inf} = \frac{L_{inf}}{V_{pc} \times 365}$$

C_{inf} = API concentration in influent wastewater [mg/L]

V_{pc} = Per capita water consumption [L/d]

(4) $$C_{eff} = \frac{L_{inf} \times (1 - RR)}{V_{pc} \times 365}$$

C_{eff} = API concentration in effluent wastewater [mg/L]

2.2.2. Load estimation to river mouths and to the Baltic Sea

The cell-specific effluent load into the water environment was used in estimating the load to the river mouth, and subsequently to the BS, taking into account degradation and environmental conditions, such as water temperature and flow speed during transport.

Delay estimations in river basins

The flow route network (see p. 12) was used in estimating the time it takes for emissions originating in a certain grid cell to reach the BS. This network gives an estimate on the distance from each grid cell to the BS. To estimate how long it takes for an emission to reach the BS, the distance was divided with the estimated flow speed. Different scenarios (see chapter 2.3.2) were developed, with different flow speeds, to account for variations between seasons.

The estimates derived based on these background data were combined with information on selected lakes located in the calculation area and their estimated retention times. The flow network was used in identifying which grid cells are located upstream from which lakes. The retention time of each lake was added to the flow times of each cell located upstream from the discharge point of the lake. If there were several consecutive lakes, the lake retentions were summed (see Figure 7). The lakes included into the model are presented in Annex 2.

Lakes were selected from each country by CWPharma project partners in respective countries. Lake selection was carried out based on lake retention times and locations: lakes with longer retention times or locations downstream from significant population centers were prioritised. During this selection process, it was concluded that there are no lakes that would have a relevant impact on retention times to the BS in Denmark and Germany.

As an example, in Finland a preliminary set of lakes was selected from a national database (WSFS-VEMALA, e.g. Huttunen et al. 2016) by selecting the lakes with the highest retention times. Retention time for each lake was evaluated by dividing the volume of the lake by the outflow of the lake. This set was further supplemented with a set of smaller lakes located downstream from towns with significant population (e.g. Kuortaneenjärvi in western Finland), and some of the lakes with highest retention times were excluded if they were upstream from towns and cities (e.g. Kilpisjärvi in northern Finland).

Information on the retention time and location of the discharge point was collected for each lake. Based on the coordinates, the discharge points were placed manually into grid cells best corresponding to the general location of the lake and the calculated flow network.

Delays were calculated using Eq. (5).

(5) $$T_t = \frac{\frac{D}{V_{flow}}}{86\,400} + T_L$$, where

T_t = Total delay from emission cell to the BS [d]

D = Distance from emission cell to the BS [m]

V_{flow} = Flow speed [m/s]

T_L = Cumulative retention time in lakes located downstream from the emission cell [d]

86400 = 60 x 60 x 24 (coefficient needed for unit change between days and seconds)

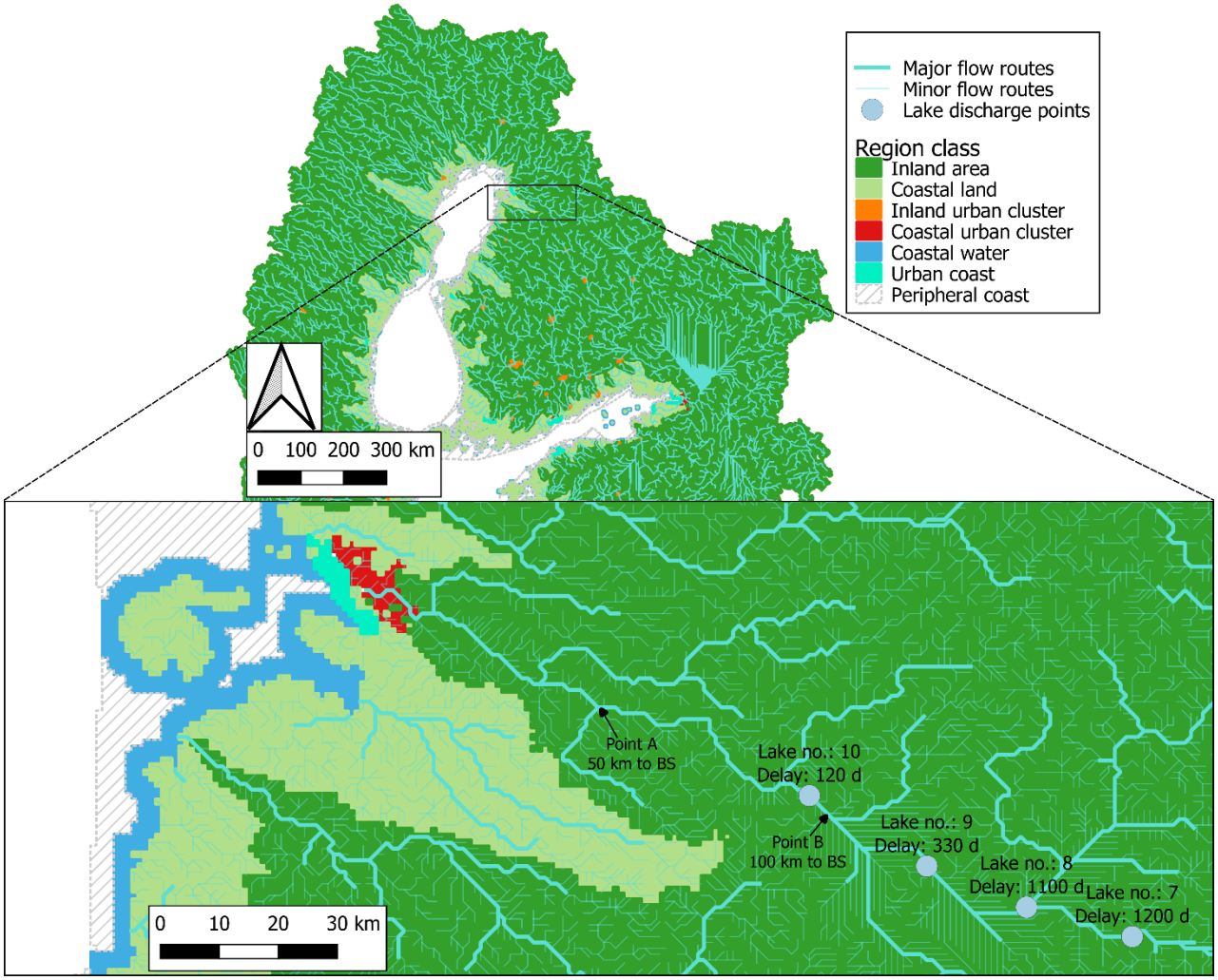

Figure 7. An example of how lakes and distance from the BS were taken into consideration in the delay-estimates. In Point A, the total delay was calculated by dividing the distance to the BS (50 km) with the flow speed (0.15 m/s), resulting in a delay of 3.86 d. However, since there is a lake below point B, the retention in this lake must be accounted for. Therefore, the delay from Point B is not 7.72 d, but 127.72 d. The retention times in lakes no. 10 to 7 seem to increase, due to the retention in each lake being added to the retentions of lakes located downstream.

Estimation of removal rates in the environment

During the transport from river basin grids cells to the BS, part of API load is dissipated due to photolysis and microbiological degradation. In the BPL model, these two processes were assumed to be the most relevant dissipation ways for most APIs in rivers and lakes.

In the BPL model, water flow in rivers and lake is divided into photoactive layer F_{photo} and non-photoactive layer. Degradation is calculated separately in these parts (see Eq. (6)). The total loads to the BS, to its sub basins, and to river mouths were aggregated from the loads from individual grid cells.

(6) $$L_{BS} = L_{eff} \times [F_{photo} \times e^{(-k_F \times D_t)} + (1 - F_{photo}) \times e^{(-k_{bF} \times D_t)}]$$

, where

L_{BS} = Load to the Baltic Sea [mg/a]

F_{photo} = Fraction of surface water, where APIs are exposed to photodegradation [-]

k_F = Degradation rate in the photoactive water fraction [1/d]

k_{bF} = Degradation rate in the non-photoactive water fraction [1/d]

D_t = Transport time from grid cell to the BS [d]

While photodegradation is assumed to occur only in the surface layer of the water column, biodegradation is assumed to occur in the whole volume (see Eq. (7) and (8)). The dissipation processes are described by pseudo first order kinetics, where the different processes are combined by summing their rates (see Eq. (8)). The impact of water temperature on biodegradation is calculated using a simple approximation based on Arrhenius equation (Eq. (9)). This approach is similar to the one suggested in the European Chemicals Agency (ECHA) guidance for biocide registration (2017).

(7) $k_{bF} = k_{bioT}$, where

k_{bioT} = Biodegradation rate in temperature T [1/d]

(8) $k_F = k_{photo} + k_{bioT} = \frac{\ln(2)}{DT50_{photo}} + \frac{\ln(2)}{DT50_{bioT}}$

k_{photo} = Photodegradation rate (direct + indirect) in optimum radiation conditions [1/d]

$DT50_{photo}$ = Photodegradation half-life [d]

$DT50_{bioT}$ = Biodegradation half-life [d]

(9) $DT50_{bioT} = DT50_{bioRefT} \times e^{\alpha \times (T_{ref} - T)}$

$DT50_{BioRefT}$ = Biodegradation half-life in reference temperature d]

α = A parameter including natural constants and activation energy etc. (see below) [1/°C]

T_{ref} = Reference temperature for biodegradation [°C]

T = Temperature in the environment [°C]

According to the opinion of European food safety authority (EFSA 2008), Arrhenius activation energy 65.4 kJ/mol should be used, if no substance specific information exists. Pesticides and pharmaceuticals are both organic synthetic compounds and the groups are not expected to differ in this perspective. The suggested Arrhenius activation energy corresponds to a Q10 value of 2.58 1/°C and thus $\alpha = (\ln Q_{10})/10 = 0.0948$ 1/°C. On the other hand, in the EU biocide registration, an older value 0.08 1/°C is used. In this project value 0.09 1/°C is used in calculations for APIs.

Temperatures used for different areas, and the water fraction exposed to photodegradation are presented in Table 4. The fraction of photoactive water volume (F_{photo} in Eq. (6)) is difficult to determine. It sums many different processes from river geometry to radiation intensity and water quality (DOC and Secchi depth). On a sunny summer day (high radiation intensity) in a 20 m and 5 m deep canal-type river profile, photoactivity can be assumed highest in a five cm surface layer of the water column. Similarly, light intensity can be assumed to decrease by 50% for each five cm step deeper into the water column. Using these assumptions, F_{photo} gets value 0.025. If the river were wider and shallower, F_{photo} would be higher (e.g. for a river 100 m wide and 2 m deep, F_{photo} would be 0.05). However, in cloudy days the value is smaller and during nights it is zero. There is also high seasonal variation in the radiation – and ice cover in winter in many rivers. For the calculation implementation, F_{photo} was treated as a constant for the whole BSR, with the value varying from 0 to 0.045, depending on calculation scenario (see chapter 2.3.2).

Potentially relevant removal processes, overlooked in the BPL model, are hydrolysis and sedimentation. The relevant part of hydrolysis is assumed to occur already before API is released to river water from WWTP. Therefore, it is not included as separate process in the model. Although sedimentation may be important for some compounds in some water bodies, it is not included into the model. It is assumed, that the most sorptive APIs will adsorb to particles in WWTPs. Additionally, while APIs from effluent may adsorb on particles, both dissolved and particle bound APIs may transport via river to BSE. Including sedimentation into the river processes in the model would also

have required river specific information on sedimentation rate. Therefore, for the very sorptive APIs the model is expected to give a slight overestimation on API loads and concentrations.

2.2.3. Calculation of concentration in river mouths and coastal areas

Predicted environmental concentrations (PECs) were estimated for 240 river mouths located within the BSR. These concentrations at river mouths were estimated based on the loads calculated for the cells located upstream from the river mouth cell. These cells could be identified based on the flow accumulation grid (see p. 12). The PECs represent average annual concentrations, and as such is expected to differ from individual measurement results. The river mouths covered by the BPL model and river-specific annual flows are presented in Annex 3.

As the calculation grid contains the estimated total transport times from each grid cell to the BS, the transport times to the river mouths could be calculated as well. To estimate the loads to the river mouths, Eq. (6) was modified by replacing D_t with D_{tRM} (see (Eq. (10) and (11)). The estimated load was converted to annual average concentration by dividing it with the annual average river flow for in each respective river (Eq. (12)).

(10) $$L_{RM} = L_{eff(i)} \times \begin{bmatrix} F_{photo} \times e^{(-k_F \times D_{tRM(i)})} + \\ (1 - F_{photo}) \times e^{(-k_{bF} \times D_{tRM(i)})} \end{bmatrix}$$

, where

L_{RM} = Load to the river mouth [mg/a]

$D_{tRM(i)}$ = Transport time from emission cell i to the river mouth

(11) $$D_{tRM(i)} = D_{t(i)} - D_{t(r)}$$

, where

$D_{t(i)}$ = Transport time from emission cell i to the BS [d]

$D_{t(r)}$ = Transport time from river mouth cell r to the BS [d]

(12) $$c_{RM} = \frac{\sum L_{RM}}{V} \times 1000$$

, where

C_{RM} = Concentration in river mouth [ng/L]

L_{RM} = Loads from cells located within the river basin [mg/a]

V = Annual average flow in the river [m³/a]

The API concentrations in coastal areas are approximated from the calculated annual average loads to the BS using two different approaches. The first approach is similar to the one used in estimating concentrations at river mouths (see Eq. (12)). Using this approach, C_{raw} is calculated by simply diluting the annual load to the coastal water volume (see Eq. (13)). The equation is especially suitable for areas where water changes during the year (e.g. estuaries).

The second approach estimates a long-term plateau concentration (C_{AA}), assuming that APIs are not transported out from the recipient coastal area. However, sedimentation, photodegradation and biodegradation are included into the calculation. The concentration is calculated by mixing the calculated plateau mass to water volume (see Eq. (14), (15) and (16)).

The input load is the sum of the loads from all cells discharging to that specific coastal area. Within each area, total and instant mixing of load in coastal water volume is assumed to take place. The concentrations in coastal waters were calculated for two different areas: urban coasts and coastal waters in general (see Table 1). The latter represents the background concentration, assuming the load to that coastal region is distributed uniformly in the area. The former, on the other hand,

assumes that the emission from the coastal urban cluster remains within the coastal waters within a 3 km perimeter from the cluster. Background concentration caused by the load from areas outside the coastal urban cluster are taken into account as well. Discussion on different dissipation routes is presented in the next chapter.

(13) $$C_{raw(i)} = \frac{L_{BS(i)}}{V(i)}$$

, where

$C_{raw(i)}$ = Concentration in coastal area *i*, estimated from annual load

$L_{BS(i)}$ = Annual load to coastal area *i* [kg/a]

$V(i)$ = Water volume in the coastal area *i* [m³]

(14) $$C_{AA(i)} = \frac{M(i)}{V(i)}$$

$C_{AA(i)}$ = Long-term plateau concentration in coastal area *i*

$M(i)$ = Plateau mass in Baltic Sea coastal area *i* [kg]

$V(i)$ = Water volume in the coastal area *i* [m³]

(15) $$M = \frac{1}{4} \times \sum_{q=1}^{4} \sum_{l=1}^{3} \times \frac{\frac{D_l}{D_{tot}} \times \frac{L_{BS} - m_{API\,s}}{365}}{k(q,l)}$$

q = Season in focus [-]
(1=Q1 (Jan-Mar),..., 4=Q4 (Oct-Dec))

l = Water layer in focus [-]
(1 = surface, 2 = mid-layer, 3 = bottom layer)

D_l = Depth of layer l [m]

D_{tot} = Total depth in the focus area [m]

$m_{API\,s}$ = Mass of sedimented API [kg/a]

$k(q,l)$ = total degradation rate in layer l during season q

(16) $$k(q,l) = a(q,l) \times \frac{ln(2)}{DT50_{photo}} + \frac{ln(2)}{DT50_{bio} \times e^{\alpha \times (T_{ref} - T_{ql})}}$$

k_{ql} = Degradation rate in layer l during season q

a_{ql} = Fraction of photolysis activity in layer l in season q in relation to the maximum potential photolysis [-]
(in June the fraction is 1,0 in layer l_1; the value of l_3 is 0 in all seasons)

$DT50_{photo}$ = Photolysis half-life [d]

$DT50_{bio}$ = Biodegradation half-life in reference temperature T_{ref} [d]

T_{ref} = reference temperature [°C]

T_{ql} = Temperature in layer l in season q [°C]

α = temperature correction factor [1/°C]

Dissipation processes in the BSE

Sedimentation

Sedimentation can be an important dissipation pathway from water phase especially for APIs having high adsorption affinity. The real sedimentation processes in BSE are rather complicated (e.g. Blomqvist & Heiskanen 2011) but a simple approach is used in the BPL model. The annual incoming load is divided into adsorbed phase and water phase. APIs are assumed to adsorb only on particulate organic carbon (POC) and, further, to be buried into sediment with it, with no resuspension. A

constant value for organic carbon burial rate is used for whole BS (see p. 27). Eq. (17) presents the equation used in estimating the mass of sedimented APIs in the BPL model, and Box 1 shows the derivation of this equation.

(17) $$m_{API\ s} = \frac{L_{BS(i)}}{1 + \frac{V_i \times \rho}{K_{OC} \times A \times k_{SEDPOC}}}$$

, where

$L_{BS(i)}$ = API load to coastal area *i* [kg/a]

V_i = Water volume in coastal area *i* [m³]

ρ = water density [kg/m³]

K_{OC} = API's partitioning factor between dissolved and adsorbed phases (adsorption coefficient) in proportion to organic carbon [l/kg]

A_i = Area of coastal area *i* [m²],

k_{SEDPOC} = Burial rate of particulate organic carbon in sediment [kg/m²/a]

Box 1. Derivation of the sedimentation equation (17).

Equation	Explanation
$K_D = \frac{c_S}{c_D}$	K_D = partitioning coefficient (linear adsorption) It is defined as the quotient of concentrations in adsorbed (c_S) and in dissolved (c_D) phases.
$c_{API\ s} = K_D \times c_{API\ D}$	$c_{API\ s}$ = concentration of API in sediment $c_{API\ D}$ = concentration of API in dissolved phase
$\frac{m_{API\ s}}{m_s \times f_{OC}} = \frac{K_D}{f_{OC}} \times \frac{m_{API\ D}}{m_W}$	Concentration is given as API mass per matrix mass: m_s is sediment mass and m_w is water mass. Values of both sides are divided by f_{oc} (fraction of organic matter) $K_D/f_{oc} = K_{oc}$ (by definition)
$\frac{m_{API\ s}}{m_{POC}} = K_{OC} \times \frac{m_{API\ L} - m_{API\ s}}{m_W}$	The non-adsorbed part of total API is the API in dissolved phase. Here, because the focus is in the API sedimentation during a year and its relation to one year API loading, the annual API load ($m_{API\ L}$) is used as total API. Consequently, only one year sedimentation is used as sediment mass. Assuming adsorption occurs on organic carbon only, the fraction of organic carbon of the one year sedimented material is the mass of annually buried particulate organic carbon $m_{POC} = m_s \times f_{oc}$.
$\frac{m_{API\ s}}{(m_{API\ L} - m_{API\ s})} = \frac{K_{OC} \times m_{POC}}{m_W}$	The equation is re-organized to solve the $m_{API\ s}$.
$m_{API\ s} = \frac{L_{BS}}{1 + \frac{V \times \rho}{K_{OC} \times A \times k_{SEDPOC}}}$	After some re-organizing steps and using markings: $m_{POC} = k_{SEDPOC}$ and $m_W = V \times \rho$, the result is Eq. (17).

API degradation in BSE

When API-load and the first order degradation rates are expected to be constant, a steady state "plateau" concentration is going to be reached in a system. The plateau principle (steady state concentration = input rate/dissipation rate) was originally developed in the 1940's in pharmacy to

calculate the right dose for patients and later expanded to different areas, including environmental modeling. The API loading into coastal areas can be seen as constant in this context, but degradation rates are known to vary with depth and season. Despite the varying dissipation rate, a steady state situation with seasonal fluctuation is expected to be reached. The plateau equation is typically used if dissipation processes follow first order kinetics. However, in this simplified approach sedimentation is assumed to occur instantly and to be a linear process. Therefore, the sedimented part of the annual API load is calculated first and only the rest (non-sedimented) part of annual API load is used for plateau calculation. This is an oversimplification of the actual process and it underestimates the sedimentation of persistent APIs, but given the high uncertainties in the input parameters, this simplification was considered to give an estimate of sufficient quality.

The fraction of the annul load, remaining in the water phase after sedimentation is divided to daily loads (annual load/365) to have the same time unit as used in the dissipation. The daily load is instantly mixed to the water volume of the focus region at the loading day. No further mixing (e.g. due to changing temperature gradient) between layers is assumed to happen. This API-mass is assumed to undergo degradation processes through biodegradation and photolysis.

Photodegradation and other radiation-initiated degradation processes are usually faster than biodegradation, but they can occur only in surface layer where enough radiation energy is available. In the model, the sea water profile is divided into three layers according to photoactivity capacity. In the surface layer the photoactivity is expected to have its full capacity in summer. In the second layer there is some photoactivity but radiation energy and photoactivity is only a portion of that in surface layer. Photoactivity is not relevant in the third layer located below the second layer. Radiation attenuation in sea water depends on wavelength. The UV-wave length (<400 nm), which has more energy than visible light and thus is more important for degradation processes, penetrate only into surface water while longer wavelength can reach to depths deeper than measured Secchi depth (Simis et al. 2017).

Biodegradation in BSE is assumed to occur in the same way as in freshwater and the same temperature correction equation is used (see river processes, Eq. (9)). However, for the coastal area, different temperatures are used for different latitudes and depths. Temperature correction is carried out for different seasons. For each season, the mass is calculated and averaged to produce an annual average plateau mass (see Eq. (15)). Using the first order kinetics and assuming no differences in the load, the plateau concentration is mathematically reached within 8 times half-life since the start of the loading, and rather good estimate is reached within 5 half-life times.

2.2.4. Risk identification

The predicted concentrations in river mouths and coastal waters estimated for the eight APIs presented in Table 2 were compared to API-specific predicted no effect concentrations (PNEC) reported by Ek Henning et al. (2020), presented in Table 6. This comparison was carried out by dividing the PEC with the API-specific PNEC-value (see Eq. (18)). Whenever the resulting risk quotient (RQ) exceeds the threshold value 1 (i.e. PEC > PNEC), there is a potential environmental risk.

(18) $$RQ = \frac{PEC}{PNEC}$$

, where

RQ = Risk quotient [-]

PEC = Predicted environmental concentration [ng/L]

$PNEC$ = Predicted no effect concentration [ng/L]

Since the APIs in focus in this work represent only a very small fraction of all the APIs on the market, and being emitted into the environment, this exercise cannot be used in estimating the overall risk posed by pharmaceutical emissions to the environment. Therefore, the approach presented above was applied only to individual APIs.

2.3. Input data & scenarios

2.3.1. National input data

The APIs to be modelled were selected based on previous information about their occurrence and possible risks to the environment. Strong emphasis was given to the screening campaign carried out in the project CWPharma (Ek Henning et al. 2020). The APIs selected to be simulated in this work, as well as their national sales, are presented in Table 2. The API sales were largely combined in a parallel activity of the project CWPharma and reported by Ek Henning et al. (2020), and further supplemented with the data published by the MORPHEUS-project (Kaiser et al. 2019) and by the The Danish Health Data Authority (2020). Sales information for all APIs looked into in the project CWPharma is presented in Annex 4.

Table 2. API-specific annual sales (average for the tears 2015-2017).

API	Sales										Per capita avg [5]
	Sales	DE[1]	EE[1]	FI[1]	LV[1]	SE[1]	PL[2]	LT[2]	DK[3]	RU	
DCF	kg/a	27,000	1,500	2,500	2,000	2,800	8,000	510	910	20,000[4]	0.61
	mg/d/pers.	0.90	3.1	1.2	2.7	0.78	0.58	0.71	0.44	0.37	
CLM	kg/a	11,000	410	220	450	630	8,600	130	470		0.41
	mg/d/pers.	0.37	0.86	0.11	0.63	0.17	0.62	0.18	0.23		
MTF	kg/a	1,600,000	23,000	150,000	29,000	110,000	670,000	19,000	92,000		51
	mg/d/pers.	54	47	75	41	32	48	26	44		
IBU	kg/a	340,000	15,000	120,000	20,000	120,000	8,500	3,900	64,000		13
	mg/d/pers.	11	32	61	28	32	0.61	5.5	31		
OFL	kg/a	480	3.7	11	27	0,013			0,017		0.013
	mg/d/pers.	0.02	0.008	0.005	0.04	3.59e-06			8.2e-06		
TRD	kg/a	21,000	320	1,700	360	3,500			6,400		0.87
	mg/d/pers.	0.72	0.67	0.86	0.5	0.97			3.1		
VFX	kg/a	19,000	120	2,000	57	3,600			2,400		0.70
	mg/d/pers.	0.64	0.24	0.98	0.08	0.99			1.1		
CBZ	kg/a	37,000	1,000	3,000	1,400	5,900	27,000	400	1,800		1.4
	mg/d/pers.	1.2	2.2	1.5	2.0	1.6	2.0	0.56	0.88		

1) Ek Henning et al. 2020 (data averaged over years 2015–2017)
2) Kaiser et al. 2019 (data for year 2015)
3) The Danish Health Data Authority 2020 (data averaged over years 2015–2017)
4) HELCOM 2014 (data for early 2010's, exact year unknown)
5) Calculated as population weighted per capita consumption based on countries with sales statistics available. This value was used whenever no country-specific value was available.

Information on pharmaceutical sales in Denmark was available in defined daily doses (DDD) and in sold packages. Ek Henning et al. (2020) noted that converting DDD values into mass units contains several uncertainties. Therefore, the Danish sales data was converted from sold packages to mass units. The information available on the Medstat.dk website (The Danish Health Data Authority 2020) made it possible to produce a seemingly good estimate of the total sales. However, it was not possible to validate these estimates within this project.

The weighted per capita sales figure was calculated as the sum of the masses sales in the BSR countries, where sales information was available, divided by the population in those countries. For countries, for which no sales statistics were collected (BY, CZ, NO, SK and UA), this value was used.

As the calculations were carried out for the whole BSR, national information on sewage treatment and waste management was also utilized in order to account for the regional differences. Information on sewer network coverage was collected for all countries with regions within the Baltic Sea catchment area. Information on waste management was collected in a parallel activity of project CWPharma (Mehtonen et al. 2020). The national input data on waste and sewage management are presented in Table 3. Since waste management statistics in all countries were either lacking or

outdated, no information on which fraction of improperly managed unused pharmaceuticals are eventually flushed into the sewer network. Therefore, a constant of 0.5 was applied to the whole BSR.

Table 3. Country-specific information on pharmaceutical waste management and sewer network coverage.

Country (ISO 3166)	Fraction of sold pharmaceuticals left unused [1)]	Fraction of pharmaceutical waste treated properly [1)]	Fraction of domestic wastewater treated [2)]
BY	0.08	0.28	0.83
CZ	0.08	0.28	0.99
DE	0.08	0.28	0.99
DK	0.08	0.28	0.99
EE	0.08	0.28	0.99
FI	0.04	0.65	0.99
LT	0.08	0.12	0.96
LV	0.08	0.08	0.92
NO	0.08	0.28	0.75
PL	0.08	0.07	0.99
RU	0.08	0.05	0.67
SE	0.05	0.72	0.99
SK	0.08	0.28	0.95
UA	0.08	0.28	0.61

1) Mehtonen et al. 2020. When no national value was available, an average based on available values was issued.
2) UNICEF & WHO 2019

2.3.2. Scenarios for API dissipation in inland and coastal waters

Bio- and photodegradation were taken into consideration when estimating the removal rates in rivers and lakes, and in coastal waters. The seasonal differences in the rates were taken into consideration by carrying out the calculations with five different scenarios for the inland processes. The riverine dissipation processes were included into three of these (scenarios 1, 2 & 3), while scenario 0 included only removal due to metabolism, waste management and WWTP processes. Scenario -1 presented the "total residue approach" used in the environmental risk assessment of pharmaceuticals (EMA 2006) and included no removal processes. These scenarios are presented in Table 4. The estimated variation in coastal temperature and light conditions were averaged to produce one estimate on annual the average concentration (see chapter 2.2.3 and Eq. (15)).

Table 4. Scenarios for degradation in inland waters.

Scenario	Removal processes (biodegradation & photodegradation)	River flow conditions[a)]	Water temperature in inland areas
-1 *All sold mass is assumed to be discharged into environment*	• No removal processes taken into consideration.	• No flow conditions taken into consideration	• Temperature not taken into consideration
0 *Effluent mass in waste-waters is assumed to reach the Baltic Sea*	• Metabolism and removal at WWTP included • Environmental removal processes not taken into consideration	• Flow speed (m/s) not used in calculation • Flow rate (m^3/s) at river mouths assumed to be the average of annual averages	• Biodegradation not taken into consideration, so temperature has no impact on results
1 *Effluent load is reduced by environmental processes before reaching the Baltic Sea (annual average)*	• Biodegradation rate is corrected to scenario temperature. • Photodegradation (incl. radiation initiated degradation) takes place in 1.5% of the total water volume.	• Flow speed assumed to be annual average (0.15 m/s) • Flow rate at river mouths assumed to be the annual average	• North from GoF[b)]: 7 °C • South from GoF[b)]: 9 °C
2 *Effluent load is reduced by environmental processes before reaching the Baltic Sea (summer conditions)*	• Biodegradation rate is corrected to scenario temperature. • High radiation energy and long days leads to the best possible photoactivity. Photoactivation takes place in 4.5% of the total flow volume.	• Flow speed assumed to be 80% of the annual average (0.12 m/s) • Flow rate at river mouths assumed to be 80% of the annual average	• Whole BSR: 18 °C
3 *Effluent load is reduced by environmental processes before reaching the Baltic Sea (winter/spring conditions)*	• Biodegradation rate is low due to low temperature. Biodegradation rate is corrected with temperature. • Photolysis not included	• Flow speed assumed to be 120% of the annual average (0.18 m/s) • Flow rate at river mouths assumed to be 120% of the annual average	• Whole BSR: 5 °C

a) Annual average flow rates for each river in the BPL model are presented in Annex 3.
b) GoF = Gulf of Finland, the threshold line was set to Y-coordinate 4 300 000

Water flow in inland scenarios

Flow rate values used in the BPL model are based on the average of the annual averages as reported by HELCOM (HELCOM 2018b). These values were then modified for each river, using a scenario-specific multiplier. The scenario-specific multipliers were estimated using literature data on river flow rates, and their variation. For example, the long-term average discharge from the area of Finland was 3,293 m^3/s during 1912-2004 (Korhonen 2007). The annual was about 18%. In Finland the lowest monthly mean discharges were roughly 80% of the annual long-term average (Korhonen 2007). The discharge in high flow situations in spring was up to 200% of the mean. However, as the calculation approach in BPL aims to estimate the annual average loads and concentrations, only moderate flow rate values were chosen for the scenarios. In reality some of the flow peaks in different rivers may be much more than 120% of the mean, resulting in the calculated concentrations exceeding those measured in the actual environment during those flow peaks.

Based on these considerations, in scenario 2 (low flow situation) flow rate and flow speed at river mouths were assumed to be 80% of the average (see Table 1). In scenario 3 (high flow situation) flow rate and flow speed were assumed to be 120% of the average.

Water temperature in inland scenarios

Using the equations presented in chapter 2.2, water temperature affects the degradation of substances in the environment. The temperatures used in inland scenarios are presented in Table 4, while the considerations behind those values are presented in the following paragraphs.

Temperature in scenario 1

Air temperature data from DWD (Deutcher Wettendienst) temperature maps were used to evaluate the mean water temperatures in the study area. South from the latitude of Gulf of Finland (Y-coordinate <4 300 000) the annual mean air temperature for 1981–2010 was about 5–10 °C according to DWD maps. North from this latitude the mean air temperature was about 0–5 °C.

However, the difference between mean air and mean water temperatures is greater in the north because of the longer ice-covered period. In Finland the mean annual temperatures of river waters are approximately 6–8 °C (Hertta database). Similar values were available also for lakes. For example, in lake Saimaa in Finland, the mean surface water temperature was about 8 °C in 1995–1998 while the water temperature was assumed to be 1 °C during the ice-covered period (Hertta database).

A mean value of 12 °C is suggested to be used when calculating the degradation of substances in Europe (European Chemicals Agency, 2017). The mean annual water temperature of the River Vistula in Poland is 8 °C in the upper reaches and 9 °C in the middle and lower reaches. In the middle and lower parts of the river the water is about 2 °C warmer than the mean annual air temperature of Poland (Parczewski & Pruchnicki 2017). In Latvian rivers the mean water temperature for period 2000–2019 was also about 9 °C (LEGMC 2020).

Based on these data, 9 °C was selected as the water temperature for scenario 1 in regions south from the latitude of Gulf of Finland. 7 °C was selected for the area north from this latitude. The lower value is relevant mainly for Finland and Northern Sweden.

Temperature in scenario 2

Mean long-term surface water temperatures in some Finnish lakes (e.g. Lake Pielinen, Lake Kallavesi, Lake Lappajärvi) are about 18 °C in July. The mean temperature in surface waters is about 2 °C higher than the mean air temperature in July (Korhonen 2002). Mean river water temperatures are 18–19 °C in Finland in July (biggest rivers in Hertta database).

The water temperature of River Vistula varies from 12 °C to 15 °C in summer. In river sections that are thermally affected by nearby industries, however, the water temperature is as much as 6 to 10 °C

higher (Parczewski & Pruchnicki 2017). Mean water temperatures in Latvian rivers in the Daugava, Gauja, Lielupe and Venta river basin districts were about 19–21 °C in July during 2000–2019 (LEGMC 2020).

According to DWD temperature maps the mean air temperature in July in 1981–2010 was 15–20 °C throughout the study area except in the northern parts of Finland and Sweden. Therefore, water temperature of 18 °C was used in scenario 2 in the whole study area.

Temperature in scenario 3

In River Prosna in Poland and in River Daugava in Latvia the high flow peaks occur in springtime (European Environmental Agency, 2016). In Finland high flow situations usually occur during the snow melt or afterwards from April to June (Korhonen 2007). High flow situations seem to occur later in northernmost parts of the study area than in the lower latitudes.

During 1961–2000 the surface water temperature reached 5 °C in southern Finland in the beginning of May and in northern Finland at the end of May or in early June. In spring the average air temperature is a couple of degrees higher than the water temperature (Korhonen 2002).

According to DWD temperature maps the mean air temperature reached 5–10 °C in the study area south from the latitude of Gulf of Finland in April and north from that latitude in May in 1891–2010. The timing of the high flow situations also varies spatially. Scenario 3 represents the situation during flow peaks. Therefore, a temperature of 5 °C was chosen for this scenario for the whole study area. Because the study area is large, this scenario occurs in different months in different regions.

Sedimentation rate in coastal areas

The sedimentation rate around BSE (sediment profiles accumulated after 1963- 1986 until 1995-2003) were 60–6,160 g/m² per year (Mattila et al. 2006). E.g. in Gdansk bay, the annual sediment accumulation has shown to be 176–966 g/m² (literature referred by Damrat et al. 2013). The organic carbon content of BSE sediments varies from 0.1% to 16% (Leipe et al. 2010). The burial rate of particulate organic carbon in mud areas around BSE was 14–35 g/m² per year (Leipe et al. 2010). They also calculated that 3.5 +/- 2.9 MT of particulate organic carbon is annually buried in the whole BSE area (including sediment accumulation areas and areas with no sedimentation). Based on the values presented by Leipe et al. (2010), k_{SEDPOC} was assigned the value 20 g/m²/a.

Photoactivity – radiation penetration in coastal areas

As was presented earlier in chapter 2.2.3 (p. 22), the water column in coastal waters was divided into three layers, varying on the estimated photoactivity. Layers h1 and h2 are assumed to be photoactive, while the bottom layer (h3) is assumed not to receive enough light to sustain photolysis in any meaningful extent. The proportion of the depths of photoactive layers h1 and h2 to the total depth are significant for photodegradable APIs.

Although UV radiation penetrates only few centimeters, the very thin surface layer is mixed with waves and the depth of sea water exposed to full spectra of solar radiation is higher than that of still water. The first layer depth (h1) is selected to represent the significant wave height in June, when radiation – and photodegradation is at its highest. The monthly average of significant wave height has its minimum (about 0.5 m) in June (e.g. Pettersson et al. 2019) in all BSE areas.

Secchi depth was planned to be used as the bottom depth of the second layer. The secchi depths vary between BSE regions (av. 4–8 m in open sea areas). However, the variation from on shore to open sea is even higher. In estuaries the secchi-depth may be very low (sometimes <0.5 m). Because the focus of the model is the coast 0–3 km from on-shore, it was decided that no regional secchi-depth scenarios were used but a value of 2,5 m is used for all coastal areas. Radiation and thus

photodegradation is significantly lower in the second layer than in the surface and thus its thickness (bottom depth) is not as significant as that of the surface layer.

The radiation available for photosynthesis (for algae and aquatic plants) in different sea water depths is studied e.g. by Simis et al. (2017). They found that the radiation energy decreases fast with depth. This idea was applied to photodegradation in this model. Photoactivity factor ($a(q,l)$ in Eq. (16)) was assumed to decrease to 1/z when moving from layer h1 to h2. The parameter z is a factor describing the assumed decrease in photoactivity when moving to deeper water columns. In this work, z was assigned a constant value of 4, corresponding to exponential decrease in radiation activity, as demonstrated in Figure 8.

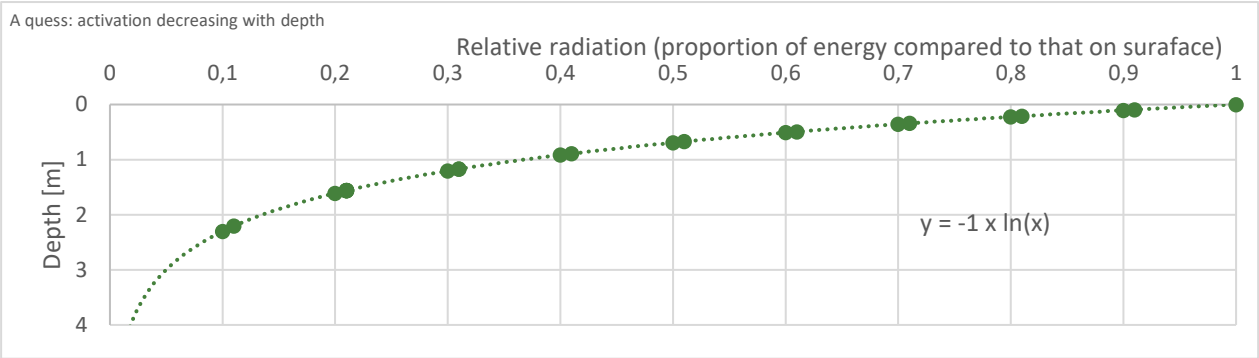

Figure 8. Radiation energy decreases with depth. According to the selected depths of layers 1 and 2, the radiation energy in layer 2 (0.5 m–2.5 m) is about ¼ => z=4.

Seasonal variation

Seasonal variation in photodegradation activity was estimated based on the seasonal variation of radiation energy. It is highest in June (mid-summer) and lowest in December, when no photodegradation was assumed. Some photoactivity is assumed to take place from March to September. The seasonal variation of photodegradation activity, as used in the BPL model, is presented in Table 5.

Water temperature in coastal areas

The Baltic Sea surface water temperature has increased during the last 30 years at a rate of about 0.59 °C/decade. During 2014–2018 the annual mean surface temperature has varied between 8.0 and 9.0 °C (Siegel and Gerth 2019). The maximum difference in annual temperatures between areas is about 3 degrees Botnian Bay being the coldest and southern parts of BS being the warmest. In coastal areas temperatures are higher than in open sea areas especially in summer time. Taking into account the simplifications contained in the BPL model, it was not considered worthwhile to create very detailed scenarios. Thus, the regional variations in temperature were simplified by dividing the BSE area into three temperature regimes.

Surface temperature is measured daily – also from satellites. However, in deeper depths, the amount of data is lower. On average it seems that thermocline is in 30–50 m depth. Water temperature varies seasonally above thermocline. The annual variation of temperature and radiation causes faster degradation than the annual averages of the same values but the actual difference between annual average and seasonal variation depends on the depths. Temperatures used in the calculations are presented in Table 5.

Table 5. Temperatures used in the three depth-layers and different latitudes. (Q1: Jan-Mar, Q2: Apr-Jun, Q3: Jul-Sep, Q4: Oct-Dec)

Scenario	Layer h1[a] (0–0.5 m)				Layer h2[a] (0.5–2.5 m)				Layer h3 (2.5 m–bottom)			
Month	Q1	Q2	Q3	Q4	Q1	Q2	Q3	Q4	Q1	Q2	Q3	Q4
Sedimentation[b]												
k_{SEDPOC} [g/m²/a]	20											
Photodegradation[c]												
$a(q,l)$ [-]	0.05	1	0.5	0	0.0125	0.25	0.125	0	0	0	0	0
Temperature [°C]												
Northern parts (Bothnia bay & Bothnia sea, North from Y-coordinate 4 300 000)	0	10	19	2	0	9	16	1.6	0.4	4.6	12	2.5
Middle areas (including Gulf of Finland & Gulf of Riga, Y-coordinates between 3 700 000-4 300 000)	0.4	12	20	4	0.3	12	17	3.5	0.9	6.2	12	4
Southern parts (e.g. Arkona sea, south from Y-coordinate 3 700 000)	2	14	21	6	2	14	19	6	3	8	14	5

a) Layer depths are capped at total depth. I.e., if total depth is 1.4 m, layer h1 is 0–0.5 m and layer h2 is 0.5–1.4 m.
b) Sedimentation is assumed to take place only when the load from land areas enters the BS. Sedimentation rate is assumed not to vary from seasonally or regionally.
c) Photodegradation is assumed to be similar in all regions. Values presented for layer h2 are calculated from values assigned to layer h1, using factor z, as described on p. 28. If factor z is assigned values other than four, $a(q,l)$ will change for layer h2.

2.3.3. API-specific properties

The APIs selected to be modeled in this work, as well as their sales data for the BSR countries are presented in Table 2 in chapter 2.3.1. API-specific property data required by the BPL model were compiled through a literature review. Various search engines were utilized (e.g. Web of Science, Google Scholar) and results from studies with an experimental design relevant for the BSR were collected. API-specific property data, such as information about degradation pathways and half-lives, binding to solids and excretion rate were compiled. The partitioning coefficients (K_{oc}) and PNEC-values collected by Ek Henning et al. (2020) were used. Properties relevant for the BPL model for the selected APIs are presented in Table 6. The considerations in selecting these values is presented in the following sub-chapter.

Table 6. API-specific input data selected for the calculations.

API	Excreted fraction [%]	Removal at WWTPs [%] [a)]	$DT50_{photo}$ [d]	$DT50_{bio}$ [d]	T_{ref_bio} [°C]	K_{oc} [L/kg]	PNEC [ng/L]
CBZ	3	12.0[1)]	450[2)]	-	-	324[1)]	128,000[1)]
CLM	30	29.1[1)]	40[3)]	-	-	457[1)]	3.91[1)]
DCF	61.5[b)]	6.42[1)]	2.4[4)]	60[5)]	31.5[5)]	219[1)]	85.2[1)]
IBU	1	95.0	96.3[5)]	24.8[5)]	31.5[5)]	2,090[1)]	0.12[1)]
MTF	100	99.8[1)]	28.3[6)]	-	-	19.1[1)]	1,350[1)]
OFL	90	86.5[1)]	10.6[2)]	-	-	2,040[1)]	20.4[1)]
TRD	10	3.10[1)]	4.7[7)]	121[7)]	23[7)]	617[1)]	170,000[1)]
VFX	5	19.8[1)]	3.5[7)]	114[7)]	23[7)]	191[1)]	3,220[1)]

a) Removal at WWTPs is defined here as removal from the water phase (influent concentration vs. effluent concentration). This parameter includes removal due to biodegradation and hydrolysis, as well as due to adsorption onto particles and potential volatilization.

b) Excretion rate for orally administered DCF is estimated to be 1%. However, due to a high fraction of overall sales being used topically, the effective excretion rate is higher. In Finland it is estimated, that 65% of DCF is used topically. Only 6% is of topically administered DCF is estimated to be absorbed. Using these data, the excretion rate was calculated following the method presented by Äystö et al. 2020.

1) Ek Henning et al. 2020
2) Andreozzi et al. 2003
3) Vione et al. 2009
4) Fass.se
5) Arajuo et al. 2014
6) Straub et al. 2019
7) Rúa-Gómez & Püttmann 2013

Selection of API-specific input data

Carbamazepine

In CWPharma, CBZ removal was calculated for 21 pairs of influent and effluent wastewater samples. The removal rates ranged from -360% to 98% (Ek Henning et al. 2020). The median and average removal rates were 12% and -7.6%, respectively. The removal rate of 12% was used for the calculations.

Björlenius et al. (2018) estimated an overall removal half-life of 1,294 d in the Baltic Sea environment. However, many sources report shorter half-lives, such as 37.8 d (Andreozzi et al. 2002) and 73 d (Álvarez-Ruiz et al. 2020). In another paper Andreozzi et al. (2003) concluded that CBZ photolysis in northern regions is slow, and the half-life for direct photolysis in central Europe is in the range of 450 d in the autumn. The photolysis half-life of 450 d was used for the calculations.

Clarithromycin

In CWPharma, CLM was estimated to be removed in conventional WWTPs on average by 22.3% (Ek Henning et al. 2020), while the median removal rate was estimated to be 29.1%. The latter value, 29.1%, was selected to be used here.

Information on CLM removal in environmental processes is scarce. However, some information on its photodegradation is available. Vione et al. (2009) concluded that the photodegradation half-lives

for CLM range from 10 to 40 days under clear sky conditions. Thus, photolysis half-life was set to 40 d.

Diclofenac

DCF removal rates based on the samples taken in CWPharma (Ek Henning et al. 2020) ranged between WWTPs from -150% to 33%. The average rate was -14.6%, while the median value was 6.42%. There is high variability in DCF removal in WWTPs. However, the removal rates are usually slightly positive. Therefore, the median value, 6.42% was selected here.

DCF has long been an API of interest, and therefore there is more information on its environmental properties than on many other APIs. Photodegradation half-lives for DCF in Central Europe have been estimated to range from <1 to 5 d. According to the Fass.se database, photolysis half-life for DCF is 2.4 d, while according to Arajuo et al. (2014) reported DCF photolysis half-lives to range from 5.76 to 2.15 d, depending on whether the sample was filtered or unfiltered. The value 2.4 d was selected to represent the photolysis half-life.

DCF is also known to be slowly biodegradable. According to Arajuo et al. (2014) the biodegradation half-life is 60 d.

Ibuprofen

IBU removal at WWTPs is high according to most literary sources. In CWPharma project the removal rate could only be calculated for one sampling occasion at one WWTP. The removal rate was estimated to be 86% (Ek Henning et al. 2020). However, the removal rates are often >90% (e.g. Miehe 2010, Äystö et al. 2020). Therefore, a removal rate of 95% was used for the calculations.

According to Packer et al. (2003), IBU degrades through photolysis in river water, with a half-life of 0.11 d. This is in stark contrast with the results reported by Arajuo et al. (2014) who tested the persistence of four APIs in filtered and unfiltered waters using different light conditions. The half-life they reported for IBU in filtered lake water under sunlight was 96.3 d. In addition to testing photodegradation of selected APIs, Arajuo et al. (2014) also tested their degradation in filtered water in darkness. In this test, they estimated a half-life of 248 d for IBU. However, considering the high degradability of IBU often demonstrated in WWTPs, this value seems very high for biodegradation. They also reported an overall half-life of 19.7 d in unfiltered lake water under natural sunlight (Arajuo et al. 2014). Using the k-values reported by Arajuo et al. (2014), a biodegradation half-life of 24.8 d was estimated. This value was used in combination with the photodegradation half-life of 96.3 d.

Metformin

Between 98-100% of MTF was estimated to be removed during WWTP processes (Ek Henning et al. 2020). The value 99.8% was selected to be used here. However, there is relatively little information on its environmental properties. Straub et al. (2019) estimated its photolysis half-life to be 28.3 d. This value was used for the calculations. No information on MTF biodegradation was available.

Ofloxacin

In the project CWPharma, OFL removal values could only be estimated for two data points. The average removal rate was 86.5% (range: 83–90%) (Ek Henning et al. 2020). However, according to Ek Henning et al., the removal rates reported in literature vary a lot, ranging from -157% to 99%. Therefore, a removal rate of 86.5% was used for the calculations.

Andreozzi et al. (2003) reported OFL to go through photodegradation in relatively northern areas (50 °N), with half-lives ranging from 1.6 to 10.6 d. As the Baltic Sea catchment area is located between 49–70 °N, the highest reported value was used to represent photodegradation in the region. No information was found on biodegradation rates for OFL, but there are some indications that it is

biodegraded relatively efficiently (Jung et al. 2009). Nevertheless, OFL was considered to go through photodegradation only and no biodegradation was assumed to take place.

Tramadol

Previously TRD removal rates have been reported to range from -26% (Hörsing ym. 2014) to 50% (Rúa-Gómez & Püttmann 2011). In the CWPharma project, TRD removal rates in WWTPs ranged from -105 to 90% (Ek Henning et al. 2020) with the median removal rate of the 20 data points being 3.1% (avg -1.5%). The range of the removal rates is wide, but the average and median values are well in line with the removal rates reported by Fick et al. (2011) and Verlicchi et al. (2012), -3% and 4%, respectively. In the calculations the median removal rate (3.1%) calculated in CWPharma was used.

According to Rúa-Gómez & Püttmann (2013), indirect photodegradation is the dominant process for TRD degradation in natural waters. They tested the degradation of five APIs in different types of waters (ultrapure, river water, river water with no biotic processes) in different conditions. The half-life of TRD in natural river water was reported to be 3.7 d. The values selected for the calculations for half-life attributed to photodegradation by sunlight was 4.7 d, and biodegradation half-life at 23 °C was 121 d.

Venlafaxine

VFX removal rates in WWTPs were estimated to vary between -90 and 63% (Ek Henning et al. 2020). The median and average removal rates were 14.5 and 19.8%, respectively. Previously reported values have ranged from 7.7% (Gurke et al. 2015) to 21% (Fick et al. 2011) and 49% (Rúa-Gómez & Püttmann 2011). The removal rate selected for calculations was 19.8%.

According to Rúa-Gómez & Püttmann (2013), indirect photodegradation is the dominant process for VFX degradation in natural waters. The overall half-life in natural river water was reported to be 2.4 d. The values selected for the calculations for half-life attributed to photodegradation in sunlight was 3.5 d, and biodegradation half-life at 23 °C was 114 d.

3. Results and discussion

3.1. Loads to river mouths

To identify the rivers with the highest API loads to the BS, the river-specific loads were divided with the load from the river with the highest load. This quotient was then used in ranking the rivers based on how high or low the API-specific load was compared to other rivers. These values were then averaged between different APIs and different calculation scenarios to produce a concise estimate on which rivers carry the highest API loads to the BS. The rivers with generally the highest API loads are presented in Figure 9 and Table 7.

The rivers with generally the highest loads included rivers with very high population density in the river basin (e.g. Damhusåen, 3 100 pers./km^2), but also rivers with very low population density (e.g. Oulujoki, 6.8 pers./km^2). Based on the BPL model, loads to the mouths of rivers correlate well with the population in river basin. However, national and regional differences, such as differences in consumption patterns and environmental conditions, also have an impact on the load to the river mouth.

The simulated loads in scenario -1 were higher than those in any other scenario (for scenario descriptions, see Table 4). The simulated loads in scenario 0 varied from 1% (IBU) to 56% (DCF) of those in scenario -1 depending on the API. This indicates the high importance of metabolism and wastewater treatment, which are included into scenario 0 but not in -1. The difference between simulated loads in scenario 0 and those estimated using scenarios 1, 2 and 3 was rather small in most cases, indicating that degradation in rivers and lakes plays a minor role in the total dissipation. The importance of environmental dissipation processes varied between APIs and sites.

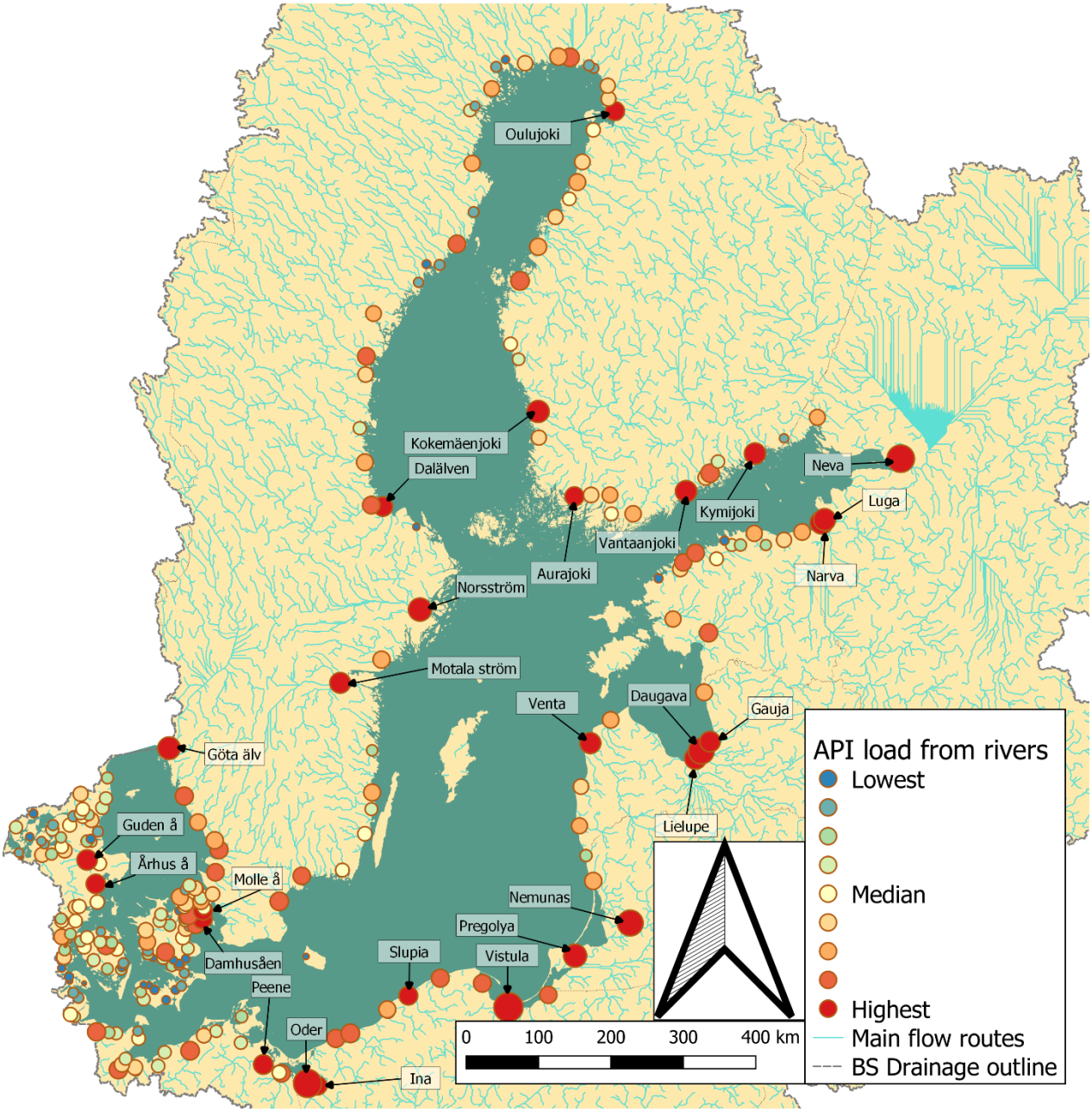

Figure 9. API loads from each river included into the BPL model relative to emissions from other rivers. The rivers with the highest API loads are flagged.

Table 7. Estimated API Loads to the mouths of 15 rivers receiving the highest API loading within the BSR. The loads were generally highest to the mouth of rivers with the highest population in their river basins (see Annex 3).

River	Scn[a)]	Load to river mouth [kg/a]							
		CBZ	CLM	DCF	IBU	MTF	OFL	TRD	VFX
Vistula, PL	1	922	1,140	2,530	108	15,300	16.2	835	357
	0	923	1,150	2,770	138	15,500	16.4	919	395
	-1	16,300	5,120	4,900	13,900	411,000	114	7,380	5,920
Oder, PL	1	603	742	1,740	24.2	3,130	9.42	558	238
	0	604	748	1,890	29	3,160	9.55	610	261
	-1	10,700	3,360	3,350	12,100	276,000	76.9	4,910	3,950
Neva, RU	1	171	196	228	232	30,000	9.22	117	53.5
	0	173	198	553	425	30,200	9.29	225	104
	-1	3,020	787	966	37,200	111,000	26.3	1,810	1,520
Nemunas, LT	1	78.4	101	524	76.5	6,380	3.81	148	63.2
	0	78.5	102	563	87.6	6,430	3.85	160	68.4
	-1	1,490	444	999	12,900	56,800	20.5	1,320	1,060
Daugava, LV	1	80.8	102	773	109	5,210	4.29	66.3	19.4
	0	80.9	102	813	122	5,260	4.32	71.2	21.2
	-1	1,460	443	1,440	17,700	38,800	21.9	586	328
Norrström,SE	1	33.0	24.6	150	8.92	247	3.02e-04	32.6	14.4
	0	33.3	24.8	295	21.7	250	3.05e-04	65.5	29.6
	-1	1,060	119	533	22,100	21,800	0.00246	663	676
Pregolya, RU	1	33.1	40.3	87.3	29.3	2,240	0.970	34.3	15.1
	0	33.1	40.4	91.4	29.7	2,250	0.975	35.7	15.8
	-1	569	174	161	1,830	16,000	4.39	283	227
Narva, RU	1	29.6	42.6	115	8.94	2,710	1.02	11.3	3.79
	0	29.8	43.2	285	47.9	2,750	1.03	29.2	10.3
	-1	545	187	509	6,630	15,100	3.79	237	147
Göta älv, SE	1	23.9	18.1	109	7.99	247	0.0238	24.3	10.9
	0	24.1	18.2	212	16.3	249	0.0242	47.3	21.3
	-1	765	87.4	383	15,800	15,800	0.0815	477	485
Kokemäenjoki, FI	1	13.9	6.47	82.8	4.86	248	0.193	10.0	4.88
	0	14.0	6.55	199	17.4	250	0.195	24.9	12.6
	-1	445	31.2	357	17,600	21,600	1.56	250	284
Luga, RU	1	11.3	13.4	26.9	26.6	2,080	0.632	13.8	6.3
	0	11.3	13.5	28.2	28.8	2,090	0.639	14.4	6.63
	-1	188	53.3	48.7	1,680	6,600	1.75	113	91.0
Lielupe, LV	1	13.5	16.9	147	11.0	390	0.781	12.7	3.77
	0	13.5	17.2	181	17.3	395	0.792	15.9	4.81
	-1	237	75.3	319	3,150	6,260	4.70	128	72.9
Vantaanjoki, FI	1	7.83	3.65	104	8.86	140	0.109	13.0	6.54
	0	7.84	3.66	111	9.7	140	0.109	13.9	7.01
	-1	248	17.4	199	9,820	12,100	0.870	139	159
Kymijoki, FI	1	9.48	4.42	41.8	3.42	169	0.131	5.18	2.59
	0	9.58	4.47	136	11.9	171	0.133	17.0	8.57
	-1	304	21.3	243	12,000	14,800	1.06	170	194
Venta, LV	1	7.63	9.72	98.6	8.85	227	0.450	10.7	3.59
	0	7.63	9.74	102	9.24	228	0.452	11.1	3.74
	-1	134	42.8	180	1,730	3,890	2.74	89.4	56.8

a) The load estimated with the total residue approach (scn -1) is equal to the estimated consumption in the river basin.

3.2. Loads to the Baltic Sea

3.2.1. Carbamazepine

Annual CBZ sales within the Baltic Sea drainage basin were estimated to be 50 tonnes. CBZ loads were estimated to originate mainly from inland areas. Inland areas and inland urban clusters accounted for 80% of the load reaching the BS, while coastal cities (i.e. coastal urban clusters) accounted for 15% of the total annual load of 2.6 tonnes. Most of the emissions reaching the BS (61%) were estimated to originate from Poland (Figure 10).

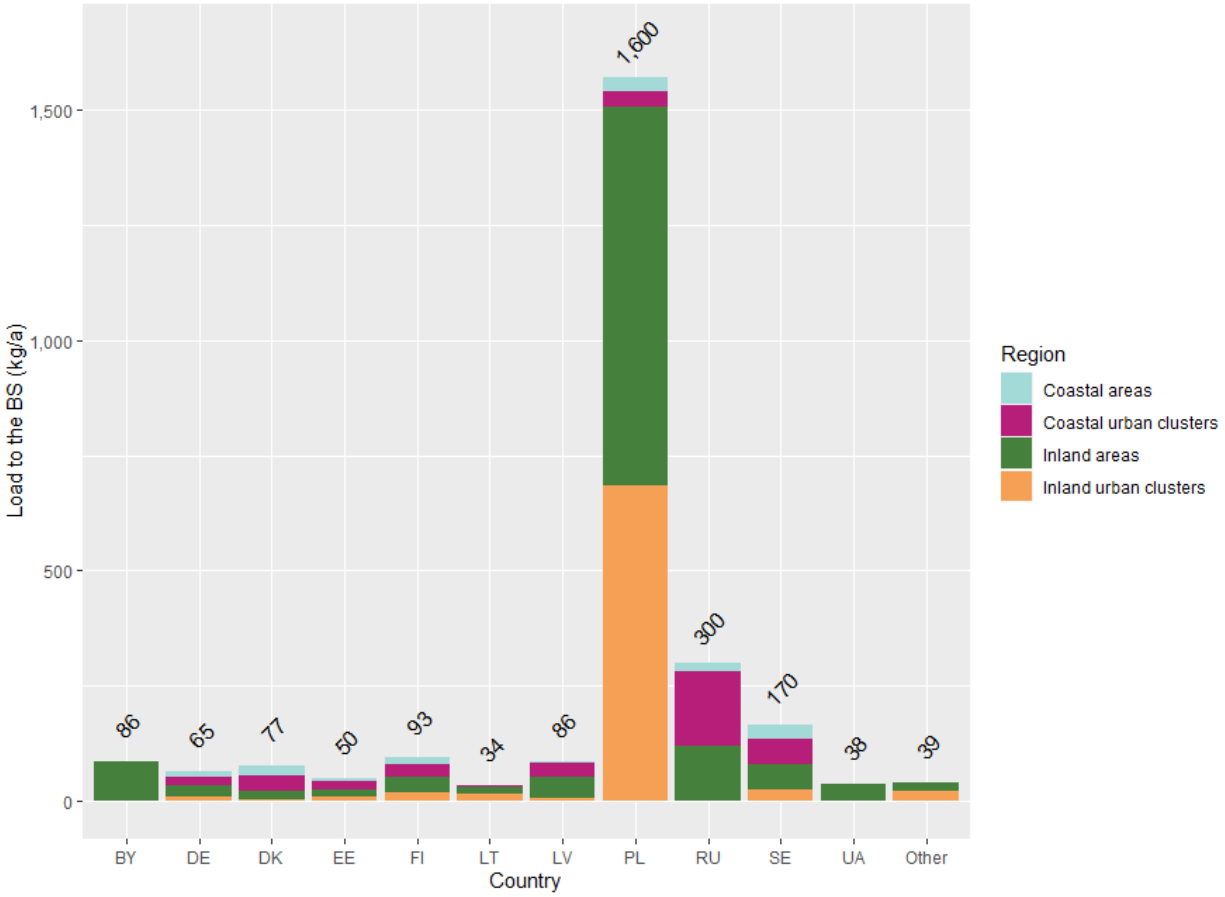

Figure 10. Carbamazepine loads reaching the Baltic Sea from each country and region, estimated according to scenario 1.

Circa 47% of the CBZ emissions within the Baltic Sea drainage area were estimated to originate from its use, while the rest was estimated to originate from the improper treatment of unused pharmaceuticals (Figure 11). However, due to poor data on pharmaceutical wastage and treatment of that waste, this estimate contains large uncertainties. Estimates on the mass of pharmaceuticals flushed into the sewer network are uncertain. Here it was assumed, that 50% of the pharmaceutical waste that is not treated properly, is flushed into the sewer network. Changing this fraction would have a parallel impact on the significance of improper waste management as a source of CBZ into the environment.

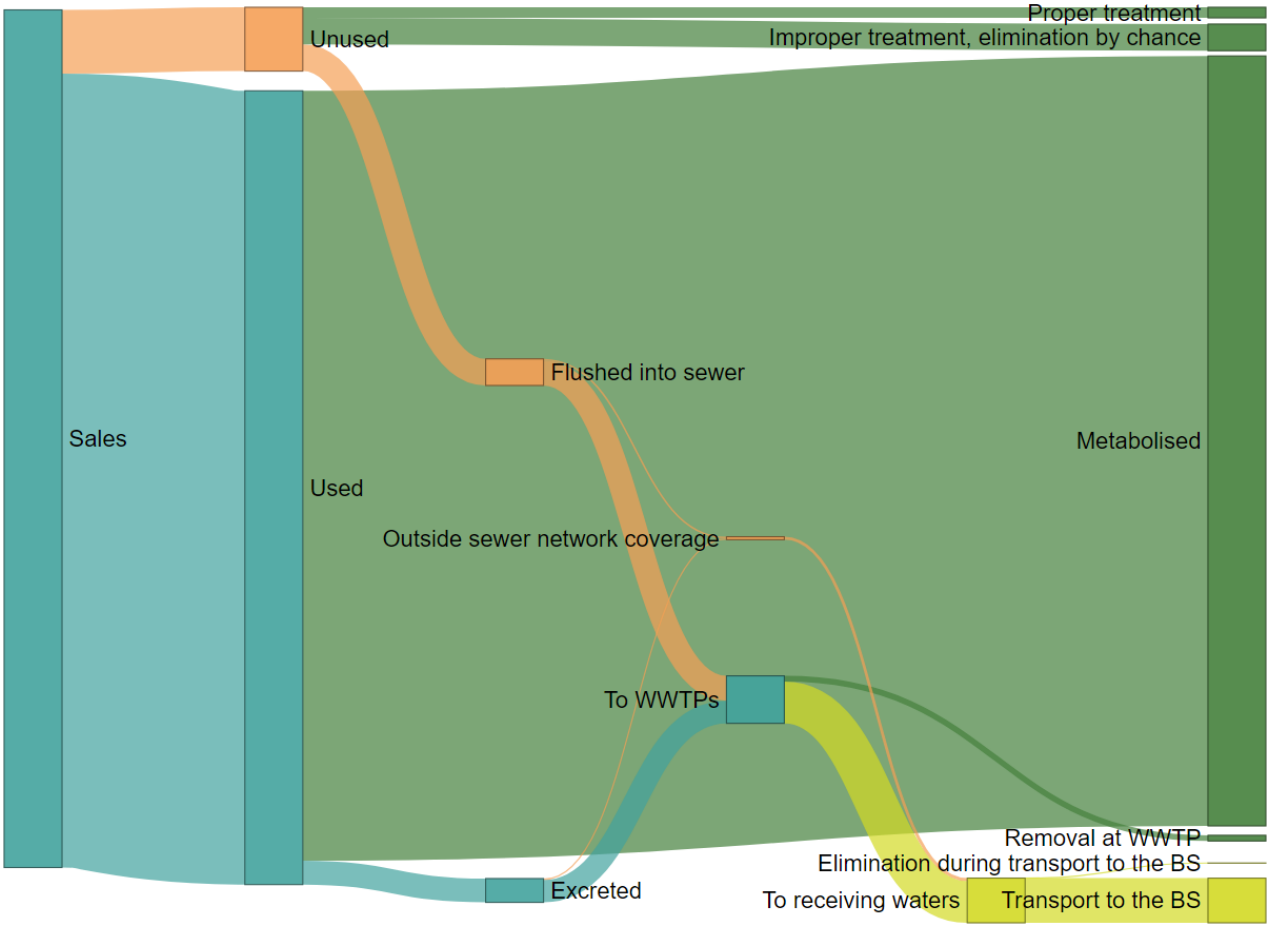

Figure 11. Carbamazepine flows according to scenario 1. Green boxes present end-points/processes, where the load is destroyed before reaching the environment. Orange boxes present suboptimal management practices, while yellow boxes present emissions into the water environment.

The total CBZ loads reaching the Baltic Sea from each grid cell are presented in Figure 12. The load estimates are highly dependent on the sales information. When looking at sales figures presented in Table 2, or the cell-specific loads presented in Figure 12, Lithuanian consumption and subsequent emissions seem rather low compared to other countries. The Lithuanian consumption information used in the calculations was compiled by the project MORPHEUS for a smaller part of Lithuania, and it is unclear how well this information presents the situation in the whole country.

National per capita loads to the BS ranged from 11 mg/a in Lithuania to 39 mg/a in Estonia and 41 mg/a in Poland and Latvia. When calculating per capita loads by calculation areas, the highest emissions were estimated to originate from coastal Latvia (see Figure 13). When looking at the calculation area-specific per capita emissions, it must be noted that the calculation areas mainly follow the outlines of river basins, giving no regard to country borders. For instance, despite the national per capita emissions being the lowest in Lithuania, the per capita emissions within the calculation areas covering large parts of Lithuania are much higher. This is caused by those calculation areas also covering regions in other countries, with higher per capita CBZ consumption (i.e. Latvia and Belarus).

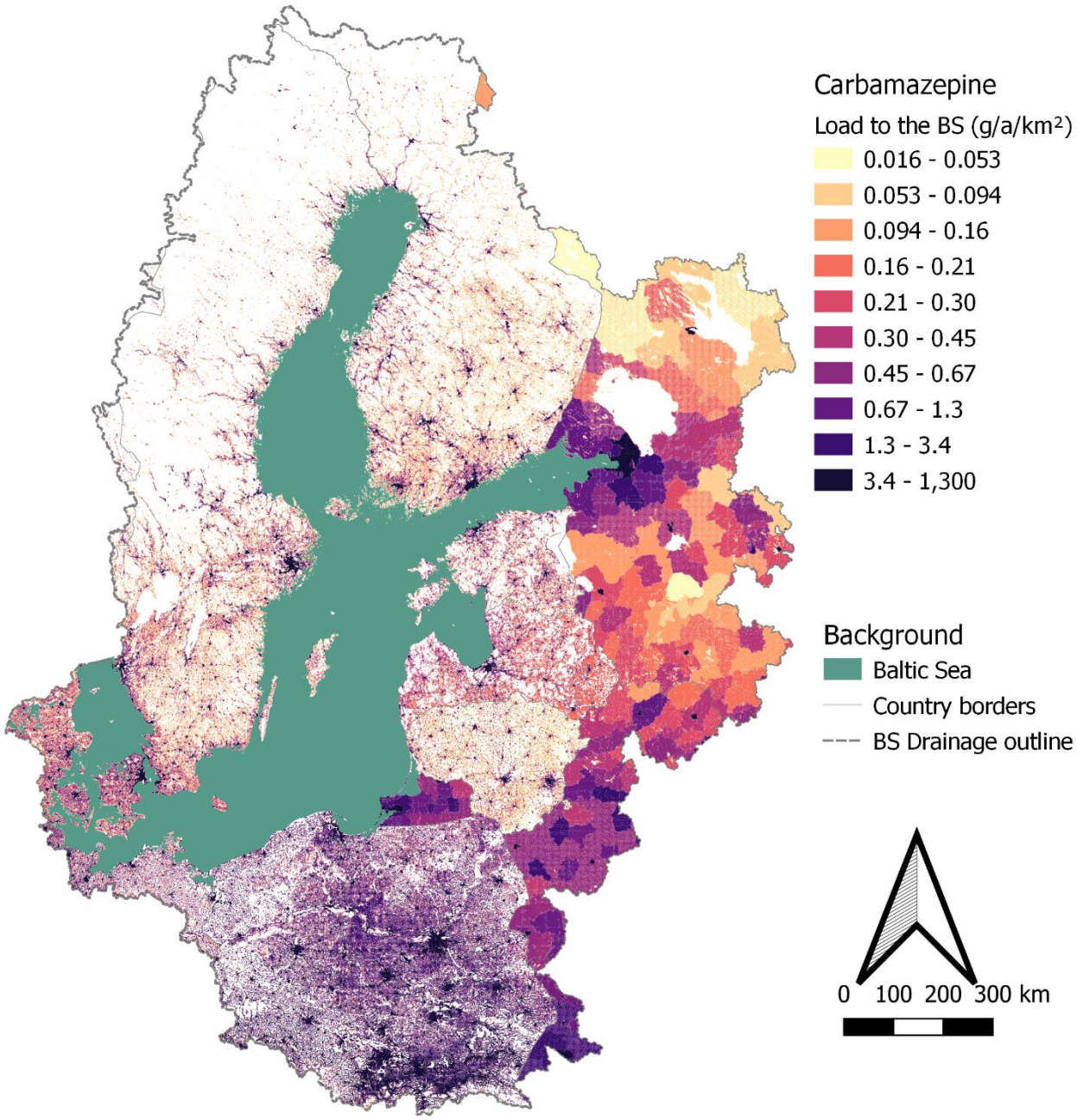

Figure 12. Carbamazepine load (g/a/km²) reaching the Baltic Sea, originating from individual grid cells.

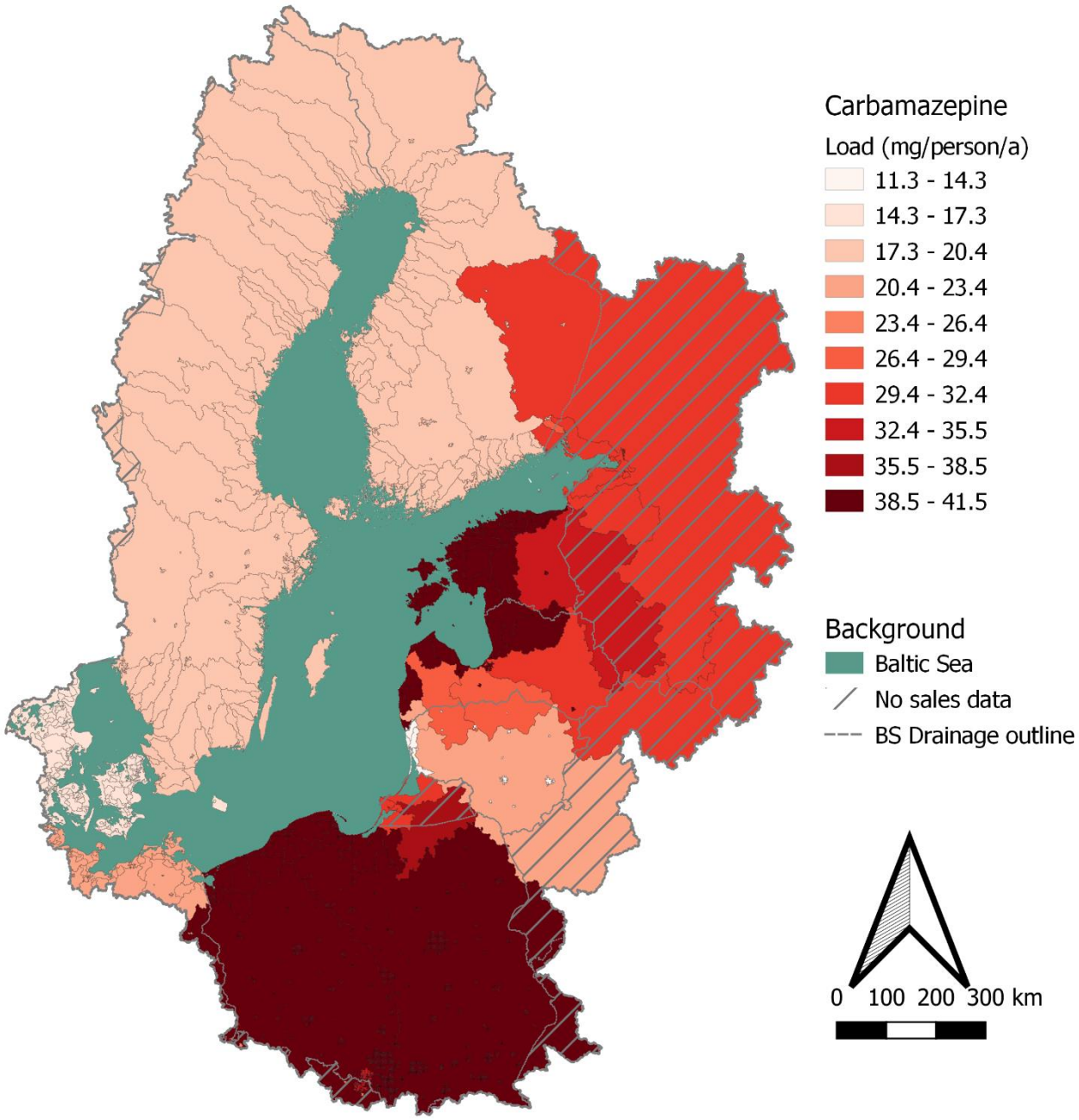

Figure 13. Mean per capita CBZ load reaching the Baltic Sea, aggregated by calculation areas. The dashed area shows the countries for which no national sales data was available, but a population weighted average value was used.

When looking at individual urban clusters emitting wastewaters into the Baltic sea, the highest emissions are estimated to originate from St. Petersburg. Although the assumed per capita consumption of CBZ does not differ greatly between Russia and other countries (see Table 2), the estimated CBZ emissions from other coastal cities are generally less than one fifth of the emissions originating from St. Petersburg (Figure 14). However, since the consumption value is an average based on countries from which information is available, the emissions from St. Petersburg should be further investigated.

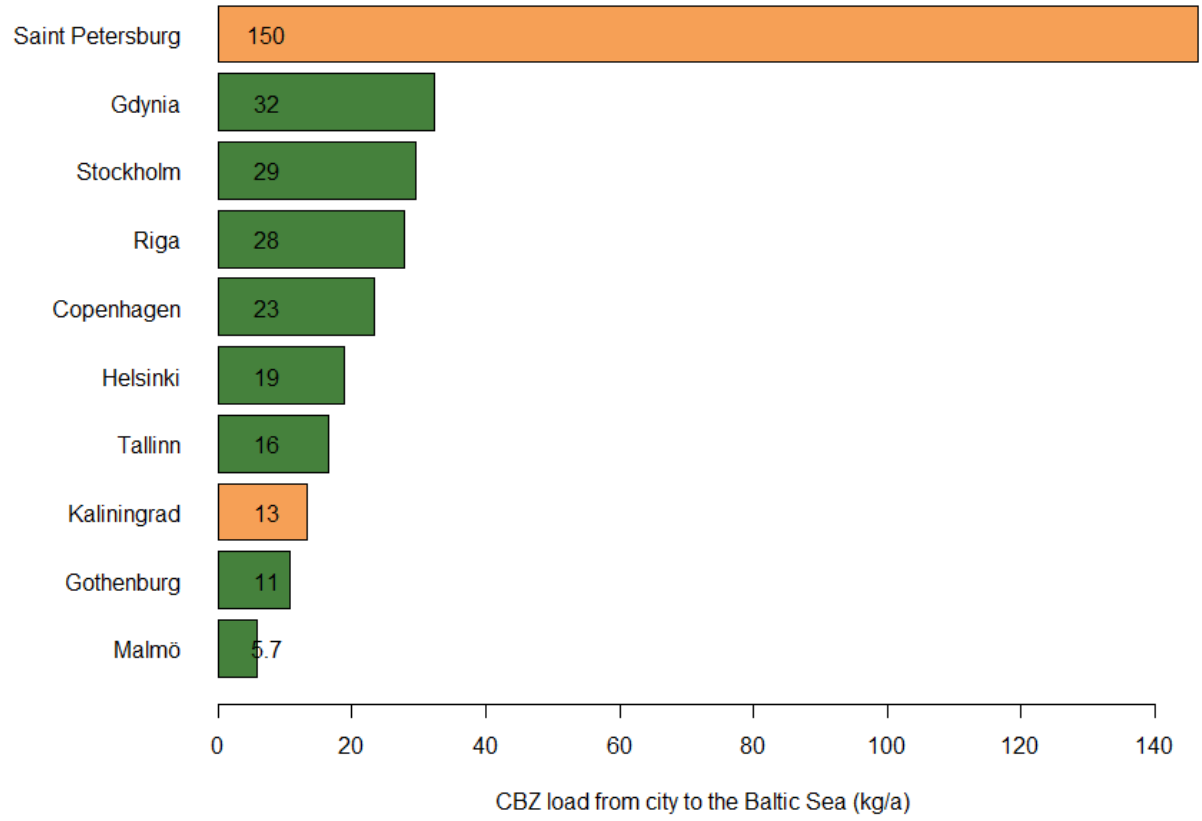

Figure 14. Ten coastal urban clusters with the highest CBZ emission reaching the Baltic Sea. The green bars present the cities in countries with sales statistics available, while orange bars represent cities in countries where an average per capita sales value was used. The numerical value presents the calculated load in kilograms, using two significant numbers.

The coastal areas with the highest incoming CBZ loads were estimated to be located in Poland, in the Gdansk and Bornholm basins, as well as on the coast of St. Petersburg, in eastern Gulf of Finland (see Figure 15). The loads to these coastal waters were estimated to be 990, 650 and 260 kg/a, respectively.

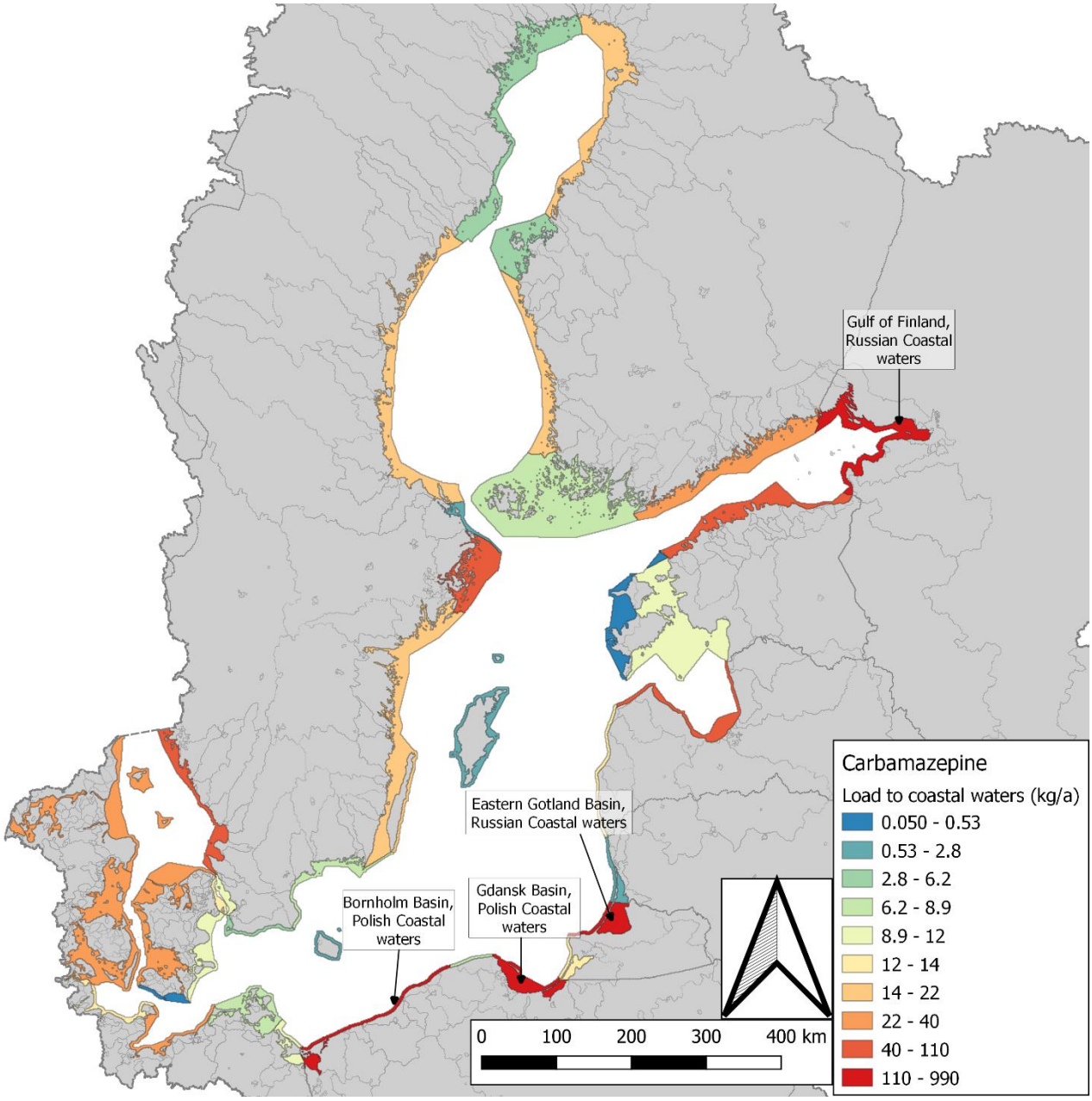

Figure 15. Carbamazepine load (kg/a) reaching the coastal waters in different parts of the Baltic Sea.

3.2.2. Clarithromycin

The overall sales of CLM in the Baltic Sea drainage area were estimated to be 14 tonnes, resulting in a total load of 3.1 tonnes being emitted into the aquatic environment. The annual load eventually reaching the Baltic Sea was estimated to range from 3 to 3.1 tonnes. This high portion of effluent load estimated to reach the Baltic Sea reflects the fact, that no biodegradation was taken into consideration for CLM, but that it was assumed to only degrade through photolysis. Circa 63% of the load reaching the Baltic Sea was estimated to originate from Poland, followed by emissions from Russia (12%) and Sweden (4%). The emissions were estimated to originate mainly from inland areas and inland urban clusters (circa 81%), while coastal cities accounted for 14%. National loads are presented in Figure 16.

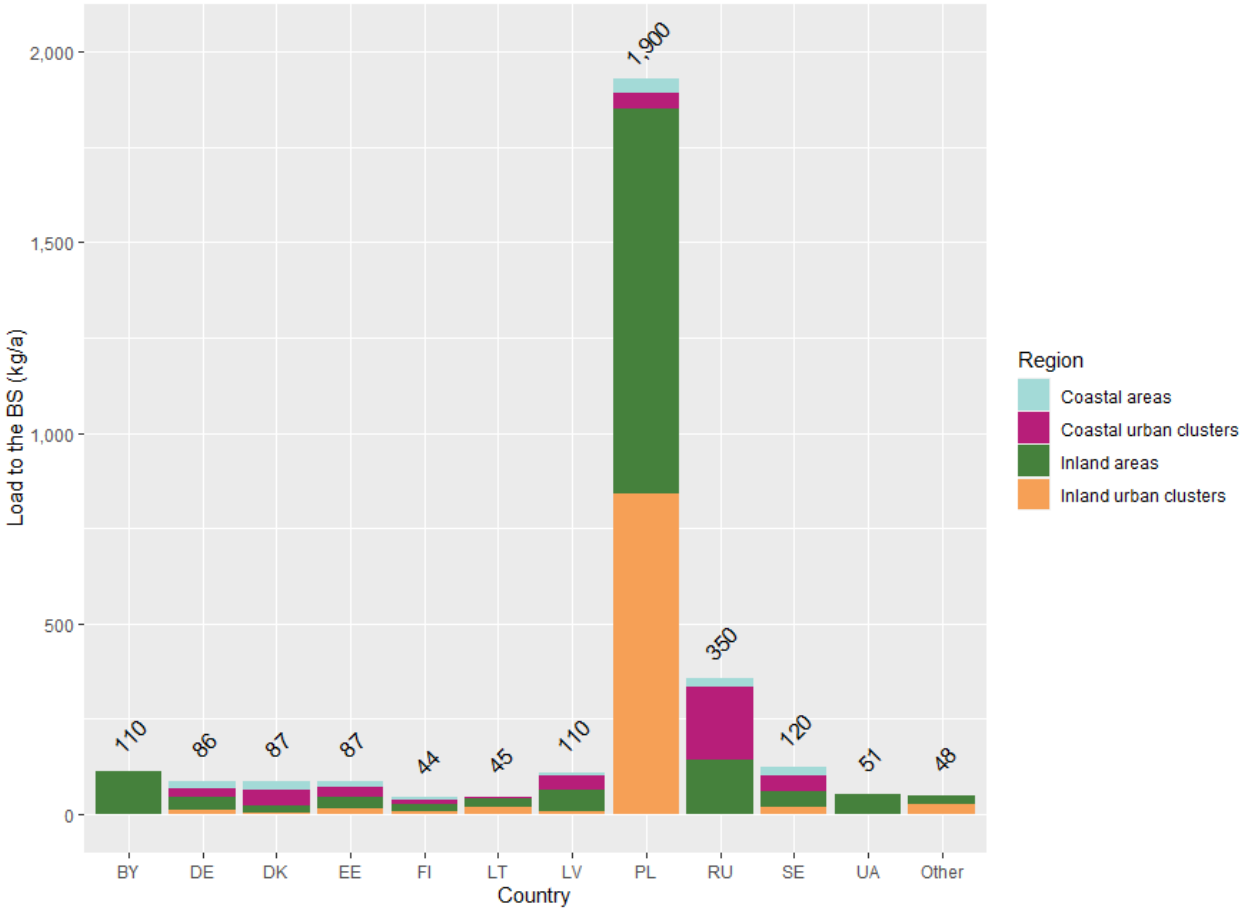

Figure 16. Clarithromycin loads reaching the Baltic Sea from each country and region class, estimated according to scenario 1.

CLM was estimated to originate mainly from consumption and subsequent excretion in areas connected to centralized wastewater treatment (Figure 17). The load to surface waters from areas outside sewer network coverage accounted for only 8% of all emissions.

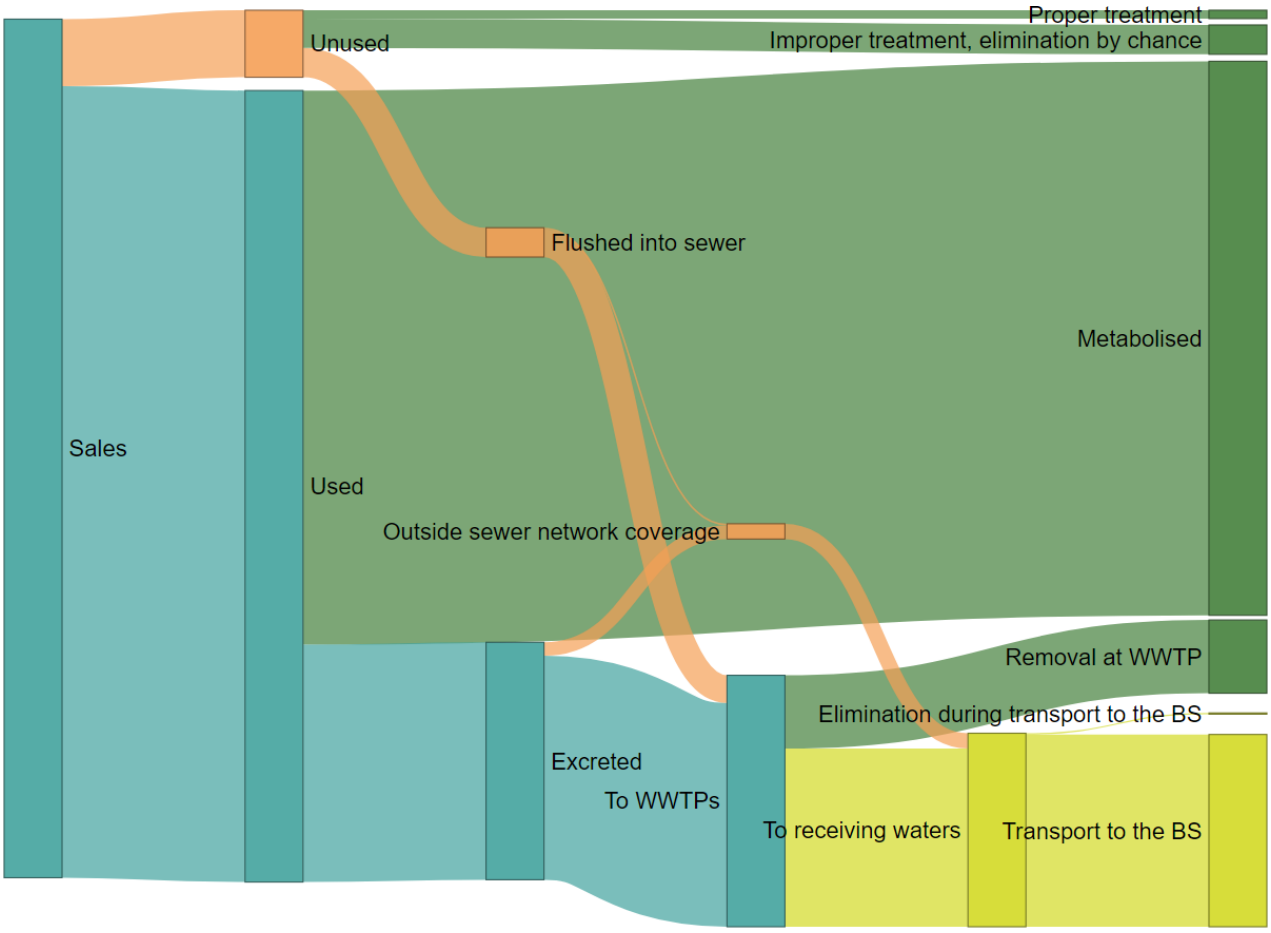

Figure 17. Clarithromycin flows according to scenario 1. Green boxes present end-points/processes, where the load is destroyed before reaching the environment. Orange boxes present suboptimal management practices, while yellow boxes present emissions into the water environment.

As no biodegradation was taken into consideration, the overall degradation rate was rather low. Therefore, the regional distribution of the emissions reaching the Baltic Sea, presented in Figure 18 are rather similar as those estimated for CBZ (Figure 12), but differ from those of e.g. DCF (Figure 24). As the degradation rate decreases, the significance of flow time from emission source to the Baltic sea decreases. This makes emissions from e.g. inland urban clusters more important.

The national per capita loads to the Baltic Sea from coastal countries ranged from 8.2 mg/a in Finland to 68 mg/a in Estonia. This difference is in line with national per capita sales presented in Table 2. Regionally the highest per capita emissions were estimated to originate from coastal areas in Estonia (see Figure 19).

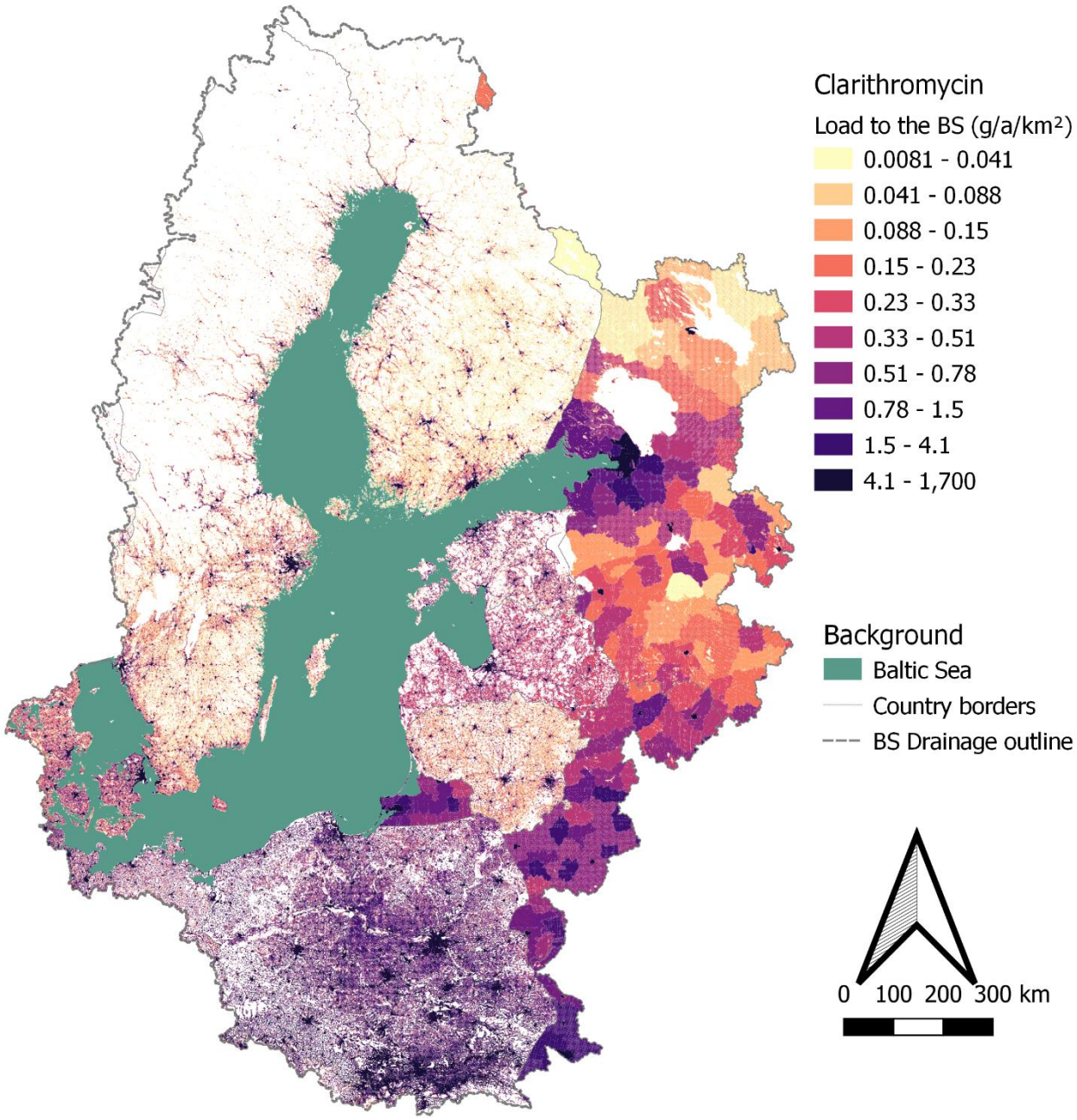

Figure 18. Clarithromycin load (g/a/km²) reaching the Baltic Sea, originating from individual grid cells.

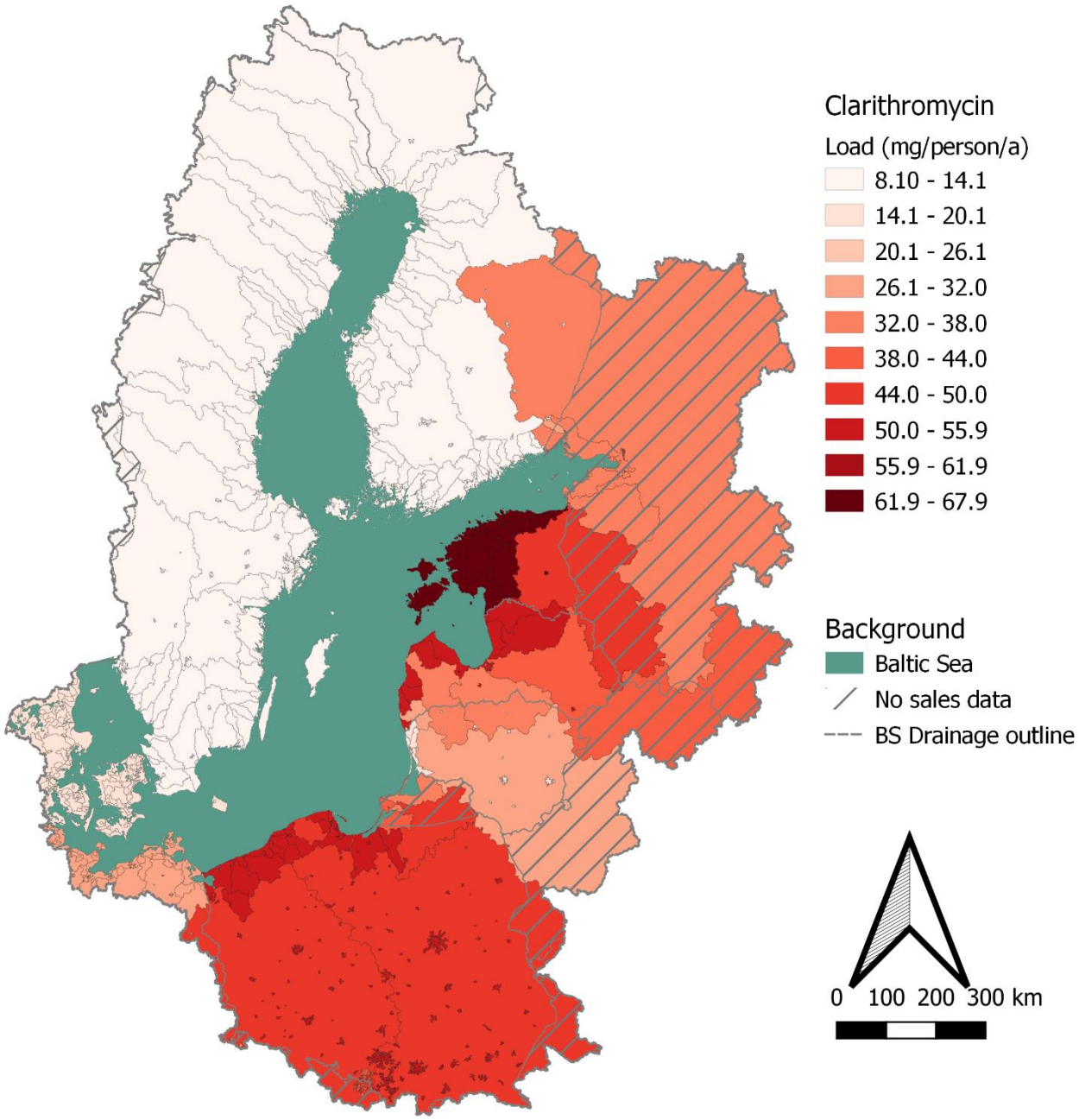

Figure 19. Mean per capita clarithromycin load reaching the Baltic Sea, aggregated by calculation areas. The dashed area shows the countries for which no national sales data was available, but a population weighted average value was used.

The ten coastal cities estimated to emit the highest load or CLM into the Baltic Sea are presented in Figure 20. The city emitting the highest CLM load to the Baltic Sea was estimated to be St. Petersburg. However, as there is no information available on actual sales of CLM in Russia, but an average has been used, the results are very uncertain. Replacing the average per capita sales used for Russia (0.41 mg/d/person) with the minimum and maximum per capita sales values reported from other countries, 0.11 mg/d/person and 0.86 mg/d/person (see Table 2), can help us estimate the range of emissions from St. Petersburg. Thus, the emissions would likely range from 46 kg/a to 370 kg/a. In both scenarios, St. Petersburg is likely the city emitting the highest load of CLM into the Baltic Sea.

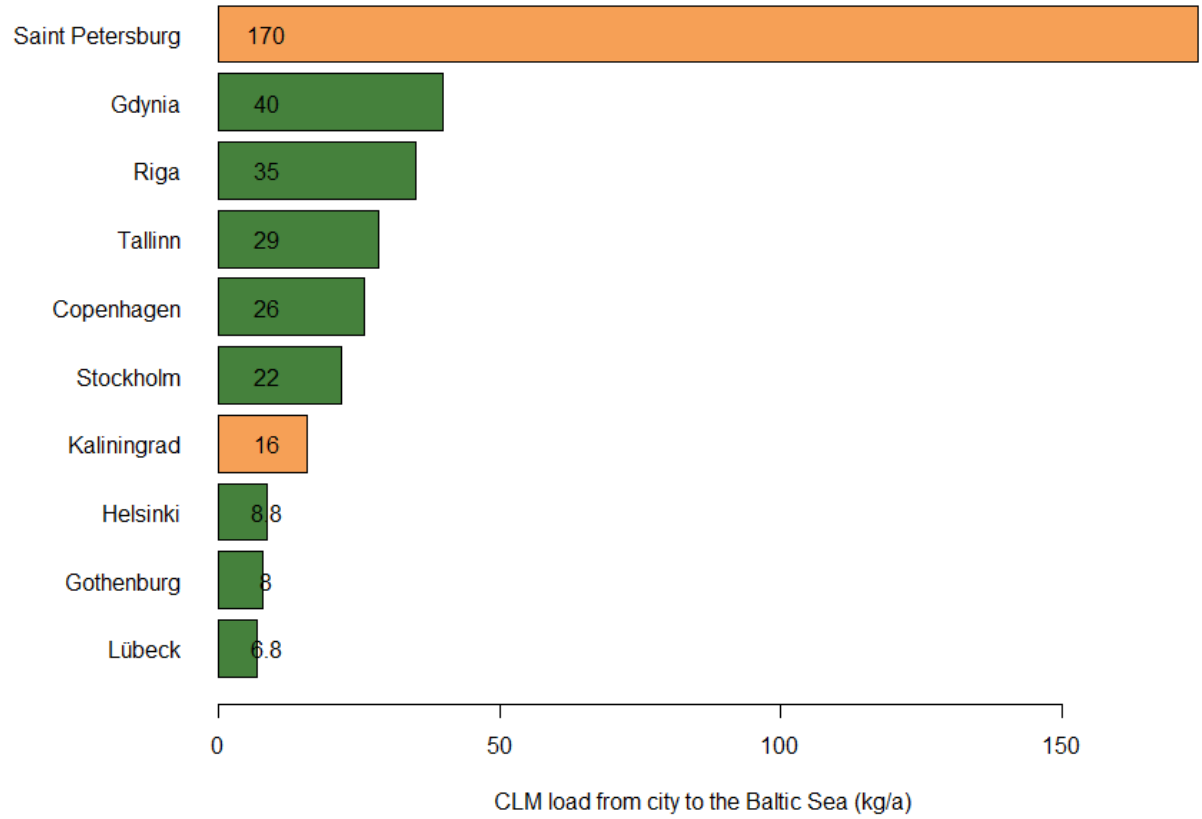

Figure 20. Ten coastal urban clusters with the highest clarithromycin emission reaching the Baltic Sea. The green bars present the cities in countries with sales statistics available, while orange bars represent cities in countries where an average per capita sales value was used. The numerical value presents the calculated load in kilograms, using two significant numbers.

The load reaching coastal waters in different areas is presented in Figure 21. CLM was estimated to be emitted in highest total quantities to the coastal areas in Poland, in the Gdansk basin (1,200 kg) and Bornholm basin (780–800 kg), and to the coastal waters outside the city of St. Petersburg (300 kg).

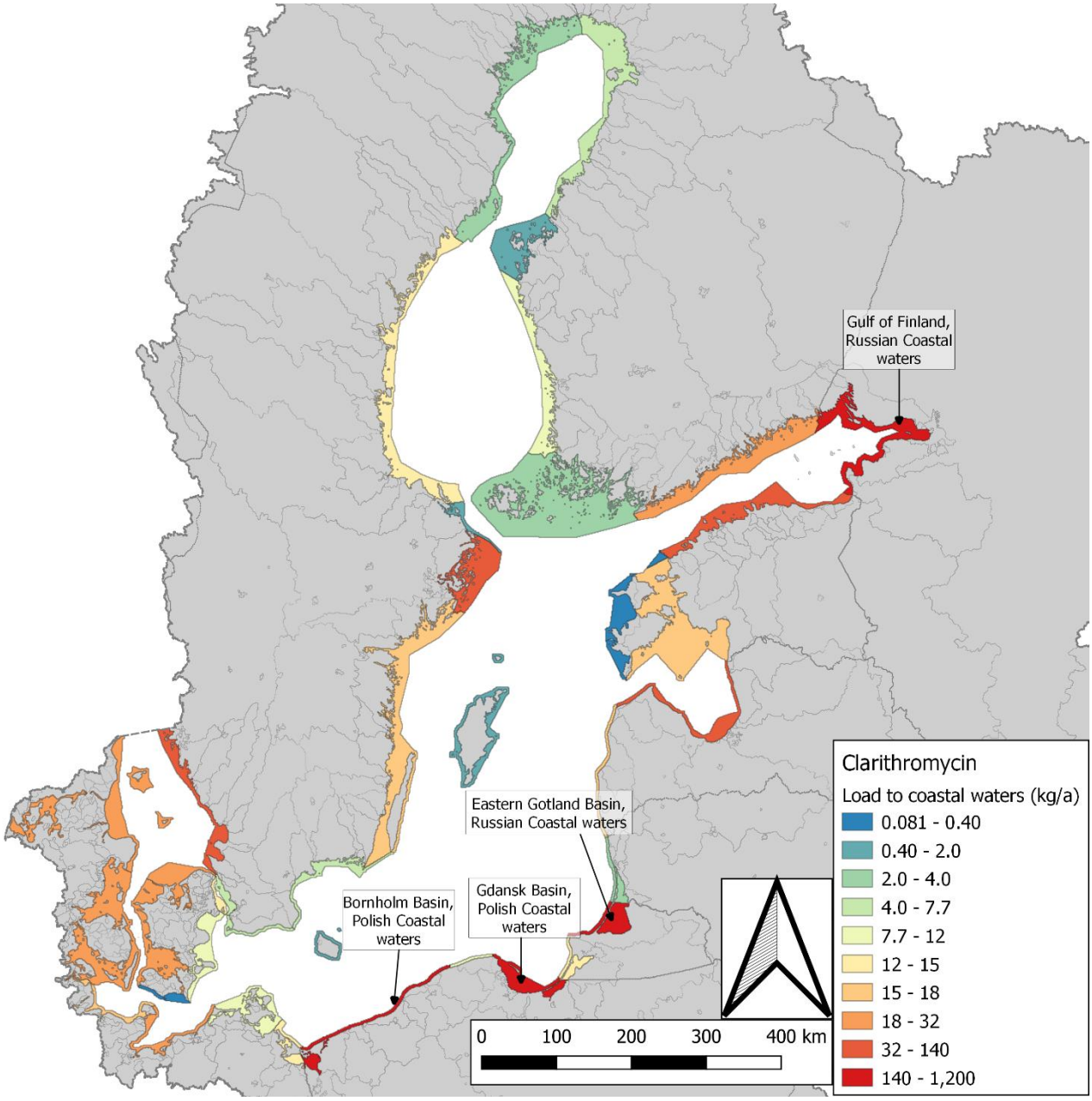

Figure 21. Clarithromycin load (kg/a) reaching the coastal waters in different parts of the Baltic Sea.

3.2.3. Diclofenac

Annual DCF sales within the Baltic Sea drainage basin were estimated to be 22 tonnes. The total loads to the Baltic Sea, estimated for DCF varied from 9.6 tonnes/a to 12 tonnes/a, estimated using scenarios 2 and 0, respectively, while the emission estimated using the whole residue approach suggested by EMA (2006) reached 22 tonnes. The Country emitting the highest DCF loads was estimated to be Poland, in all scenarios (Figure 22). Circa 20% - 25% of the DCF load reaching the BS was estimated to be emitted from coastal cities (coastal urban clusters), while the majority (64–69%) was estimated to originate from inland areas. The overall high emissions from inland areas are largely due to Poland, where inland emissions accounted for 96% of the total load to the BS. Coastal cities had a much higher impact on the total load e.g. in Denmark (45%), Finland (42%), Sweden (41%) and Latvia (38%).

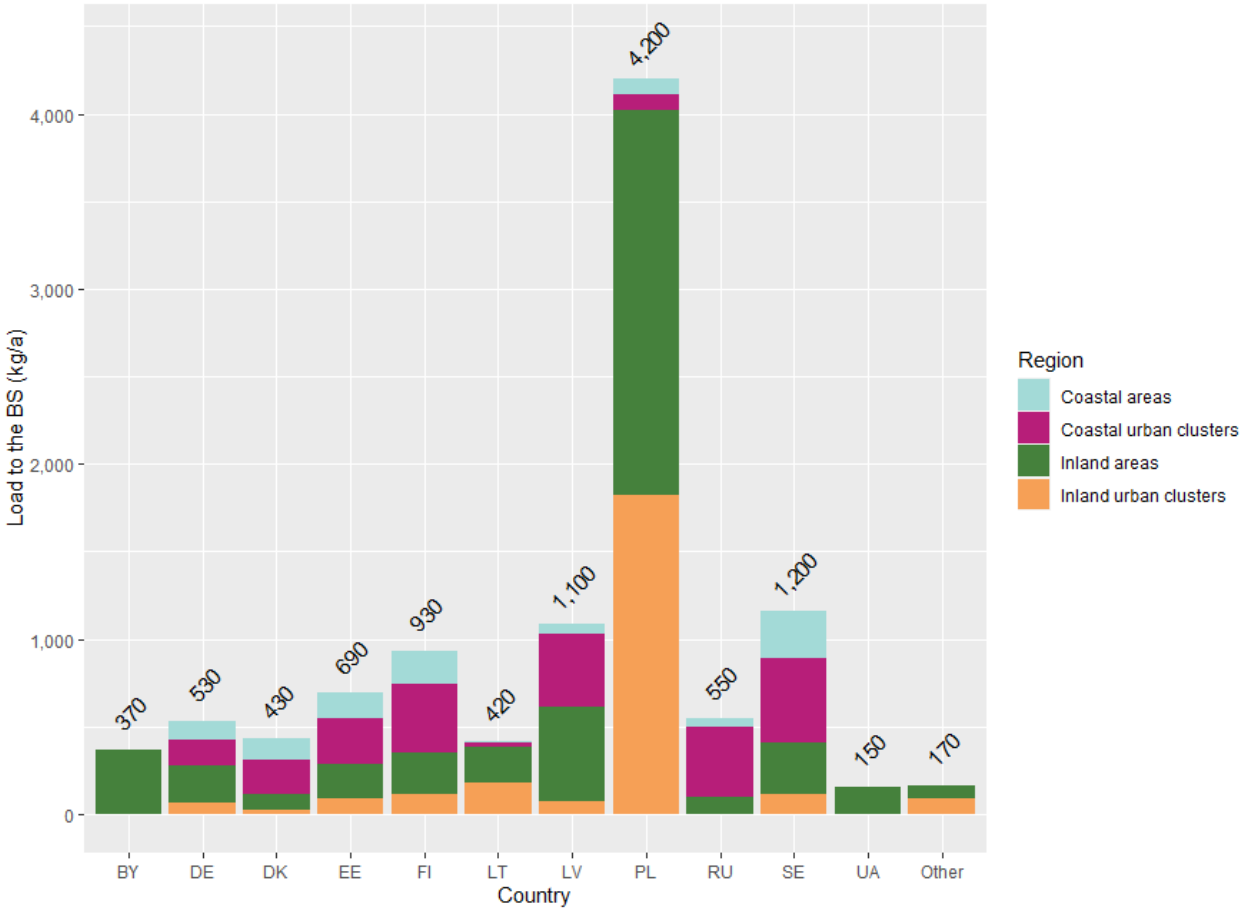

Figure 22. Diclofenac loads to the Baltic Sea from each country and region class, estimated according to scenario 1.

DCF emissions reaching the Baltic Sea were estimated to originate mainly from the use of DCF within regions connected to centralized sewage treatment (Figure 23). Estimating the importance of waste management is much more uncertain, due to poor waste statistics. However, only a relatively small portion of DCF load to the Baltic Sea was estimated to originate from improper waste management.

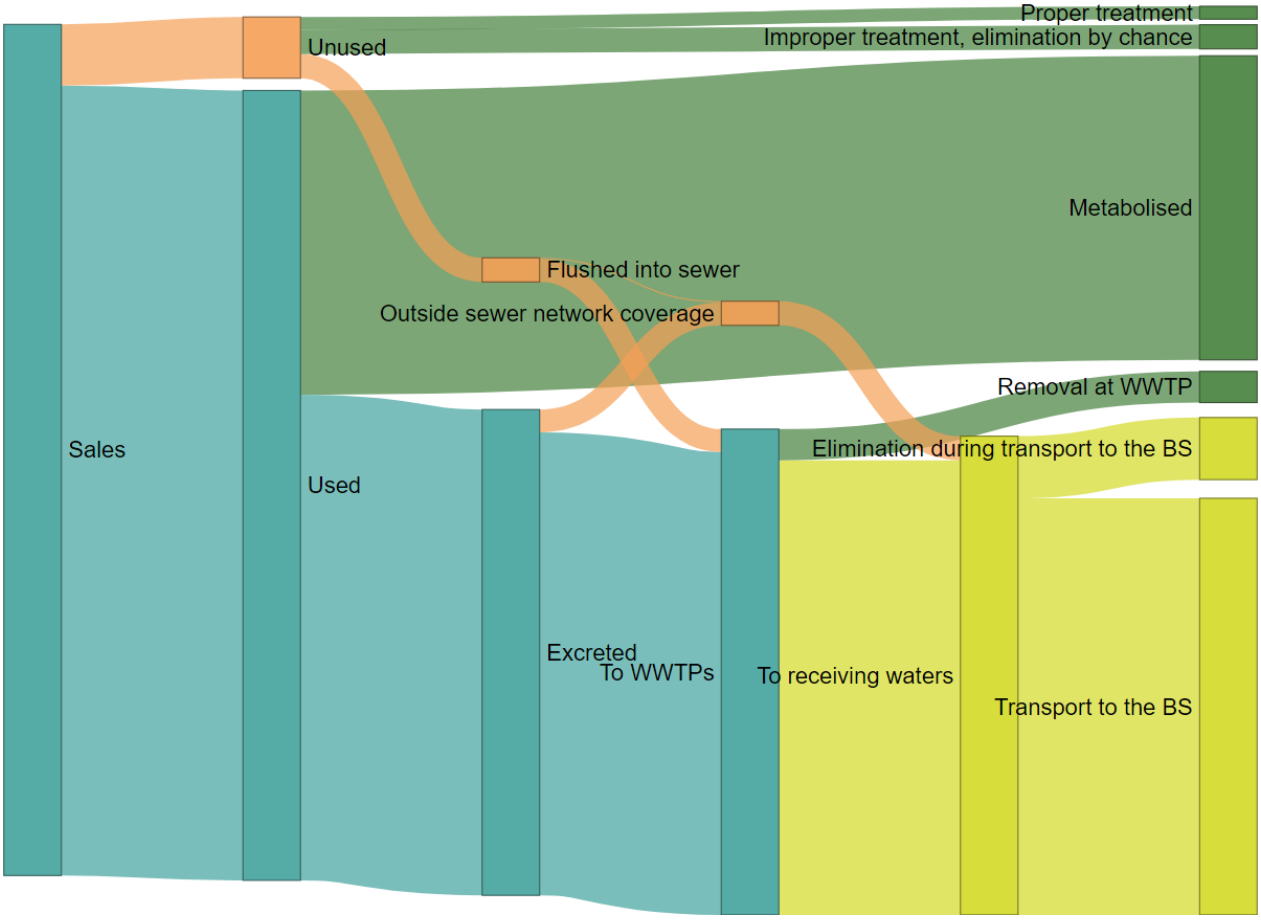

Figure 23. Diclofenac flows according to scenario 1. Green boxes present end-points/processes, where the load is destroyed before reaching the environment. Orange boxes present suboptimal management practices, while yellow boxes present emissions into the water environment.

The grid cell-specific estimated DCF loads to the BS are presented in Figure 24. The emissions from areas with high travel times (see Figure 5) and significant lakes, in e.g. Central Finland, southern parts of Sweden, and areas in Russia, upstream from lakes Ladoga and Onega were estimated to be relatively low.

The national per capita emissions reaching the Baltic Sea ranged from 15 mg/a (Norway) and 58 mg/a (Russia), to 520 mg/a (Latvia) and 540 mg/a (Estonia). When looking at individual calculation areas (Figure 25), the highest per capita DCF emissions reaching the Baltic Sea (640 mg/person/a) were estimated to originate in coastal areas in Estonia. The relatively high per capita emissions from Estonia are in line with the comparably high per capita consumption of DCF (see Table 2).

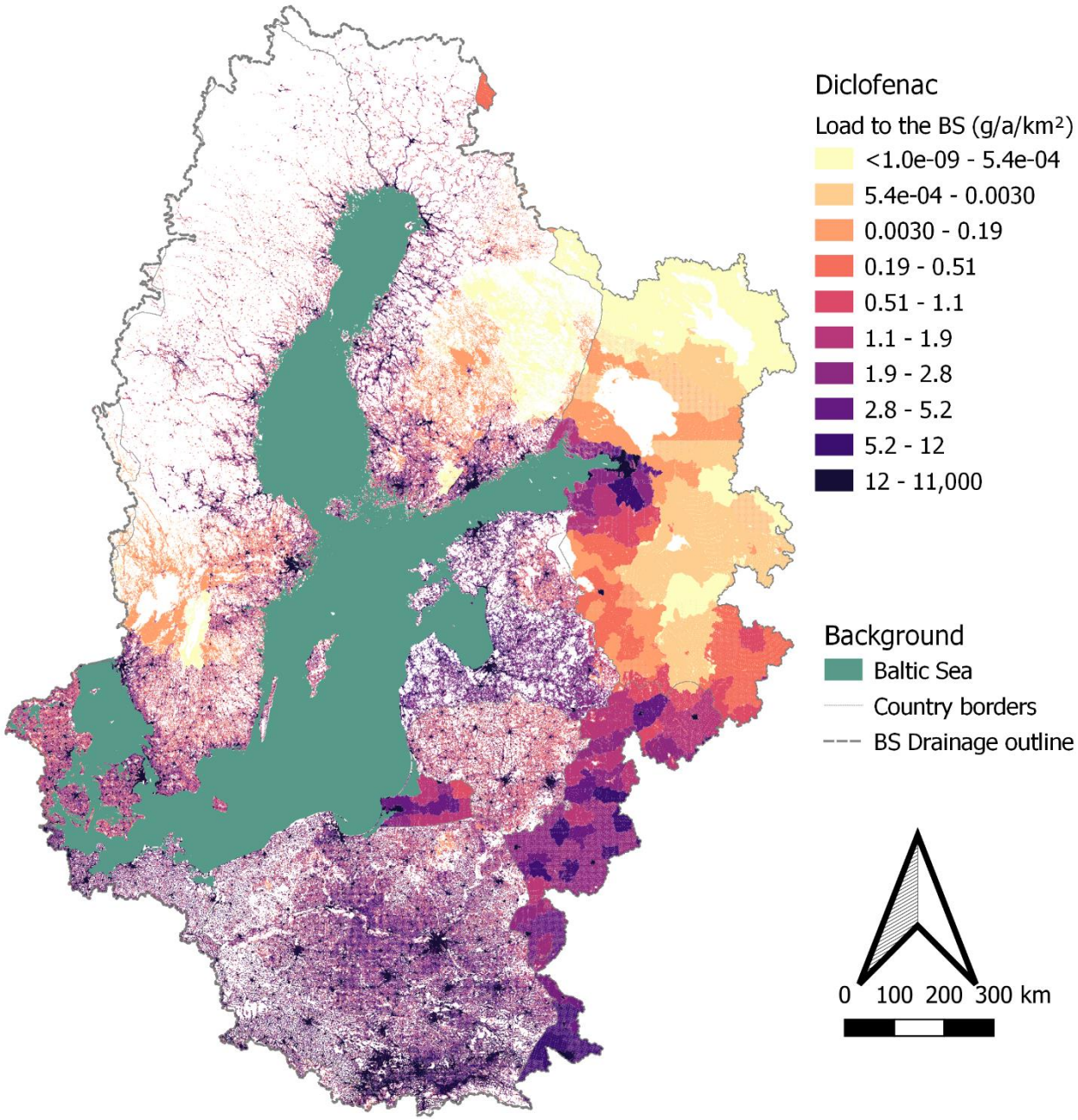

Figure 24. Diclofenac load (g/a/km²) to the Baltic Sea, originating from each of the grid cells.

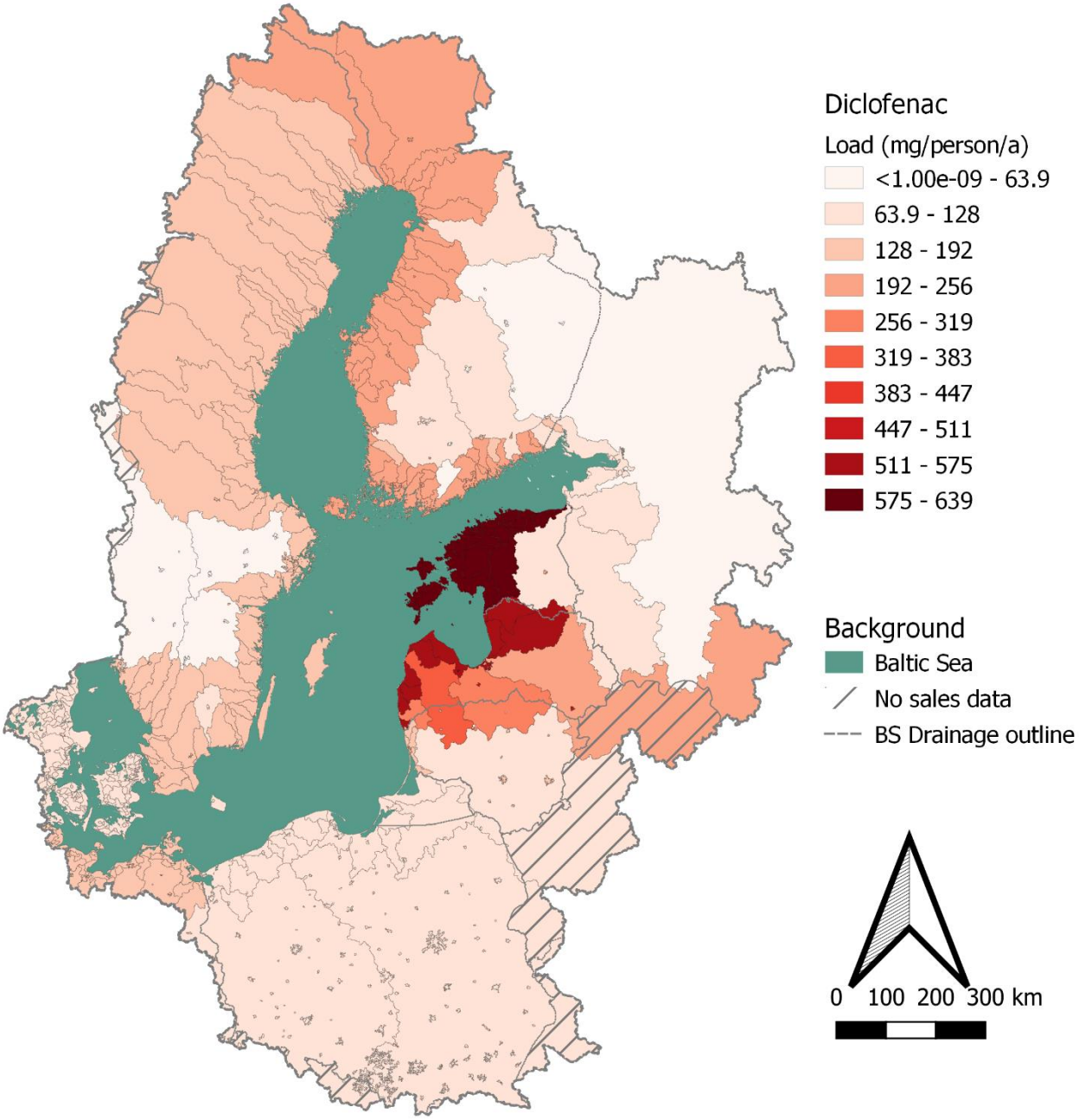

Figure 25. Mean per capita diclofenac load reaching the Baltic Sea, aggregated by calculation areas (AlueId). The dashed area shows the countries for which no national sales data was available, but a population weighted average value was used.

The cities with the highest total load to the Baltic Sea were estimated to be Riga and St. Petersburg with the annual emissions reaching 380 kg and 370 kg, respectively. Ten coastal cities with the highest emission to the Baltic Sea are presented in Figure 26. As the calculation scenarios assumed that coastal cities emit their treated wastewaters directly into the BS, these emissions do not undergo environmental removal processes. Thus, the urban loads do not differ between calculation scenarios.

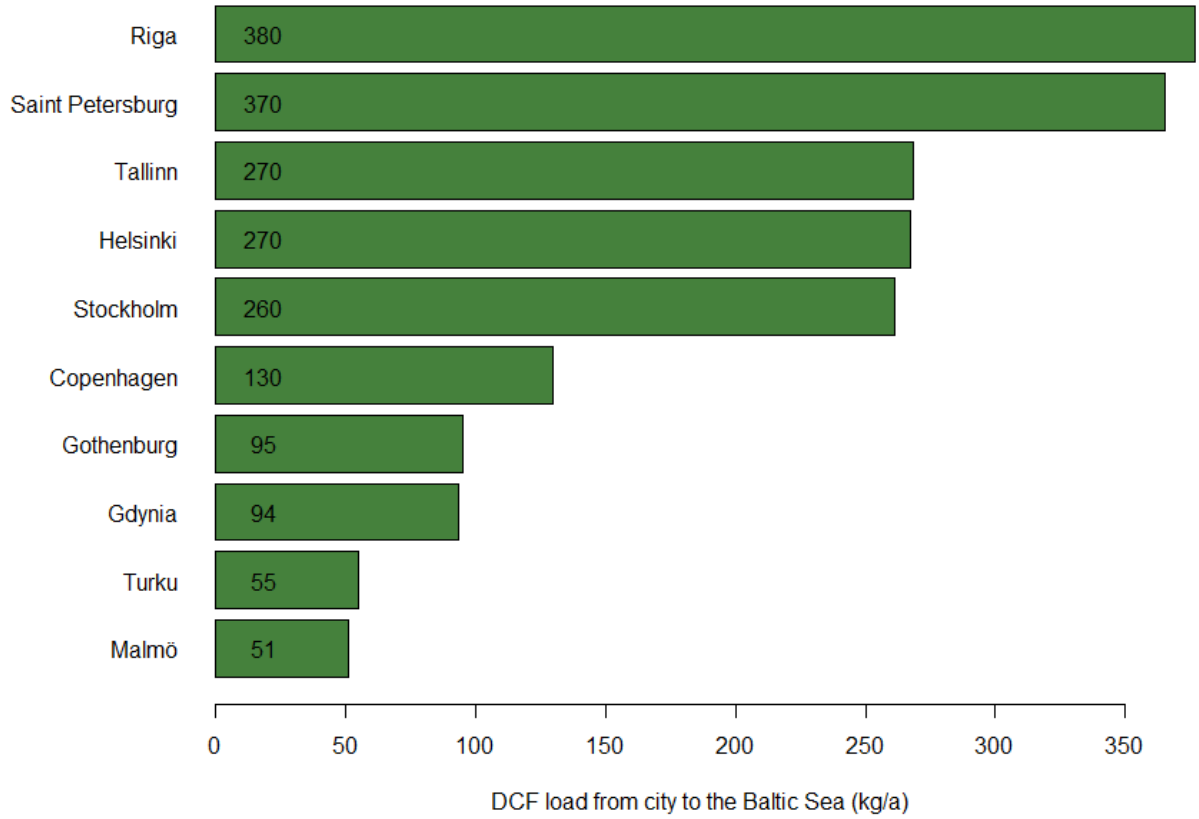

Figure 26. Ten coastal urban clusters with the highest diclofenac emission to the Baltic Sea. The numerical value presents the calculated load in kilograms/a, using two significant numbers.

The coastal areas receiving the highest loads were estimated to be located in Poland. The DCF load to the coastal waters in the Gdansk basin were estimated to be 2,300–2,800 kg/a, depending on the calculation scenario. For reference, the DCF load to the coastal waters of the Gulf of Riga was estimated to range from 1,000 to 1,100 kg/a, and from 440 to 450 kg/a for the Finnish coast on the Gulf of Finland.

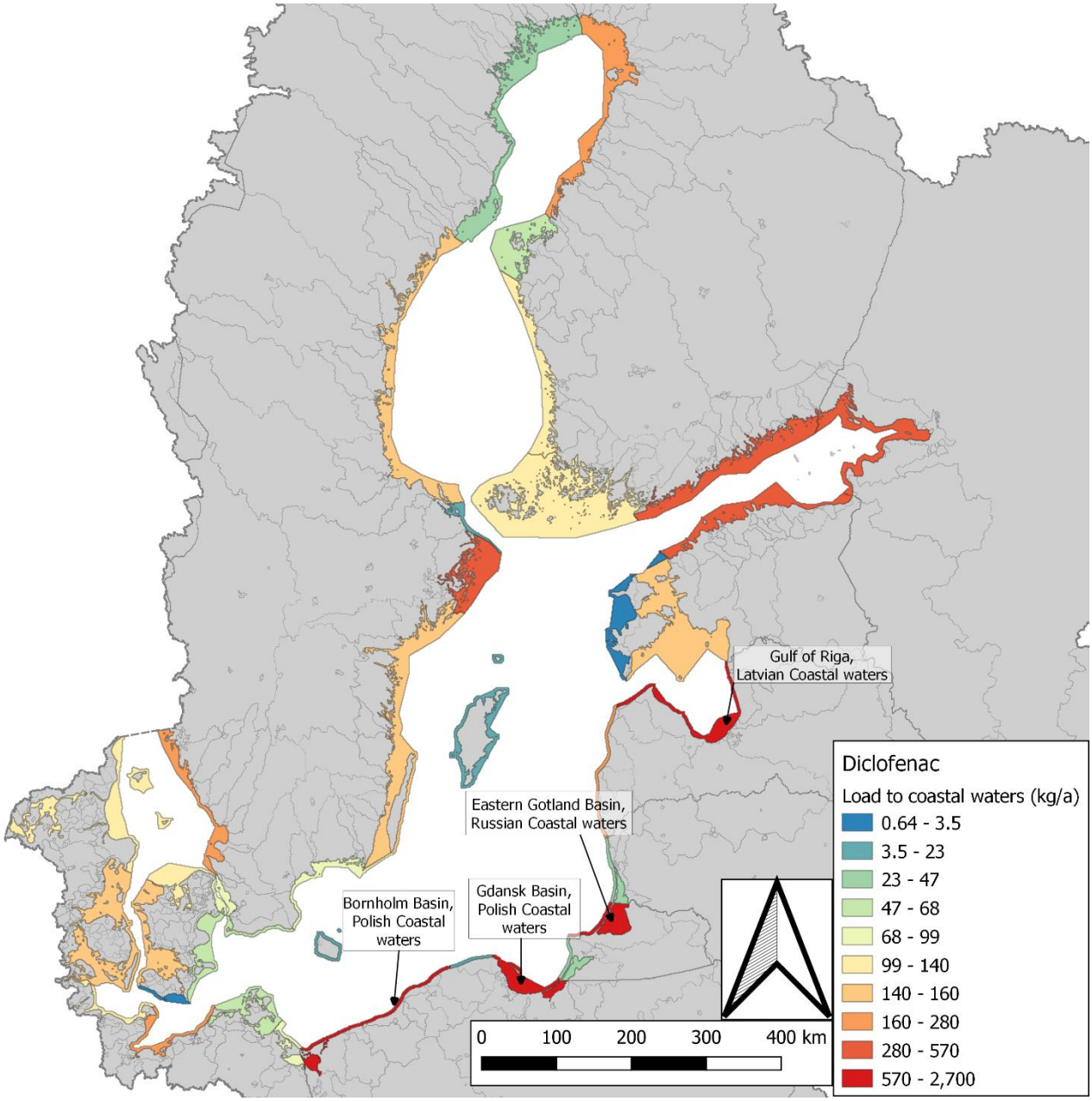

Figure 27. Diclofenac load to the coastal waters in different parts of the Baltic Sea.

3.2.4. Ibuprofen

The annual sales within the Baltic Sea drainage area was estimated to be 420 tonnes. The estimated load to the BS was 1.6 tonnes/a. This is a small fraction of the load (420 tonnes) estimated using the total residue approach (EMA 2006). The total IBU load reaching the Baltic Sea, estimated using scenarios 1-3 (see Table 4), ranged from 1,100 to 1,300 kg/a. The emissions were estimated to originate mainly from coastal urban clusters, this region accounting for 48–53% of the load to the BS. National loads are presented in Figure 28. Russia was estimated to account for 43–47% of the total load reaching the Baltic Sea.

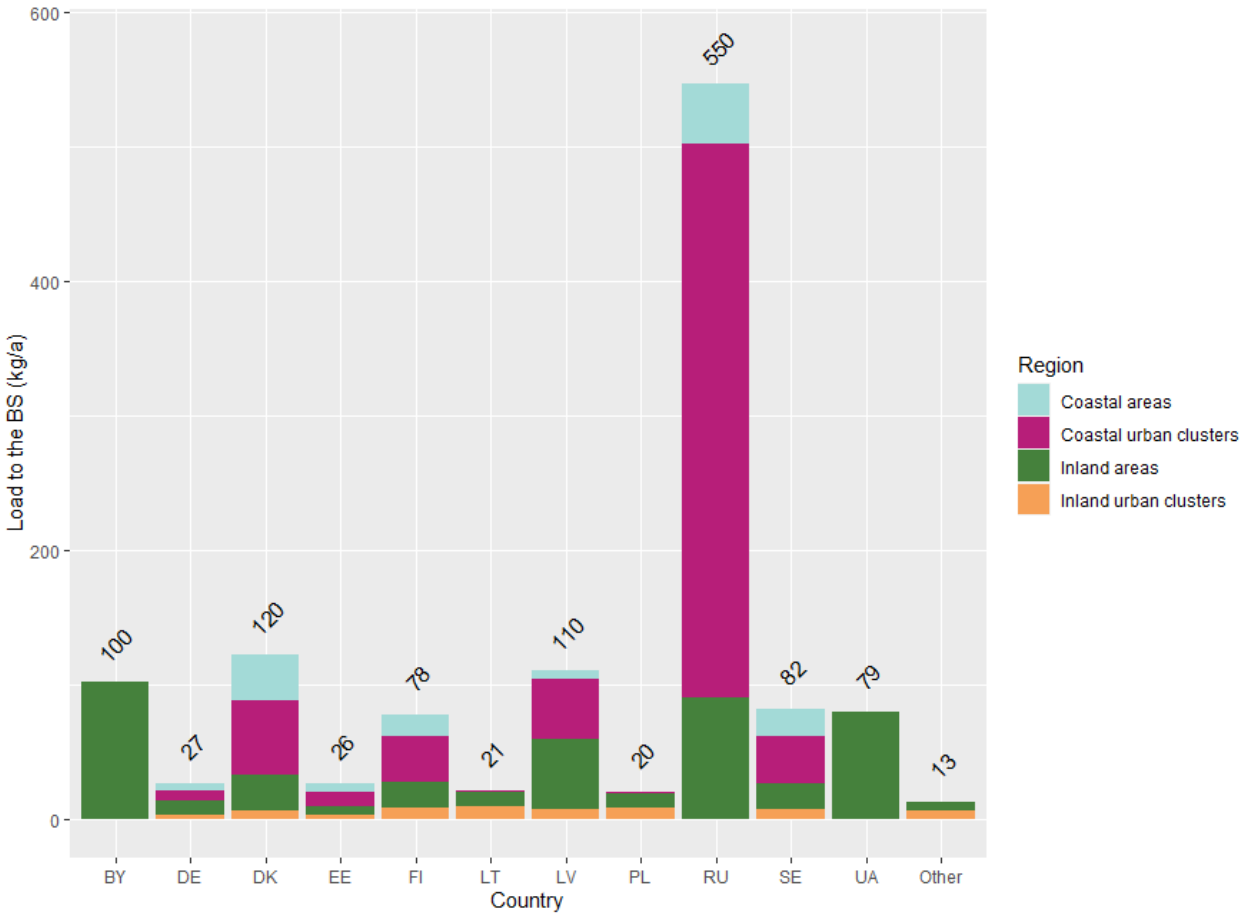

Figure 28. Ibuprofen loads reaching the Baltic Sea from each country and region, estimated according to scenario 1.

Circa 66% of the IBU load in wastewaters within the Baltic Sea drainage basin was estimated to originate from improper treatment of unused medicines (see Figure 29). This is due to the very low fraction of IBU excreted unchanged (1%, see Table 6). Although the mass of consumed IBU is several times higher than the mass estimated to be left unused, wastage was estimated to be a significant emission source since that mass will never undergo metabolic processes. However, the mass of pharmaceuticals flushed into the sewer network contains large uncertainties. To allow for more elaborate estimates, more comprehensive statistics on pharmaceutical wastage and waste management would be required.

Similarly, circa two thirds (1,100 kg) of the IBU mass emitted into the water environment was estimated to originate from untreated wastewaters. Although the load in influent wastewater at WWTPs is ten-fold (11,000 kg) compared to the one in wastewater generated outside sewer network coverage, the very high removal rate compensates for this.

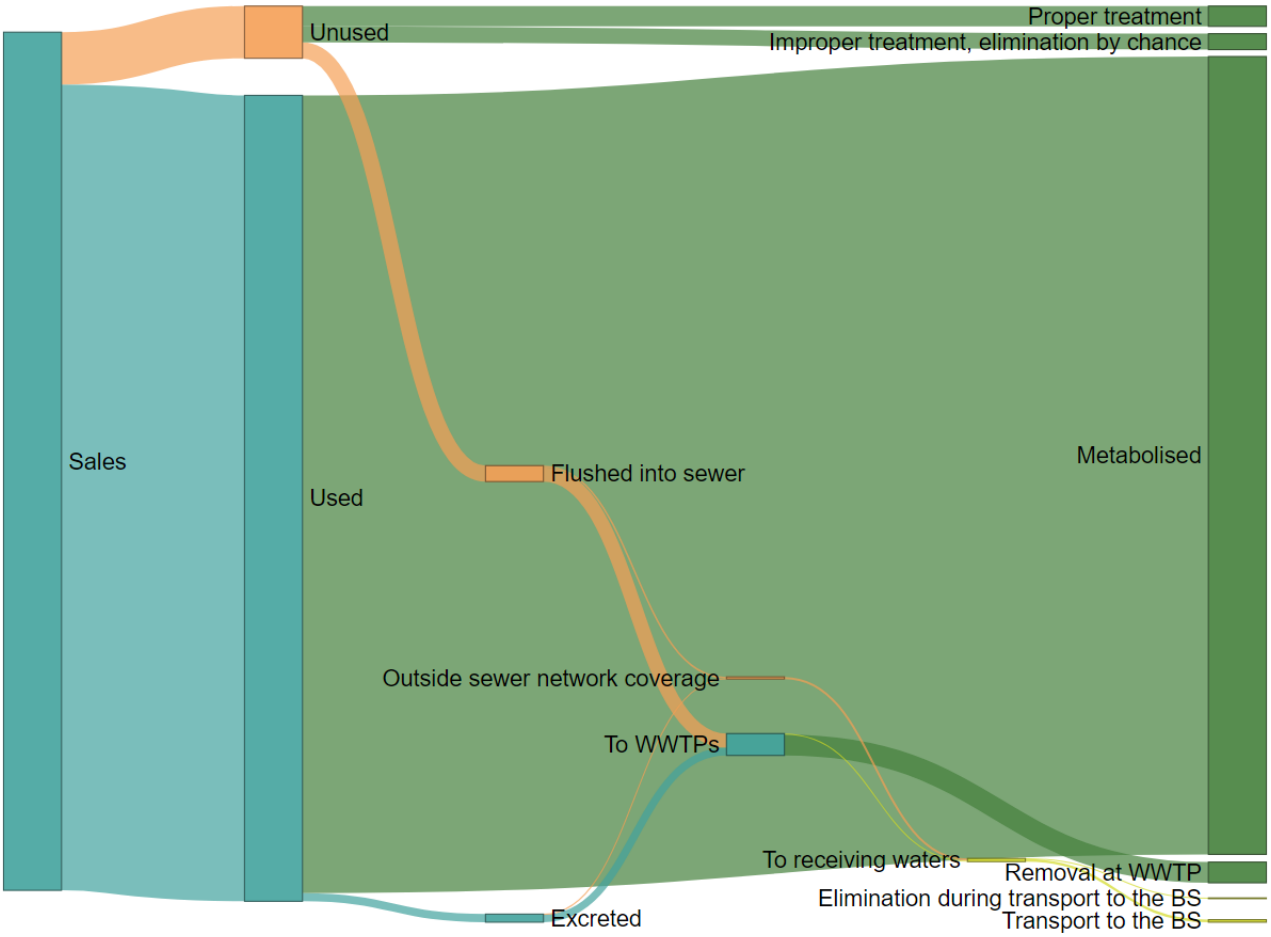

Figure 29. Ibuprofen flows according to scenario 1. Green boxes present end-points/processes, where the load is destroyed before reaching the environment. Orange boxes present suboptimal management practices, while yellow boxes present emissions into the water environment.

Regional distribution of the emissions reaching the Baltic Sea is presented in Figure 30. Emissions from coastal Russia were estimated to be relatively high, due to a high fraction of wastewater being left untreated (see Table 3).

The national per capita emissions reaching the Baltic Sea ranged from coastal countries ranged from 0.5 mg/a in Poland to 8.8 mg/a in Sweden, 16 mg/a in Finland, and 58 mg/a in Russia. When looking at individual calculation areas, the highest per capita emissions were estimated to originate from coastal cities in Russia (Figure 31). The high emissions from Russia, Belarus and Ukraine are in line with low sewer network coverage (see Table 3). As IBU is removed efficiently in conventional wastewater treatment processes, the coverage of the sewer network has a big impact on total load.

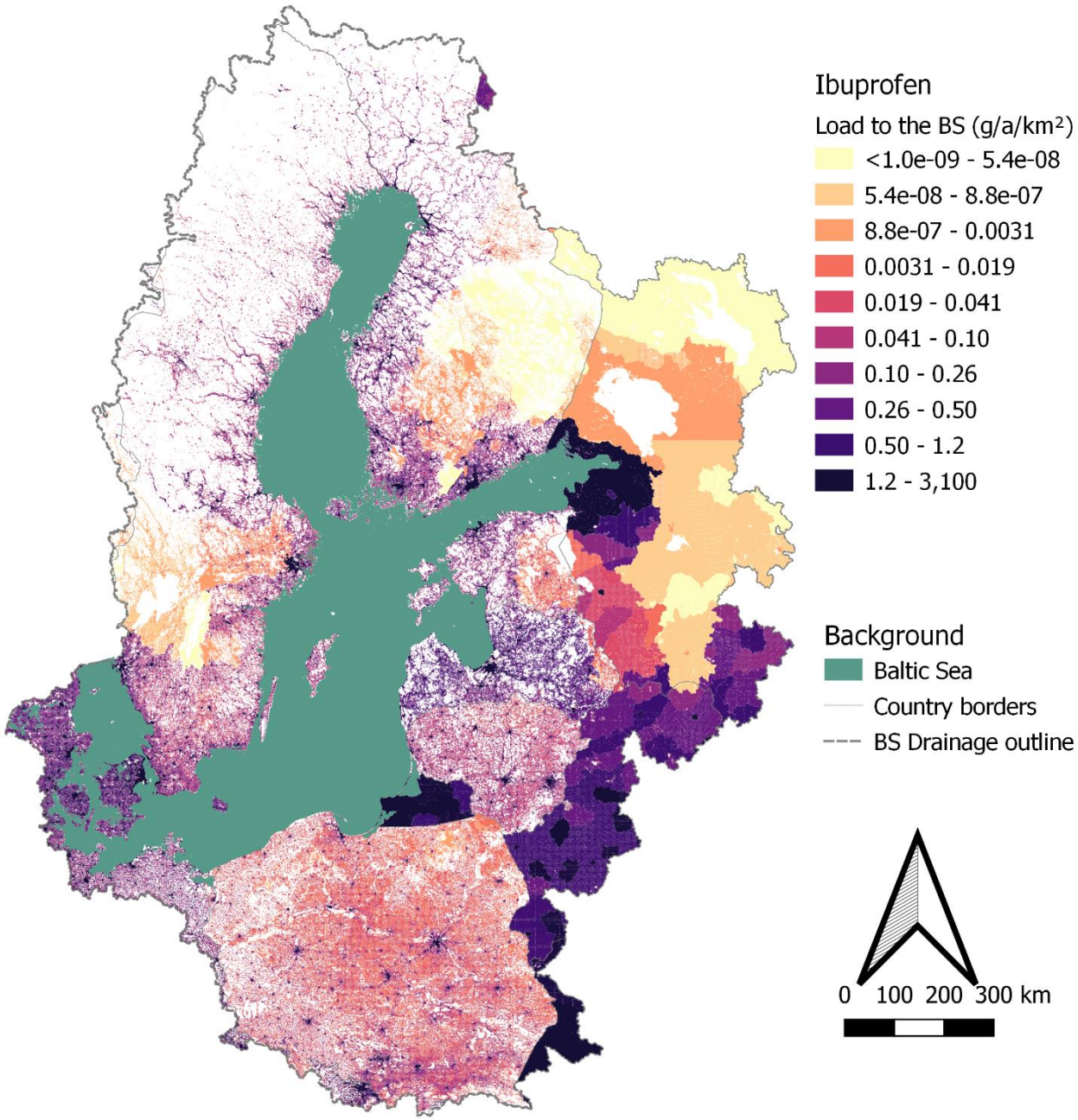

Figure 30. Ibuprofen load (g/a/km²) reaching the Baltic Sea, originating from individual grid cells.

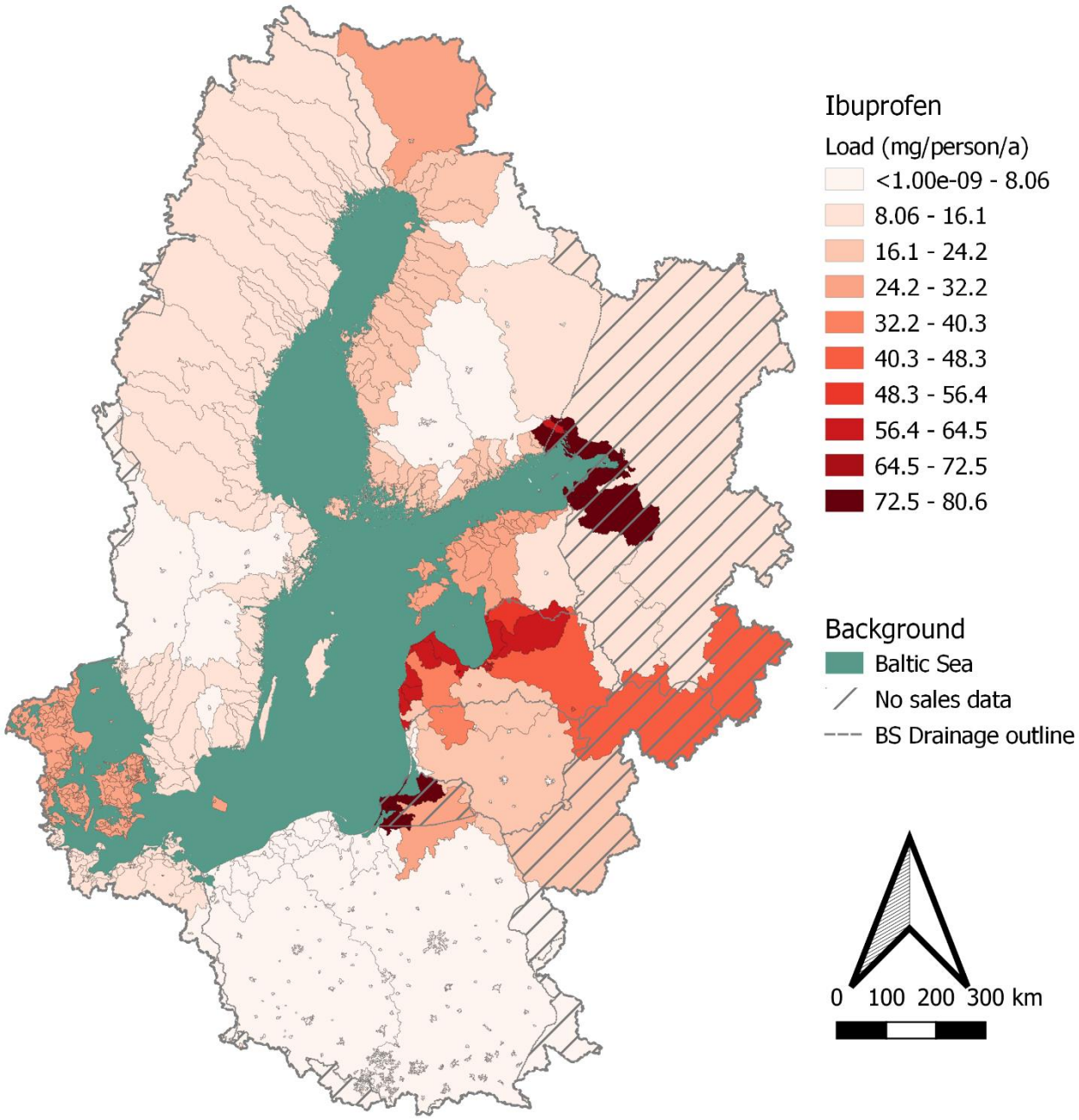

Figure 31. Mean per capita ibuprofen load reaching the Baltic Sea, aggregated by calculation areas. The dashed area shows the countries for which no national sales data was available, but a population weighted average value was used.

The highest load originating from individual cities varied drastically, with St. Petersburg being the city emitting the highest load of IBU into the Baltic Sea. The city-specific IBU loads are presented in Figure 32. The country with the highest per capita IBU consumption in the region is Finland. The mass of sales were estimated to be 24 tonnes in Helsinki, and 22 tonnes in St. Petersburg. However, due to more pharmaceuticals being left unused, a smaller fraction of pharmaceutical waste being managed properly (see assumptions in Table 3), and a lower fraction of wastewater being treated, the load originating from St. Petersburg was estimated to be circa 16-fold.

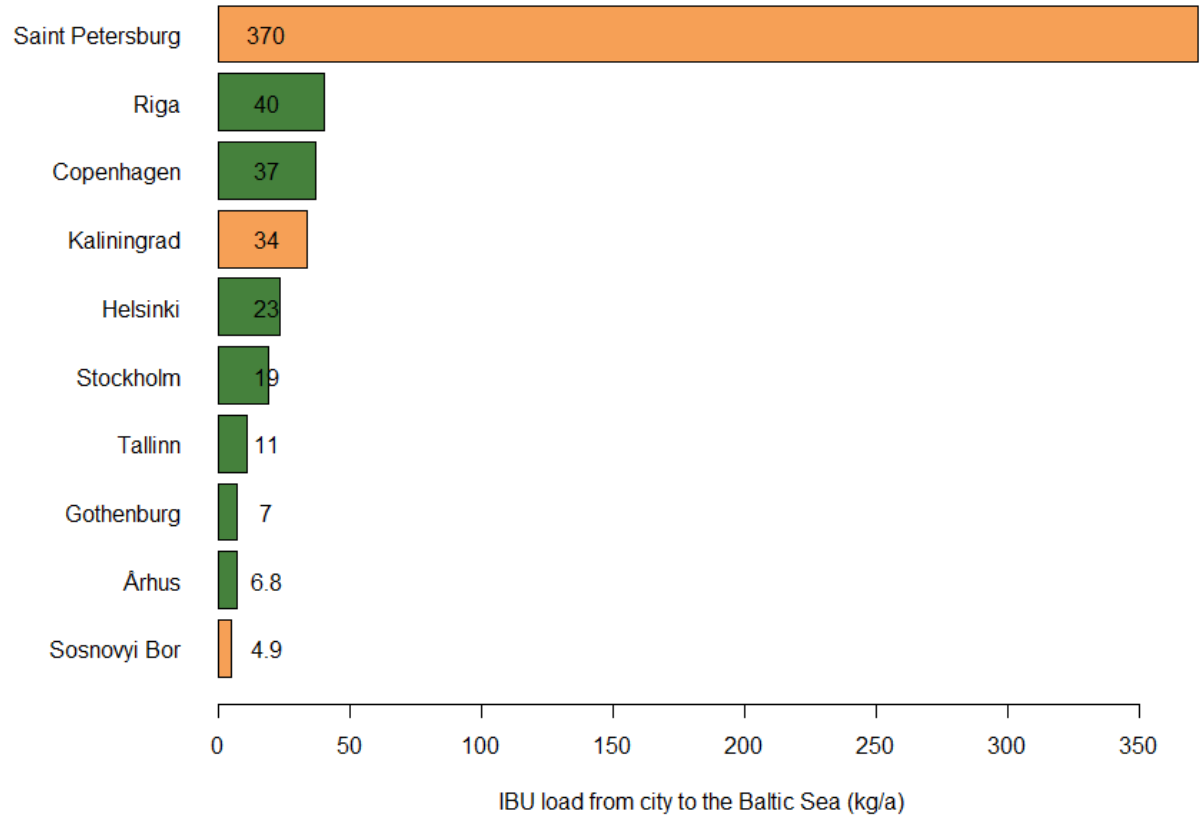

Figure 32. Ten coastal urban clusters with the highest ibuprofen emission reaching the Baltic Sea. The green bars present the cities in countries with sales statistics available, while orange bars represent cities in countries where an average per capita sales value was used. The numerical value presents the calculated load in kilograms, using two significant numbers.

IBU was estimated to be emitted in highest quantities to the coastal waters outside St. Petersburg, in eastern Gulf of Finland. These emissions were estimated to reach 450 kg/a. Other areas with high IBU loads were e.g. coastal waters outside Riga and Gdansk, with loads of 140 kg and 110, respectively. The IBU loads emitted to coastal waters in different parts of the BSR are presented in Figure 33.

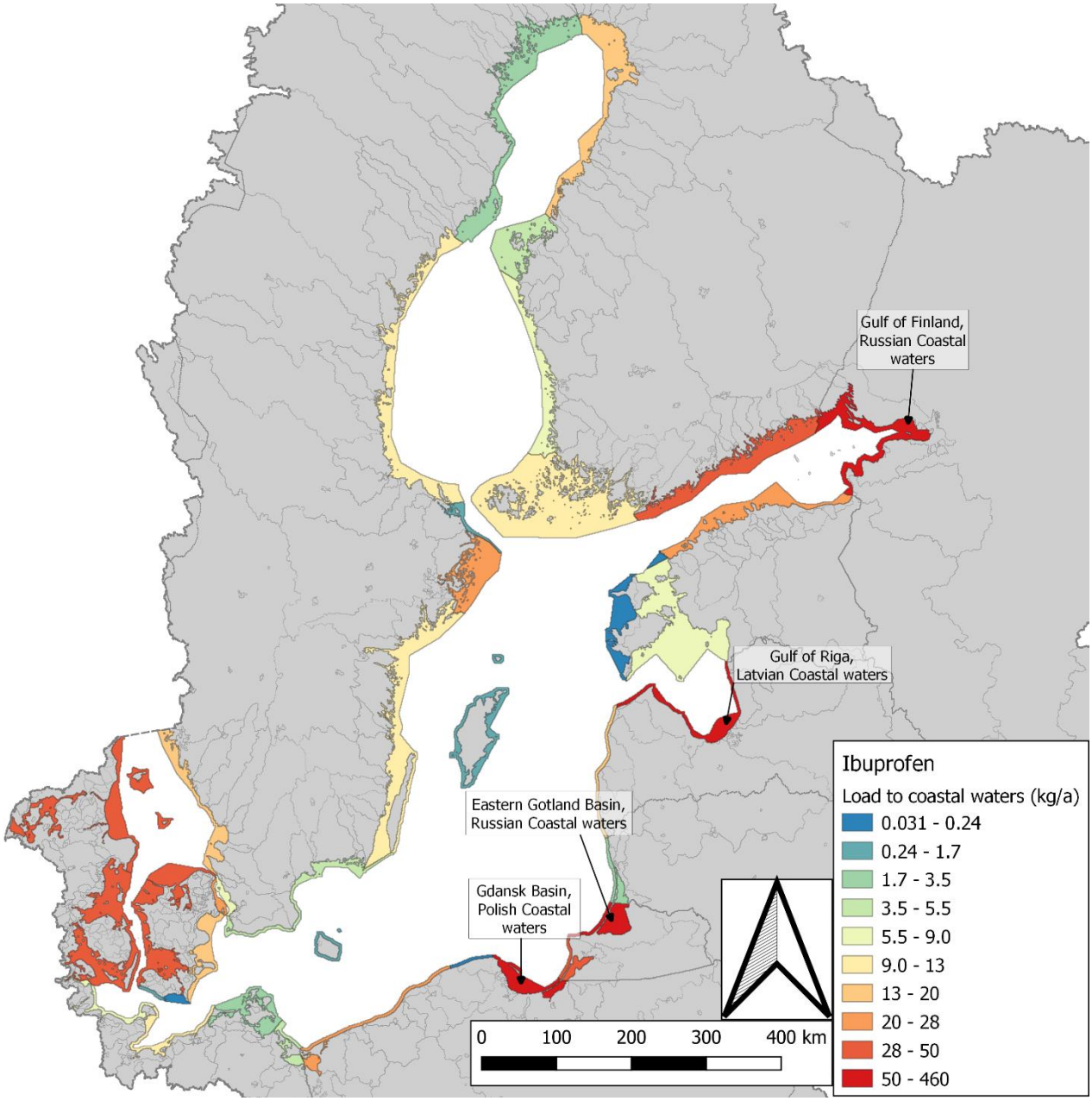

Figure 33. Ibuprofen load (kg/a) reaching the coastal waters in different parts of the Baltic Sea.

3.2.5. Metformin

Annual MTF sales within the Baltic Sea drainage basin were estimated to be 1,400 tonnes. The overall annual MTF load estimated to reach the Baltic Sea was estimated to be 91 tonnes. This estimated load is significantly lower than the one (1,400 tonnes) suggested by the whole residue approach (EMA 2006). The highest annual emissions (54–55 tonnes) were evaluated to originate from Russia, followed by emissions from Belarus and Ukraine (Figure 34).

Circa 36% of the load to the BS were estimated to originate from coastal urban clusters. There were large differences between countries. For instance, in Poland, emissions coastal cities were estimated to account for only 2% of the load reaching the Baltic Sea.

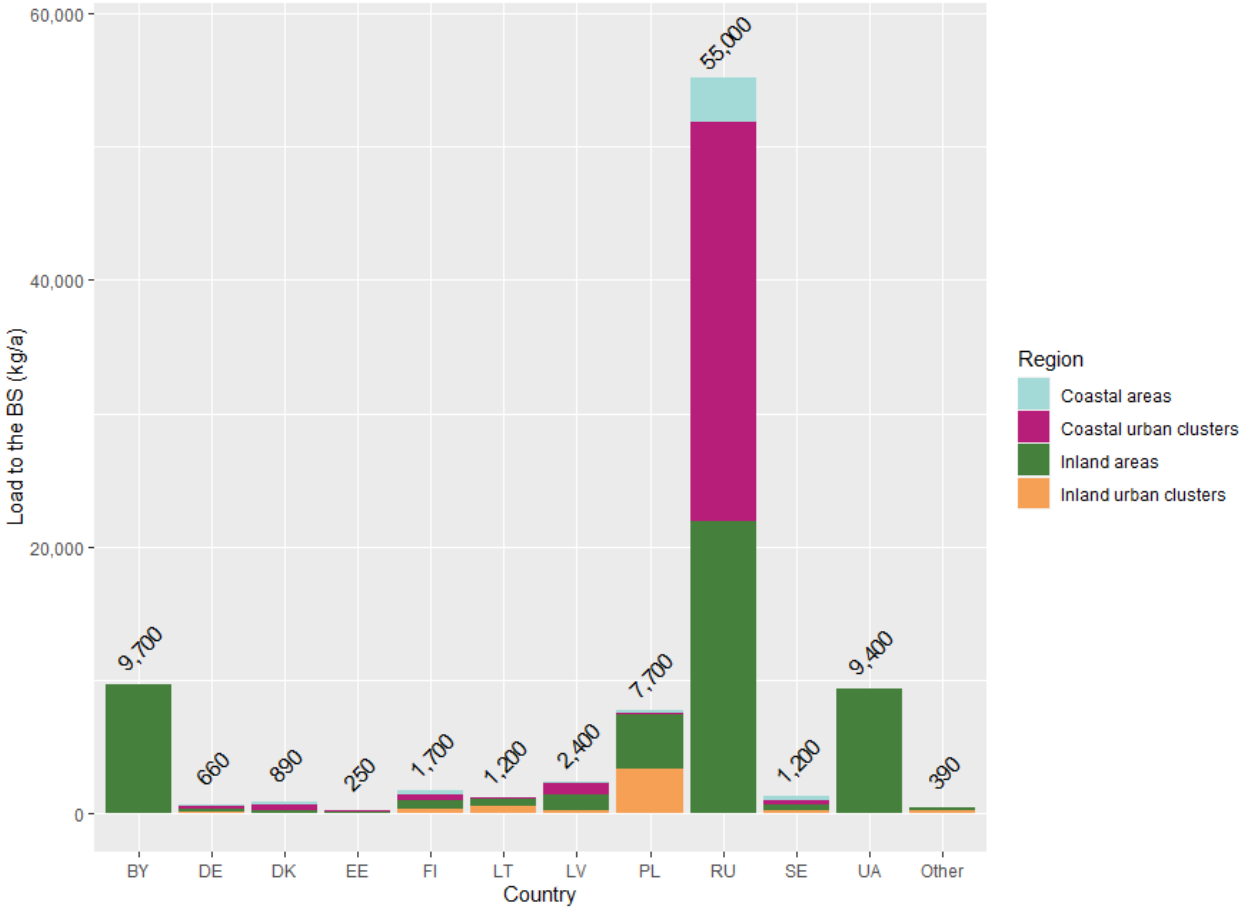

Figure 34. Metformin loads reaching the Baltic Sea from each country and region, estimated according to scenario 1.

The load to the BS was estimated to originate largely from its use in areas not connected to centralized wastewater treatment (Figure 35). This is in line with results presented in Figure 34, which clearly reflect the coverage of sewer network in these countries. In the three countries accounting for the highest loads to the BS (RU, BY, UA), the fraction of population connected to wastewater treatment is less than 85%. This has a high impact on estimated MTF emissions, due to the API being efficiently removed in conventional WWTP processes (removal rate >99%). Emissions from WWTPs were estimated to account for only circa 3% of the load to the water environment, while the remaining 97% is emitted in wastewaters that are left untreated. This result is in line with those published by Bollmann et al. (2019), who identified untreated wastewaters to be significant sources for micropollutants that are removed to a high extent in WWTPs.

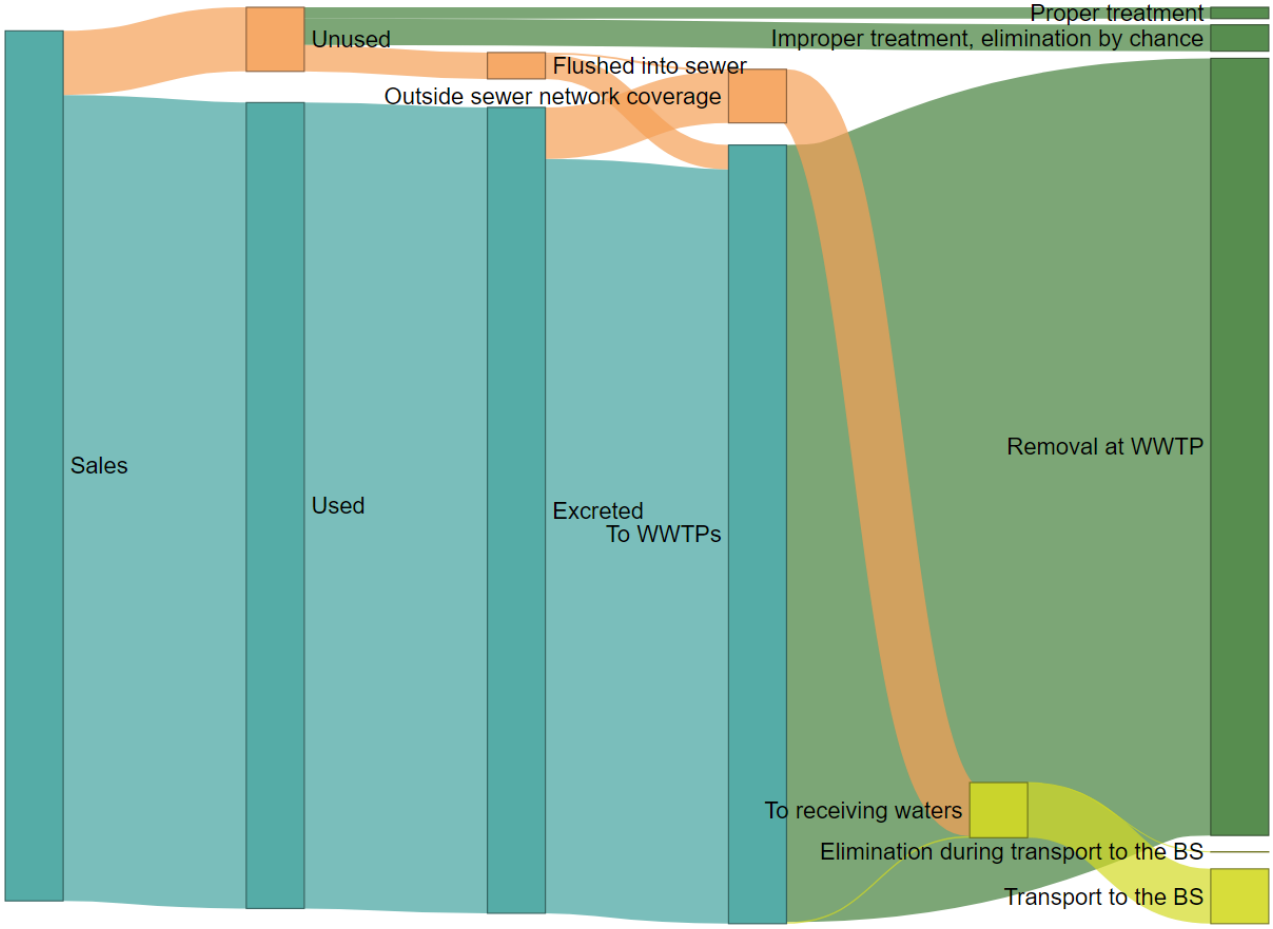

Figure 35. Metformin flows according to scenario 1. Green boxes present end-points/processes, where the load is destroyed before reaching the environment. Orange boxes present suboptimal management practices, while yellow boxes present emissions into the water environment.

The grid cell-specific MTF loads to the BS are presented in Figure 36. The areas in countries with relatively low fraction of wastewater is treated are highlighted as important emissions sources. On the other hand, areas with high population density are also shown as emission hotspots.

The national per capita load reaching the Baltic Sea ranged from 130 mg/a in Sweden to 6,600–6,800 mg/a in Ukraine. The per capita emission was highly dependent on the fraction of sewage that is lead to proper wastewater treatment. The highest per capita emissions in individual calculation areas (5,800 mg/a) reaching the Baltic Sea were estimated to be in coastal Russia (Gulf of Finland & Kaliningrad). However, as no actual sales figures are available for e.g. Russia or Ukraine (see Table 2), these results rely strongly on the assumption, that the per capita consumption of MTF in these countries is similar to that in the eight coastal countries for which we have sales figures.

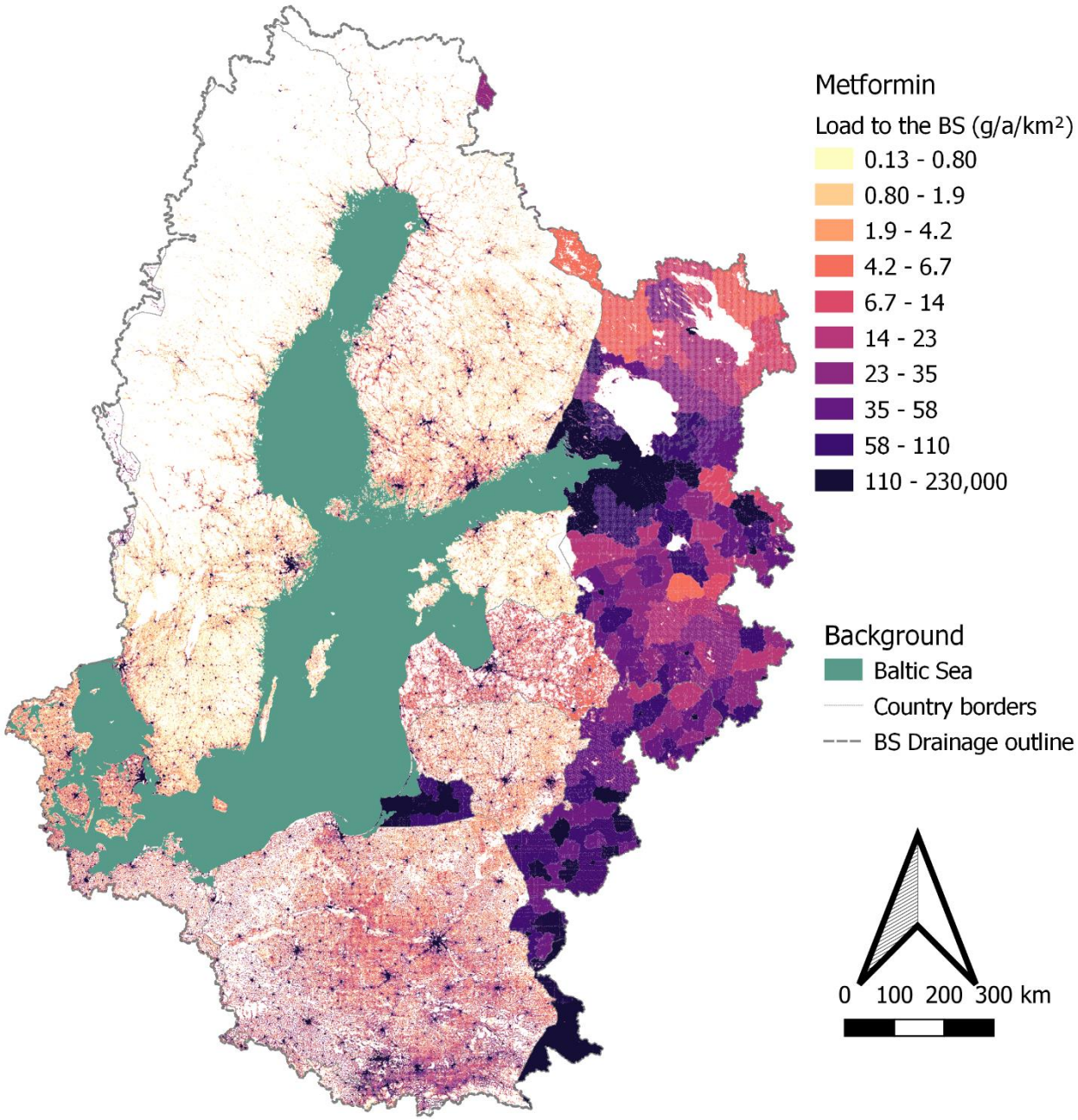

Figure 36. Metformin load (g/a/km²) reaching the Baltic Sea, originating from each of the grid cells.

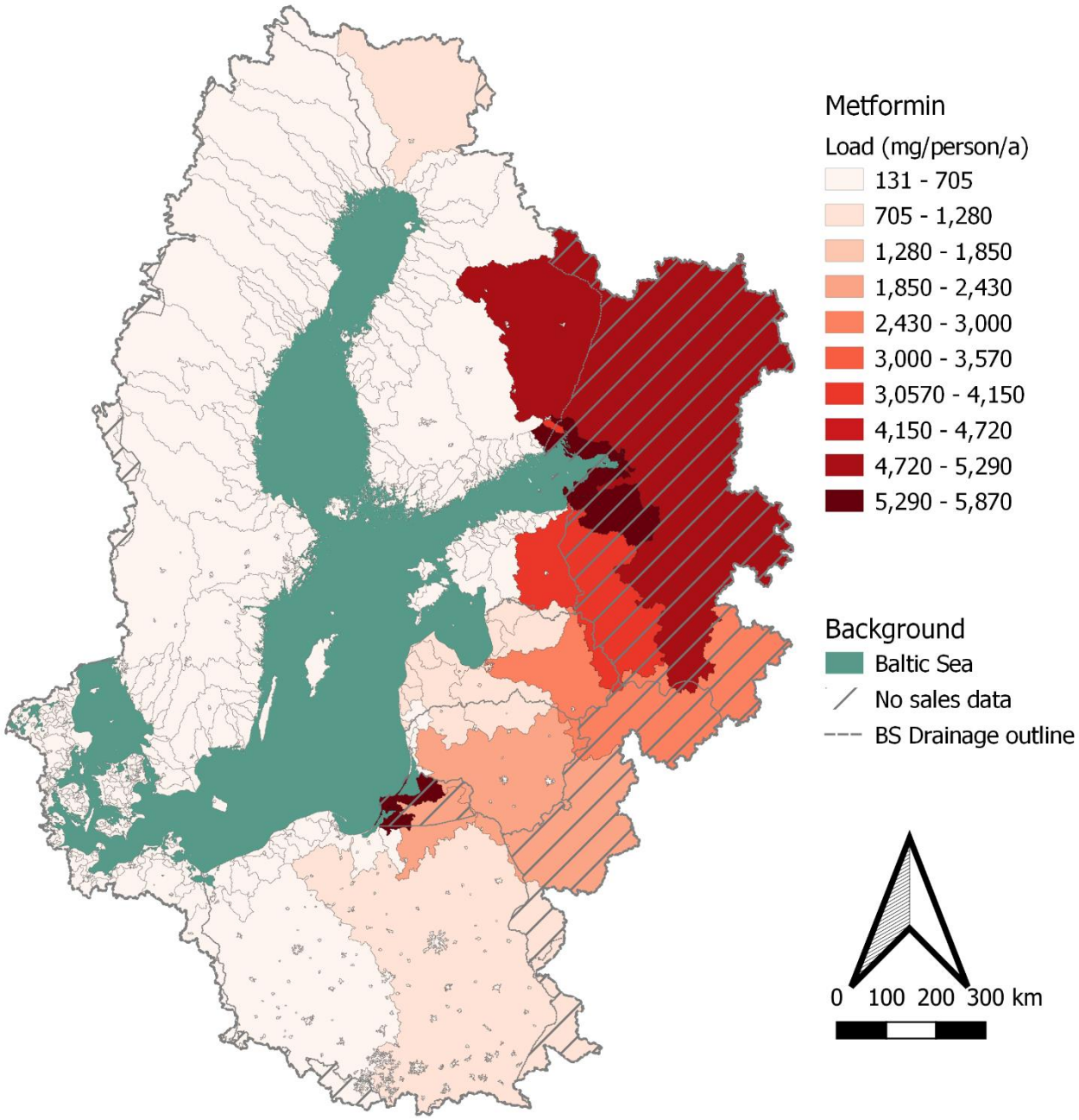

Figure 37. Mean per capita metformin load reaching the Baltic Sea, aggregated by calculation areas (AlueId). The dashed area shows the countries for which no national sales data was available, but a population weighted average value was used.

The coastal cities with the highest MTF load reaching the Baltic Sea were estimated to be St. Petersburg and Kaliningrad. However, emissions from Russia are based on uncertain assumptions. For instance, as presented in Figure 1, the information on population density available in areas in Russia, and other areas outside the EU is very much less exact than for EU-member states. This may result in inaccurate estimations on spatial emissions. Ten coastal cities with the highest emission reaching the Baltic Sea are presented in Figure 38.

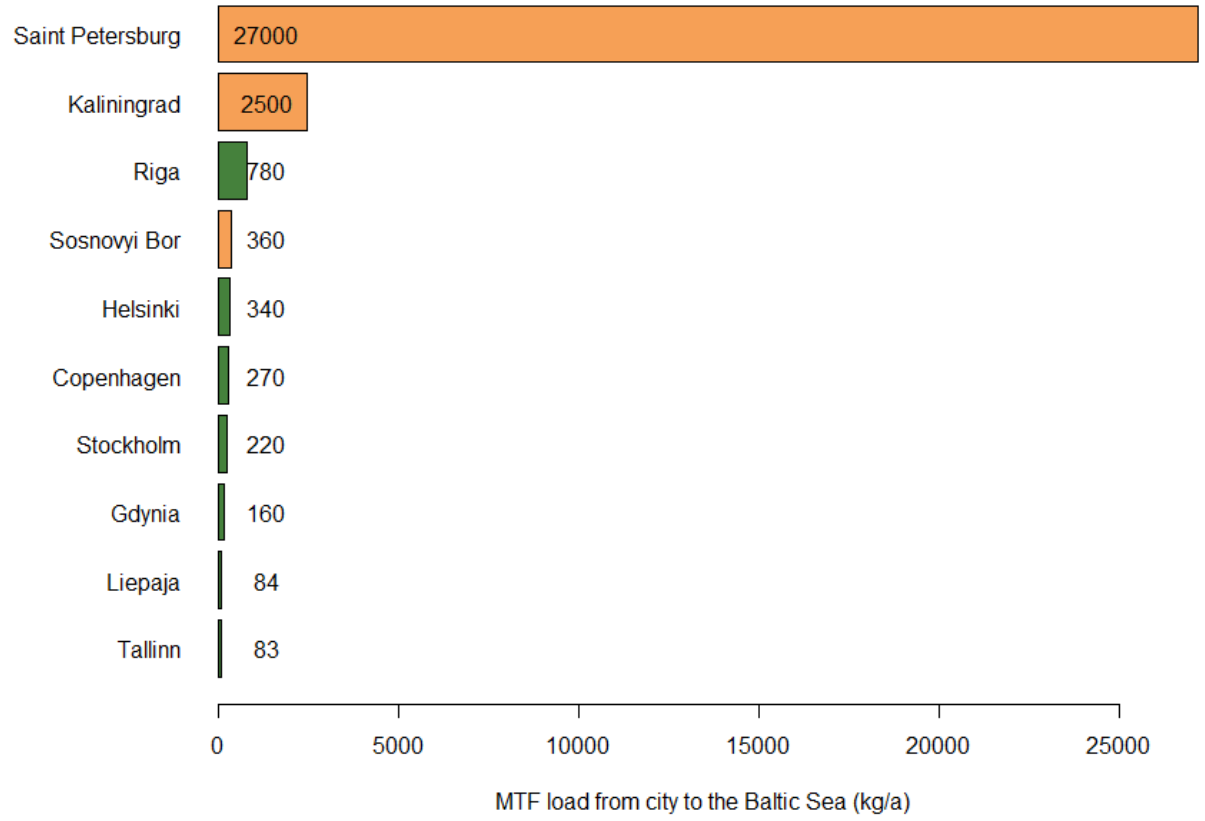

Figure 38. Ten coastal urban clusters with the highest metformin emission reaching the Baltic Sea. The green bars present the cities in countries with sales statistics available, while orange bars represent cities in countries where an average per capita sales value was used. The numerical value presents the calculated load in kilograms, using two significant numbers.

The coastal areas with the highest incoming MTF load were estimated to be in the eastern Gulf of Finland, off the coast of St. Petersburg. The MTF load entering this coastal area was estimated to reach 46 tonnes annually. For reference, the MTF load entering the coastal waters in the Swedish coastal waters in the northern Baltic Proper off the coast of Stockholm were estimated to be around 390 kg/a.

The estimated loads to coastal waters in different parts of the Baltic Sea are presented in Figure 39. These estimated loads varied only slightly between scenarios. This is likely due to no biodegradation being taken into account for MTF.

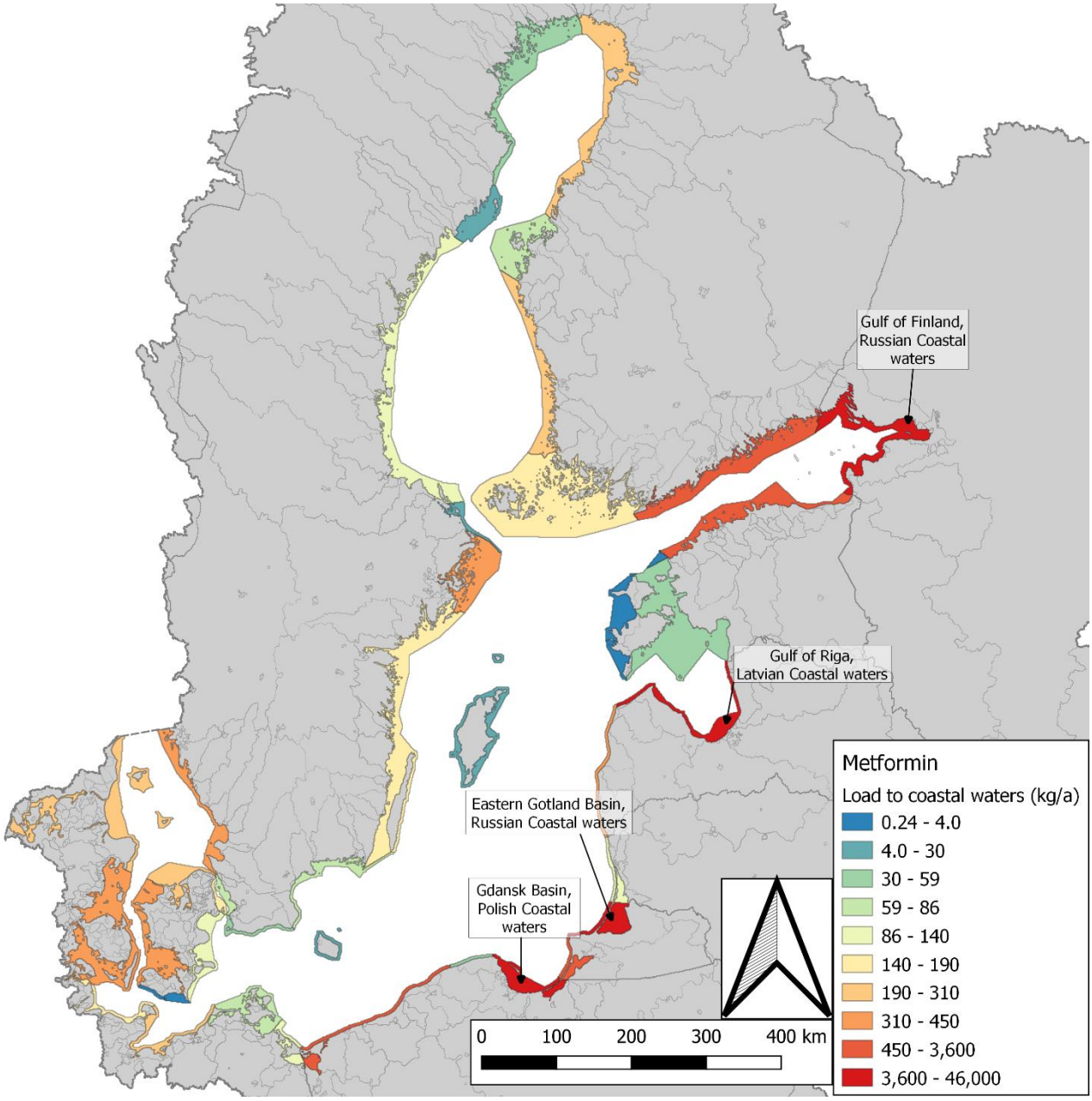

Figure 39. Metformin load (kg/a) reaching the coastal waters in different parts of the Baltic Sea.

3.2.6. Ofloxacin

The total mass of annual sales of OFL within the Baltic Sea drainage area was estimated to be 340 kg. This would result in 58 kg being emitted into the water environment, assuming that the removal rate at MWWTPs is 86.5%. The total load reaching the Baltic Sea was estimated to range from 57 to 59 kg/a, depending on the calculation scenario. This estimate covers only the emissions from the use of the racemic mixture (ofloxacin), and not those from the use of the enantiopure form levofloxacin. More discussion on this is presented in chapter 4.2 The high portion of emission to the surface waters eventually reaching the BS reflects the slow photodegradation and no biodegradation being incorporated into the calculations.

The emissions reaching the Baltic Sea from individual countries is presented in Figure 40. Emissions were estimated to originate mainly from Poland and Russia, these countries accounting for 44% and 32%, respectively. According to the calculations, coastal cities accounted for 20% of the load, while inland areas (including inland urban clusters) accounted for 76%.

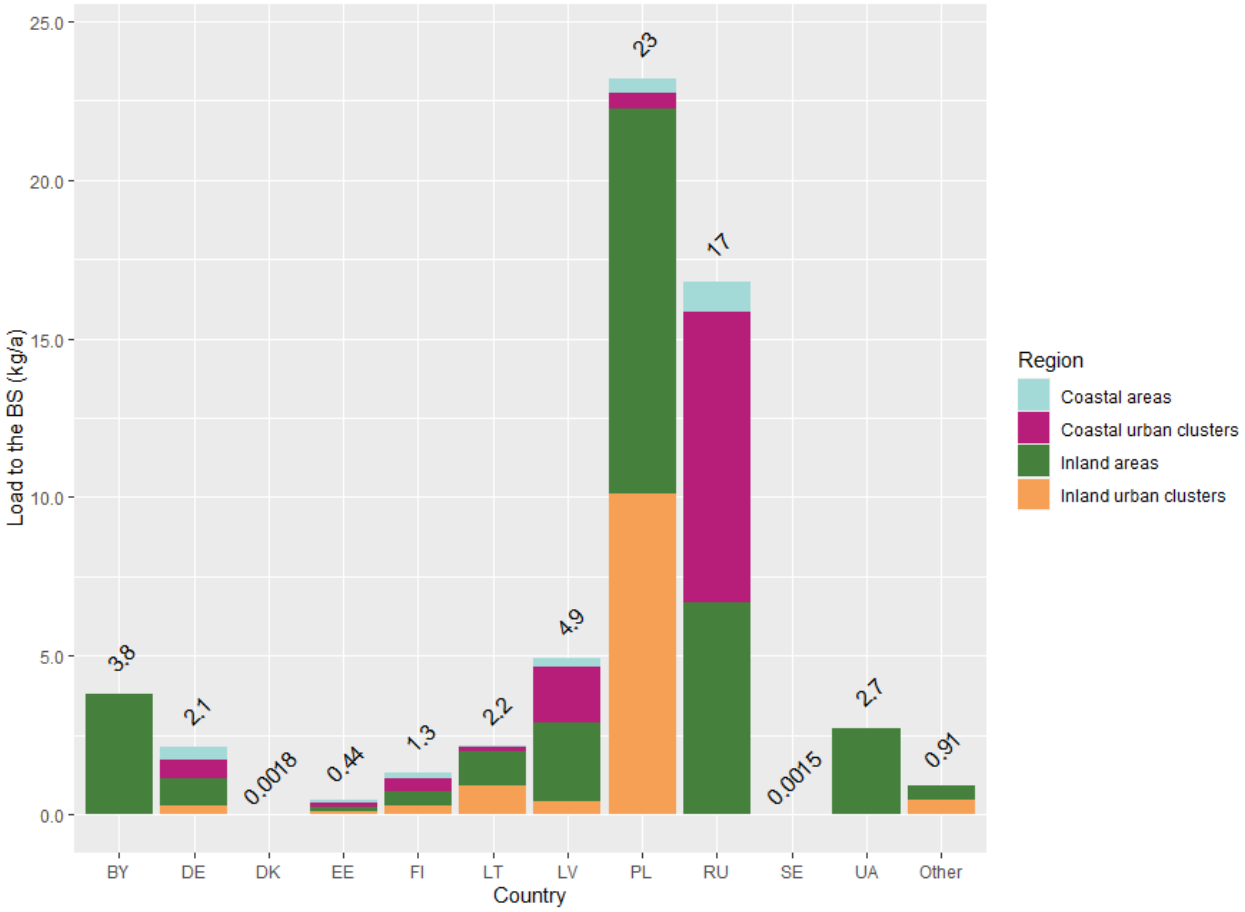

Figure 40. Ofloxacin loads reaching the Baltic Sea from each country and region class, estimated according to scenario 1.

The majority of OFL emitted into water environment was estimated to originate from usage within sewer network coverage (Figure 41). However, circa 37% was estimated to originate from areas outside sewer network coverage. Improper management of pharmaceutical waste was estimated to account for circa 3.5% of the load in untreated wastewaters.

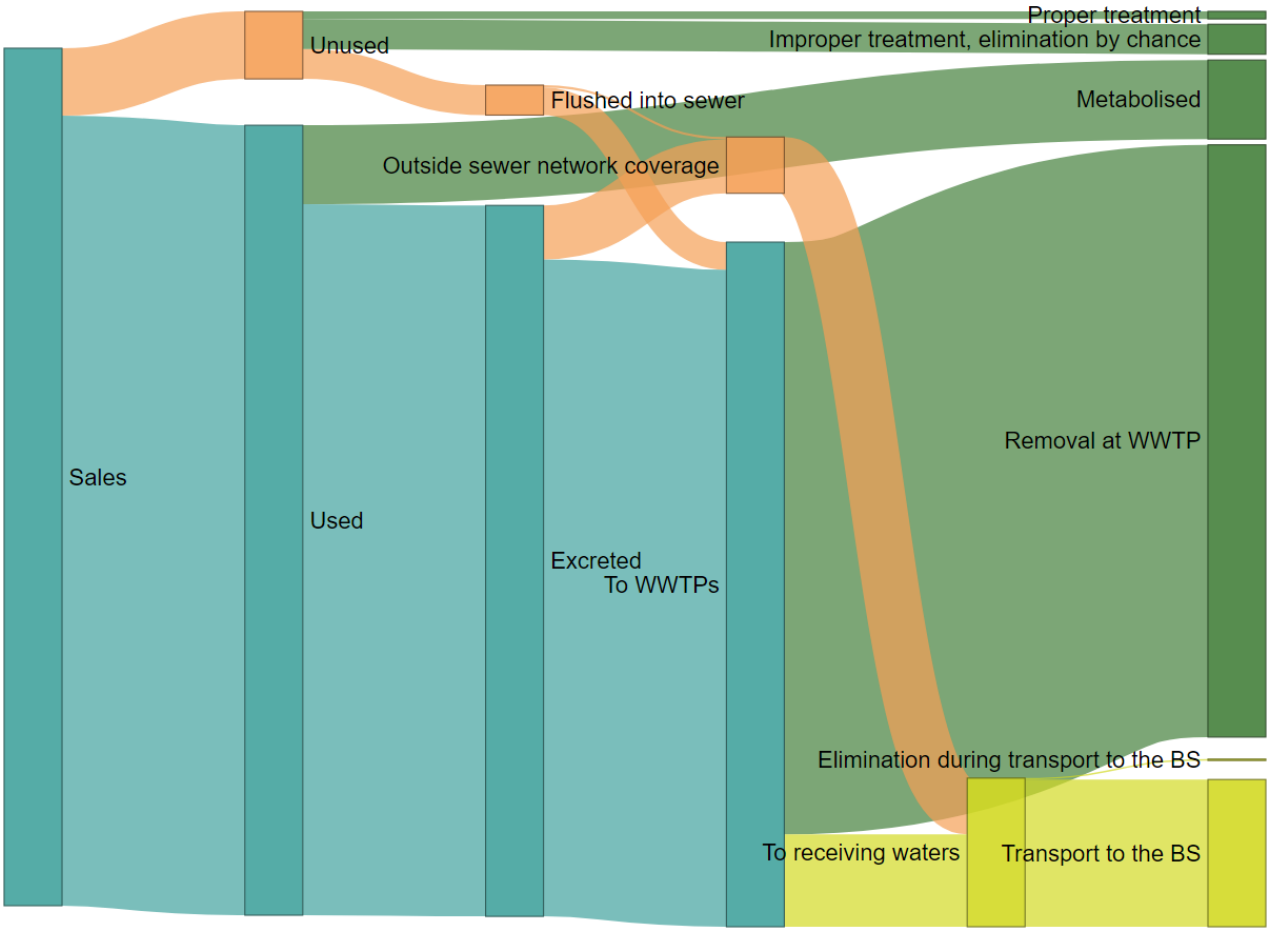

Figure 41. Ofloxacin flows according to scenario 1. Green boxes present end-points/processes, where the load is destroyed before reaching the environment. Orange boxes present suboptimal management practices, while yellow boxes present emissions into the water environment.

The estimated emissions from each grid cell are presented in Figure 42. The per capita load to be Baltic Sea varied between countries from 0.16 µg/person/a in Sweden and 0.37 µg/person/a in Denmark to circa 2.0 mg/person/a in Ukraine and 2.4 mg/person/a in Latvia. The relatively high emissions from Latvia are in line with consumption information (see Table 2). However, Ukrainian emissions are very uncertain due to no sales statistics being compiled for Ukraine. A population weighted average per capita consumption (0.013 mg/person/d) was used for Ukraine. However, the estimated high emissions from Ukraine reflect the relatively low level of sewer network coverage. As over 85% of OFL is removed in WWTPs, but removal in the environment is slow, the level of sewer network coverage has a direct impact on overall load to the Baltic Sea.

When looking at regional emissions the highest per capita loads to the Baltic Sea (2.4 mg/person/a) were estimated to originate from coastal regions in Latvia (see Figure 43). Areas with the lowest per capita emissions were located in Sweden.

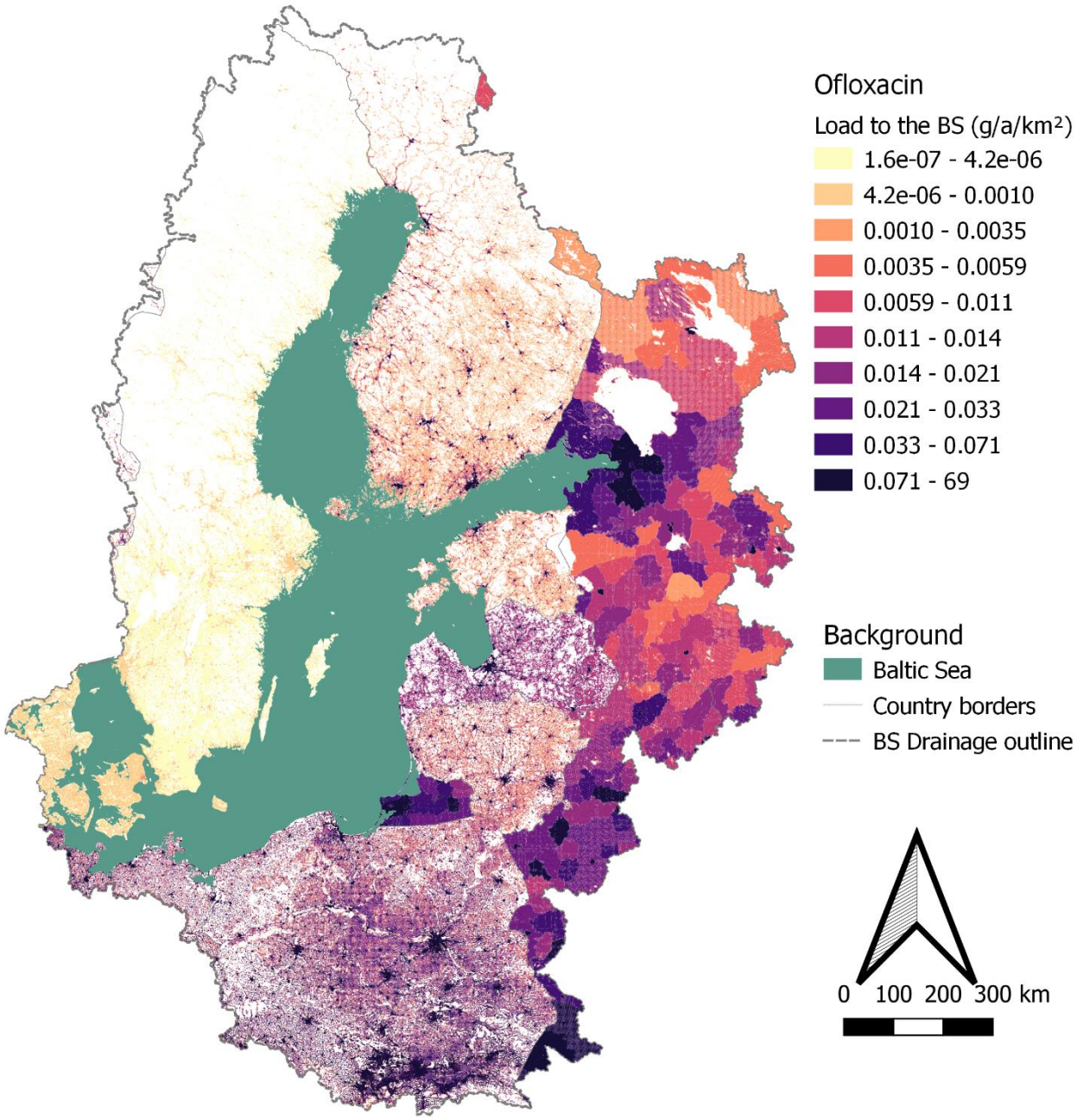

Figure 42. Ofloxacin load (g/a/km²) reaching the Baltic Sea, originating from individual grid cells.

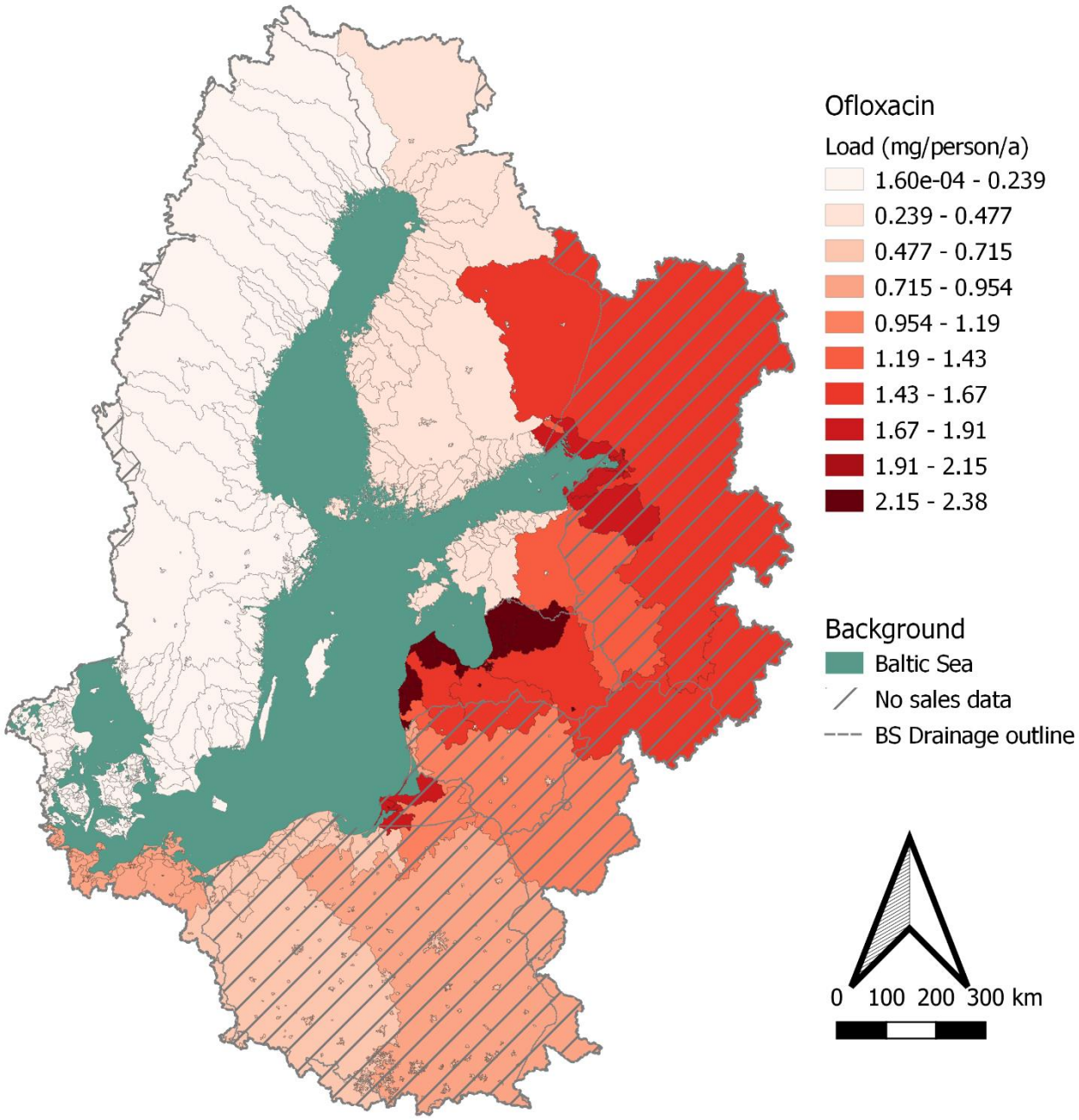

Figure 43. Mean per capita ofloxacin load reaching the Baltic Sea, aggregated by calculation areas. The dashed area shows the countries for which no national sales data was available, but a population weighted average value was used.

Figure 44 presents the ten coastal cities with the highest OFL loads to the Baltic Sea. The highest load to the Baltic Sea was estimated to originate from St. Petersburg. It is noteworthy, that the OFL load estimated to originate from St. Petersburg accounts for roughly 49% of the total load originating from Russia. However, the absolute load from Russia, and its relation to emissions from other countries is very uncertain, due to no sales statistics being available.

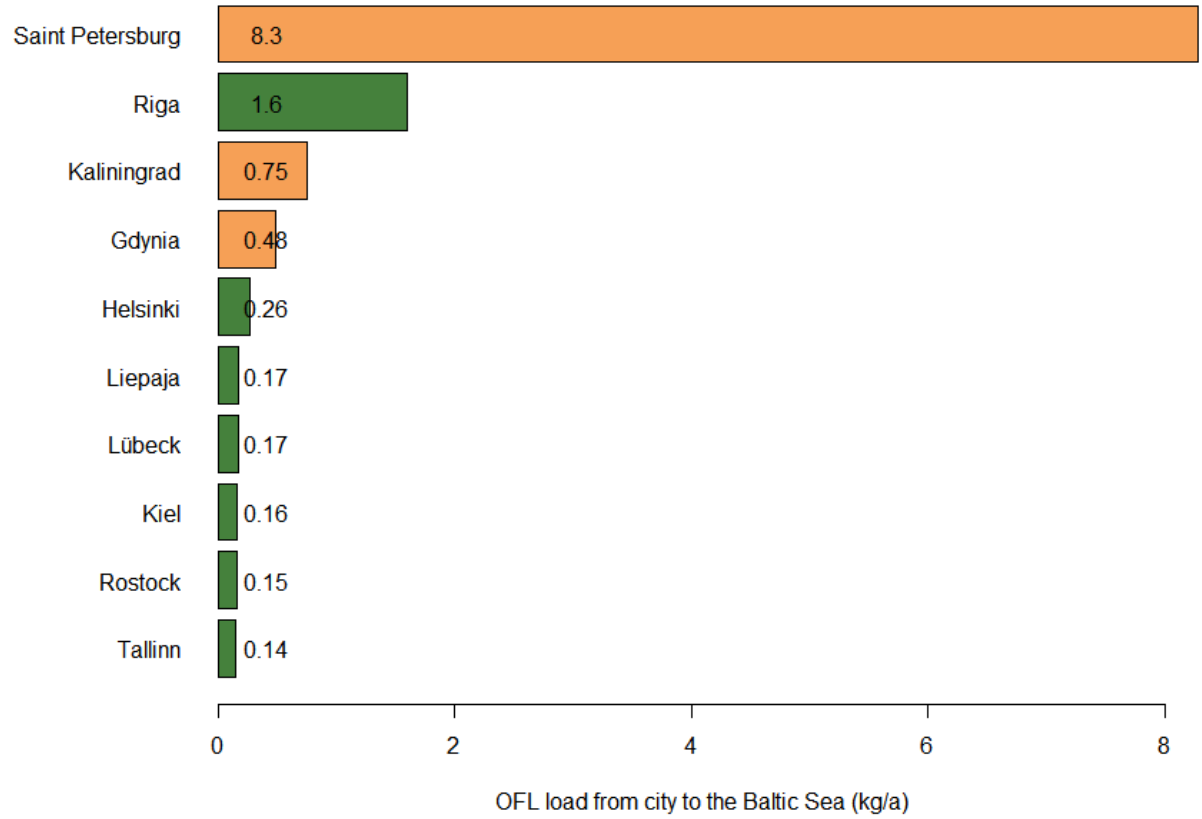

Figure 44. Ten coastal urban clusters with the highest ofloxacin emission reaching the Baltic Sea. The green bars present the cities in countries with sales statistics available, while orange bars represent cities in countries where an average per capita sales value was used. The numerical value presents the calculated load in kilograms, using two significant numbers.

The highest OFL load was estimated to be emitted to the coasts off the cities of Gdansk and St. Petersburg, 170 kg/a and 140 kg/a, respectively. However, as these estimates are highly dependent on the sales data, which we do not have for Poland or Russia, the loads should be further investigated. To produce more elaborate estimates, better sales statistics would be required. When looking at loads to coastal areas in countries where sales statistics were collected, the highest load was estimated to be received in the Gulf of Riga (58 kg/a).

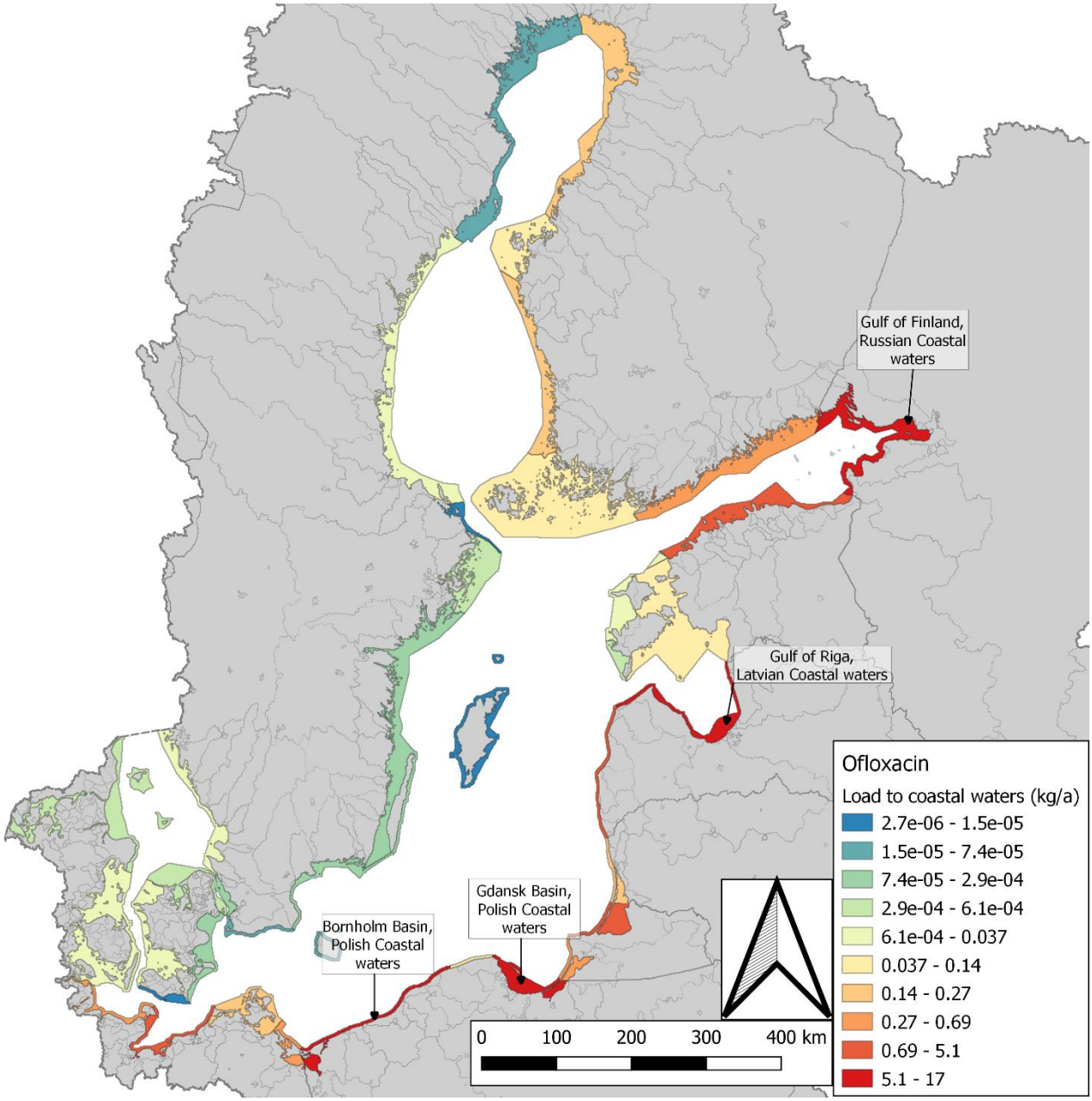

Figure 45. Ofloxacin load (kg/a) reaching the coastal waters in different parts of the Baltic Sea.

3.2.7. Tramadol

The annual total TRD sales within the Baltic Sea catchment area were estimated to be 30 tonnes. The load estimated to be emitted to waters receiving sewage, was 3.6 tonnes. Load reaching the Baltic Sea was estimated to range from 2.9 to 3.3 tonnes, with emission from Poland accounting for 42-45% of this mass. Coastal cities (i.e. coastal urban clusters) were estimated to account for 23% of the total load reaching the Baltic Sea. According to the calculations, 63-67% of TRD loads originate from inland areas. National emissions are presented in Figure 46.

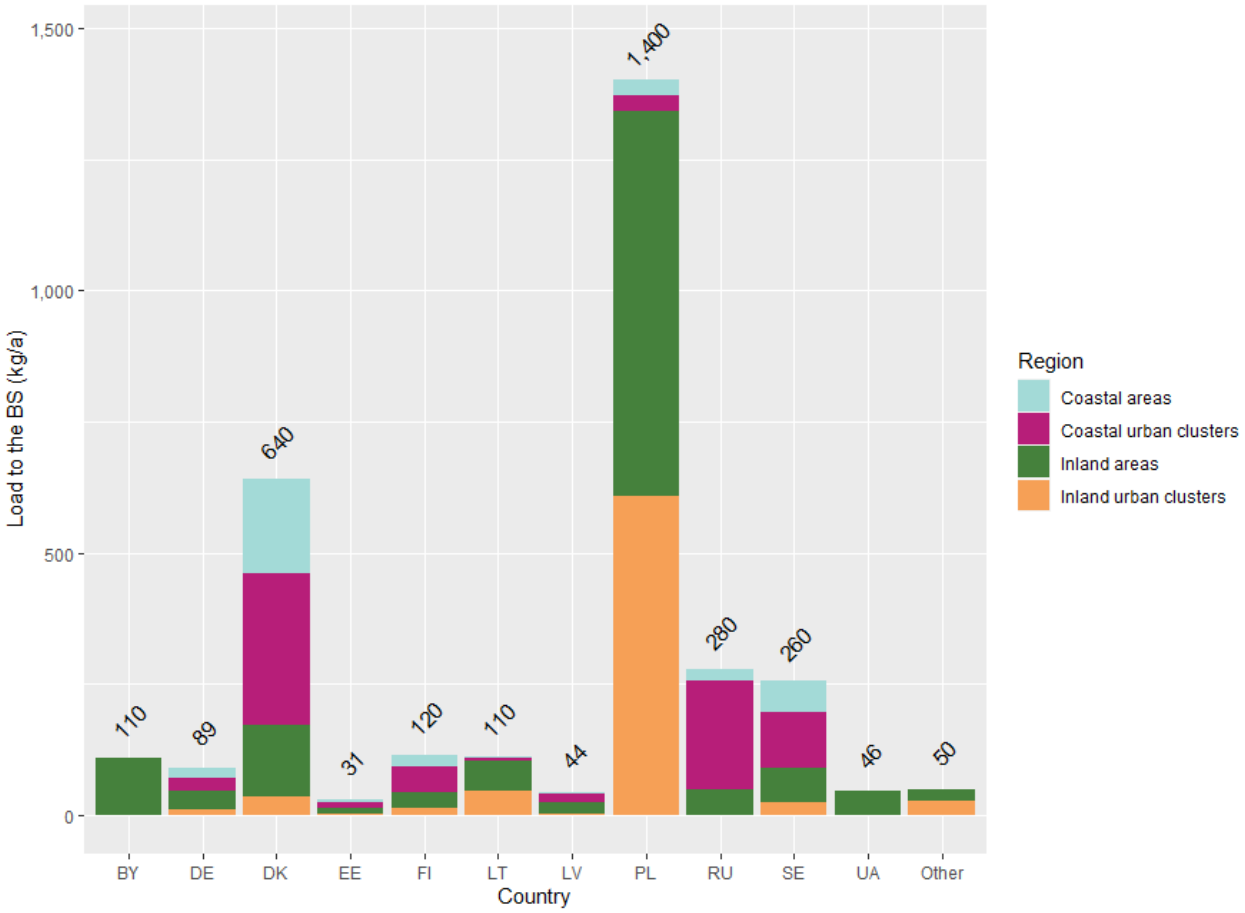

Figure 46. Tramadol loads reaching the Baltic Sea from each country and region, estimated according to scenario 1.

TRD emissions were estimated to originate to a large extent from the usage and excretion of the API (Figure 47). Circa 24% of the load to wastewaters was estimated to originate from improper management of unused pharmaceuticals. Due to the poor removal at conventional WWTPs (3.1%, see Table 6), a vast majority of the load in influent wastewaters was estimated to reach the water environment. Thus, emissions outside sewer network coverage accounted only for a small fraction (circa 6%).

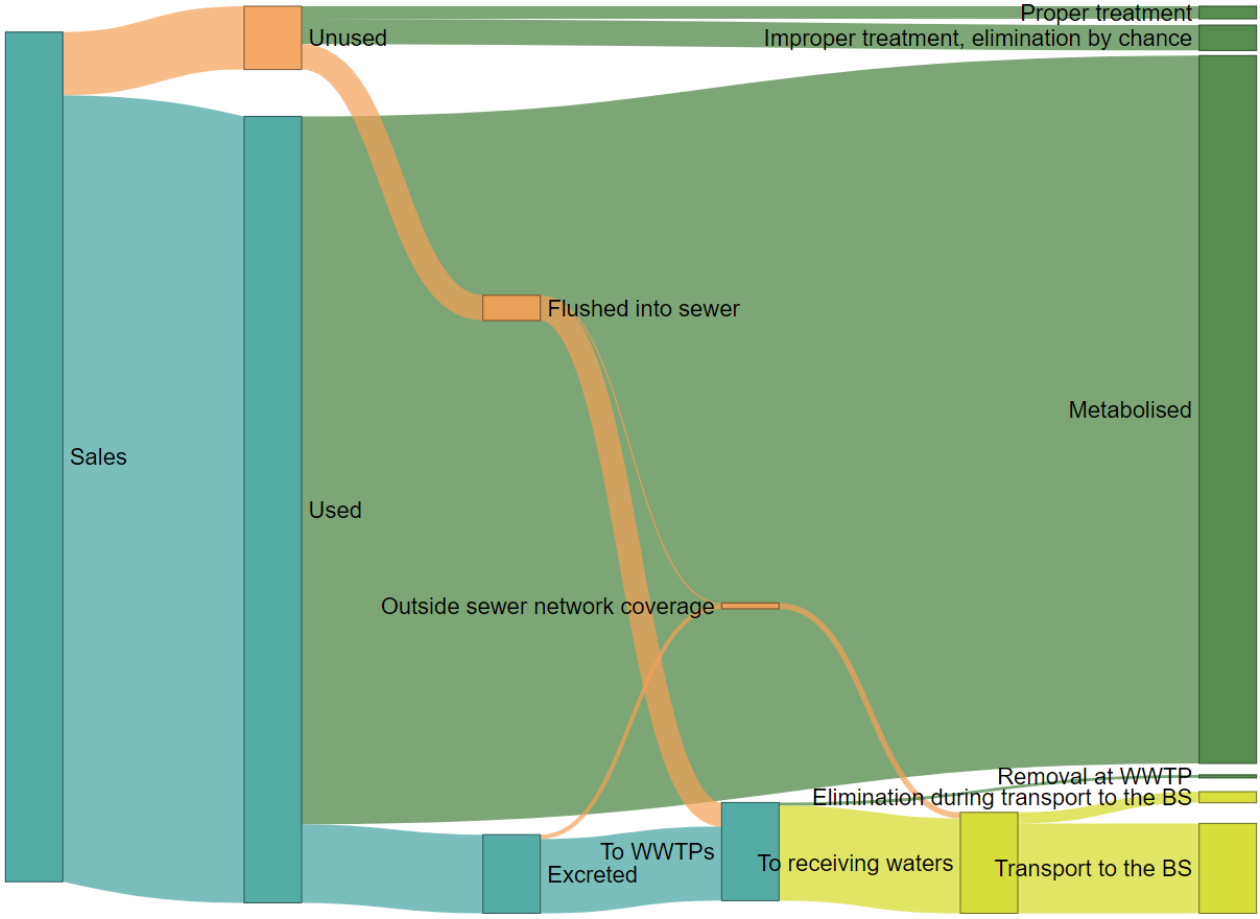

Figure 47. Tramadol flows according to scenario 1. Green boxes present end-points/processes, where the load is destroyed before reaching the environment. Orange boxes present suboptimal management practices, while yellow boxes present emissions into the water environment.

The national per capita emission reaching the Baltic Sea from coastal countries ranged from 21 mg/a in Latvia, to 130 mg/a in Denmark. The Danish per capita emission is roughly 3.6 times higher than the second highest per capita emission (Lithuania, 37 mg/a). The relatively high emissions are in line with the high per capita consumption in Denmark, presented in Table 2.

The grid cell-specific emissions are presented in Figure 48 and calculation area-specific per capita loads are presented in Figure 49. The emissions were estimated to be much lower in areas, that flow through big lakes. These areas include e.g. Central Finland, Russian areas flowing though the lake Ladoga, and Swedish areas flowing though the lakes Vänern and Vättern. The highest regional per capita loads were estimated to be emitted from coastal areas in Denmark, circa 130 mg/a/person.

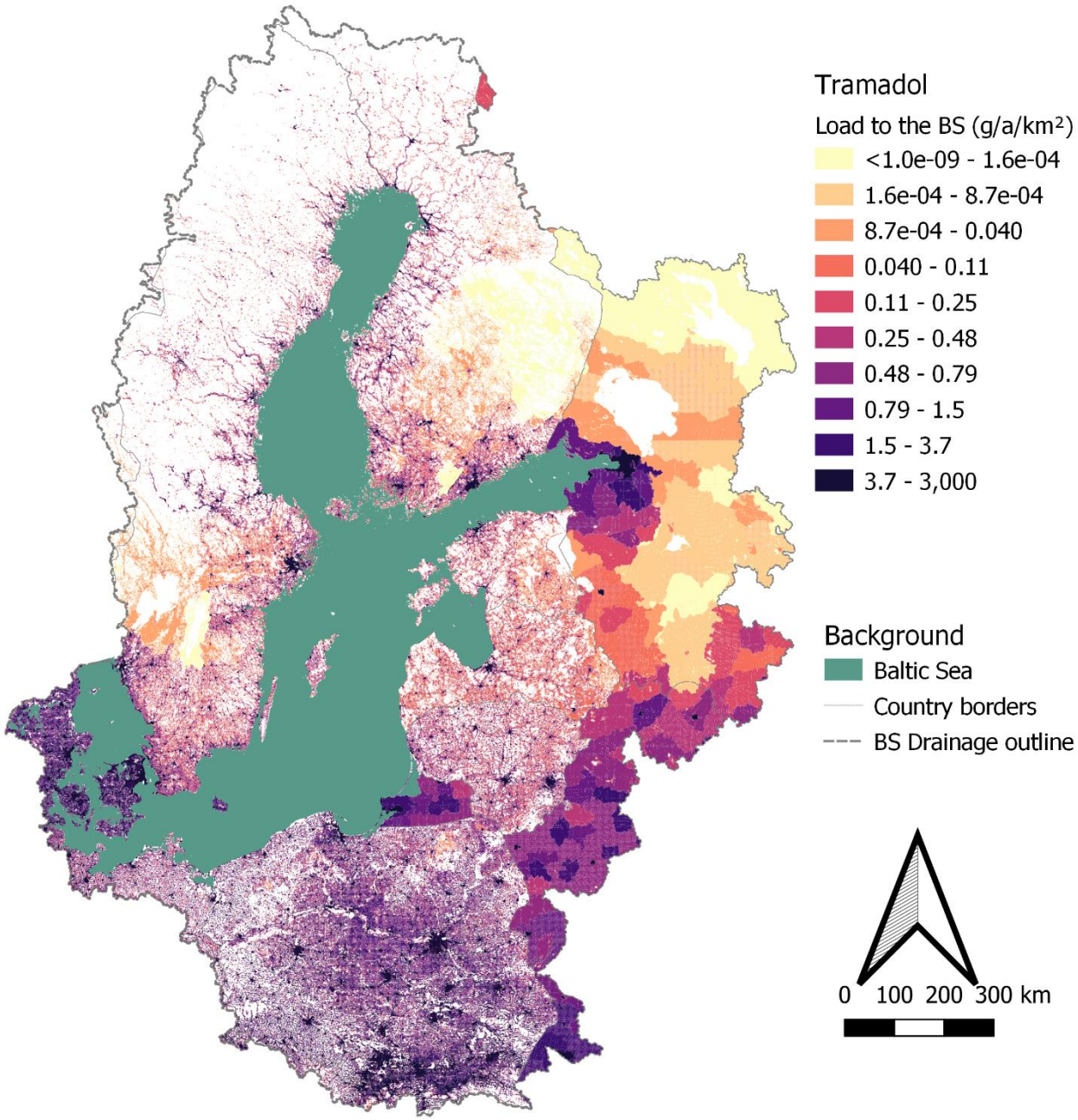

Figure 48. Tramadol load (g/a/km²) reaching the Baltic Sea, originating from individual grid cells.

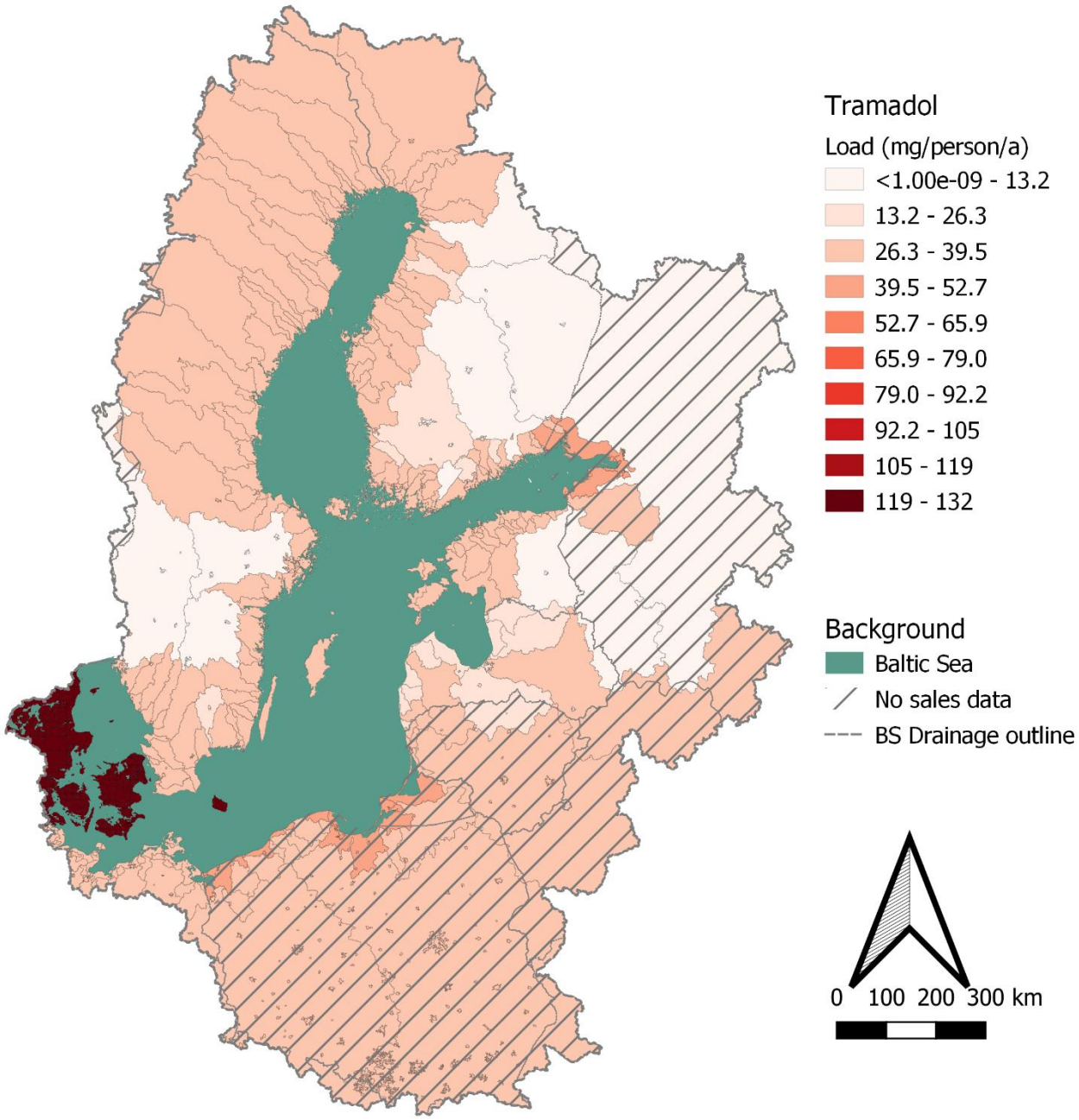

Figure 49. Mean per capita tramadol load reaching the Baltic Sea, aggregated by calculation areas. The dashed area shows the countries for which no national sales data was available, but a population weighted average value was used.

The highest load originating from individual cities was estimated to come from Copenhagen, followed closely by emissions from St. Petersburg. The mass of sales was estimated to be 1,600 kg in Copenhagen, and 1,500 kg in St. Petersburg. Due to a large difference in per capita sales, the emissions from e.g. St. Petersburg were much lower than those from Copenhagen.

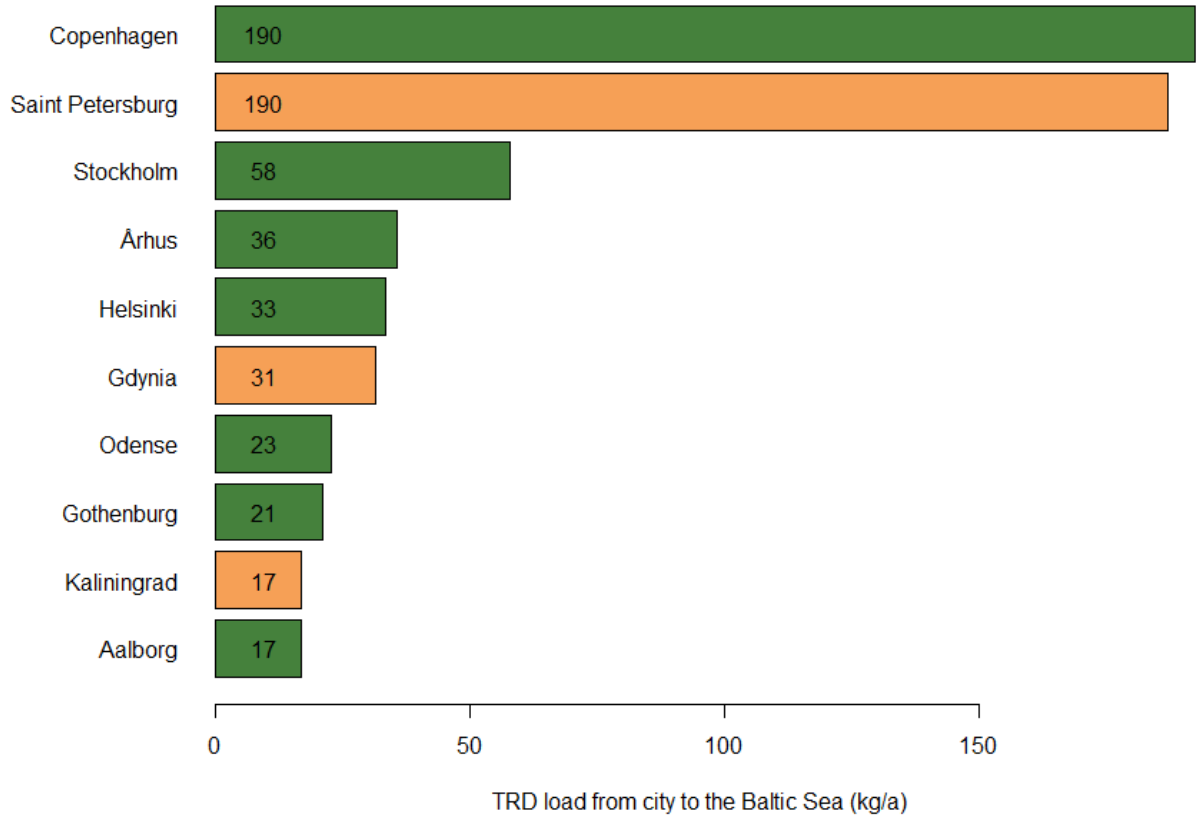

Figure 50. Ten coastal urban clusters with the highest tramadol emission reaching the Baltic Sea. The green bars present the cities in countries with sales statistics available, while orange bars represent cities in countries where an average per capita sales value was used. The numerical value presents the calculated load in kilograms, using two significant numbers.

Despite the largest per capita emissions, and highest city-specific emissions being emitted in Denmark, the coastal areas receiving the highest TRD loads were estimated to be located in Poland. The estimates of the load reaching the coastal waters in the Gdansk basin ranged from 770 to 940 kg/a, using scenarios 2 and 3, respectively. This high load is well in line with the high number of people (25 million), whose emissions flow into that coastal area. For comparison, the emissions reaching the coastal areas outside the city of Copenhagen were estimated to be 400 kg/a, while these emissions were generated by 3.1 million people.

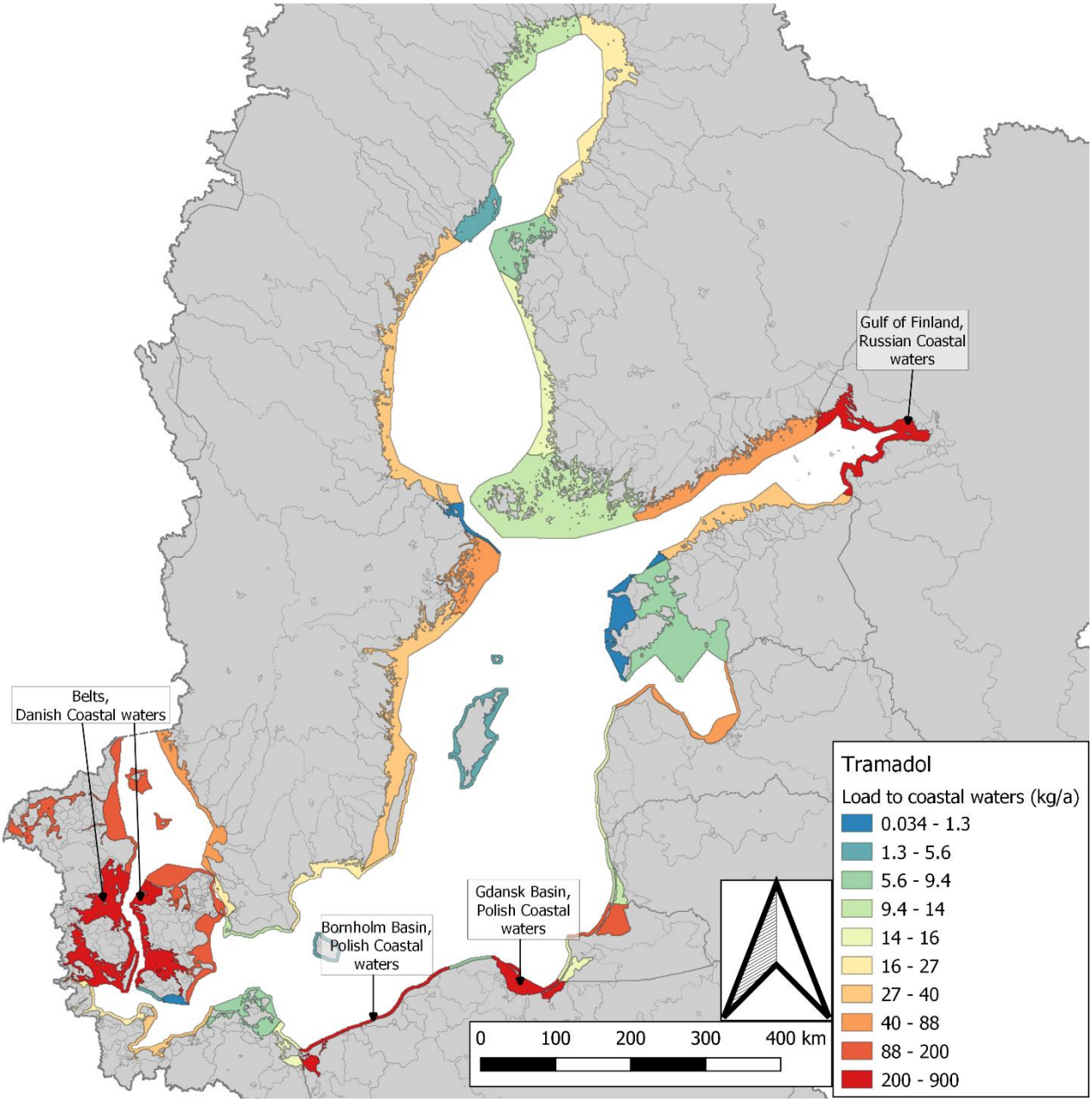

Figure 51. Tramadol load (kg/a) reaching the coastal waters in different parts of the Baltic Sea.

3.2.8. Venlafaxine

The total annual sales of VFX were estimated to be 23 tonnes. However, due to no national information being available from Poland, Lithuania and Russia, the estimate is uncertain. The national per capita sales range from 0.08 mg/d/person in Latvia to 1.1 mg/d/person in Denmark, resulting in an overall population weighted average of 0.70 mg/d/person. If minimum national sales were assumed to be applicable for the countries with no sales data, the total sales in the BSR would decrease to 9.8 tonnes/a. Similarly, assuming the maximum national sales would be applicable for the countries with no sales data, the total sales would reach 32 tonnes/a.

The load reaching the recipient waters was estimated to reach 1.4 tonnes/a, using the average sales value when no data was available. The load would range from 520 kg to 2,000 kg/a, using the assumptions presented above. The load reaching the Baltic Sea was estimated to range from 1,100 kg to 1,200 kg/a, using scenarios 2 and 3, respectively. The national loads to the Baltic Sea are presented in Figure 52. Poland accounted for circa 50% of the total load reaching the Baltic Sea. However, if we assume that the Latvian low sales best reflect the sales in Poland, the total load reaching the Baltic Sea would be 440 kg. In this case, the emissions from Poland would decrease to 67 kg, resulting in Denmark being the country with the highest national emissions to the Baltic Sea.

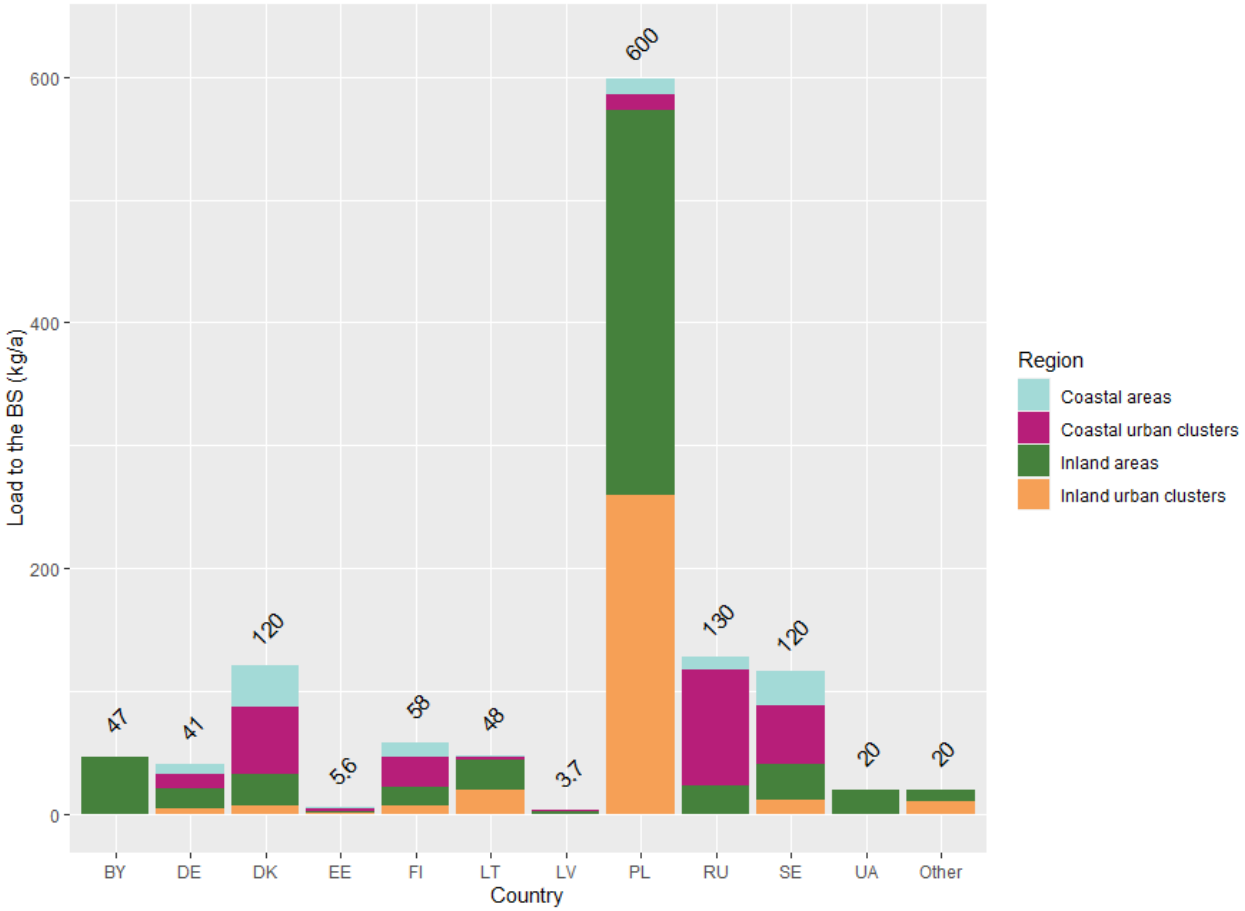

Figure 52. Venlafaxine loads reaching the Baltic Sea from each country and region, estimated according to scenario 1.

As the population weighted average per capita sales value is considered the best estimate, when no national data is available, further discussion will concentrate on results obtained using that value. VFX was estimated to originate mainly from consumption of the API (Figure 53). However, flushing unused pharmaceutical into the sewer was estimated to account for circa 38% of the load in influent wastewaters.

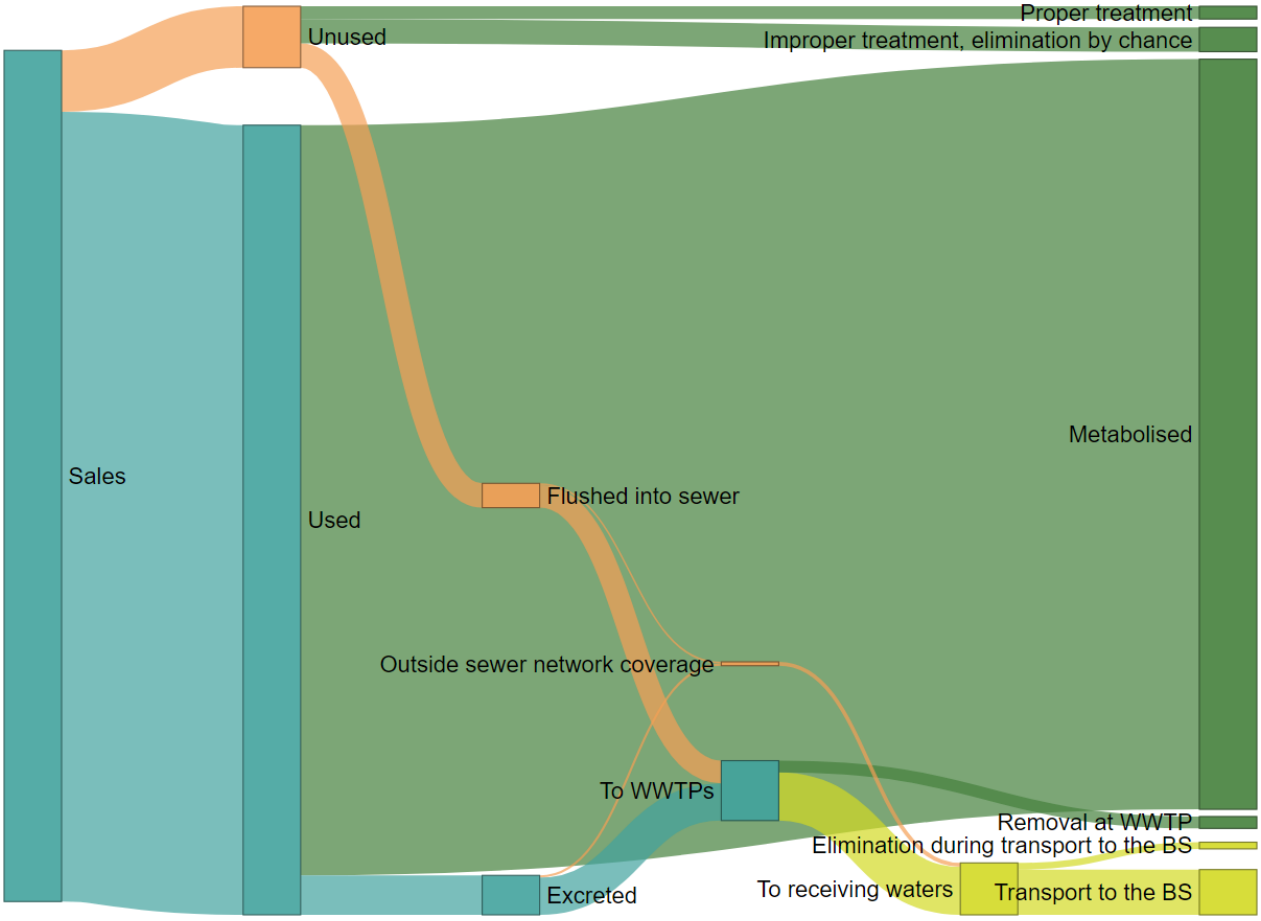

Figure 53. Venlafaxine flows according to scenario 1. Green boxes present end-points/processes, where the load is destroyed before reaching the environment. Orange boxes present suboptimal management practices, while yellow boxes present emissions into the water environment.

The total estimated VFX loads reaching the Baltic Sea from each grid cell are presented in Figure 54, and calculation area-specific per capita emissions are presented in Figure 55. The national per capita load reaching the Baltic Sea ranged from 1.8 mg/a in Latvia to 25 mg/a in Denmark. Highest regional per capita emissions were estimated to originate from coastal Denmark.

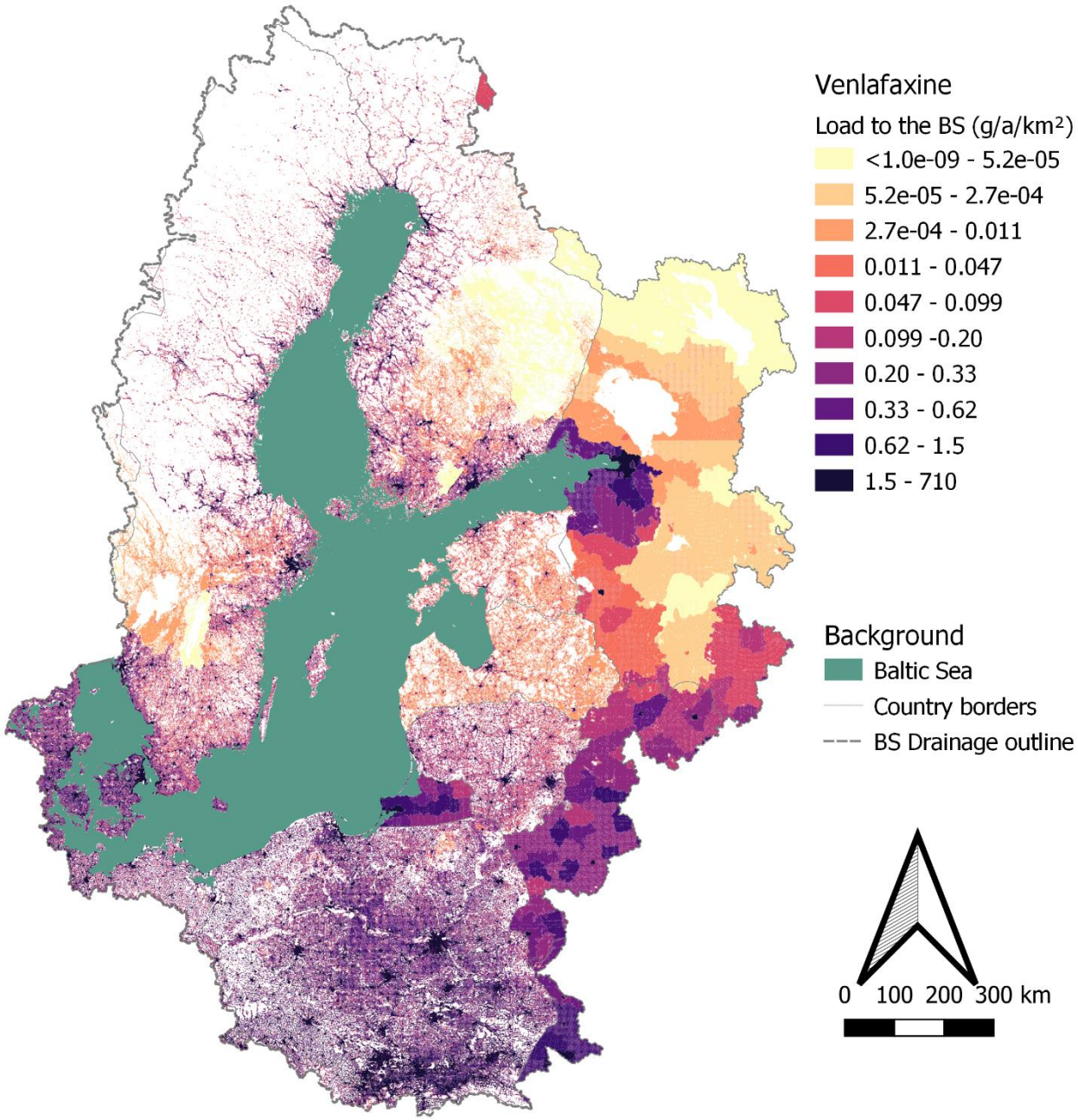

Figure 54. Venlafaxine load (g/a/km²) reaching the Baltic Sea, originating from individual grid cells.

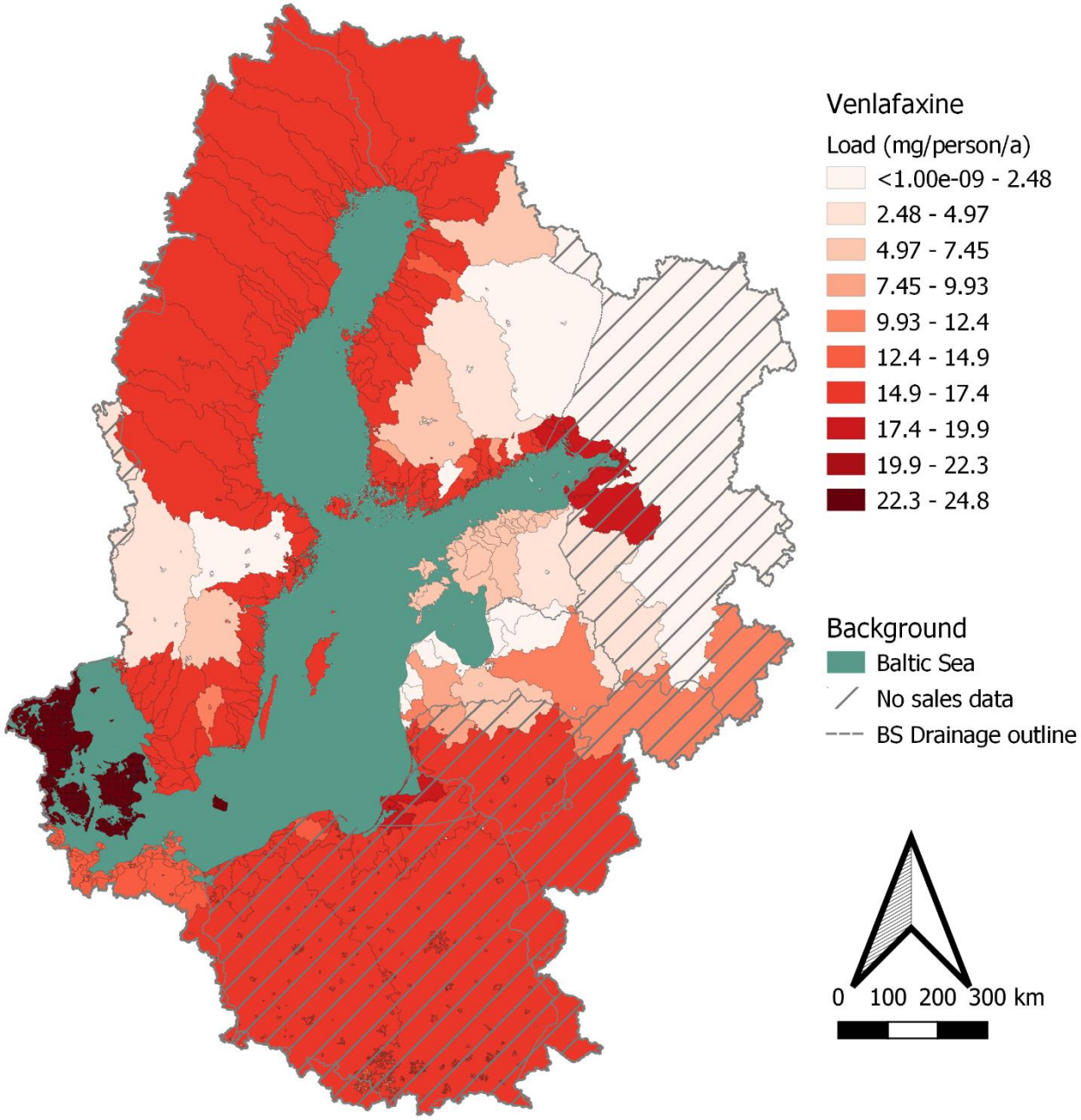

Figure 55. Mean per capita venlafaxine load reaching the Baltic Sea, aggregated by calculation areas. The dashed area shows the countries for which no national sales data was available, but a population weighted average value was used.

Loads from individual cities are presented in Figure 56. The highest load originating from individual cities was estimated to come from St. Petersburg. However, the loads from Copenhagen, Stockholm and Helsinki, where national sales statistics were available, were estimated to be relatively high as well.

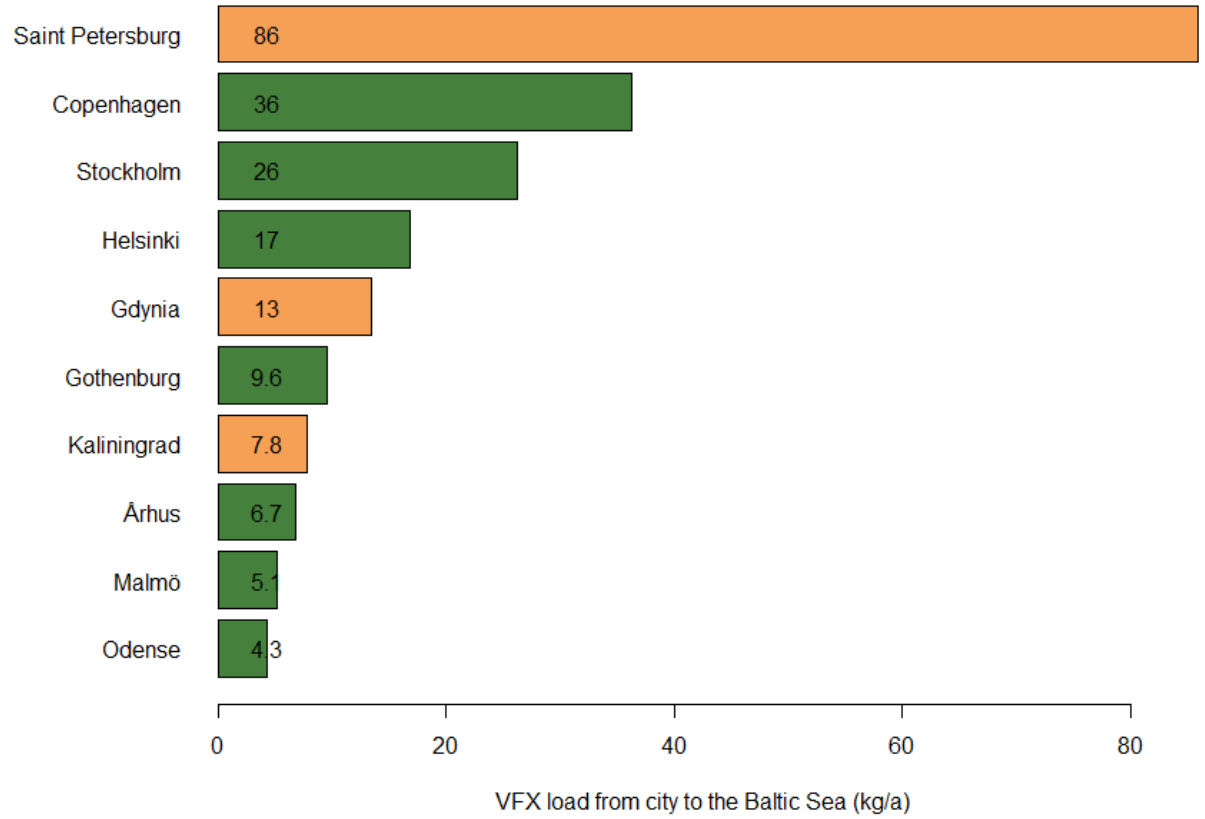

Figure 56. Ten coastal urban clusters with the highest venlafaxine emission reaching the Baltic Sea. The green bars present the cities in countries with sales statistics available, while orange bars represent cities in countries where an average per capita sales value was used. The numerical value presents the calculated load in kilograms, using two significant numbers.

The loads to coastal waters in different parts of the Baltic Sea are presented in Figure 57. The coastal areas estimated to receive the highest loads were located in Poland and Russia. The Polish coastal waters in Gdansk and Bornholm basins, and Russian coastal waters in eastern Gulf of Finland were the only coastal waters receiving more than 100 kg VFX annually. Outside Russia and Poland, the coastal area with highest incoming load was located in Denmark (The Belts). The strait between Zealand and Funen was estimated to receive an annual load of 43 kg of VFX.

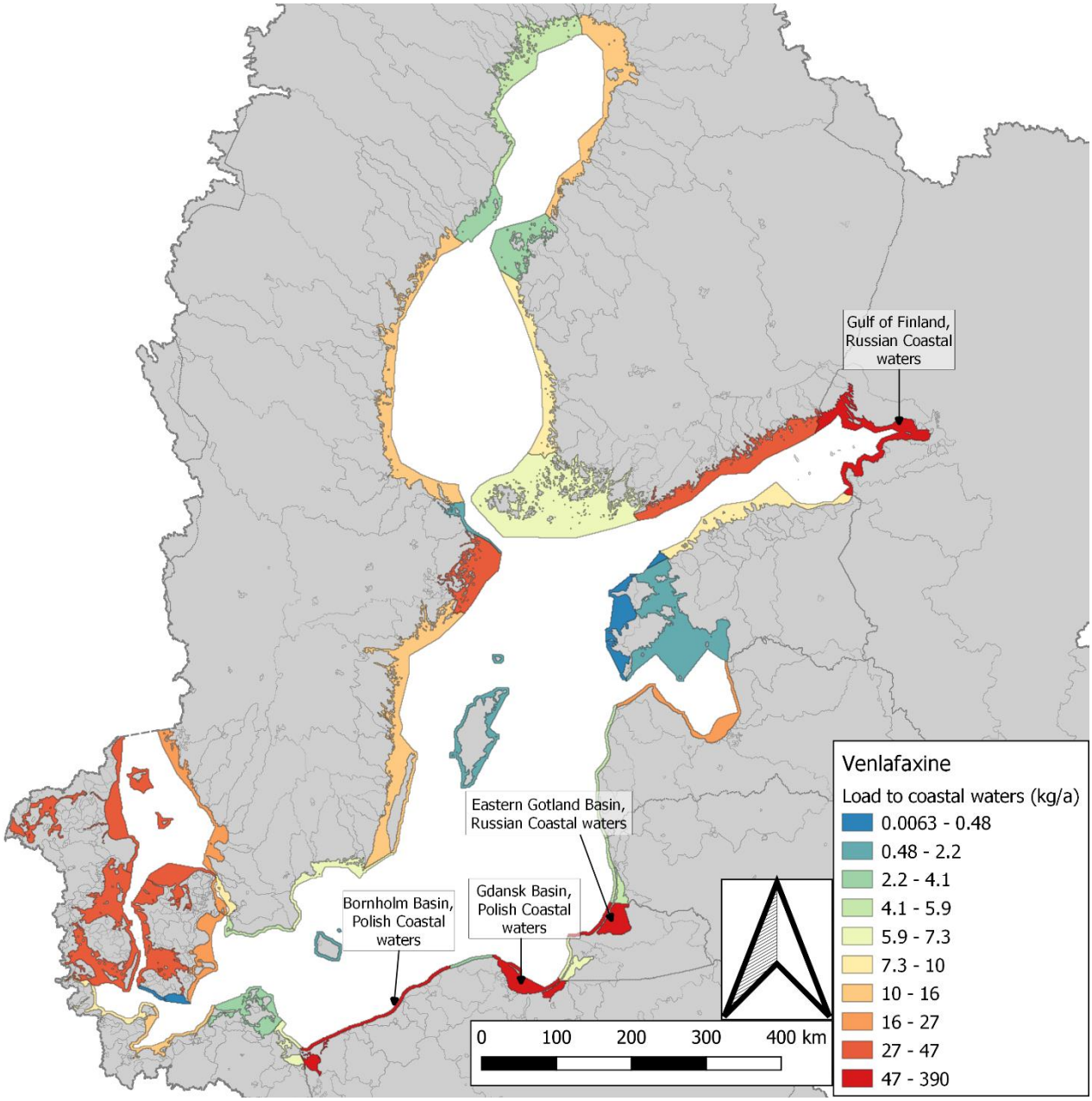

Figure 57. Venlafaxine load (kg/a) reaching the coastal waters in different parts of the Baltic Sea.

3.2.9. Summary of loads to the Baltic Sea

The national loads to the BS were estimated to be highest from Poland for DCF, CBZ, TRD, CLM, OFL and VFX. Similarly highest emissions were estimated to occur from Russia for MTF and IBU. However, there was more variation in the national per capita loads for each API (see Table 8). The highest per capita emissions were estimated to occur from Denmark for TRD and VFX, from Estonia for DCF and CLM, from Latvia for OFL and from Russia for IBU and MTF. Per capita emissions for CBZ were estimated to similar in Latvia and Poland, and only slightly lower in Estonia.

Table 8. National per capita loads to the BS from each BS coastal country.

Country	Population within the BSR[a)]	Per capita emission reaching the Baltic Sea (mg/a/person)							
		CBZ	**CLM**	**DCF**	**IBU**	**MTF**	**OFL**	**TRD**	**VFX**
DE	2 945 092	22	29	180	9.2	220	0.72	30	14
DK	4 879 992	16	18	89	25	180	3.7e-04	130	25
EE	1 290 739	39	68	540	20	200	0.34	24	4.4
FI	5 313 289	18	8.2	180	15	310	0.24	22	11
LT	3 026 584	11	15	140	7.0	380	0.71	37	16
LV	2 079 911	41	52	520	53	1,200	2.4	21	1.8
PL	38 431 200	41	50	110	0.52	200	0.60	36	16
RU	9 443 010	32	37	58	58	5,800	1.8	30	14
SE	9 349 371	18	13	120	8.8	130	1.6e-04	28	12

a) Population aggregated from the calculation grid. The data used in the grid (Eurostat 2016b) refers to year 2011.

The API with the highest variation in country-specific per capita emissions was MTF. However, the highest MTF emissions were estimated to originate from Russia, where no sales statistics were available. On the other hand, relatively high per capita emissions of TRD were estimated to originate from Denmark. A similar difference is present in the national consumption statistics (Table 2).

The coastal waters with highest API loading were estimated to be on the northern coast of Poland (Gdansk basin and Bornholm basin). For instance, the DCF load to Polish coastal waters in the Gdansk basin ranged from 2,300 kg/a to 2,800 kg/a, using scenarios 2 and 3, respectively. On the other hand, the MTF load to the Russian coastal waters in the Gulf of Finland was several times higher than the loads to any other coastal area within the BSR. The coastal waters with the highest relative API loads are presented in Figure 58 and Table 9.

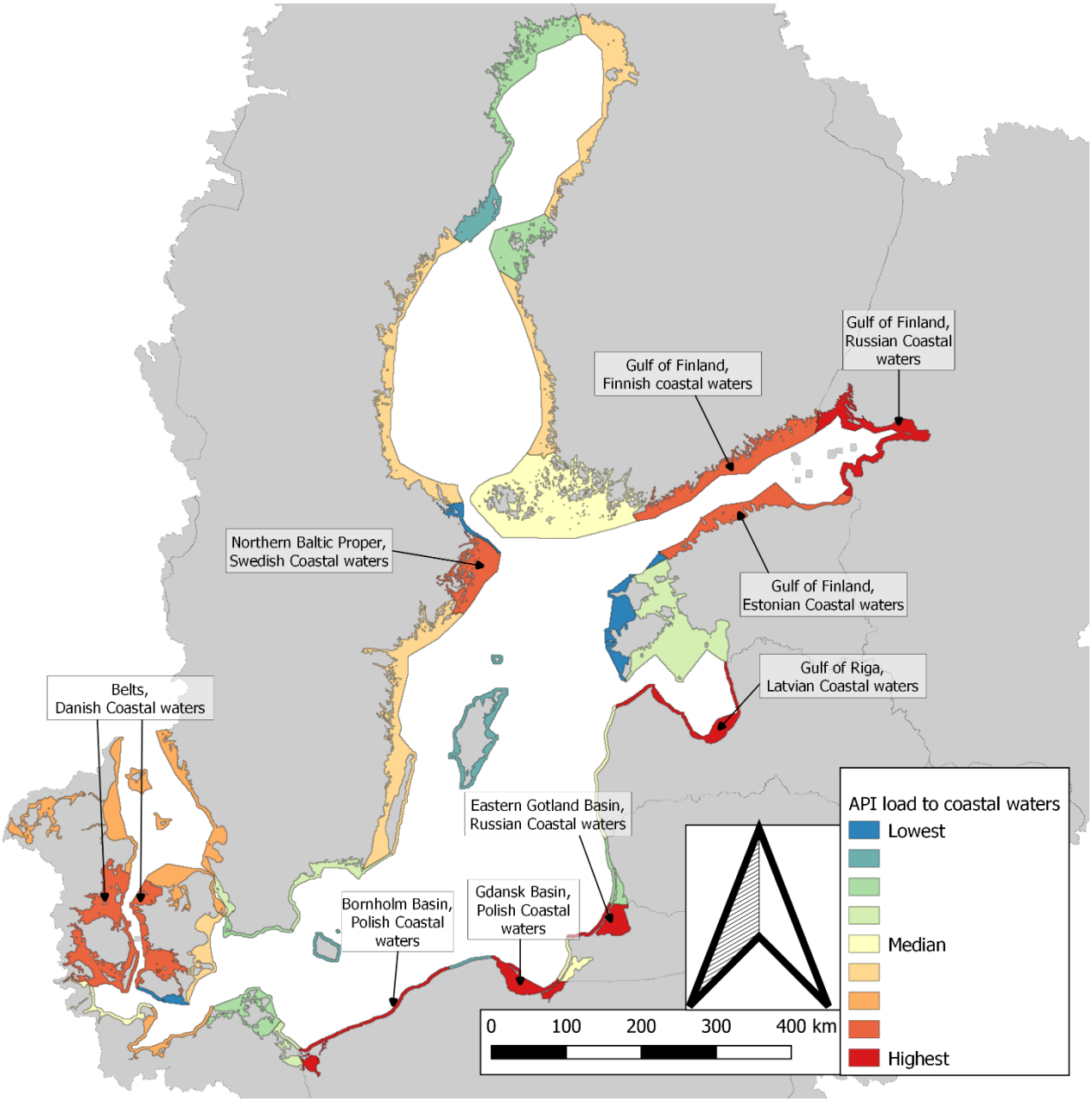

Figure 58. Coastal waters with the highest API loads relative to loads to other coastal waters (averaged over APIs and scenarios).

Table 9. Estimated API loads to coastal waters in different parts of the BSR receiving the highest API loading.

Coastal area	scn[a)]	Load to coastal waters [kg/a]							
		CBZ	CLM	DCF	IBU	MTF	OFL	TRD	VFX
Gdansk Basin, PL Coastal waters	1–3	989–993	1,200–1,230	2,340–2,850	70.3–121	15,200–15,800	16.8–17.5	770–943	326–404
	-1	17,500	5,500	5,260	14,300	441,000	123	7,920	6,350
Bornholm Basin, PL Coastal waters	1–3	645–647	781–801	1,620–1,940	18.5–26.7	3,270–3,380	9.79–10.2	519–625	220–267
	-1	11,500	3,600	3,570	12,400	295,000	82.1	5,240	4,220
Gulf of Finland, RU Coastal waters	1–3	258–262	299–303	451–457	451–457	45,900–46,600	14.1–14.3	228–231	105–106
	-1	4,510	1,210	1,360	51,000	163,000	40.1	2,710	2,240
Eastern Gotland Basin, RU Coastal waters	1–3	115	143–146	554–639	95.6–119	9,150–9,360	4.86–5.03	167–193	71.4–82.8
	-1	2,120	635	1,170	15,300	75,000	25.4	1,640	1,320
Gulf of Riga, LV Coastal waters	1–3	108	135–137	1,020–1,130	119–146	5,870–6,030	5.75–5.9	75.9–89.9	19.9–25.1
	-1	1,940	595	2090	24300	50,000	31	776	411
Gulf of Finland, FI coastal waters	1–3	39.2–39.5	18.2–18.4	436–450	37.7–38.5	698–706	0.542–0.549	54.6–56.1	27.4–28.2
	-1	1,250	87.9	1000	49,600	60,900	4.39	703	800
Gulf of Finland, EE Coastal waters	1–3	56.3–57.1	88.8–90.5	502–593	24.3–30.6	2,780–2,890	1.23–1.27	25.4–34.7	5.49–8.69
	-1	1,090	406	1310	14,700	27,100	5.74	407	208
Belts, DK Coastal waters	1–3	27.6	30.9	153–154	43.5–43.7	317–318	6.0e-04	228–229	42.9–43.1
	-1	555	143	277	19,300	27,900	0.00517	1950	717
Northern Baltic Proper, SE Coastal waters	1–3	50.8–51.6	37.8–38.5	285–334	20.6–21.4	381–387	5.0e-04	63.1–73.2	28.4–32.7
	-1	1,650	185	827	34,300	33,800	0.00382	1030	1,050
Kattegat, DK Coastal waters	1–3	24.3	27.3	134–136	38.1–38.5	280	6.0e-04	199–202	37.5–38
	-1	490	126	245	17,100	24,700	0.00457	1720	633
Kattegat, SE Coastal waters	1–3	41.7–42.3	31.3–31.8	264–273	19.4–19.8	378–386	0.02	58.9–60.5	26.5–27.3
	-1	1,350	153	675	27,900	27,700	0.0828	839	854
The Sound, DK Coastal waters	1–3	135	15.1	75.5	21.4	155	3.0e-04	112	21.1–21.1
	-1	272	69.8	136	9,460	13,700	0.00253	956	351
Mecklenburg Bight, DE Coastal waters	1–3	24	31.4–31.5	194–197	10–10.1	242	0.779–0.781	32.7–33.1	14.9–15.1
	-1	483	145	354	4,480	21,300	6.35	283	251
Bothnian Bay, FI Coastal waters	1–3	15.4–15.5	7.5–7.57	186–198	16.1–17	302–307	0.212–0.215	23.9–25.5	11.9–12.7
	-1	487	35.9	382	18,700	23,000	1.65	275	310
Bothnian Sea, FI Coastal waters	1–3	16.7–17.1	7.72–7.96	92.9–135	7.68–8.75	295–304	0.229–0.237	11.5–16.4	5.77–8.1
	-1	540	37.9	433	21,400	26,300	1.89	303	345

a) The load estimated with the total residue approach (scn -1) is equal to the estimated consumption in the area discharging to each coastal area.

The simulated API-specific end-points presented in figures 11, 17, 23, 29, 35, 41, 47 and 53, are summarized in Table 10 as fractions of the total sales within the BSR. Degradation during transport to the BS was most important for DCF. However, DCF was also estimated to be the API with the highest fraction of sales reaching the BS.

The most relevant removal processes from ingestion of API to reaching the BS were estimated to be metabolism and removal in WWTPs. Elimination during transport had a minor impact on the selected APIs.

Table 10.Overview on API-specific end-points according to scenarios 1–3.

End-point [%]	**API**							
	CBZ	CLM	DCF	IBU	MTF	OFL	TRD	VFX
Eliminated in waste management	4.3	4.4	4.4	4.2	4.3	4.4	4.5	4.4
Metabolized	89.8	64.5	35.7	93	0	9.2	83.3	88.1
Eliminated in WWTP	0.7	8.5	3.7	2.4	89.3	69.1	0.4	1.4
Eliminated during transport to the BS	0	0-0.5	5.7–11.7	0.1	0–0.1	0–0.5	1.0–2.2	0.6–1.3
Reaches the BS	5.2	22.1–22.5	44.6–50.5	0.3	6.2–6.3	16.8–17.3	9.7–10.9	4.8–5.5

3.3. Concentrations in wastewater and surface water

3.3.1. Predicted influent and effluent concentrations

Calculated national average concentrations in influent and effluent wastewaters for all APIs analysed in CWPharma WP2 are presented in Annexes 5 and 6, respectively. The PECs for the selected 8 APIs for influent and effluent wastewaters are presented in tables 11 and 12, respectively. The tables also present the range of concentrations detected in the sampling campaigns carried out in CWPharma (Ek Henning et al. 2020). During the screening campaign samples were collected from Estonian, Finnish, German, Latvian, Polish and Swedish wastewaters.

The concentrations in influent and effluent wastewaters were calculated assuming, that the water flow at WWTPs is 140 L/person/day. This approach will overestimate concentration in situations where the water flow is higher, e.g. due to higher per capita water usage or when a significant sewage volume originates from industrial activities or stormwaters.

All PECs for CBZ, CLM, DCF and VFX in influent wastewater were within the range of detected concentrations. Similarly, PECs in influent wastewaters for MTF and TRD were within the range of detected concentrations, except in Finland and Denmark, respectively. However, the screening campaigns carried out by Ek Henning et al. (2020) did not cover Denmark. Concentration data from Denmark would be required to estimate whether the concentrations are actually higher in Denmark than in other BSR countries, as could be assumed based on our calculations.

Table 11. Predicted average influent concentrations of modeled substances for each country and the range, median and number of measured influent concentrations reported by Ek Henning et al. (2020). The green background color tells that predicted value is within the observed range.

	Predicted influent concentration (ng/L)							
	CBZ	**CLM**	**DCF**	**IBU**	**MTF**	**OFL**	**TRD**	**VFX**
FI	390	230	5,200	7,200	520,000	33	630	380
SE	390	360	3,300	3,800	220,000	0.022	710	380
DE	490	800	3,800	3,100	370,000	98	620	340
LV	910	1,400	12,000	9,300	280,000	230	460	47
EE	870	1,900	13,000	8,600	320,000	47	580	130
PL	910	1,400	2,500	200	330,000	83[a)]	800[a)]	410[a)]
LT	250	400	3,000	1,700	180,000	83[a)]	790[a)]	400[a)]
DK	350	490	1,900	8,300	300,000	0.050	2,700	600
RU	670[a)]	920[a)]	1,600	4,300[a)]	350,000[a)]	83[a)]	810[a)]	420[a)]
Measured influent concentration (ng/L)[b)] (Ek Henning et al. 2020)								
Min-max	26–3,500	37–1,900	640–16,000	2,300–8,000	15,000–480,000	430–3,800	140–1,400	30–1,500
Median	720	330	4,500	3,600	100,000	710	600	600
N	28	31	36	6	36	20	27	30

a) Based on the weighted average per capita sales, presented in Table 2.
b) Results above the limit of quantification, as reported by Ek Henning et al. (2020)

All PECs in effluent wastewaters, except those for IBU and OFL in all countries and TRD in Denmark, were within the range of detected concentrations (Table 12). PECs for DCF matched relatively well with the detected concentrations, being 0.34 (Russia) to 2.8 (Estonia) -fold compared to the median of detected concentrations.

Table 12. Predicted average effluent concentrations of modeled substances for each country and the range, median and number of measured effluent concentrations reported by Ek Henning et al. (2020). The results falling within the range of detected concentrations is presented in green background.

	Predicted effluent concentration (ng/L)							
	CBZ	**CLM**	**DCF**	**IBU**	**MTF**	**OFL**	**TRD**	**VFX**
FI	350	160	4,900	360	1,000	4.5	610	310
SE	350	260	3,700	190	430	0.003	680	310
DE	430	570	3,600	150	730	13	600	270
LV	800	990	11,000	470	560	31	450	37
EE	760	1,300	12,000	420	640	6.3	560	100
PL	800	980	2,300	10	660	11[a)]	780[a)]	330[a)]
LT	220	290	2,800	87	360	11[a)]	770[a)]	320[a)]
DK	310	350	1,700	410	600	0.007	2,600	480
RU	590[a)]	650[a)]	1,500	220[a)]	700[a)]	11[a)]	780[a)]	340[a)]
Measured effluent concentration (ng/L)[b)] (Ek Henning et al. 2020)								
Min-max	150-2,500	35–2,200	1,400–38,000	3,700–44,000	21–2,600	300–740	170–1,500	23–960
Median	670	220	4,500	14,000	820	550	520	420
n	33	32	34	8	6	3	33	29

a) Based on the weighted average per capita sales, presented in Table 2.
b) Results above the limit of quantification, as reported by Ek Henning et al. (2020)

3.3.2. Predicted surface water concentrations

River mouths

The estimated API-specific annual concentrations, averaged across all rivers in the BPL model from the results from scenarios 1-3, ranged from 48–72 pg/L for OFL to 82–120 ng/l for MTF. The scenario 3 predicted lowest and the scenario 2 highest concentrations for all APIs in estuarian river waters in all countries (for scenario descriptions, see Table 4). The rivers with generally the highest overall API concentrations are presented in Figure 59 and Table 13.

While the loads to the BS through each river (see chapter 3.1) correlated strongly with population in the river basin and national sales statistics, concentrations at river mouths were strongly linked to flow rates in the rivers, and flow rate modifiers used in scenarios 2 and 3. The highest API concentrations were estimated to occur in southern parts of the BSR.

The rivers with the generally the highest concentrations in Estonia, Finland, Latvia, Lithuania and Sweden were estimated to be Pühajõgi, Vantaanjoki, Lielupe, Akmena-Dane and Råån, respectively. Many of the rivers estimated to have highest concentrations were different from the rivers estimated to carry the highest loads (see chapter 3.1.) For instance, although the river with the highest flow rate, Neva, was estimated to carry the fifth highest DCF load to the BS (230 kg/a), the predicted concentration was relatively low (2.6–3.9 ng/L).

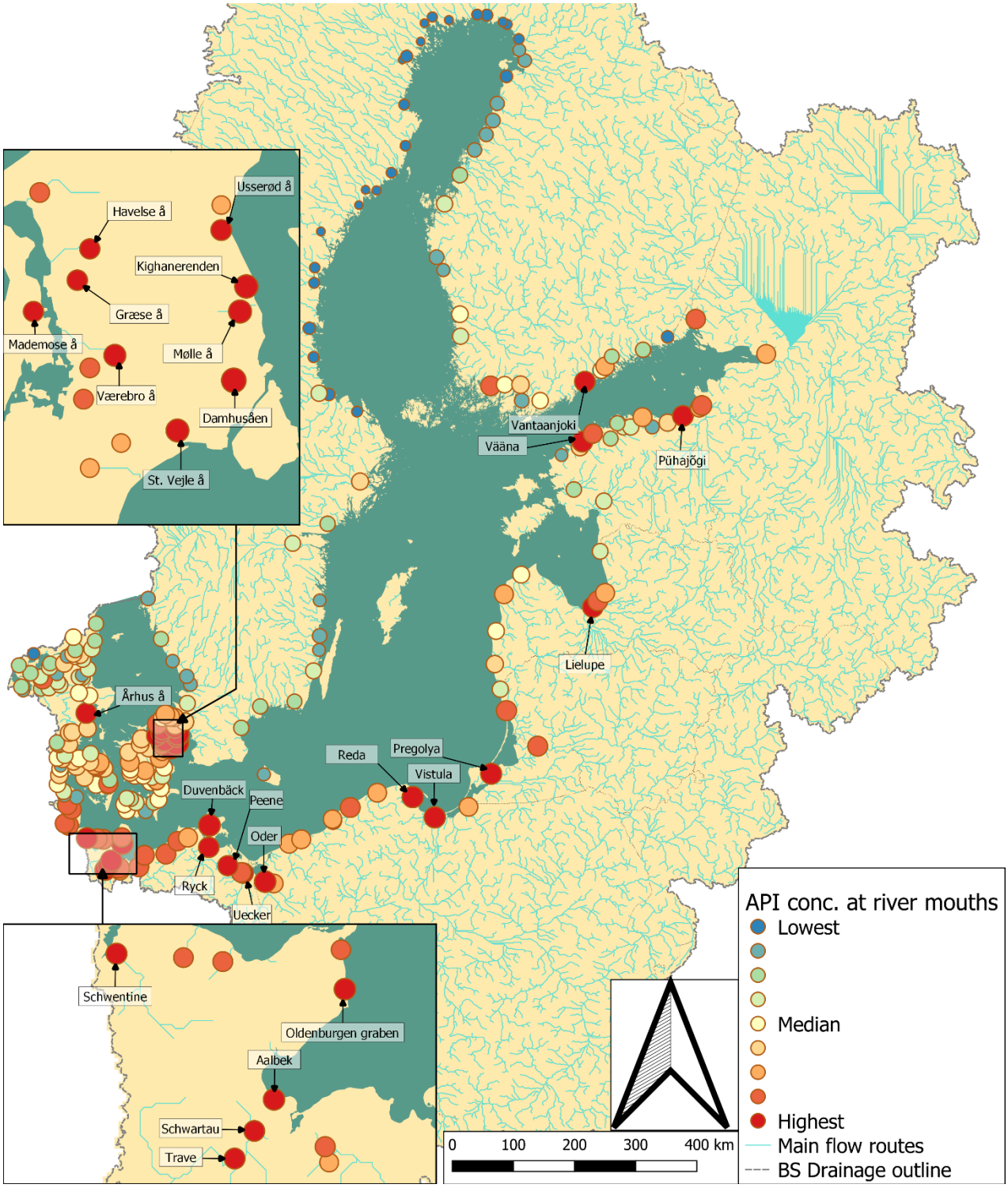

Figure 59. API concentrations at each river mouth included into the BPL model relative to concentrations at other river mouths. The rivers with the highest API loads are flagged.

Table 13. Estimated API concentrations at the mouths of 15 rivers with the highest predicted concentrations within the BSR.

River	Scn	Concentration at river mouth (ng/L)							
		CBZ	CLM	DCF	IBU	MTF	OFL	TRD	VFX
Damhusåen, DK	1-3	230–340	260–380	1,300–1,900	360–540	2,600–3,900	0,0053–0,0079	1,900–2,800	360–530
	-1	5,500	1,400	2,700	190,000	280,000	0,051	19,000	7,100
Kighanerenden, DK	1-3	110–170	130–190	620–940	180–270	1,300–1,900	0,0026–0,0039	920–1,400	170–260
	-1	2,700	690	1,300	94,000	140,000	0,025	9,500	3,500
Mølle å, DK	1-3	94–140	100–160	520–780	150–220	1,100–1,600	0,0022–0,0032	780–1,200	150–220
	-1	2,300	580	1,100	79,000	110,000	0,021	8,000	2,900
St. Vejle å, DK	1-3	87–130	97–150	490–730	140–210	1,000–1,500	0,002–0,003	720–1,100	140–200
	-1	2,100	540	1,000	73,000	110,000	0,02	7,400	2,700
Værebro å, DK	1-3	52–78	58–87	290–440	82–120	600–900	0,0012–0,0018	430–650	81–120
	-1	1,300	320	630	44,000	63,000	0,012	4,400	1,600
Duvenbäk, DE	1-3	18–27	24–36	150–220	7,7–11	180–280	0,6–0,89	25–37	12–17
	-1	440	130	320	4,100	19,000	5,8	260	230
Oder, PL	1-3	30–45	37–54	89–110	1,3–1,3	160–230	0,47–0,68	29–35	12–15
	-1	630	200	200	720	16,000	4,6	290	230
Oldenburger graben, DE	1-3	16–23	20–31	130–190	6,6–9,8	160–240	0,51–0,76	21–32	9,8–14
	-1	380	110	280	3500	17,000	4,9	220	200
Aalbek, DE	1-3	15–22	19–29	120–180	6,2–9,3	150–220	0,48–0,72	20–31	9,3–14
	-1	360	110	260	3,300	16,000	4,7	210	190
Reda, PL	1-3	28–42	35–52	81–120	0,42–0,63	140–210	0,42–0,63	27–40	12–17
	-1	590	190	170	180	15,000	4	260	210
Vistula, PL	1-3	23–34	28–41	65–79	2,9–2,6	380–550	0,4–0,58	21–26	9,2–11
	-1	480	150	140	410	12,000	3,4	220	170
Pregolya, RU	1-3	12–18	14–21	32–44	10–15	800–1200	0,35–0,51	12–17	5,5–7,6
	-1	240	74	68	780	6,800	1,9	120	97
Schwentine, DE	1-3	12–17	15–23	95–140	4,9–7,2	120–180	0,38–0,56	16–24	7,3–11
	-1	280	84	210	2,600	12,000	3,7	160	150
Usserød å, DK	1-3	27–41	31–46	150–230	43–65	310–470	6.3e-04–9.5e-04	230–340	43–64
	-1	660	170	330	23,000	33,000	0,0061	2,300	850
Trave, DE	1	11–16	14–21	86–120	4,4–6,4	110–160	0,34–0,51	14–21	6,6–9,6
	-1	250	76	190	2,400	11,000	3,3	150	130
Median	1	2,9	3,3	20	2,8	35	2.0e-04	10	3
	-1	65	15	37	1,300	2,800	0,0016	90	52
Average	1	7,9	9,1	50	9,6	98	0,058	47	9,6
	-1	160	42	92	4,400	7,200	0,43	400	160
90% of all results	1	0,11–23	0,057–30	1–150	0,079–28	0,96–320	1.6e-06–0,33	0,17–150	0,05–28
	-1	3,2–480	0,27–140	1,9–270	43–13,000	83–20,000	1.2e-05–2,3	1,7–1,300	1,2–470

PECs for coastal waters were compared to the concentrations measured during the sampling campaign carried out as a part of the project CWPharma (Ek Henning et al. 2020). The MECs for the estuaries of rivers covered by the BPL model were compared to respective PECs. This comparison is presented in Figure 60.

All PECs for CBZ in Peene and Vistula and for MTF and VFX in Motala ström were within the range of detected estuarian concentrations of those same rivers. On the other hand, the concentrations were generally overestimated to a varying extent. On average, the calculated concentrations were 11–15 times higher than the measured values. However, this error was highly variable between APIs and rivers. For instance, the average error for CBZ ranged from 2.3 to 4.3-fold, while the error ranged from 28 to 41-fold for CLM. The PECs were occasionally lower than the ones detected in the rivers Motala Ström, Peene and Vistula.

Due to the variability of the error-quotients and low number of measured concentrations in the simulated areas, the available dataset does not allow for proper calibration of the BPL model. Calibrating the model would require more samples, with a better coverage of the annual cycle.

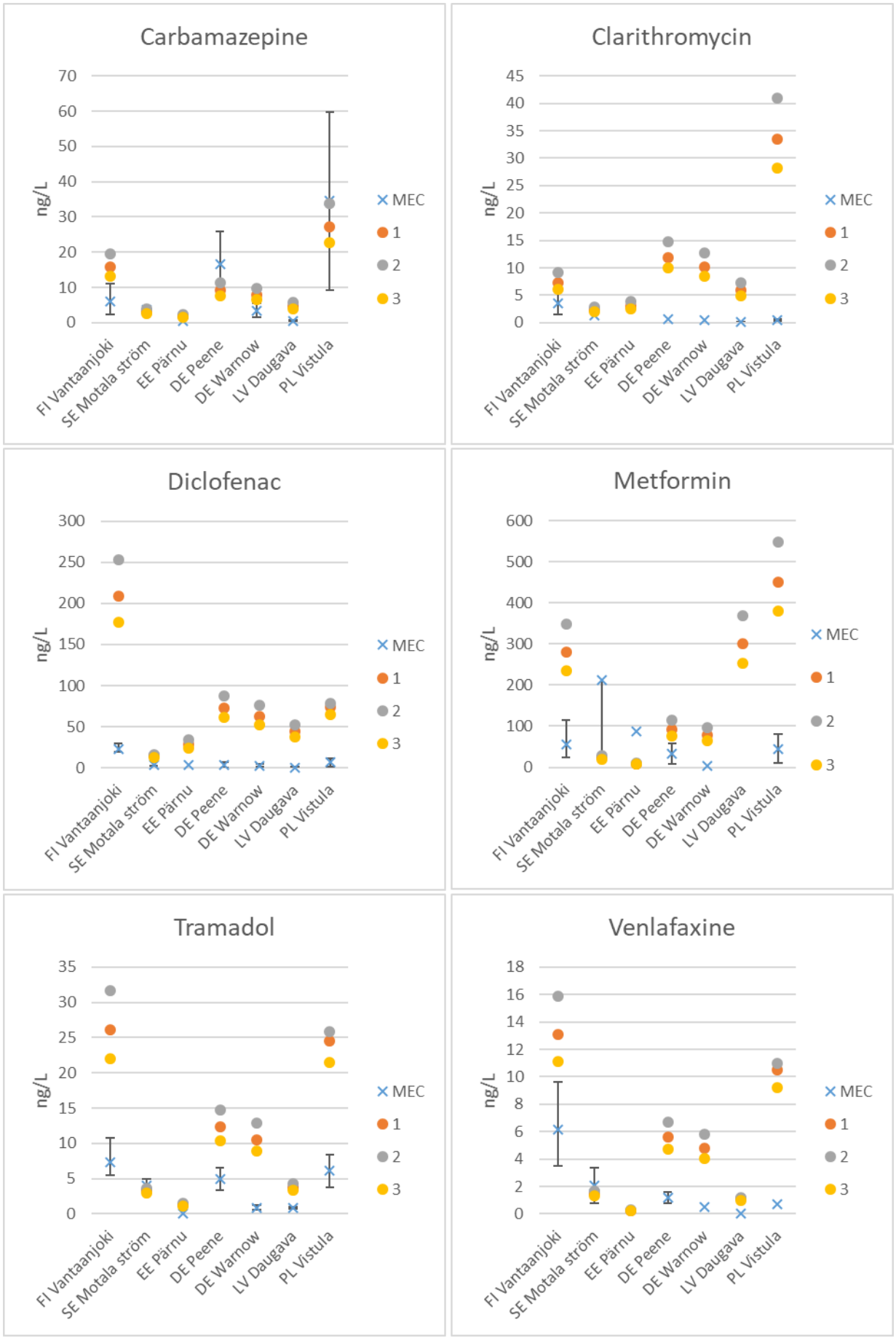

Figure 60. Predicted concentrations (scenarios 1–3), average concentrations (MEC) and the range of measured concentrations (whiskers) of APIs in the estuarian surface waters of studied rivers.

Coastal concentrations

The estimated background concentrations in coastal waters in different parts of the BS ranged from the median concentration of 0.3 pg/L estimated for OFL to 16 ng/L estimated for MTF. The estimated median concentrations at urban coasts for these APIs were 12 pg/L and 220 ng/L, respectively.

The concentrations at urban coasts were several times higher than the estimated background concentrations. As in case of estuarian concentrations, the scenario 2 (winter/sping) predicted highest concentrations for all APIs, while scenario 3 predicted the lowest.

The PECs for coastal waters were compared to the concentrations measured during the CWPharma sampling campaign (Ek Henning et al. 2020) and those presented by HELCOM (UNESCO & HELCOM 2017). PECs for scenarios 1–3 in both background areas and urban coasts, as well as the MEC values are presented in the Table 14. The city-specific PEC values for urban coasts are presented in Figures 61 and 62.

Median PECs in background areas for DCF, TRD, VFX and IBU were within or almost in the range of MECs. Median PECs for TRD and VFX corresponded very well with the median of their measured concentrations. The C_{raw} concentrations were generally closer to the MECs than the C_{AA}. The predicted concentrations for the urban coasts were generally higher than the MEC-values.

Table 14. Predicted and measured environmental concentrations in the BS coastal waters.

API		PEC (Scn. 1–3) [ng/L] [a]		MEC [ng/L] [a), b)]
		Background conc.	Conc. at urban coasts	
CBZ	Min	C_{raw}: 0.0091	C_{raw}: 1.1	CWPharma: 0.6 (n=13) HELCOM: 0.25 (n=132)
	Med.	C_{raw}: 0.69	C_{raw}: 8.1	CWPharma: 1.5 (n=13) HELCOM: 3.4 (n=132)
	Max	C_{raw}: 60–61	C_{raw}: 100	CWPharma: 6.3 (n=13) HELCOM: 160 (n=132)
CLM	Min	C_{raw}: 0.014	C_{raw}: 1.1	CWPharma: 0.59 (n=5) HELCOM: 0.27 (n=2)
	Med.	C_{raw}: 0.43	C_{raw}: 6.5	CWPharma: 1.2 (n=5) HELCOM: 0.27 (n=2)
	Max	C_{raw}: 63–65	C_{raw}: 100	CWPharma: 1.6 (n=5) HELCOM: 0.27 (n=2)
DCF	Min	C_{raw}: 0.17, C_{AA}: 0.36	C_{raw}: 7–7.1, C_{AA}: 13	CWPharma: 0.43 (n=11) HELCOM: 0.1 (n=61)
	Med.	C_{raw}: 5.2–5.3, C_{AA}: 8.8–9.3	C_{raw}: 92–93, C_{AA}: 140	CWPharma: 2.8 (n=11) HELCOM: 0.2 (n=61)
	Max	C_{raw}: 160–200, C_{AA}: 300–370	C_{raw}: 1100, C_{AA}: 1700	CWPharma: 22 (n=11) HELCOM: 54 (n=61)
IBU	Min	C_{raw}: 0.0019, C_{AA}: 0.0018	C_{raw}: 0.39, C_{AA}: 0.3	HELCOM: 0.25 (n=17)
	Med.	C_{raw}: 0.14, C_{AA}: 0.12	C_{raw}: 1.8–1.9, C_{AA}: 1.6–1.8	HELCOM: 3.4 (n=17)
	Max	C_{raw}: 4.2–4.3, C_{AA}: 4.2–4.3	C_{raw}: 38, C_{AA}: 33	HELCOM: 158 (n=17)

API		PEC (Scn. 1–3) [ng/L] [a)]		MEC [ng/L] [a), b)]
		Background conc.	Conc. at urban coasts	
MTF	Min	C_{raw}: 0.073	C_{raw}: 20	CWPharma: 3.4 (n=10)
	Med.	C_{raw}: 16	C_{raw}: 220	CWPharma: 17 (n=10)
	Max	C_{raw}: 2400	C_{raw}: 45000	CWPharma: 230 (n=10)
OFL	Min	C_{raw}: 8.4e-08	C_{raw}: 8.5e-06	CWPharma: 15 (n=1)
	Med.	C_{raw}: 3.3e-04–3.4e-04	C_{raw}: 0.012	CWPharma: 15 (n=1)
	Max	C_{raw}: 0.34–0.35	C_{raw}: 0.89–0.9	CWPharma: 15 (n=1)
TRD	Min	C_{raw}: 0.0049, C_{AA}: 0.0097	C_{raw}: 2.6–2.7, C_{AA}: 3.8	CWPharma: 0.12 (n=12) HELCOM: 0.69 (n=2)
	Med.	C_{raw}: 0.89–0.94, C_{AA}: 1.5–1.6	C_{raw}: 12, C_{AA}: 20	CWPharma: 1.0 (n=12) HELCOM: 0.69 (n=2)
	Max	C_{raw}: 35–43, C_{AA}: 62–76	C_{raw}: 200, C_{AA}: 160	CWPharma: 5.5 (n=12) HELCOM: 0.69 (n=2)
VFX	Min	C_{raw}: 0.0015, C_{AA}: 0.0028	C_{raw}: 0.79–0.84, C_{AA}: 1.4–1.5	CWPharma: 0.14 (n=12) HELCOM: 1.0 (n=2)
	Med.	C_{raw}: 0.56–0.6, C_{AA}: 0.93–0.98	C_{raw}: 8.1, C_{AA}: 12	CWPharma: 0.9 (n=12) HELCOM: 1.0 (n=2)
	Max	C_{raw}: 24–29, C_{AA}: 39–48	C_{raw}: 110, C_{AA}: 81	CWPharma: 4.8 (n=12) HELCOM: 1.0 (n=2)

a) Only PEC-values higher than zero, and MEC-values higher than the LOQ were taken into consideration.
b) Sources: CWPharma (Ek Henning et al. 2020), HELCOM (UNESCO & HELCOM 2017)

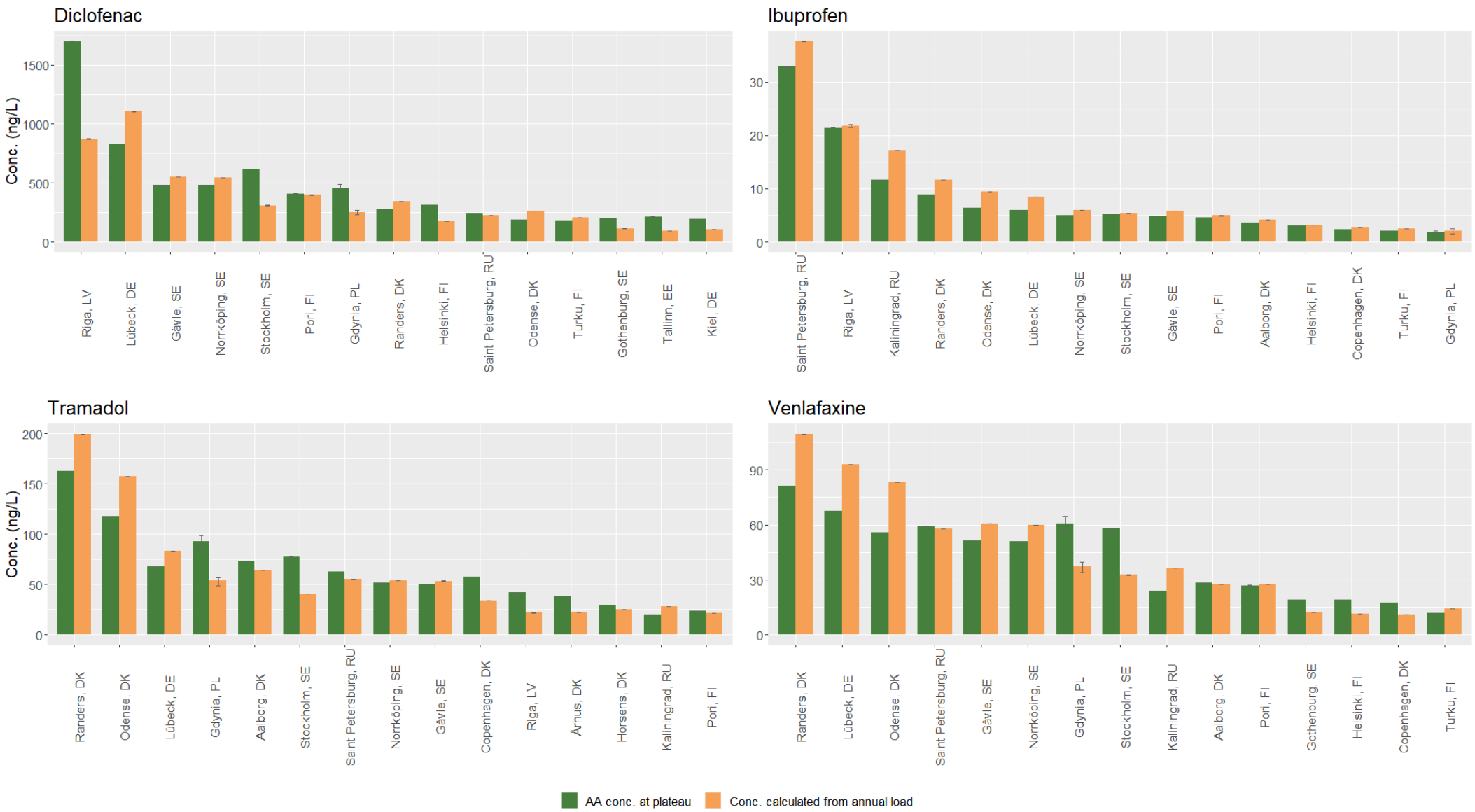

Figure 61. Predicted concentrations at urban coasts for DCF, IBU, TRD and VFX. The whiskers present the variation between different scenarios (1-3).

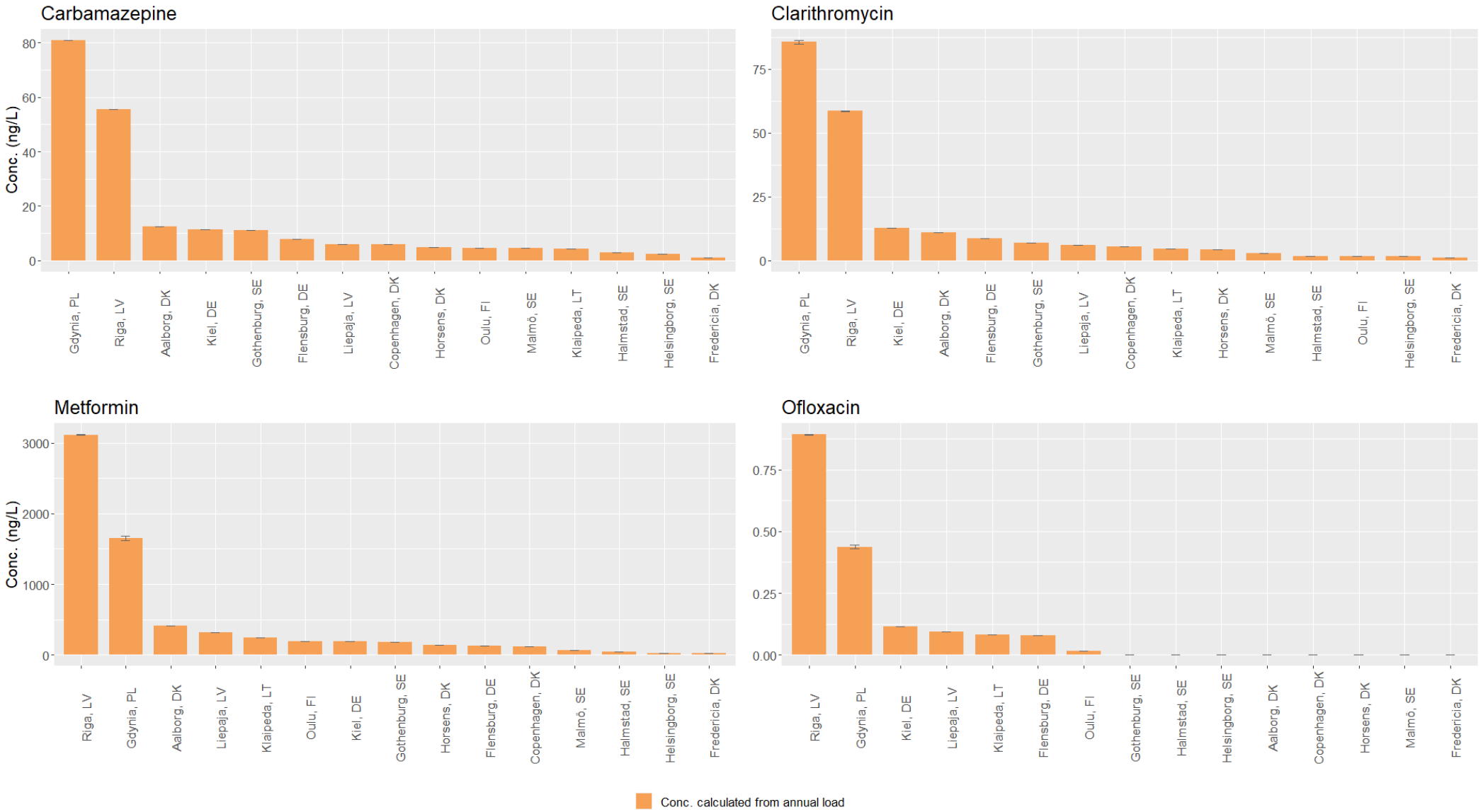

Figure 62. Predicted concentrations at urban coasts for CBZ, CLM, MTF and OFL. The whiskers present the variation between different scenarios (1-3).

3.3.3. Predicted concentrations in surface waters vs. PNEC

CLM, DCF, IBU and MTF were estimated to exceed their PNEC-values in river waters and coastal waters within the BSR. The risk quotients are presented in Figure 63. Additionally, with scenario -1, CBZ and VFX exceeded their concentrations in individual rivers in Denmark (Damhusåen, Kighanerenden, Mølle å and St. Vejle å). PNEC-exceedances were more common in southern parts of the BSR than in the northern parts.

The API with the highest PNEC-exceedances was IBU. However, the PNEC-values presented in literature for IBU contain a lot of variation. The PNEC-value used here, 0.12 ng/L (Ek Henning et al. 2020), is somewhat lower than those commonly presented. For instance, Orias & Perrodin (2013) used a PNEC-value 200 ng/L, and Korkaric et al. (2019) presented a revised EQS of 1 ng/L. If those PNEC-values were to be used, the RQ-values would be significantly lower. However, the estimated IBU concentrations in two rivers would still exceed even the value presented by Orias & Perrodin (2013).

As the RQ-value is highly dependent on the PNEC-value, the high RQs for this API should be considered a signal that IBU ecotoxicity should be further investigated to help derive a robust PNEC.

At least one API was estimated to exceeded its PNEC-value in each of the urban coasts covered by the BPL model. However, there were many wider coastal areas, where the dilution factor was high enough to lower the PECs below the PNEC-levels.

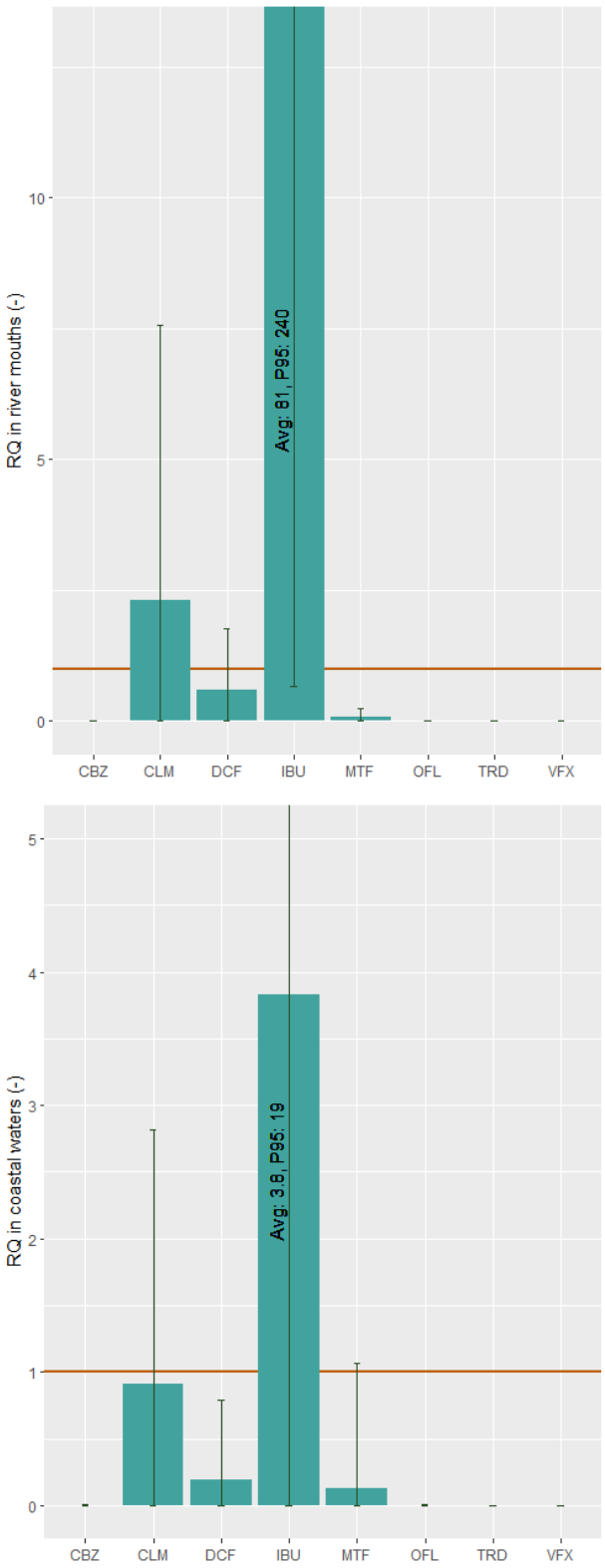

Figure 63. Risk quotients for the eight APIs in river mouths and coastal waters according to scenario 1. The whiskers present the range of concentrations in 90% of river mouths. Note that the risk quotients for ibuprofen exceed the y-scale. The RQs for coastal waters were calculated using C_{raw}.

4. Model evaluation

4.1. Critical overview of the model processes

The model calculates API emissions originating from approximately 1.9 million 1 km² grid cells representing the BSR catchment area, dissipation of APIs during the transport from the emission source to the BS coast, and the eventual loads to the BS. The driving parameter was API consumption which was based on national sales and divided into grid cells according to population. The estimated API loads emitted in wastewater effluents were based on coefficients (e.g. API-specific excretion rate and removal rate at WWTP). A pseudo first order equation was used to estimate dissipation during transport to the BS in inland surface waters. The time available for transport was calculated using simulated flow-path model created in this project for the whole BSR from elevation and other open source data. The model itself is not dynamic, but seasonal changes were taken into account by running different simulation scenarios. The outputs are annual loads and annual average concentrations (during a typical year) in selected areas. Loads were transformed into concentrations by using typical water volumes e.g. in river mouths. In coastal areas two approaches were used to estimate concentrations, as presented in chapter 2.2.3.

During the last decade several similar models and their applications have been published. Some of them are more specific but may require external hydrological model to obtain good results e.g. STREAM-EU (Lindim et al. 2016, Lindim et al. 2019, van Gils et al. 2020). Some of the models have incorporated catchment data but they do not cover the whole BSR like ePiE (Oldenkamp et al. 2018). On the other hand, e.g. GLOBAL-FATE (Font et al. 2019, Acuña et al. 2020) calculates concentrations in the whole world but process description is more simple than in the BPL model presented here.

The inbuilt GIS-model makes BPL a stand-alone model and independent of external hydrological models. The transport time calculations are based on the calculated flow-path lengths. The estimated transport time combined with the simple approach used in estimating the dissipation during transport, together with the WWTP processes incorporated into each grid cell, create the basis for the calculation approach. It is relatively simple and efficient compared e.g. to those approaches where mass is routed over the whole chain from one node to the next.

The main known limitations in the process description of the current model are related to the definition of the fraction of water where photodegradation occurs, the dissipation processes and dilution of APIs in coastal areas, and to sedimentation. Photodegradation is the most important process for the degradation of many APIs (e.g. Oldenkamp et al. 2019). In the BPL model, a scenario-specific constant (F_{photo}) describes the portion of water flow where photodegradation takes place in inland waters. In coastal waters corresponding value ($a(q,l)$) is depth and season specific portion of photoactivity compared to optimal conditions. The impact of parameters affecting photodegradation is higher for the APIs that are easily degraded by sunlight, as highlighted by the univariate sensitivity analysis carried out for the BPL model (see Annex 7). Consequently, the impacts of F_{photo} and $a(q,l)$ would increase with decreasing $DT50_{photo}$ values. Thus, the shorter the photolysis half-life, the more sensitive the model is to changes in parameters related to photodegradation. Therefore, more studies are needed on the photodegradation of APIs in natural conditions in different depths of the water column, and during different seasons.

API concentrations in coastal areas were calculated using two approaches. In the first approach, coastal area was considered as a continuum of a river: annual API load was divided by the water volume of the area. This estimation assumed uniform mixing and dissipation of an API in the coastal area during the loading year. In the second approach sedimentation, biodegradation and photodegradation were included (using simple process descriptions), but API transport from the recipient area was not taken into account. To improve these estimates, and to possibly merge the two approaches, more MEC data would be required, including well described, representative sampling points and depths, frequent sampling for at least two years, and comprehensive information on the API loading to the area.

Sedimentation was not considered in inland waters. This may cause overestimation of the loads of APIs with high sorption affinity, especially in sites of high sediment deposition on the flow-path. The steady state concentration in coastal water was calculated using the plateau principle. We found no good examples on how to apply pseudo first order kinetics (combined temperature related biodegradation and depth related photodegradation) and zero-order sedimentation with the plateau concentration calculation. To keep the calculation simple, the API-specific fraction estimated to be eliminated from the water phase due to sedimentation was deducted already from the annual load. The sedimentation rate is assumed to be constant throughout the BS coast. This is a simplification of the sedimentation process, and it does not take into account the continuous nature of the process, or its variations due to regional conditions. The approach might underestimate the sedimentation of persistent APIs and lead to overestimation of their concentration in coastal water. On the other hand, even higher error may be caused by using the constant sedimentation rate along BS coastline. It is clear that the simulation of API sedimentation is not site specific using this approach.

In addition to how sedimentation was incorporated into the coastal calculations, the scenarios used in the calculations and the degradation calculation approach may need re-evaluation. For instance, the current approach does not allow the water to mix in coastal areas after initial emission. As the lower parts of the water column are assumed to have no photoactivity, the plateau-principle is applicable only to biodegradable APIs. Therefore, if the BPL model is used in estimating not only the locations of hotspots but also the actual concentrations, the calculation approach should be modified.

Considerations for persistent APIs

A numerical degradation rate coefficient is needed to simulate the loading scenarios 1-3 (see Table 4) and to calculate plateau concentration in coastal waters. For very persistent APIs there might be no degradation rate value available in literature. For these compounds, the calculation can technically be carried out using a very long half-life, or the loading can be simulated using scenario 0, which excludes the riverine processes.

According to the plateau principle, the steady state concentration will be reached after around five half-life times since the start of the loading. If a persistent API has been on the market for less than five times its pseudo first order degradation half-life, the steady state concentration is not yet reached and comparison to measured values is not relevant. Additionally, the approach assumes API-specific consumption to remain constant from year to year. Despite its shortcomings, the steady state simulation gives valuable information. It may highlight the need for mitigation measures not only to those APIs having concentrations above PNEC values now, but also to apply them to persistent APIs whose concentrations are increasing and may exceed the PNEC in the future. The long-term accumulation of CBZ and its slow recovery in BS coastal areas after a hypothetical end of loading was well demonstrated by Björlenius et al. (2018).

4.2. Model performance and suggestions for future work

The model performance was studied stepwise, first comparing the predicted and measured concentrations in WWTP influent, then in effluent, and finally in the surface waters (river mouths and estuaries). The main results are presented in chapter 3.3. and some comparison is presented already there.

When comparing the PEC-values with MEC-values, it must be taken into account that while the PECs represent annual national averages, the MEC-values are always bound to a certain time and location. Thus, the representativeness of measured data is limited. Moreover, the transformation from load to concentration depends on water volumes.

In this calculation exercise, the per capita wastewater flow was assumed to be 140 L/d/person. The estimated water volume was based on the number of inhabitants, and therefore the industrial wastewaters and urban storm water which may dilute the API concentrations at WWTPs were not taken into account.

The predicted influent concentrations of the five (CBZ, CLM, DCF and VFX) out of the eight selected test APIs fitted well into the range of measured concentrations in all countries (Table 11). Also, the predicted influent concentrations of TRD and MTF fitted within the range of detected concentrations with individual exceptions. The rather good overall performance of most APIs in influent simulation indicates that the API consumption was well estimated in the project. However, when comparing the PECs and MECs for individual countries, there was more variation. For instance, MTF PECs in influent water (520 µg/L) were about five times higher than the observed range (43–110 µg/L) in two Finnish WWTPs (Ek Henning et al. 2020). Therefore, it is possible that MTF load in Finland was overestimated. On the other hand, TRD consumption was estimated to be relatively high in Denmark compared to any other BSR country (Table 2). However, the sampling campaign carried out in CWPharma (Ek Henning et al. 2020) did not cover Denmark, and the MEC-dataset contained no data from Denmark. Thus, more information would be required to assess whether the concentrations in Danish wastewaters are higher than in other BSR countries.

Despite the rather good overall performance, PECs for two APIs did not fit within the MEC range (OFL and IBU). Predicted IBU concentrations in influent were out of the observed range in several countries (higher in LV, EE, DK; lower in PL, see Table 11). Predicted OFL concentrations in influent water were underestimated by several orders of magnitude. The lower level of the measured OFL concentration range in influent was barely reachable by changing the parameters describing portion of non-used OFL or human excreted factor, without modifying OFL sales. This exercise prompted a further study on OFL use. It was found out that while the usage of OFL itself is rather small, the use of its s-enantiomer levofloxacin is much higher (e.g. in Finland OFL usage was about 11 kg/a while that of levofloxacin varied from 270 to 303 kg/a during 2015-2017). The excreted factor in humans is about the same for the two enantiomers. In the laboratory analysis, the method does not separate between different enantiomers but measures the concentration of the racemic mixture. Thus, the OFL loads into the environment presented in this report are inherently underestimates, due to the sales data covering only the racemic mixture, and not the enantiopure forms. If we were to include the Finnish levofloxacin sales into the OFL sales value, the PEC value for influent wastewaters would be 940 ng/L, falling well within the Finnish MEC values (430–970 ng/L, Ek Henning et al. 2020). However, compiling further sales statistics on levofloxacin for all BSR-countries was not within the scope of this work. Nevertheless, this observation highlights the importance accessibility of comprehensive sales statistics.

The predicted effluent concentrations of six out of eight APIs were within the MEC-ranges (See Table 12). As presented above, OFL loads to WWTPs were underestimated due to incomprehensive sales statistics, resulting in underestimated effluent concentration as well. The IBU concentration in effluent was underestimated in all countries although its estimated influent concentration was in the range of measured concentration in half of the countries. However, the measurement data reported by Ek Henning et al. (2020) covered only six data points for influent and eight data points for effluent wastewaters. According to the few data points presented in the study, concentrations were higher in effluent wastewaters than in influent wastewaters, which is in stark contrast with previous results presented in the literature. As a result, a reliable removal rate could not be calculated from this data. Thus, the removal rate (95%) used in the calculations was derived as expert judgement based on literature sources. To better assess the performance of the BPL in estimating IBU loads and concentrations, more measurement data points would be required.

In addition to the eight selected APIs, the predicted effluent concentrations of 25 other APIs were compared to the country-specific measured effluent concentrations presented by Ek Henning et al. (2020). The APIs were set in order according to their performance. The 16 best performing APIs were gabapentin, **venlafaxine**, **tramadol**, losartan, **carbamazepine,** hydrochlorothiazide, telmisartan, **clarithromycin,** mesalazine, **diclofenac**, citalopram, bisoprolol, naproxen, valsartan, progesterone

and **metformin**, for which the average concentration ranged from 50% to 200% of the measured concentration in at least half of the countries included. This criterion is rather tight due to the limited data and the high variation of measured concentrations in effluent waters. This API ranking indicates that the substances selected for simulations were not the ones performing best or worst but represent a somewhat random sample of all the APIs investigated in the project CWPharma.

Surface water

As shown in chapter 3.3.2, concentrations in river mouths and coastal waters were usually overestimated to a varying extent. Estimating river mouth concentrations contains more uncertainties than estimating effluent concentrations. However, any errors in effluent estimations may be multiplied when estimating environmental concentrations.

The predicted concentrations in river mouths were typically 11–15 times higher than measured ones. The medians of predicted coastal concentrations fitted in the range of measured concentrations for all tested APIs except OFL, due to problems in sales statistics, as discussed on p. 101. However, the site-specific API concentrations were often overestimated but usually less than 10-fold.

On average, a good fit between a predicted and measured environmental micropollutant concentration is within an order of magnitude. For example, van Gils et al. (2020) noticed that 65% of the concentrations predicted using the model STREAM-EU were within one order of magnitude of the measured concentrations, but in 10% cases the difference was higher than 100-fold.

Summary of performance and suggestions to future work

In model assessment attention should be given to the question: How well does the model suit its purpose? This includes not only the accuracy of simulated outputs, but the whole chain. Are the simulation results useful? Does the use of the model have any advantages over other methods?

The current model approach was created to (1) estimate pharmaceutical load from BS catchment area to the BS, (2) find areas with high loadings and (3) identify potential hotspots for API occurrence. We think that the goals of the model are met. The model estimates the current annual loadings of selected APIs to the BS. Additionally, it identifies the most important source areas as well as areas where API concentrations can be assumed to be highest. Moreover, in a parallel activity of the project CWPharma, the model has been utilized in estimating the load reduction potential of selected scenarios (Äystö et al. 2020). Comparison between predicted and measured values indicated that predicted values are realistic and do not differ many orders of magnitudes from the measured ones. Taking into account the high uncertainties in input data and the limitations in measured comparison data, the model results can be assessed as good enough for its purpose.

The predicted loads and concentrations presented in this report are obtained without any calibration. More realistic surface water concentrations could be achieved by calibrating the model. A univariate sensitivity analysis (Annex 7) gives a good starting point to select parameters for calibration. The parameters having the highest linear impact on predicted concentrations were sales modifier (tested in the sensitivity analysis, not included in the process description), excretion rate, removal rate at WWTP and sewer network coverage (see Table A7.2 in the Annex 7). These parameters affect API concentration in wastewater, but they are not related to environmental fate. A stepwise calibration approach, starting with these parameters (within their uncertainty areas) and using concentration in wastewater as an object function, might be the most efficient way to start. Pharmaceutical consumption data is the driving force of the simulations. Therefore, the extra parameter “sales modifier”, presented in Annex 7, should be utilized in calibration to account for the uncertainties and regional differences in API sales. This kind of parameter is used in other models as well (e.g. Acuña et al. 2020). Once the predicted concentrations in wastewater are acceptable, the parameters describing environmental fate can be calibrated.

For a robust calibration of the BPL model, comprehensive and good quality measured datasets are required from WWTPs, river mouths and coastal waters. The corresponding water volumes should be defined to convert measured concentrations into mass units. The sampling frequency and the length of data series should be sufficient for calculating the typical annual average value, and the

uncertainties of these averages should be estimated. A rough first step calibration of API loads from wastewater treatment plants to surface waters could be carried out for some API & country -combinations using data already available.

If remarkable differences between PEC and MEC were to occur after calibration, the model process description would require improvements. Some possible points to improve process description are pointed in chapter 4.1. Further model development from reviewing the process descriptions to calibration and further validation may be useful in identifying knowledge gaps. Uncertainty assessment of predicted values might bring additional information as well (see e.g. Gimeno et al. 2017).

To increase the applicability of the BPL model, it should be looked into, whether additional processes could be incorporated into the calculation method. These processes could include e.g. emissions caused by veterinary medication, leaching from land areas where sewage sludge has been utilized in agriculture or landscaping, and elimination from the water phase due to sedimentation during transport from emission cell to the BS coast.

The BPL model could also be implemented to a wider set of APIs. The mass flow simulations (e.g. Table 10) demonstrates that degradation in riverine system plays a minor role for the selected APIs. Thus, the model, using the assumptions in scenario 0, could be assumed to give relatively good estimates on overall loads to the BS.

5. Conclusions

A new GIS-based model, BPL, was created to estimate pharmaceutical loads to the Baltic sea and concentrations in river mouths and along the coast. The model was applied to eight APIs selected e.g. based on their occurrence and relatively high concentrations in the BSR.

According to the BPL model and the input data utilized in this calculation exercise, the coastal areas with the highest API load are the Polish coastal waters in Gdansk and Bornholm basins. Similarly, the highest loads from individual countries originated most commonly from Poland and Russia. The high loads from Poland were caused by the high number of inhabitants in the basin area. However, as the sales statistics were lacking especially for Russia, the estimated high emissions from Russia are largely based on average consumption values, and as such contain significant uncertainties.

The rivers with the highest predicted concentrations were in southern parts of the Baltic Sea region. Predicted concentrations of ibuprofen, clarithromycin and diclofenac exceeded the PNEC in many rivers and coastal areas. As expected, the predicted concentrations were higher in urban coasts than in wider coastal areas. Selected simulation results are demonstrated in a web map application (SYKE 2020).

The predicted influent and effluent concentrations of four out of eight APIs (carbamazepine, clarithromycin, diclofenac and venlafaxine) were within the range of measured concentrations. The discrepancies between the predicted and measured concentrations of the other four APIs can be explained by incomprehensive sales statistics or unrepresentative samples. The medians of predicted annual average surface water concentrations fit well into the range of measured concentrations for seven out of eight APIs. However, the site-specific surface water concentrations were usually two- to 15-fold overestimated. Similar performance has been reported with other models (e.g. van Gils et al. 2020).

The predicted ofloxacin concentrations differed dramatically from those measured in wastewaters. The contrast between predicted and measured ofloxacin concentrations in influent wastewater was likely caused mainly by the input sales statistics covering only the racemic mixture (ofloxacin) but not its enantiopure form levofloxacin, which is used in higher quantities at least in Finland. Previously Oldenkamp et al. (2016) identified API consumption, along with ecotoxicological data (e.g. PNEC values), as the most important and uncertain parts affecting the assessment of API risks. Our modelling exercise supports their conclusion. These observations highlight the importance of accessible and comprehensive pharmaceutical sales statistics. Such data is the prerequisite for any computational estimates on the environmental loads of pharmaceuticals.

According to this calculation exercise, degradation in the environment is not a major dissipation process for the eight APIs looked into in this report. Its impact was very low compared to metabolism and removal in wastewater treatment plants. Thus, preliminary calculations could be carried out for a wider set of APIs without the need for extensive literary reviews on API-specific behaviour in the environment.

The BPL model can be further refined by improving and supplementing the input data. These data should include more comprehensive statistics on pharmaceutical sales and management of unused medicines. Additionally, the model could be further improved by calibrating it using good quality datasets. However, the calibration of the parameters affecting environmental fate can be carried out only if the data on pharmaceutical sales is correct and there is a sufficient amount of measurement data available.

Based on this work, computational approaches can help identify emission and occurrence hotspots. The identified sites could then be utilized when designing screening campaigns. The BPL model works well for demonstrating the potential emission hotspots and for identifying the parts in the emission chain, where emission reduction measures could have the biggest reduction potential. In future work, the model could be calibrated to achieve more reliable estimates of API concentrations.

6. References

Álvarez-Ruiz, R., McLachlan, M.S., Gallen, M., Hawker, D.W., Kaserzon, S. & Mueller, J.F. 2020. Measuring the half-life of PPCPs and PFASs in the Brisbane River estuary using a mass balance model and benchmarking. Poster, presented in SETAC 2020.

Andreozzi, R., Raffaele, M. & Nicklas, P. 2003. Pharmaceuticals in STP effluents and their solar photodegradation in aquatic environment. Chemosphere 50: 1319–1330. https://doi.org/10.1016/S0045-6535(02)00769-5

Arajuo, L., Troconis, M.E., Espina, M.B. & Prieto, A. 2014. Persistence of Ibuprofen, Ketoprofen, Diclofenac and Clofibric Acid in Natural Waters. Journal of Environment and Human, 1: 32–38.

Aus der Beek, T., Weber, F. A., Bergmann, A., Hickmann, S., Ebert, I., Hein, A. & Küster, A. 2016. Pharmaceuticals in the environment-Global occurrences and perspectives. Environmental Toxicology and Chemistry, 35(4), 823–835. https://doi.org/10.1002/etc.3339

Björlenius, B., Ripszám, M., Haglund, P., Lindberg, R.H., Tysklind, M. & Fick, J. 2018. Pharmaceutical residues are widespread in Baltic Sea Coastal and offshore waters – Screening for pharmaceuticals and modelling of environmental concentrations of carbamazepine. Science of the Total Environment 633: 1496–1509. https://doi.org/10.1016/j.scitotenv.2018.03.276

Blomqvist, S. & Heiskanen, A.S. 2001. The Challenge of Sedimentation in the Baltic Sea. In: Wulff F.V., Rahm L.A., Larsson P. (eds) A Systems Analysis of the Baltic Sea. Ecological Studies (Analysis and Synthesis), vol 148. Springer, Berlin, Heidelberg.

Bollmann, U.E., Simon, M., Vollersten, J. & Bester, K. 2019. Assessment of input of organic micropollutants and microplastics into the Baltic Sea by urban waters. Marine Pollution Bulletin, 148: 149-155. https://doi.org/10.1016/j.marpolbul.2019.07.014

CIESIN 2016. Gridded Population of the World, Version 4 (GPWv4): Population Count. Center for International Earth Science Information Network - CIESIN - Columbia University. Palisades, NY: NASA Socioeconomic Data and Applications Center (SEDAC). https://doi.org/10.7927/H4X63JVC

Damrat, M., Zaborska, A. & Zajączkowski, M. 2013. Sedimentation from suspension and sediment accumulation rate in the River Vistula prodelta, Gulf of Gdańsk (Baltic Sea). Oceanologia 55(4): 937–950. https://doi.org/10.5697/oc.55-4.937

Danielson, J.J. & Gesch, D.B. 2011. Global multi-resolution terrain elevation data 2010 (GMTED2010): U.S. Geological Survey Open-File Report 2011–1073, 26 p. http://pubs.usgs.gov/of/2011/1073/

Deutcher Wettendienst (DWD). Website: https://www.dwd.de/EN/climate_environment/climatemonitoring/europe/europe_node.html [cited on 7.5.2020]

EC 2019. Communication from the commission to the European Parliament, the Council and the European Economid and Social Committee. European Union Strategic Approach to Pharmaceuticals in the Environment. Brussels 11.3.2019. COM(2019) 128 final.

EEA 2019. Waterbase - UWWTD: Urban Waste Water Treatment Directive – reported data. Website: https://www.eea.europa.eu/data-and-maps/data/waterbase-uwwtd-urban-waste-water-treatment-directive-6 [Cited on 17.11.2020]

EFSA 2008. Opinion on a request from EFSA related to the default Q10 value used to describe the temperature effect on transformation rates of pesticides in soil - Scientific Opinion of the Panel on Plant Protection Products and their Residues (PPR Panel). EFSA Journal 6 (1): 1–32. https://doi.org/10.2903/j.efsa.2008.622

Ek Henning, H., Putna.Nimane, I., Kalinowski, R., Perkola, N., Bogusz, A., Kublina, A., Haiba, E., Barda, I., Karkovska, I., Schütz, J., Mehtonen, J., Siimes, K., Nyhlén, K., Dzintare, L., Äystö, L., Sinics, L., Laht, M., Lehtonen, M., Stapf, M., Stridh, P., Poikāne, R., Hoppe, S., Lehtinen, T., Kõrgma, V.,

Junttila, V. & Leisk, Ü. 2020. Pharmaceuticals in the Baltic Sea Region – emissions, consumption and environmental risks. Report no. 2020:28, Länsstyrelsen Östergötland, Linköping. Available at: https://www.lansstyrelsen.se/4.f2dbbcc175974692d268b9.html

EMA 2006. Committee for medicinal products for human use (CHMP). Guideline on the environmental risk assessment of medicinal products for human use. London, 01 June 2006. Doc. Ref. EMEA/CHMP/SWP/4447/00 corr 2.

Eurographics 2018. EuroGlobalMap, Hydrography. Available at: https://eurogeographics.org/maps-for-europe/open-data/

European Chemicals Agency 2017. Guidance on the Biocidal Products Regulation, Volume IV Environment – Assessment and Evaluation (Parts B + C). ECHA-17-G-23-EN.

European Environmental Agency, 2016. Indicator Assessment. Prod-ID: IND-103-en. CLIM 016. Available at: https://www.eea.europa.eu/data-and-maps/indicators/river-flow-3/assessment

Eurostat 2016a. GEOSTAT_POP_2011_V2_0_1. European Commission. Available at: https://ec.europa.eu/eurostat/web/gisco/geodata/reference-data/population-distribution-demography/clusters

Eurostat 2016b. GEOSTAT_POP_2011_V2_0_1. European Commission. Available at: https://ec.europa.eu/eurostat/web/gisco/geodata/reference-data/population-distribution-demography/geostat

Fass.se. Diklofenak T Apofri. Website: https://www.fass.se/LIF/product?userType=2&nplId=20040607004036 [Cited on 18.11.2020]

Fick, J., Lindberg, R.H., Kaj, L. & Brorström-Lundén, E. 2011. Results from the Swedish National Screening Programme 2010. Subreport 3. Pharmaceuticals. IVL Report B2014.

Font, C., Bregoli, F., Acuña, V., Sabater, S. & Marcé, R. 2019. GLOBAL-FATE (version 1.0.0): A geographical information system (GIS)-based model for assessing contaminants fate in the global river network. Geoscientific Model Development 12: 5213-5228. https://doi.org/10.5194/gmd-12-5213-2019

Gimeno, P., Marcé, R., Bosch, L., Comas, J. & Corominas, L. 2017. Incorporating model uncertainty into the evaluation of interventions to reduce microcontaminant loads in rivers. Water Research 124: 415-424. https://doi.org/10.1016/j.watres.2017.07.036

Greskowiak, J., Kühne, R., Kutsarova, S., Lindim, C., Markus, A., van de Meent, D., Munthe, J., Schueder, R., Schüürmann, G., Slobodnik, J., de Zwart, D. & van Wezel, A. 2020. Computational material flow analysis for thousands of chemicals of emerging concern in European waters. Journal of Hazardous Materials 397: 122655. https://doi.org/10.1016/j.jhazmat.2020.122655

Gurke, R., Rößler, M., Marx, C., Diamond, S., Schubert, S., Oertel, R. & Fauler, J. 2015. Occurrence and removal of frequently prescribed pharmaceuticals and corresponding metabolites in wastewater of a sewage treatment plant. Science of the Total Environment 532: 762–770. https://doi.org/10.1016/j.scitotenv.2015.06.067

HELCOM 2005. Raster grid of the Baltic Sea bathymetry computed with ArcGIS Spatial Analyst (KRIGING) from the original Digital Topography of the Baltic Sea (IOWTOPO) database produced by the Baltic Sea Research Institute of Warnemunde. Available at: http://metadata.helcom.fi/geonetwork/srv/eng/catalog.search#/metadata/5dcf182a-517a-4599-be0d-626bea8e058d

HELCOM 2011. HELCOM Pollution Load Compilation. Municipal wastewater treatment plants 2006.

HELCOM 2014. BASE project 2012-2014: Pilot activity to identify sources and flow patterns of pharmaceuticals in St. Petersburg to the Baltic Sea.

HELCOM 2017. HELCOM subbasins with coastal and offshore division 2018. HELCOM. Available at: http://metadata.helcom.fi/geonetwork/srv/eng/catalog.search#/metadata/e5a59af9-c244-4069-9752-be3acc5dabed

HELCOM 2018a. HELCOM Pollution Load Compilation. Sub-catchments of transboundary and border rivers. Available at: http://metadata.helcom.fi/geonetwork/srv/eng/catalog.search#/metadata/0e718846-f0a6-4aa8-8c66-0337bac68461

HELCOM 2018b. PLC-Water database. River flow data 1995-2016. Available at: http://nest.su.se/helcom_plc/

HELCOM 2020. Map and data service. Website: https://maps.helcom.fi/website/mapservice/ [Cited on 17.11.2020]

Hertta database. Finnish Environment Institute. Available at: https://www.ymparisto.fi/en-US/waters

Huttunen, I., Huttunen, M., Piirainen, V., Korppoo, M., Lepistö, A., Räike, A., Tattari, S. & Vehviläinen, B. 2016. A national scale nutrient loading model for Finnish watersheds – VEMALA. Environmental Modelling and Assessment 21(1), 83–109. https://doi.org/10.1007/s10666-015-9470-6

Hörsing, M., Wahlberg, C., Falås, P., Hey, G., Ledin, A. & la Cour Jansen, J. 2014. Reduktion av läkemedel i svenska avloppsreningsverk – kunskapssammanställning. Svenskt Vatten Utveckling, Rapport Nr 2014–16.

JRC 2007. CCM River and Catchment Database. European Commission.

Jung, C.M., Heinze, T.M., Strakosha, R., Elkins, C.A. & Sutherland, J.B. 2009. Acetylation of fluoroquinolone antimicrobial agents by an Escherichia coli strain isolated from a municipal wastewater treatment plant. Journal of Applied Microbiology, 106: 564–572. https://doi.org/10.1111/j.1365-2672.2008.04026.x

Kaiser, A., Tränckner, J., Björklund, E., Svahn, O., Suzdalev, S., Langas, V., Gamaga-Budré, G., Szopinska, M., Fudala-Ksiazek, S. & Jankowska, K. 2019. Pharmaceutical consumption patterns in four coastal regions of the South Baltic Sea. Project MORPHEUS 2017-2019, Deliverable 3.1.

Korhonen, J. 2002. Suomen vesistöjen lämpötilaolot 1900-luvulla. Suomen ympäristökeskus. Suomen ympäristö 566. 116 p. https://helda.helsinki.fi/handle/10138/40478

Korhonen, J. 2007. Suomen vesistöjen virtaaman ja vedenkorkeuden vaihtelut. Suomen ympäristökeskus. Suomen ympäristö 45/2007. 120 p. http://hdl.handle.net/10138/38428

Korkaric, M., Junghans, M., Pasanen-Kase, R. & Werner, I. 2019. Revising Environmental Quality Standards: Lessons Learned. Integrated Environmental Assessment and Management, 16: 948–960. https://doi.org/10.1002/ieam.4192

LEGMC 2020. Clidata database: Hydrological monitoring data of Latvian Environment, Geology and Meteorology Centre.

Leipe, T., Tauber, F., Vallius, H., Virtasalo, J., Uścinowicz, S., Kowalski, N., Hille, S., Lindgren, S. & Myllyvirta, T. 2011. Particulate organic carbon (POC) in surface sediments of the Baltic Sea. Geo-Marine Letters 31 (3): 175–188. https://doi.org/10.1007/s00367-010-0223-x

Lindim, C., de Zwart, D., Cousins, I. T., Kutsarova, S., Kühne, R. & Schüürmann, G. 2019. Exposure and ecotoxicological risk assessment of mixtures of top prescribed pharmaceuticals in Swedish freshwaters. Chemosphere 220: 344 – 352. https://doi.org/10.1016/j.chemosphere.2018.12.118

Lindim, C., van Gils, J. & Cousins, I. T. 2016. A large-scale model for simulating the fate & transport of organic contaminants in river basins. Chemosphere 144: 803–810. https://doi.org/10.1016/j.chemosphere.2015.09.051

Mattila, J., Kankaanpää, H. & Ilus, E. 2006. Estimation of recent sediment accumulation rates in the Baltic Sea using artificial radionuclides 137Cs and 239,240PU as time markers. Boreal Environmental Research 11:95-107.

Mehtonen, J., Äystö, L., Junttila, V., Perkola, N., Lehtinen, T., Bregendahl, J., Leisk, Ü., Kõrgmaa, V., Aarma, P., Schütz, J., Stapf, M., Kublina, A., Karkovska, I., Szumska, M., Bogusz, A., Kalinowski, R., Spjuth, S., Nyhlén, K., Jakobsson, T., Suzdalev, S. & Kaskelainen, E. 2020. Good practices for take-

back and disposal of unused pharmaceuticals in the Baltic Sea region. Clear Waters from Pharmaceuticals (CWPharma) Activity 4.1 Report. Reports of the Finnish Environment Institute 34/2020. 103 p. http://hdl.handle.net/10138/319009

Miehe, U., 2010. Wirksamkeit technischer Barrieren zur Entfernung von anthropogenen Spurenstoffen. Kläranlagen und Raumfilter. von der Fakultat III - Prozesswissenschaften - der Technischen Universitat Berlin. Genehmigte Dissertation.

Oldenkamp, R., Beusen, A. & Huijbregts, M. 2019. Aquatic risks from human pharmaceuticals—modelling temporal trends of carbamazepine and ciprofloxacin at the global scale. Environmental Research Letters 14 (3): 034003. 10.1088/1748-9326/ab0071. https://doi.org/10.1088/1748-9326/ab0071

Oldenkamp, R., Hoeks, S., Čengić, M., Barbarossa, V., Burns, E.E., Boxall, A.B.A. & Ragas, M.J. 2018. A High-Resolution Spatial Model to Predict Exposure to Pharaceuticals in European Surface Waters: ePiE. Environental Science & Technology, 52: 12494-12503. https://doi.org/10.1021/acs.est.8b03862

Orias, F. & Perrodin, Y. 2013. Characterisarion of the ecotoxicity of hospital effluents: A review. Sci Tot Environ, 454–455, 250–276. https://doi.org/10.1016/j.scitotenv.2013.02.064

Packer, J.L., Werner, J.J., Latch, D.E., McNeill, K. & Arnold, W.A. 2003. Photochemical fate of pharmaceuticals in the environment: Naproxen, diclofenac, clofibric acid, and ibuprofen. Aquat. Sci. 65: 342–351. https://doi.org/10.1007/s00027-003-0671-8

Parczewski & Pruchnicki. 2017. Vistula River. Encyclopædia Britannica, inc. Website: https://www.britannica.com/place/Vistula-River [Cited on 11.5.2020]

Pettersson, H., Brüning, T., Larsson, M. & Kalén, O. 2019. Wave climate in the Baltic Sea 2018. HELCOM Baltic Sea Environment Fact Sheets. Website: http://www.helcom.fi/baltic-sea-trends/environment-fact-sheets [Cited on 15.5.2020]

R Core Team 2020. R: A language and environment for statistical computing. R Foundation for Statistical Computing, Vienna, Austria.

Rúa-Gómez, P. & Püttmann, W. 2013. Degradation of lidocaine, tramadol, venlafaxine and the metabolites O-desmethyltramadol and O-desmethylvenlafaxine in surface waters. Chemosphere 90: 1952–1959. https://doi.org/10.1016/j.chemosphere.2012.10.039

Siegel, H. & Gerth, M. 2019. Sea Surface Temperature in the Baltic Sea in 2018. HELCOM Baltic Sea Environment Fact Sheets. Website: http://www.helcom.fi/baltic-sea-trends/environment-fact-sheets/hydrography/development-of-sea-surface-temperature-in-the-baltic-sea [Cited on 1.6.2020]

Simis, S. G., Ylöstalo P., Kallio, K., Spilling, K. & Kutser, T. 2017. Contrasting seasonality in optical biogeochemical properties of the Baltic Sea. PLoS ONE 12 (4): e0173357. https://doi.org/10.1371/journal.pone.0173357

Straub, J.O., Caldwell, D.J., Davidson, T., D'Aco, V., Kappler, K., Robinson, P.F., Simon-Hettich, B. & Tell, J. 2019. Environmental risk assessment of metformin and its transformation product gualynurea. I. Environmental fate. Chemosphere 216: 844–854. https://doi.org/10.1016/j.chemosphere.2018.10.036

SYKE 2020. CWPharma - Pharmaceutical emissions to the Baltic Sea. Web Map Application: https://syke.maps.arcgis.com/apps/MapSeries/index.html?appid=85d441bdc8e04354bdd7c7257b211b9f [Cited on 30.11.2020]

The Danish Health Data Authority 2020. Website: www.medstat.dk [Cited 31.3.2020]

UNESCO & HELCOM 2017. Pharmaceuticals in the aquatic environment of the Baltic Sea region – A status report. Baltic Sea Environment Proceedings No. 149.

UNICEF & WHO 2019. Progress on household drinking water, sanitation and hygiene 2000-2017. Special focus on inequalities. New York: United Nations Children's Fund (UNICEF) and World Health Organization (WHO).

van Gils, J., Posthuma, L., Cousins, I. T. Brack, W., Altenburger, R., Baveco, H., Focks, A., Greskowiak, J., Kühne, R., Kutsarova, S., Lindim, C., Markus, A., van de Meent, D., Munthe, J., Schueder, R.,

Schüürmann, G., Slobodnik, J., de Zwart, D. & van Wezel, A. 2020. Computational material flow analysis for thousands of chemicals of emerging concern in European waters. Journal of Hazardous Materials 397: 122655. https://doi.org/10.1016/j.jhazmat.2020.122655

Verlicchi, P., Al Aukidy, M. & Zambello, E. 2012. Occurrence of pharmaceutical compounds in urban wastewater: Removal, mass load and environmental risk after a secondary treatment–A review. Science of the Total Environment 429: 123–155. https://doi.org/10.1016/j.scitotenv.2012.04.028

Vione, D., Feitosa-Felizzola, J., Minero, C. & Chiron, S. 2009. Phototransformation of selected human-used macrolides in surface water: Kinetics, model predictions and degradation pathways. Water Research 42: 1959–1967. https://doi.org/10.1016/j.watres.2009.01.027

Vogt, J., Soille, P., de Jager, A., Mehl, W., Foisneau, S., Bódis, K., Dusart, J., Paracchini, M.L., Haastrup, P. & Bamps, C. 2007. A pan-European River and Ctachment Database. JRC reference report. Report EUR 22920 EN. 120 p.

Äystö, L. & Stapf, M. 2020. Scenarios for reducing pharmaceutical emissions – Estimated load reductions, greenhouse gas emissions & costs. Project CWPharma Activity 5.1 + 5.2 report. https://helda.helsinki.fi/handle/10138/322549

Äystö, L., Vieno, N., Fjäder, P., Mehtonen, J. & Nystén, T. 2020. Pharmaceutical load to wastewater treatment plants and their primary emission sources. Vesitalous 1/2020: 5–8. In Finnish with an abstract in English.

Annex 1 – Structure of the calculation grid

Variable name	Content
Id_nro	Grid cell-specific identifier (running number)
Point_x	X-coordinate (ETRS_1989_LAEA)
Point_y	Y-coordinate (ETRS_1989_LAEA)
AreaId	Area-specific identifier issued to each cluster, river basin and coastal area (running number)
RegionId	Flag used to differentiate between different types of regions 1 = Coastal urban cluster 2 = Main river basins 3 = Coastal areas & sea 4 = Coastal sea areas, not included in the original HELCOM-data 5 = Inland urban clusters
Country	Country ('FI', 'LV', 'SE', etc.)
ToSea_m	Distance to the sea along the calculated flow route (unit: m)
Elevation_m	Elevation from sea level (unit: m)
Population	Population per cell
SourceCode	Baltic Sea river basin code (HELCOM, PLC-6 subcatchments)
Name	Baltic Sea river basin name (HELCOM, PLC-6 subcatchments)
AreaName	Area-specific name
LakeOutlet_id	Identifier for lake discharge points
LakeOutlet_name	Name for lake discharge points
UpCatch_id	Flag used to identify an upper catchment areas of a lake (cells that flow through a specific lake. Each cell flowing through a lake has the "LakeOutlet_id" as its "UpCatch_id")
UpCatch_name	Name used to used to identify an upper catchment areas of a lake (cells that flow through a specific lake. Each cell flowing through a lake has the "LakeOutlet_name" as its "UpCatch_name")
Upcatch_km2	Value presenting the size of the upper catchment area of each grid cell (km^2)
Retention	Cumulative retention time from lakes (unit: d)
Sea_Land	Flag used to differentiate cells located land areas and sea (Land = 1, Sea = 2)
Coast3km	Flag to identify a 3 km sea zone from the coast for further calculations (values 1, NA)
SeaDepth3p	Sea depth (unit: m)
SeaDepth3_m3	Sea volume in grid cell (unit: m^3)
ClassMax	Value given to urban clusters (*RegionId* 1 & 5) representing the highest class of the WWTPs linked to that cluster

SumPE	Value given to urban clusters (*RegionId* 1 & 5) representing the sum of person equivalents for the WWTPs linked to the cluster
WWTP_count	Value given to urban clusters (*RegionId* 1 & 5) representing the number of WWTPs linked t othe cluster
RiverBasin	Flag used to identify calculated catchment areas of the main river basins. Each cell is given the "RiverBasin_outlet" value given for the cell discharging the water from that catchment area.
RiverBasin_Flow_ka1995_2006	Average of annual average water flows in discharge cells for the years 1995-2006. Source: HELCOM (unit: m^3/s)
RiverBasin_outlet	Flag used to identify discharge cells for calculated catchment basins.
Shape_Area	Area of each grid (constant: 1e+06 m^2)
UC_Flag	Flag used to identify urban coasts (1/0)
CoastCluster	Flag used to identify coastal waters of each urban cluster (AreaId of the nearest coastal urban cluster)
Tot_cons	Consumption of a specific API in the grid cell (unit: mg). Calculated from the per capita consumption in each country multiplied by the population in the cell.
Delay2Purku_d	Flow time from the cell to the discharge cell. Used in estimating the load reaching the discharge cell. Calculated as the cell-specific *Delay_d* subtracted by the *Delay*_d calculated for the *RiverBasin*-specific discharge cell. (unit: d)
SeaAreaId	Information of sea areas (AreaId) into which cell flows.

Annex 2 – Lakes included into the BPL model

Lake ID	Name	Country	Retention time (d)[a)]	Population upstream (persons)[b)]	Area upstream (km^2)[b)]	Coordinates	
						X	Y
1	Ladoga	RU	4,015	1,057,799	88,790	5479500	4268500
2	Ilmen	RU	4,105	850,029	69,930	5541500	4131500
3	Onega	RU	9,125	363,259	55,136	5648500	4458500
4	Kemijärvi (N43 146.50)x1	FI	40	28,417	27,572	5090500	4915500
5	Kiantajärvi (N43 199.30)	FI	1,413	4,253	3,492	5210500	4763500
6	Lammasjärvi	FI	1,209	6,242	3,470	5261500	4690500
7	Rehja-Nuasjärvi	FI	1,160	20,865	4,027	5178500	4678500
8	Oulujärvi (N43 122.20)x3	FI	1,064	40,548	6,533	5160500	4683500
9	Oulujärvi (N43 122.20)x2	FI	334	500	435	5143500	4690500
10	Oulujärvi (N43 122.20)x1	FI	118	3,824	2,046	5123500	4702500
11	Pielinen	FI	11,920	33,439	13,843	5336500	4571500
12	Hiirenvesi	FI	10,747	12,258	6,712	5337500	4558500
13	Höytiäinen	FI	12,969	7,363	1,554	5317500	4537500
14	Viinijärvi	FI	14,308	8,784	869	5296500	4528500
15	Pyhäselkä (Saimaa N60+75.80)	FI	9,572	81,844	2,144	5322500	4496500
16	Kiteenjärvi	FI	4,272	6,353	344	5364500	4480500
17	Pyhäjärvi	FI	11,585	4,627	940	5352500	4446500
18	Simpelejärvi (N60 68.80)	FI	4,492	2,328	429	5349500	4420500
19	Ylä-Enonvesi	FI	9,513	2,537	319	5309500	4458500
20	Juojärvi	FI	14,624	6,489	1,839	5272500	4512500
21	Syväri	FI	13,183	7,714	2,382	5232500	4575500
22	Nerkoonjärvi	FI	15,440	39,954	4,755	5178500	4587500
23	Onkivesi	FI	15,431	7,601	827	5189500	4559500
24	Maaninkajärvi	FI	15,371	2,982	246	5190500	4552500
25	Kallavesi (N60 81.70)	FI	12,940	127,171	6,244	5228500	4498500
26	Unnukka	FI	12,246	8,552	408	5242500	4474500

Lake ID	Name	Country	Retention time (d)[a)]	Population upstream (persons)[b)]	Area upstream (km²)[b)]	Coordinates	
						X	Y
27	Haukivesi (Saimaa N60+75.80)	FI	11,428	53,884	5,353	5305500	4440500
28	Pihlajavesi (Saimaa)	FI	9,270	39,404	6,718	5279500	4393500
29	Ukonvesi (Saimaa)	FI	7,570	38,357	296	5233500	4383500
30	Saimaa	FI	7,412	65,355	5,569	5320500	4369500
31	Kivijärvi	FI	1,771	3,950	495	5262500	4326500
32	Vuohijärvi	FI	395	1,708	1,014	5215500	4328500
33	Kallavesi	FI	819	1,466	516	5216500	4366500
34	Lahnavesi	FI	425	5,765	505	5204500	4363500
35	Ryökäsvesi-Liekune	FI	4,271	9,566	2,138	5203500	4386500
36	Kyyvesi	FI	5,049	5,208	1,333	5206500	4421500
37	Pieksänjärvi	FI	8,589	14,067	116	5203500	4472500
38	Suontienselkä-Paasvesi	FI	8,238	4,125	441	5193500	4498500
39	Niinivesi	FI	4,072	11,062	2,263	5168500	4507500
40	Iisvesi	FI	4,703	3,331	579	5171500	4512500
41	Pielavesi	FI	5,155	4,159	1,093	5154500	4555500
42	Pyhäjärvi	FI	2,635	5,044	617	5106500	4603500
43	Ylä-Keitele (N60 99.50)	FI	4,947	8,928	2,800	5117500	4528500
44	Ala-Keitele (N60+99.50)	FI	5,451	11,398	575	5130500	4498500
45	Keski-Keitele (N60 99.50)	FI	4,653	9,086	2,911	5155500	4504500
46	Konnevesi	FI	3,932	3,219	1,286	5155500	4488500
47	Kynsivesi-Leivonvesi	FI	3,526	7,674	1,099	5152500	4460500
48	Lievestuoreenjärvi	FI	5,520	3,327	232	5150500	4451500
49	Saraavesi	FI	3,406	20,736	1,170	5141500	4456500
50	Leppävesi	FI	3,244	15,212	567	5144500	4437500
51	Palokkajärvi	FI	3,206	45,247	332	5134500	4442500
52	Muuratjärvi	FI	4,464	6,328	374	5133500	4427500
53	Päijänne (pohj. N60+78.10)	FI	3,182	79,622	666	5137500	4412500
54	Jääsjärvi	FI	3,210	6,670	1,499	5167500	4370500
55	Konnivesi	FI	36	8,343	597	5188500	4320500
56	Ruotsalainen	FI	71	12,457	564	5176500	4331500

Lake ID	Name	Country	Retention time (d)[a)]	Population upstream (persons)[b)]	Area upstream (km²)[b)]	Coordinates	
						X	Y
57	Vesijärvi	FI	3,457	45,010	478	5152500	4322500
58	Päijänne (etel. N60+78.10)	FI	118	3,584	337	5151500	4334500
59	Päijänne (kesk. N60+78.10)	FI	2,871	34,699	4,461	5148500	4337500
60	Pyhäjärvi	FI	719	6,304	475	5188500	4277500
61	Tuusulanjärvi	FI	223	37,294	83	5146500	4238500
62	Valkjärvi	FI	1,674	18,887	137	5129500	4228500
63	Enäjärvi	FI	443	10,925	35	5112500	4221500
64	Hiidenvesi	FI	6,276	25,175	932	5096500	4217500
65	Lohjanjärvi	FI	6,144	27,633	1,011	5085500	4192500
66	Kernaalanjärvi	FI	1,458	14,737	1,018	5112500	4279500
67	Äimäjärvi	FI	1,450	2,752	83	5076500	4297500
68	Ormajärvi	FI	2,689	3,603	174	5122500	4307500
69	Suolijärvi	FI	1,547	1,518	124	5114500	4310500
70	Iso-Roine	FI	1,471	1,640	300	5097500	4314500
71	Kukkia	FI	2,391	2,512	763	5105500	4325500
72	Vanajavesi (N60 79.40)x1	FI	1,055	124,653	2,904	5059500	4310500
73	Mallasvesi (N60 84.20)x1	FI	1,194	24,877	886	5071500	4315500
74	Längelmävesi	FI	1,841	17,768	1,951	5072500	4332500
75	Vesijärvi	FI	3,519	11,143	219	5070500	4337500
76	Keurusselkä (N60 105.40)x1	FI	2,350	17,627	1,672	5082500	4404500
77	Jämsänvesi-Petäjävesi	FI	3,621	4,138	670	5107500	4429500
78	Pyhäjärvi	FI	5,699	9,011	1,354	5111500	4480500
79	Pääjärvi	FI	5,787	5,561	1,222	5075500	4489500
80	Lappajärvi	FI	771	17,017	1,664	5003500	4529500
81	Kuortaneenjärvi	FI	50	15,454	1,242	5001500	4483500
82	Ähtärinjärvi	FI	3,027	1,498	486	5044500	4460500
83	Vaskivesi-Visuvesi	FI	2,200	3,244	529	5045500	4407500
84	Näsijärvi (N60 95.40)x2	FI	1,694	14,507	2,914	5045500	4368500
85	Näsijärvi (N60 95.40)x1	FI	1,580	57,686	956	5050500	4338500
86	Pyhäjärvi (N60 77.20)	FI	1,005	245,271	936	5038500	4332500

Lake ID	Name	Country	Retention time (d)[a)]	Population upstream (persons)[b)]	Area upstream (km²)[b)]	Coordinates	
						X	Y
87	Parkanonjärvi	FI	673	8,119	696	5001500	4377500
88	Kyrösjärvi	FI	609	16,877	1,959	5018500	4349500
89	Mahnalanselkä Kirkkojärvi	FI	77	8,846	490	5029500	4331500
90	Kulovesi	FI	27	15,925	540	5016500	4321500
91	Rautavesi	FI	10	13,274	381	5006500	4310500
92	Köyliönjärvi	FI	2,852	1,837	95	4986500	4278500
93	Pyhäjärvi	FI	2,433	8,434	660	4975500	4279500
94	Toisvesi	FI	2,617	10,080	1,126	5031500	4420500
95	Valkjärvi	FI	1,340	2,503	17	5143500	4286500
96	Peipsi-Pihkva	RU	730	671,238	46,706	5330500	4115500
97	Kalli järv	EE	770	96	83	5319500	4042500
98	Koosa	EE	803	155	65	5313500	4045500
99	Vagula	EE	803	3,991	415	5317500	3980500
100	Tamula	EE	1,665	14,163	87	5319500	3979500
101	Hino järv	EE	1,200	11	4	5339500	3954500
102	Aheru järv	EE	183	25	36	5286500	3954500
103	Pühajärv	EE	1,095	2,788	71	5284500	3991500
104	Saadjärv	EE	3,530	1,441	30	5283500	4049500
105	Soitsjärv	EE	3,713	21	2	5283500	4052500
106	Kaiavere järv	EE	850	1,169	81	5282500	4057500
107	Kuremaa	EE	2,050	390	25	5273500	4067500
108	Endla	EE	742	143	53	5246500	4080500
109	Võrtsjärv	EE	1,095	12,638	1,546	5256500	4027500
110	Veisjärv	EE	1,460	29	27	5243500	3988500
111	Õisu järv	EE	35	1,556	214	5225500	4000500
112	Kahala	EE	365	207	26	5195500	4139500
113	Soodla veehoidla	EE	32	3,387	209	5194500	4127500
114	Paunküla veehoidla	EE	61	700	80	5192500	4097500
116	Ülemiste	EE	120	11,098	86	5153500	4120500
117	Veskijärv (Nõva Veskijärv	EE	183	0	10	5103500	4083500

Lake ID	Name	Country	Retention time (d)[a)]	Population upstream (persons)[b)]	Area upstream (km²)[b)]	Coordinates	
						X	Y
118	Sutlepa meri / Sutlepsjön	EE	120	209	38	5096500	4067500
119	Lavassaare järv	EE	60	0	16	5150500	4024500
120	Tõhela	EE	365	30	37	5133500	4005500
121	Ermistu järv	EE	182	54	21	5133500	3997500
122	Karujärv	EE	365	17	16	5033500	3980500
123	Mullutu laht	EE	37	2,001	262	5044500	3967500
124	Suurlaht	EE	73	19	10	5048500	3968500
125	Kišezers	LV	22	85,998	82	5173500	3854500
126	Juglas ezers	LV	28	62,524	1,574	5181500	3851500
127	Slokas ezers	LV	137	12,860	75	5143500	3838500
128	Vecdaugava	LV	429	3,198	11	5169500	3855500
129	Limbažu Lielezers	LV	515	572	46	5195500	3913500
130	Mazais Baltezers	LV	1,030	3,640	114	5184500	3857500
131	Dunezers	LV	19	8,340	24	5195500	3917500
132	Liepa?jas ezers	LV	27	68,803	2,358	4999500	3765500
133	Lielais Ludzas ezers	LV	813	5,089	254	5404500	3849500
134	Indzeris	LV	327	909	31	5333500	3929500
135	Aluksnes ezers	LV	2,750	7,383	36	5339500	3938500
136	Balvu ezers	LV	20	5,170	41	5352500	3905500
137	Babites ezers	LV	118	486,910	17,501	5157500	3842500
138	Viesites ezers	LV	746	1,443	43	5278500	3799500
139	Cieceres ezers	LV	243	3,300	117	5086500	3796500
140	Cirišs	LV	96	4,044	492	5366500	3791500
141	Durbes ezers	LV	70	1,893	151	5014500	3780500
142	Burtnieku ezers	LV	61	17,883	2,116	5216500	3949500
143	Raznas ezers	LV	2,120	1,762	277	5392500	3823500
144	Pitka ezers (Ozolaines dikis)	LV	493	418	23	5207500	3794500
145	Dagdas ezers	LV	341	4,163	179	5403500	3795500
146	Dunakla ezers	LV	1,472	7,533	258	5398500	3850500
147	Lielais Stropu ezers	LV	1,301	4,240	21	5349500	3766500

Lake ID	Name	Country	Retention time (d)[a)]	Population upstream (persons)[b)]	Area upstream (km^2)[b)]	Coordinates	
						X	Y
148	Šunezers	LV	423	27,506	22	5344500	3761500
149	Lielais Subates ezers	LV	417	718	26	5305500	3765500
150	Perkonu ezers	LV	38	4,362	264	5356500	3907500
151	Kanieris	LV	30	23,362	342	5136500	3844500
152	Lielais Baltezers	LV	488	1,663	23	5182500	3854500
153	Wigry	PL	1,043	75,765	326	5174500	3517500
154	Druzno	PL	33	59,769	1,078	4934500	3486500
155	Elckie	PL	114	79,232	933	5129500	3477500
156	Sniardwy	PL	521	17,821	763	5093500	3462500
157	Nidzkie	PL	1,873	5,151	178	5082500	3454500
158	Mikolajskie	PL	657	16,099	765	5084500	3467500
160	Lebsko	PL	81	126,911	2,336	4805500	3541500
161	Gardno	PL	41	4,808	143	4776500	3528500
162	Jamno	PL	135	123,803	347	4719500	3479500
164	Mamry Pólnocne	PL	913	10,518	553	5081500	3516500
165	Wdzydze Pólnocne	PL	749	9,161	278	4838500	3460500
166	Wdzydze Poludniowe	PL	608	674	56	4839500	3456500
167	Drawsko	PL	2,439	9,763	213	4726500	3404500
168	Rynskie	PL	1,873	50,568	855	5079500	3471500
169	Kisajno	PL	6,127	5,226	60	5082500	3505500
170	Råstojaure	SE	453	0	266	4753500	5101500
171	Torneträsk	SE	3,103	448	3,454	4737500	5038500
172	Kycklingvattnet	SE	304	7	75	4520500	4612500
173	Stor-Jorm and Lill-Jorm	SE	565	253	1,288	4518500	4619500
174	Grundforsdammen	SE	8.3	18	190	4680500	4670500
175	Blåviken	SE	937	45	186	4705500	4660500
176	Rusfors Dämningsområde	SE	6.2	6,287	11,526	4716500	4646500
177	Bjurfors N Dämningsomr	SE	0.46	10,654	1,425	4788500	4587500
178	Ytterkolkselet	SE	0.20	526	472	4797500	4568500
179	Noretsjön	SE	35	9,149	9,900	4677500	4573500

Lake ID	Name	Country	Retention time (d)[a)]	Population upstream (persons)[b)]	Area upstream (km²)[b)]	Coordinates	
						X	Y
180	Hällbymagasinet	SE	12	257	851	4675500	4549500
181	Norrbyvattnet	SE	44	51	259	4624500	4527500
182	Vängelsjöns dämningso	SE	21	6,732	5,829	4633500	4524500
183	Stuguns Dämningsområde	SE	1.7	88,817	19,994	4605500	4462500
184	Bredsillret	SE	0.22	2,075	3,591	4561500	4383500
185	Bergeforsens Dämningsom	SE	0.23	13,375	6,010	4702500	4400500
186	Särnsjön	SE	14	2,661	2,935	4491500	4290500
187	Växsjön	SE	2.1	33,393	14,801	4663500	4270500
188	Stallfjärden	SE	0.05	247,696	26,009	4728500	4183500
189	Knon	SE	3,902	13	108	4531500	4123500
190	Flaxen	SE	3,297	2,149	973	4568500	4095500
191	Gunnern	SE	3,581	3,227	999	4465500	4076500
192	Stora Le/Foxen-Foxen	SE	5,015	7,399	1,522	4429500	4025500
193	Glafsfjorden	SE	3,508	36,618	3,092	4481500	4031500
194	Hjälmaren	SE	2,245	187,093	3,636	4678500	4033500
195	Mälaren	SE	1,004	1,412,372	18,953	4775500	4049500
196	Vänern	SE	3,285	607,585	40,775	4459500	3920500
197	Gesebols sjö	SE	277	253	24	4478500	3848500
198	Stråken	SE	644	513	95	4598500	3782500
199	Åsnen	SE	243	105,992	3,092	4610500	3717500
203	Tisnaren	SE	792	2,674	668	4670500	3997500
204	Långhalsen	SE	57	3,547	255	4698500	4002500
205	Nedre glottern	SE	1,066	534	23	4679500	3968500
207	Fläten	SE	737	750	122	4682500	3983500
210	Salstern	SE	676	570	83	4619500	3959500
211	Lien	SE	585	672	118	4635500	3970500
213	Ormlången	SE	164	958	375	4658500	3975500
215	Bönnern	SE	132	8,418	1,065	4654500	3970500
217	Vättern	SE	21,197	204,196	6,028	4615500	3947500
218	Tåkern	SE	21,489	2,760	385	4604500	3930500

Lake ID	Name	Country	Retention time (d)[a)]	Population upstream (persons)[b)]	Area upstream (km^2)[b)]	Coordinates	
						X	Y
220	Sommen (East and West)	SE	1,928	30,084	1,914	4618500	3904500
224	Juttern	SE	1,307	13,181	897	4665500	3875500
228	Kisasjön	SE	1,011	4,534	292	4656500	3891500
229	Åsunden	SE	1,095	4,325	694	4656500	3906500
231	Stora rängen	SE	244	3,355	330	4657500	3921500
233	Svinstadsjön	SE	752	204	35	4663500	3932500
234	Roxen	SE	168	198,651	2,662	4668500	3948500
235	Asplången	SE	98	112,257	686	4680500	3948500
236	Hällerstadsjön	SE	43	1,092	154	4679500	3942500
238	Yxningen	SE	6,131	738	310	4700500	3925500
239	Ken	SE	803	277	61	4694500	3934500
240	Strolången	SE	108	2,332	105	4698500	3936500
241	Dabie	PL	5.6	15,341,398	116,882	4629500	3389500

a) Presented retention times are additive. If water from an lake A flows through lake B, retention time for lake A would be the sum of retention times in lakes A and B. E.g. Lakes ID 7 – 10 are connected. As lake 7 is highest upstream, the additive retention time is the sum of retention times in this lake (Rehja-Nuasjärvi) and the ones downstream (1 160 d).

b) Aggregated from the calculation grid.

Annex 3 – Rivers included into the BPL model

River ID	Country	Name	River basin area (km²)[a)]	Flow (m³/a)[b)]	Pop. in riverbasin[b)]	Coordinates	
						X	Y
1	DE	Aalbek	42	1.23E+07	9,804	4373500	3431500
2	LT	Akmena-dane	521	2.14E+08	91,938	5018500	3676500
3	DK	Alling å	236	5.86E+07	13,569	4337500	3700500
4	SE	Alsterån	1,539	3.69E+08	10,355	4712500	3775500
5	SE	Alterälven	456	1.54E+08	2,623	4855500	4744500
6	DK	Arresø kanal	261	4.52E+07	50,852	4448500	3654500
7	FI	Aurajoki	880	2.49E+08	136,820	4992500	4206500
8	DK	Bagge å	22	1.09E+07	297	4622500	3572500
9	LV	Barta	2,077	6.30E+08	31,876	4999500	3752500
10	DE	Barthe	243	4.30E+07	8,887	4498500	3469500
11	DK	Binderup å	88	5.87E+07	2,734	4301500	3765500
12	DK	Bjerge å	59	1.01E+07	3,046	4404500	3575500
13	DK	Bjørnsholm å	97	3.76E+07	2,832	4273500	3753500
14	DK	Blå å - bovrup bæk	34	8.29E+06	1,120	4295500	3544500
15	SE	Botorpsströmmen	1,003	1.98E+08	5,091	4713500	3856500
16	DK	Bredkær bæk	18	6.55E+06	172	4229500	3709500
17	DK	Brende å	104	2.99E+07	12,056	4316500	3585500
18	DK	Bygholm å	154	5.15E+07	15,734	4304500	3640500
19	SE	Dalälven	28,980	1.15E+10	254,591	4728500	4192500
20	DK	Damhusåen	58	1.04E+07	178,553	4479500	3624500
21	LV	Daugava	84,982	1.73E+10	2,354,903	5167500	3855500
22	SE	Delångersån	2,000	5.51E+08	11,877	4696500	4300500
23	DE	Duvenbäk	63	8.36E+06	8,265	4533500	3489500
24	DK	Elling å	124	4.84E+07	4,210	4348500	3818500
25	DK	Elsted bæk	22	3.93E+06	735	4285500	3556500
26	DK	Elverdamsåen	34	1.48E+07	5,573	4434500	3615500
27	SE	Emån	4,483	9.76E+08	75,931	4713500	3798500
28	DK	Esrum å	125	2.68E+07	20,784	4469500	3666500
29	FI	Eurajoki	1,354	2.84E+08	24,333	4943500	4287500
30	DK	Fald å	29	1.23E+07	1,307	4226500	3715500
32	DK	Fiskbæk	12	7.01E+06	265	4296500	3538500
33	DK	Fladmose å	14	1.95E+06	467	4411500	3570500
34	DK	Fladså	23	5.71E+06	756	4439500	3567500
35	SE	Forsmarksån	368	8.32E+07	748	4774500	4164500
36	DK	Fribrødre å	48	8.87E+06	1,932	4450500	3531500
37	DE	Füsinger au	268	8.29E+07	20,008	4297500	3492500
38	LV	Gauja	9,046	2.33E+09	164,185	5179500	3868500
39	SE	Gavleån	2,490	6.00E+08	109,144	4712500	4194500
40	DK	Geels å	44	7.05E+06	4,444	4354500	3591500
41	DK	Gerå	150	5.63E+07	9,106	4341500	3777500
42	SE	Gide älv	3,442	1.20E+09	2,843	4777500	4501500
43	DE	Godderstorfer au	60	9.40E+06	2,509	4390500	3469500
44	PL	Grabowa	552	2.19E+08	15,461	4735500	3496500
45	DK	Græse å	28	4.77E+06	7,913	4454500	3640500
46	DK	Grejs å	70	3.88E+07	3,780	4284500	3624500

River ID	Country	Name	River basin area (km²)[a)]	Flow (m³/a)[b)]	Pop. in riverbasin[b)]	Coordinates	
						X	Y
47	DK	Guden å	2,648	1.02E+09	257,351	4320500	3705500
48	SE	Göta älv	50,774	1.91E+10	1,351,256	4433500	3859500
49	DK	Haderslev møllestrøm	112	5.71E+07	18,210	4288500	3571500
50	DE	Hagener au	128	2.46E+07	7,590	4350500	3467500
51	DK	Halsted å, borge bro	22	5.02E+06	423	4405500	3532500
52	DK	Hansted å	141	4.74E+07	12,634	4309500	3641500
53	DK	Haslevgårds å	86	2.39E+07	2,728	4335500	3744500
54	DK	Hasseris å	46	2.22E+07	5,937	4311500	3769500
55	DK	Havelse å	99	1.83E+07	26,049	4456500	3645500
56	SE	Helge å	4,723	1.43E+09	160,316	4585500	3648500
57	DE	Hellbach	214	3.75E+07	11,446	4427500	3440500
58	DK	Herreds å	174	3.77E+07	11,947	4296500	3753500
59	DK	Hove å	72	9.72E+06	10,689	4456500	3626500
60	DK	Hovedkanal	193	3.50E+07	7,594	4398500	3513500
61	DK	Hulebæk	10	2.24E+06	1,022	4447500	3562500
62	DK	Hundstrup å	55	1.69E+07	4,091	4348500	3555500
63	DK	Hvidbjerg å	260	9.52E+07	7,676	4222500	3750500
64	DK	Hårby å	69	2.13E+07	7,045	4329500	3567500
65	DK	Højbro å	28	7.94E+06	2,584	4456500	3664500
66	DK	Højen å	19	1.37E+07	1,422	4288500	3620500
67	FI	Iijoki	14,312	5.62E+09	21,012	5038500	4772500
68	PL	Ina	2,142	8.79E+08	175,878	4638500	3394500
69	SE	Indalsälven	26,931	1.48E+10	105,197	4705500	4399500
70	LV	Irbe	1,947	1.06E+09	23,916	5042500	3898500
71	DK	Jordbro å	114	3.77E+07	4,742	4271500	3713500
72	EE	Jägala	906	3.33E+08	7,989	5188500	4120500
73	DK	Kær mølle å	3	2.51E+06	56	4290500	3586500
74	DK	Kærs mølleå	103	5.23E+07	11,663	4314500	3765500
75	FI	Kalajoki	4,218	1.45E+09	48,190	4996500	4639500
76	SE	Kalix älv	18,141	1.03E+10	33,874	4924500	4803500
77	FI	Karjaanjoki	2,040	5.56E+08	58,707	5073500	4182500
78	DK	Karup å	654	2.32E+08	19,285	4258500	3712500
79	EE	Kasari	2,658	8.10E+08	25,243	5128500	4037500
80	DK	Kastbjerg å	101	2.70E+07	2,873	4326500	3730500
81	EE	Keila	635	2.11E+08	18,120	5138500	4106500
82	FI	Kemijoki	51,670	1.82E+10	104,509	4986500	4811500
83	DK	Kighanerenden	15	1.19E+06	10,021	4481500	3639500
84	FI	Kiiminginjoki	3,813	1.54E+09	18,375	5039500	4754500
85	FI	Kiskonjoki	1,044	3.12E+08	10,639	5043500	4182500
86	FI	Kokemäenjoki	27,011	7.07E+09	794,389	4942500	4323500
87	DK	Kolding å	298	1.20E+08	26,989	4285500	3599500
88	DK	Korup å	52	3.59E+07	1,152	4325500	3734500
89	DE	Koseler au	52	1.63E+07	5,353	4303500	3489500
90	FI	Koskenkylänjoki	897	2.65E+08	10,734	5190500	4254500
91	DE	Kossau	123	3.01E+07	10,196	4360500	3466500
92	FI	Kuivajoki	1,351	6.10E+08	1,668	5019500	4796500
93	EE	Kunda	413	1.72E+08	2,345	5256500	4139500

River ID	Country	Name	River basin area (km^2)[a)]	Flow (m^3/a)[b)]	Pop. in riverbasin[b)]	Coordinates	
						X	Y
94	FI	Kymijoki	36,588	9.68E+09	542,132	5241500	4265500
95	FI	Kyrönjoki	4,925	1.37E+09	109,659	4917500	4503500
96	DK	Køge å	133	2.34E+07	14,345	4452500	3598500
97	DK	Køng å	65	1.68E+07	3,315	4437500	3559500
98	SE	Lagan	6,455	2.51E+09	118,896	4502500	3719500
99	DK	Lammefjord s kanal	79	1.55E+07	6,349	4422500	3630500
100	DE	Langballigau	50	1.41E+07	3,483	4301500	3522500
101	DK	Langvad å	170	2.94E+07	19,768	4456500	3610500
102	FI	Lapuanjoki	4,126	1.04E+09	57,012	4942500	4550500
103	FI	Lapväärtinjoki	1,095	4.51E+08	5,938	4915500	4395500
105	DK	Lerkenfeld å	118	8.33E+07	3,118	4284500	3736500
106	FI	Lestijoki	1,372	4.08E+08	9,909	4985500	4616500
107	LV	Lielupe	17,674	2.03E+09	512,007	5159500	3845500
108	DK	Lillebæk	7	1.02E+06	841	4368500	3557500
109	DK	Lindenborg å	333	1.17E+08	19,378	4326500	3760500
110	DK	Lindholm å, voerbjerg	156	1.03E+08	10,540	4314500	3775500
111	DK	Lindved å	62	1.58E+07	21,356	4349500	3586500
112	DE	Lippingau	53	1.54E+07	3,864	4308500	3515500
113	SE	Ljungan	12,897	4.34E+09	37,253	4704500	4374500
114	SE	Ljungbyån	773	1.38E+08	22,783	4703500	3741500
115	SE	Ljusnan	19,870	7.26E+09	70,566	4703500	4253500
116	DK	Ll. Vejle å	23	4.59E+06	2,699	4461500	3614500
117	EE	Loobu	203	8.42E+07	3,897	5221500	4139500
118	RU	Luga	13,665	3.32E+09	357,012	5337500	4174500
119	SE	Lule älv	25,464	1.70E+10	43,670	4878500	4768500
121	DK	Lyby-grønning grøft	16	1.83E+06	1,511	4261500	3727500
122	SE	Lyckebyån	801	1.91E+08	16,988	4672500	3691500
123	SE	Lögde älv	1,639	6.30E+08	1,605	4788500	4526500
124	DK	Mademose å	7	5.88E+05	893	4447500	3635500
125	DK	Maglemose å	16	3.53E+06	4,103	4455500	3621500
126	DK	Marrebæksrende	20	3.50E+06	420	4398500	3533500
127	DE	Maurine	128	2.54E+07	4,879	4387500	3415500
128	DK	Mern å	38	9.35E+06	1,662	4454500	3549500
129	SE	Motala ström	15,466	3.18E+09	582,592	4669500	3949500
130	FI	Mustijoki	789	2.12E+08	24,773	5173500	4232500
131	DK	Mølle å	116	1.70E+07	120,314	4480500	3635500
132	SE	Mörrumsån	3,387	9.06E+08	114,779	4616500	3683500
133	DK	Nældevads å	30	6.69E+06	1,091	4413500	3526500
134	RU	Narva	71,822	1.30E+10	845,651	5333500	4170500
135	DK	Ndr. Halleby å	417	8.14E+07	25,335	4401500	3608500
136	LT	Nemunas	92,504	1.53E+10	4,160,035	5069500	3618500
137	RU	Neva	281,071	7.26E+10	5,707,947	5442500	4258500
138	SE	Nissan	2,705	1.40E+09	87,788	4496500	3732500
139	DK	Nive å	59	1.31E+07	7,420	4477500	3652500
140	SE	Norrström	22,634	5.28E+09	1,876,097	4779500	4050500
152	SE	Nyköpingsån	3,625	7.18E+08	84,838	4726500	3981500
153	FI	Närpiönjoki	979	3.05E+08	10,717	4904500	4416500

River ID	Country	Name	River basin area (km^2)[a)]	Flow (m^3/a)[b)]	Pop. in riverbasin[b)]	Coordinates	
						X	Y
154	DK	Odense å	536	1.56E+08	91,959	4346500	3587500
155	PL	Oder	119,544	1.69E+10	15,547,872	4624500	3397500
156	DE	Oldenburger graben	122	1.77E+07	14,896	4391500	3459500
157	FI	Oulujoki	2,3013	8.55E+09	156,938	5048500	4737500
158	FI	Paimionjoki	1,088	2.91E+08	25,656	5015500	4208500
159	PL	Parseta	3,084	8.45E+08	174,445	4683500	3466500
160	PL	Pasleka	2,280	5.05E+08	93,999	4956500	3519500
161	DE	Peene	5,041	5.99E+08	245,257	4563500	3423500
162	FI	Perhonjoki	2,538	7.48E+08	20,325	4966500	4591500
163	EE	Pirita	797	2.20E+08	52,200	5159500	4128500
164	SE	Pite älv	11,344	5.77E+09	10,059	4848500	4738500
165	FI	Porvoonjoki	1,291	3.66E+08	101,525	5179500	4238500
166	RU	Pregolya	14,086	2.35E+09	892,549	4993500	3573500
167	EE	Pudisoo	119	3.38E+07	861	5199500	4145500
168	DK	Pulverbæk	6	2.94E+06	151	4316500	3535500
169	EE	Purtse	787	2.15E+08	16,580	5281500	4146500
170	EE	Pühajõgi	213	5.54E+07	31,900	5306500	4157500
171	FI	Pyhäjoki	3,687	1.07E+09	29,047	5003500	4667500
172	EE	Pärnu	5,204	1.61E+09	73,076	5177500	4018500
173	DK	Rævs å	85	4.38E+07	13,900	4334500	3647500
174	DE	Recknitz	664	1.08E+08	26,621	4481500	3463500
175	PL	Reda	502	1.41E+08	116,200	4865500	3535500
176	PL	Rega	2,723	6.06E+08	132,533	4663500	3459500
177	SE	Rickleån	1,639	5.26E+08	3,797	4853500	4598500
178	DK	Ringe å	24	8.94E+06	1,372	4339500	3606500
179	DK	ROHDEN Å, 300 m NS Årup Mølle Dambrug	99	3.65E+07	10,028	4304500	3621500
180	DK	Romdrup å	27	1.28E+07	3,531	4322500	3767500
181	DK	Ry å	302	1.09E+08	20,728	4311500	3796500
182	DE	Ryck	199	2.44E+07	11,107	4532500	3453500
183	DK	Ryde å	93	1.44E+07	3,200	4394500	3523500
184	SE	Råne älv	4,213	1.59E+09	3,842	4884500	4798500
185	SE	Råån	190	5.41E+07	23,991	4493500	3658500
186	SE	Rönne å	1,886	6.11E+08	94,360	4497500	3688500
187	LV	Saka	1,102	6.85E+08	14,277	5001500	3806500
188	DK	Sakskøbing å	37	1.37E+07	957	4429500	3512500
189	LV	Salaca	3,422	2.24E+09	27,978	5171500	3936500
190	DK	Saltø å	154	3.10E+07	7,366	4425500	3570500
191	DE	Schwartau	227	5.79E+07	31,790	4368500	3423500
192	DE	Schwentine	753	2.00E+08	125,081	4333500	3468500
193	DK	Seerdrup å	53	1.25E+07	2,715	4404500	3580500
194	RU	Seleznevka	624	1.15E+08	26,356	5327500	4315500
195	EE	Seljajõgi	432	1.27E+08	25,082	5240500	4155500
196	FI	Siikajoki	4,332	1.38E+09	13,905	5018500	4711500
197	DK	Simested å	217	7.54E+07	9,205	4285500	3723500
198	FI	Simojoki	3,168	1.58E+09	2,748	5012500	4800500
199	DK	Skals å	556	1.47E+08	20,264	4289500	3718500

River ID	Country	Name	River basin area (km²)[a)]	Flow (m³/a)[b)]	Pop. in riverbasin[b)]	Coordinates	
						X	Y
200	SE	Skellefte älv	11,783	5.55E+09	51,174	4851500	4665500
201	PL	Slupia	1,620	5.27E+08	192,996	4763500	3518500
202	DK	Solkær å	29	8.74E+06	2,325	4293500	3597500
203	DK	Spang å	60	2.23E+07	3,827	4297500	3603500
204	DK	St. Vejle å	58	1.21E+07	79,018	4470500	3616500
205	DK	Stavis å	83	2.01E+07	6,071	4338500	3592500
206	DE	Stepenitz	702	9.06E+07	35,893	4386500	3419500
207	DK	Stokkebækken	44	1.93E+07	2,167	4370500	3563500
208	DK	Storå, bromølle	117	5.44E+07	970	4246500	3769500
209	DK	Storå, møllebro	139	3.57E+07	9,144	4320500	3598500
210	DK	Suså	759	1.83E+08	76,835	4428500	3578500
211	LT	Sventoji	501	1.69E+08	8,325	5008500	3711500
212	DK	Søborg kanal	59	1.37E+07	8,713	4461500	3670500
213	DK	Taps å	76	2.39E+07	4,163	4289500	3581500
214	DK	Tingsted å	40	1.08E+07	1,064	4442500	3526500
215	FI	Torne älv - tornionjoki	40,528	1.39E+10	71,805	4970500	4812500
216	DK	Tranegård lille å	23	5.06E+06	832	4456500	3569500
217	DE	Trave	927	2.43E+08	138,658	4363500	3416500
218	DK	Trend å	146	4.74E+07	7,769	4272500	3747500
219	DK	Tryggevaelde å	126	2.89E+07	6,248	4459500	3583500
220	DK	Tubæk	57	1.20E+07	2,184	4447500	3560500
221	DK	Tude å	260	5.78E+07	42,758	4403500	3592500
222	DK	Tuse å	104	2.25E+07	7,795	4420500	3621500
223	SE	Töre å	454	1.74E+08	1,124	4897500	4808500
224	DE	Uecker	2,477	2.21E+08	103,905	4588500	3411500
225	SE	Ume älv	27,058	1.45E+10	103,121	4830500	4554500
226	FI	Uskelanjoki	568	1.81E+08	30,102	5041500	4208500
227	DK	Usserød å	71	1.92E+07	39,535	4477500	3648500
228	DK	Værebro å	108	1.77E+07	69,542	4460500	3628500
229	EE	Valgejõgi	386	1.23E+08	4,989	5209500	4139500
230	DE	Wallensteingraben	175	4.24E+07	12,906	4418500	3421500
231	FI	Vantaanjoki	1,697	4.98E+08	443,494	5146500	4213500
232	DE	Warnow	3,111	4.51E+08	157,452	4462500	3442500
233	DK	Vejerslev bæk	19	7.53E+06	786	4241500	3737500
234	DK	Vejle å	221	1.22E+08	1,0171	4285500	3621500
235	DK	Vejstrup å	48	1.19E+07	3,254	4367500	3554500
236	LV	Venta	11,776	2.84E+09	335,509	5014500	3866500
237	DK	Viby å	29	1.43E+07	3,865	4311500	3593500
238	PL	Wieprza	2,208	5.06E+08	80,310	4734500	3499500
239	EE	Vihterpalu	471	1.37E+08	858	5108500	4093500
240	DK	Villestrup å	126	4.64E+07	5269	4320500	3731500
241	DK	Vindinge å	128	3.14E+07	11,117	4361500	3582500
242	FI	Virojoki	358	1.39E+08	1,282	5281500	4286500
243	SE	Viskan	2,222	1.33E+09	131,332	4454500	3793500
244	PL	Vistula	193,335	3.40E+10	23,232,687	4901500	3502500
245	DK	Vium mølleå	29	1.08E+07	1,350	4257500	3731500
246	DK	Voer å	244	9.64E+07	7,343	4346500	3790500
247	EE	Vääna	212	7.89E+07	44,832	5142500	4115500

River ID	Country	Name	River basin area (km^2)[a)]	Flow (m^3/a)[b)]	Pop. in riverbasin[b)]	Coordinates	
						X	Y
248	DE	Zarow	756	6.44E+07	20,993	4585500	3412500
249	SE	Ångermanälven	32,123	1.66E+10	42,949	4715500	4458500
250	DK	Århus å	329	8.91E+07	156,728	4332500	3672500
251	SE	Ätran	3,331	1.75E+09	66,203	4473500	3757500
252	SE	Öre älv	3,014	1.16E+09	4,056	4806500	4525500
253	DK	Østerbæk	10	7.88E+05	399	4476500	3665500
256	PL	Leba	2,340	6.74E+08	129,977	4807500	3542500

a) Aggregated from the calculation grid.
b) HELCOM 2018b

Annex 4 – API-sales

API	Sales	Average sales (kg/a) [a)]									
		DE[1)]	**DK[2)]**	**EE[1)]**	**FI[1)]**	**LT[3)]**	**LV[1)]**	**PL[3)]**	**RU[4)]**	**SE[1)]**	**Overall[5)]**
Antibiotics											
Ciprofloxacin	Total (kg/a)	23,400	1,160	351	290	244	659	9,530	-	2,670	38,300
	Per capita (mg/d/pers.)	0.783	0.557	0.730	0.145	0.232	0.917	0.688	-	0.743	0.714
Clarithromycin	Total (kg/a)	11,000	469	412	216	192	450	8,610	-	628	22,000
	Per capita (mg/d/pers.)	0.368	0.225	0.858	0.108	0.182	0.626	0.621	-	0.174	0.409
Doxycycline	Total (kg/a)	4,480	143	1,560	486	-	168	-	-	466	7,300
	Per capita (mg/d/pers.)	0.150	0.0687	3.24	0.243	-	0.233	-	-	0.129	0.188
Erythromycin	Total (kg/a)	14,600	361	1.5	47.7	2.6	40.9	-	-	545	15,600
	Per capita (mg/d/pers.)	0.487	0.173	0.00312	0.0238	0.00247	0.0569	-	-	0.151	0.390
Fluconazole	Total (kg/a)	433	197	15.4	123	-	23.6	-	-	186	978
	Per capita (mg/d/pers.)	0.0145	0.0946	0.0320	0.0612	-	0.0328	-	-	0.0518	0.0252
Lincomycin	Total (kg/a)	-	-	197	149	-	15.1	-	-	0	361
	Per capita (mg/d/pers.)	-	-	0.411	0.0743	-	0.0210	-	-	0	0.0531
Norfloxacin	Total (kg/a)	355	-	79.7	1.8	-	100	-	-	22.4	559
	Per capita (mg/d/pers.)	0.0119	-	0.166	8.99e-04	-	0.140	-	-	0.00623	0.0152
Ofloxacin[b)]	Total (kg/a)	481	0.017	3.67	10.8	-	26.6	-	-	0.0129	522
	Per capita (mg/d/pers.)	0.0161	8.16e-06	0.00764	0.00538	-	0.0370	-	-	3.59e-06	0.0135

API	Sales	Average sales (kg/a) [a)]									
		DE[1)]	**DK[2)]**	**EE[1)]**	**FI[1)]**	**LT[3)]**	**LV[1)]**	**PL[3)]**	**RU[4)]**	**SE[1)]**	**Overall[5)]**
Sulfadiazine	Total (kg/a)	3,070	6.85	81.5	382	-	2.55	-	-	0.477	3,540
	Per capita (mg/d/pers.)	0.103	0.00329	0.170	0.191	-	0.00355	-	-	1.32e-04	0.0912
Sulfamethoxazole	Total (kg/a)	16,700	349	407	389	137	1,020	5,680	-	0.000933	24,700
	Per capita (mg/d/pers.)	0.560	0.168	0.847	0.194	0.130	1.43	0.410	-	2.59e-07	0.460
Tetracycline	Total (kg/a)	48,300	1,590	0.26	1,090	-	2.15	-	-	270	51,300
	Per capita (mg/d/pers.)	1.62	0.761	5.41e-04	0.542	-	0.00300	-	-	0.075	1.32
Trimethoprim	Total (kg/a)	4,710	478	83.5	911	-	212	-	-	192	6,580
	Per capita (mg/d/pers.)	0.157	0.229	0.174	0.455	-	0.295	-	-	0.0532	0.170
Antiepileptics											
Carbamazepine	Total (kg/a)	36,600	1,820	1,040	3,070	589	1,430	27,200	-	5,590	77,400
	Per capita (mg/d/pers.)	1.22	0.875	2.16	1.53	0.559	1.98	1.96	-	1.55	1.44
Gabapentin	Total (kg/a)	82,800	12,700	797	8,210	-	2,150	-	-	14,800	121,000
	Per capita (mg/d/pers.)	2.77	6.08	1.66	4.10	-	2.99	-	-	4.12	3.13
Levetiracetam	Total (kg/a)	126,000	5,610	278	6,760	-	263	-	-	8,400	147,000
	Per capita (mg/d/pers.)	4.20	2.69	0.578	3.38	-	0.366	-	-	2.33	3.79
Primidone	Total (kg/a)	5,320	90.8	33.1	-	-	2.54	-	-	1.96	5,450
	Per capita (mg/d/pers.)	0.178	0.0436	0.0689	-	-	0.00353	-	-	5.43e-04	0.148
Antihypertensives											
Amlodipine	Total (kg/a)	9,470	733	161	604	-	223	-	-	945	12,100
	Per capita (mg/d/pers.)	0.317	0.352	0.335	0.301	-	0.311	-	-	0.262	0.313

API	Sales	Average sales (kg/a) [a)]									
		DE[1)]	**DK[2)]**	**EE[1)]**	**FI[1)]**	**LT[3)]**	**LV[1)]**	**PL[3)]**	**RU[4)]**	**SE[1)]**	**Overall[5)]**
Candesartan	Total (kg/a)	10,500	66	49	648	-	17.7	-	-	1,340	12,600
	Per capita (mg/d/pers.)	0.35	0.0317	0.102	0.324	-	0.0247	-	-	0.372	0.324
Enalapril	Total (kg/a)	5,550	1,200	143	788	-	167	-	-	1,960	9,810
	Per capita (mg/d/pers.)	0.185	0.576	0.297	0.393	-	0.232	-	-	0.545	0.253
Eprosartan	Total (kg/a)	7,800	-	2.39	1,040	-	2.49	-	-	82.1	8,930
	Per capita (mg/d/pers.)	0.261	-	0.00498	0.521	-	0.00347	-	-	0.0228	0.243
Hydrochlorothiazide	Total (kg/a)	53,800	1,690	264	2,060	-	265	-	-	551	58,700
	Per capita (mg/d/pers.)	1.8	0.810	0.549	1.03	-	0.368	-	-	0.153	1.51
Irbesartan	Total (kg/a)	19,000	179	0	-	-	30.1	-	-	1,140	20,300
	Per capita (mg/d/pers.)	0.635	0.0859	0	-	-	0.0419	-	-	0.317	0.553
Losartan	Total (kg/a)	10,500	8,780	177	5,450	-	194	-	-	6,700	31,800
	Per capita (mg/d/pers.)	0.352	4.22	0.368	2.72	-	0.270	-	-	1.86	0.821
Ramipril	Total (kg/a)	11,700	276	82.8	367	-	56.4	-	-	253	12,800
	Per capita (mg/d/pers.)	0.392	0.132	0.172	0.183	-	0.0784	-	-	0.0702	0.329
Telmisartan	Total (kg/a)	6,900	32	1,030	1,140	-	510	-	-	51.9	9,670
	Per capita (mg/d/pers.)	0.231	0.0154	2.14	0.571	-	0.709	-	-	0.0144	0.249
Valsartan	Total (kg/a)	87,500	150	331	4,560	-	336	-	-	1,380	94,200
	Per capita (mg/d/pers.)	2.92	0.0722	0.690	2.28	-	0.467	-	-	0.382	2.43
Asthma and allergy medications											
Cetirizine [c)]	Total (kg/a)	143	382	34	645	-	20.2	-	-	718	1,940

API	Sales	Average sales (kg/a) [a)]									
		DE[1)]	**DK[2)]**	**EE[1)]**	**FI[1)]**	**LT[3)]**	**LV[1)]**	**PL[3)]**	**RU[4)]**	**SE[1)]**	**Overall[5)]**
	Per capita (mg/d/pers.)	0.00477	0.184	0.0708	0.322	-	0.0281	-	-	0.199	0.0501
Fexofenadine	Total (kg/a)	2,420	1,660	-	639	-	0.123	-	-	535	5,260
	Per capita (mg/d/pers.)	0.0809	0.800	-	0.319	-	1.72e-04	-	-	0.149	0.137
Fluticasone	Total (kg/a)	-	13.9	0.332	14.4	-	1.31	-	-	3.28	33.3
	Per capita (mg/d/pers.)	-	0.00669	6.91e-04	0.00721	-	0.00183	-	-	9.12e-04	0.00375
Mometasone	Total (kg/a)	75	10.9	-	10.8	-	1.7	-	-	34.6	133
	Per capita (mg/d/pers.)	0.00251	0.00523	-	0.00539	-	0.00237	-	-	0.00962	0.00347
Xylometazoline	Total (kg/a)	108	25.1	13.3	14.9	-	9.9	-	-	77.1	249
	Per capita (mg/d/pers.)	0.00362	0.0120	0.0277	0.00746	-	0.0138	-	-	0.0214	0.00641
Gastrointestinal disease medications											
Omeprazole/esomeprazole	Total (kg/a)	16,100	942	260	1,340	-	455	-	-	6,050	25,100
	Per capita (mg/d/pers.)	0.538	0.452	0.541	0.667	-	0.633	-	-	1.68	0.648
Mesalazine	Total (kg/a)	108,000	17,600	762	19,100	-	459	-	-	30,800	177,000
	Per capita (mg/d/pers.)	3.62	8.47	1.59	9.54	-	0.638	-	-	8.56	4.56
Pantoprazole	Total (kg/a)	54,100	2,370	170	2,450	-	219	-	-	326	59,600
	Per capita (mg/d/pers.)	1.81	1.14	0.354	1.22	-	0.304	-	-	0.0905	1.54
Hormones											
Estriol (E3)	Total (kg/a)	478	0.678	30.5	2.63	-	0.0276	-	-	8.05	520
	Per capita (mg/d/pers.)	0.0160	3.25e-04	0.0634	0.00131	-	3.85e-05	-	-	0.00224	0.0134
Estrone (E1)	Total (kg/a)	0	-	-	-	-	-	-	-	0	0

API	Sales	Average sales (kg/a) [a)]									
		DE[1)]	**DK[2)]**	**EE[1)]**	**FI[1)]**	**LT[3)]**	**LV[1)]**	**PL[3)]**	**RU[4)]**	**SE[1)]**	**Overall[5)]**
	Per capita (mg/d/pers.)	0	-	-	-	-	-	-	-	0	0
Norethisterone	Total (kg/a)	97.8	3.88	0.476	15	-	1.15	-	-	14.8	133
	Per capita (mg/d/pers.)	0.00327	0.00186	9.92e-04	0.00747	-	0.00160	-	-	0.00412	0.00343
Progesterone	Total (kg/a)	2,250	76.1	25.8	119	-	116	-	-	127	2,710
	Per capita (mg/d/pers.)	0.0751	0.0366	0.0536	0.0593	-	0.161	-	-	0.0354	0.0698
Testosterone	Total (kg/a)	2,360	75.2	1.81	117	-	4.14	-	-	277	2,840
	Per capita (mg/d/pers.)	0.0789	0.0361	0.00377	0.0586	-	0.00576	-	-	0.0770	0.0731
Metabolic disease medications											
Allopurinol	Total (kg/a)	132,000	3,400	872	2,810	-	705	-	-	4,720	145,000
	Per capita (mg/d/pers.)	4.41	1.63	1.82	1.40	-	0.982	-	-	1.31	3.73
Atorvastatin	Total (kg/a)	12,200	2,750	174	1,620	-	655	-	-	4,020	21,500
	Per capita (mg/d/pers.)	0.409	1.32	0.362	0.806	-	0.911	-	-	1.12	0.553
Bezafibrate	Total (kg/a)	8,140	-	-	79.3	-	-	-	-	316	8,530
	Per capita (mg/d/pers.)	0.272	-	-	0.0396	-	-	-	-	0.0877	0.240
Gemfibrozil	Total (kg/a)	0	1350	-	76.2	-	-	-	-	830	2,260
	Per capita (mg/d/pers.)	0	0.650	-	0.0380	-	-	-	-	0.230	0.0601
Metformin	Total (kg/a)	1,620,000	91,800	22,800	149,000	27,700	29,200	669,000	-	115,000	2,720,000
	Per capita (mg/d/pers.)	54.0	44.1	47.5	74.6	26.3	40.7	48.2	-	31.8	50.6
Simvastatin	Total (kg/a)	40,600	4,010	88.5	2,480	-	8.76	-	-	4,090	51,200

API	Sales	Average sales (kg/a) [a)]									
		DE[1)]	**DK[2)]**	**EE[1)]**	**FI[1)]**	**LT[3)]**	**LV[1)]**	**PL[3)]**	**RU[4)]**	**SE[1)]**	**Overall[5)]**
	Per capita (mg/d/pers.)	1.36	1.93	0.184	1.24	-	0.0122	-	-	1.14	1.32
NSAIDs and analgesics											
Codeine	Total (kg/a)	653	1,170	148	1,640	-	60.6	-	-	1,630	5,300
	Per capita (mg/d/pers.)	0.0218	0.560	0.307	0.818	-	0.0844	-	-	0.453	0.137
Diclofenac	Total (kg/a)	26,900	910	1,510	2,460	744	1,950	7,980	20,000	2,800	65,200
	Per capita (mg/d/pers.)	0.898	0.437	3.14	1.23	0.706	2.72	0.576	0.374	0.779	0.608
Ibuprofen	Total (kg/a)	340,000	6,3500	15,200	122,000	5,780	20,400	8,490	-	116,000	691,000
	Per capita (mg/d/pers.)	11.4	30.5	31.6	60.7	5.48	28.3	0.613	-	32.3	12.9
Ketoprofen	Total (kg/a)	205	1.74	227	381	-	84.5	-	-	1,800	2,700
	Per capita (mg/d/pers.)	0.00687	8.36e-04	0.472	0.190	-	0.118	-	-	0.500	0.0696
Naproxen	Total (kg/a)	17,200	2,360	1,900	7,730	391	762	29,600	-	21,800	81,700
	Per capita (mg/d/pers.)	0.574	1.13	3.95	3.86	0.371	1.06	2.14	-	6.05	1.52
Oxycodone	Total (kg/a)	-	341	11.5	255	-	0.0074	-	-	625	1,230
	Per capita (mg/d/pers.)	-	0.164	0.0239	0.127	-	1.03e-05	-	-	0.173	0.139
Paracetamol	Total (kg/a)	32,400	422,000	18,700	205,000	2,800	14,900	-	-	547,000	1,240,000
	Per capita (mg/d/pers.)	1.08	202	38.8	102	2.65	20.7	-	-	152	31.2
Tramadol	Total (kg/a)	21,400	6,420	322	1,720	-	360	-	-	3,490	33,800
	Per capita (mg/d/pers.)	0.717	3.08	0.670	0.861	-	0.501	-	-	0.968	0.870
Other											
Caffeine	Total (kg/a)	492	1,780	125	59.4	-	736	-	-	148	3,340

API	Sales	Average sales (kg/a) [a)]									
		DE[1)]	**DK[2)]**	**EE[1)]**	**FI[1)]**	**LT[3)]**	**LV[1)]**	**PL[3)]**	**RU[4)]**	**SE[1)]**	**Overall[5)]**
	Per capita (mg/d/pers.)	0.0164	0.857	0.260	0.0297	-	1.02	-	-	0.0412	0.0862
Other cardiovascular medicines											
Atenolol	Total (kg/a)	3,500	412	28.4	348	12.1	24.3	733	-	2,460	7,520
	Per capita (mg/d/pers.)	0.117	0.198	0.0592	0.174	0.0115	0.0338	0.0529	-	0.683	0.140
Bisoprolol	Total (kg/a)	9,010	50.3	8.61	788	-	151	-	-	305	10,300
	Per capita (mg/d/pers.)	0.301	0.0241	0.0179	0.394	-	0.211	-	-	0.0848	0.266
Dipyridamole	Total (kg/a)	680	2,530	0.0300	3,930	-	0.211	-	-	1,700	8,840
	Per capita (mg/d/pers.)	0.0227	1.22	6.25e-05	1.96	-	2.93e-04	-	-	0.472	0.228
Metoprolol	Total (kg/a)	143,000	7,220	1,720	3,900	1,790	1,390	3,120	-	11,200	173,000
	Per capita (mg/d/pers.)	4.78	3.47	3.59	1.95	1.70	1.94	0.225	-	3.11	3.22
Nebivolol	Total (kg/a)	920	7.94	48.6	16.3	-	53.3	-	-	0.00854	1,050
	Per capita (mg/d/pers.)	0.0307	0.00382	0.101	0.00814	-	0.0742	-	-	2.37e-06	0.0269
Sotalol	Total (kg/a)	2,240	64.9	110	169	-	57.7	-	-	336	2,980
	Per capita (mg/d/pers.)	0.0749	0.0312	0.228	0.0842	-	0.0803	-	-	0.0932	0.0767
Warfarin	Total (kg/a)	25	122	25.2	243	-	30.1	-	-	234	679
	Per capita (mg/d/pers.)	8.36e-04	0.0585	0.0524	0.122	-	0.0419	-	-	0.0649	0.0175
Psycopharmaceuticals											
Citalopram (Escitalopram)	Total (kg/a)	6,840	876	14.1	729	-	10	-	-	1,620	10,100
	Per capita (mg/d/pers.)	0.229	0.421	0.0295	0.364	-	0.0140	-	-	0.450	0.260
Olanzapine	Total (kg/a)	419	66.9	8.99	119	-	9.77	-	-	768	1,390

API	Sales	Average sales (kg/a) [a)]									
		DE[1)]	**DK[2)]**	**EE[1)]**	**FI[1)]**	**LT[3)]**	**LV[1)]**	**PL[3)]**	**RU[4)]**	**SE[1)]**	**Overall[5)]**
	Per capita (mg/d/pers.)	0.014	0.0321	0.0187	0.0596	-	0.0136	-	-	0.213	0.0359
Oxazepam	Total (kg/a)	-	213	1.12	538	4.04	20.8	-	-	0.567	777
	Per capita (mg/d/pers.)	-	0.102	0.00233	0.268	0.00384	0.0289	-	-	0.000157	0.0782
Quetiapine	Total (kg/a)	23,400	2,610	438	4,250	-	462	-	-	4,150	35,300
	Per capita (mg/d/pers.)	0.783	1.25	0.912	2.12	-	0.643	-	-	1.15	0.911
Risperidone	Total (kg/a)	185	10.3	1.51	18.3	3.46	3.32	45.6	-	15	283
	Per capita (mg/d/pers.)	0.00619	0.00496	0.00315	0.00912	0.00329	0.00463	0.00329	-	0.00418	0.00526
Sertraline	Total (kg/a)	6,710	1,990	84.6	744	-	35.5	-	-	4,990	14,600
	Per capita (mg/d/pers.)	0.224	0.956	0.176	0.371	-	0.0494	-	-	1.39	0.375
Temazepam	Total (kg/a)	-	-	-	308	-	-	-	-	-	308
	Per capita (mg/d/pers.)	-	-	-	0.154	-	-	-	-	-	0.154
Venlafaxine	Total (kg/a)	19,000	2,360	116	1,960	-	56.5	-	-	3,550	27,100
	Per capita (mg/d/pers.)	0.636	1.13	0.241	0.980	-	0.0787	-	-	0.986	0.698

1) Ek Henning et al. 2020
2) The Danish Health Data Authority 2020
3) Kaiser et al. 2019
4) HELCOM 2014
5) Calculated from countries for which information was available
a) The years covered by the data vary
b) Ofloxacin sales presented here cover only sales as the racemic mixture ofloxacin. I.e. the figure does not include enantiopure forms.
c) Sales of levocetirizine and 45% of the sales of hydroxyzine have been included into cetirizine sales, due to levocetirizine being an enantiopure form of cetirizine, and 45% of hydroxyzine being metabolized into cetirizine.

Annex 5 – Calculated concentrations in influent wastewater

API	Excr[a)]	PEC_{inf} [ng/L]								
		FI	SE	DE	LV	EE	PL	LT	DK	RU
Allopurinol	0.15	1,510	1,400	5,260	1,230	2,160	4,660[b)]	4,610[b)]	1,950	4,680[b)]
Amlodipine	0.2	428	369	481	491	509	494[b)]	490[b)]	535	496[b)]
Atenolol	1	1,200	4,670	793	231	401	362	78.5	1,340	958[b)]
Atorvastatin	0.01	95.6	132	111	299	98.2	183[b)]	175[b)]	359	186[b)]
Bezafibrate	0.5	138	302	950	853[b)]	839[b)]	853[b)]	850[b)]	839[b)]	855[b)]
Bisoprolol	0.5	1,370	292	1,050	748	62.6	944[b)]	940[b)]	84.3	945[b)]
Candesartan	0.8	1,790	2,040	1,910	136	557	1,790[b)]	1,790[b)]	173	1,790[b)]
Carbamazepine	0.03	392	394	493	913	869	908	251	353	675[b)]
Cetirizine	0.6	1,340	822	19.8	118	294	211[b)]	210[b)]	762	211[b)]
Ciprofloxacin	1	1,000	5,080	5,310	6,260	4,950	4,700	1,580	3,770	4,880[b)]
Citalopram (Escitalopram)	0.15	393	480	272	17.4	35.1	325[b)]	322[b)]	501	327[b)]
Clarithromycin	0.3	227	364	800	1,400	1,870	1,390	404	490	918[b)]
Diclofenac	0.615	5,250	3,290	3,810	11,700	13,400	2,480	3,030	1,860	1,610
Dipyridamole	0.01	233	55.7	6.17	0.0964	0.017	75.5[b)]	72.2[b)]	330	76.8[b)]
Doxycycline	0.45	761	402	473	751	10,300	606[b)]	603[b)]	217	607[b)]
Enalapril	0.2	559	767	282	366	452	399[b)]	396[b)]	875	401[b)]
Eprosartan	0.9	3240	140	1,600	21.4	30.5	1,500[b)]	1,500[b)]	1,490[b)]	1,500[b)]
Erythromycin	0.1	17.5	110	420	52.3	2.7	360[b)]	2.24	150	362[b)]
Estriol (E3)	0.05	0.517	0.87	8.54	0.0227	33.9	7.96[b)]	7.77[b)]	0.174	8.04[b)]
Fexofenadine	0.8	1770	814	442	0.948	750[b)]	758[b)]	756[b)]	4,370	759[b)]
Fluconazole	0.8	339	284	79.1	181	175	139[b)]	139[b)]	517	139[b)]
Fluticasone	0.01	0.854	0.107	1.02[b)]	0.6	0.188	1.24[b)]	1.19[b)]	1.81	1.26[b)]
Gabapentin	1	28,300	28,200	18,800	20,500	11,300	21,400[b)]	21,400[b)]	41,200	21,400[b)]
Gemfibrozil	0.06	17.5	105	0	39.5[b)]	36.1[b)]	39.7[b)]	38.8[b)]	390	40[b)]
Hydrochlorothiazide	1	7,100	1,050	12,200	2,520	3,720	10,300[b)]	10,300[b)]	5,490	10,300[b)]
Ibuprofen	0.01	7,200	3,810	3,080	9,310	8,570	203	1,740	8,280	4,340[b)]

API	Excr[a)]	PEC_{inf} [ng/L]								
		FI	SE	DE	LV	EE	PL	LT	DK	RU
Irbesartan	0.05	217 [b)]	123	339	24.8	0	328 [b)]	321 [b)]	45.9	332 [b)]
Ketoprofen	0.01	22.5	58.9	1.86	38.6	128	23.1 [b)]	22.1 [b)]	0.227	23.5 [b)]
Levetiracetam	0.7	16,400	11,200	20,200	1,780	2,780	18,400 [b)]	18,400 [b)]	12,900	18,500 [b)]
Losartan	0.04	882	598	165	142	172	434 [b)]	422 [b)]	1,980	438 [b)]
Mesalazine	0.8	52,800	46,900	19,800	3,520	8,670	25,200 [b)]	25,100 [b)]	46,200	25,200 [b)]
Metformin	1	515,000	217,000	366,000	278,000	322,000	330,000	180,000	299,000	346,000 [b)]
Metoprolol	0.05	766	1,210	2,550	1,150	1,920	134	983	1,850	1,930 [b)]
Mometasone	0.5	18.8	33.1	8.75	8.41	12.1 [b)]	12.3 [b)]	12.3 [b)]	18.3	12.3 [b)]
Naproxen	0.5	13,400	20,800	2,000	3,760	13,800	7,590	1,310	3,960	5,410 [b)]
Nebivolol	0.05	3.2	9.23e-04	16.4	43.9	54.1	16 [b)]	15.6 [b)]	2.04	16.2 [b)]
Norethisterone	0.05	2.94	1.6	1.75	0.948	0.53	2.04 [b)]	1.99 [b)]	0.996	2.06 [b)]
Norfloxacin	0.35	2.2	15.1	29.7	358	416	39.1 [b)]	38.8 [b)]	38.2 [b)]	39.2 [b)]
Ofloxacin	0.9	33.4	0.0221	98.5	228	46.8	83.2	83	0.05	83.3 [b)]
Olanzapine	0.07	31.6	112	9.32	9.83	12.5	26 [b)]	25.5 [b)]	21.4	26.2 [b)]
Omeprazole/esomeprazole	0.01	79.1	198	146	208	147	215 [b)]	205 [b)]	123	218 [b)]
Paracetamol	0.03	26,200	38,500	436	9,540	15,600	14,400 [b)]	1,190	81,600	14,600 [b)]
Progesterone	0.05	23.3	13.8	40.1	95.4	28.7	41.5 [b)]	40.5 [b)]	19.5	41.9 [b)]
Quetiapine	0.05	834	449	418	380	488	541 [b)]	528 [b)]	669	547 [b)]
Risperidone	0.15	9.84	4.46	7.37	5.78	3.76	4.11	4.07	5.91	6.62 [b)]
Sertraline	0.01	44	163	60.9	16.2	47.8	124 [b)]	119 [b)]	260	127 [b)]
Simvastatin	0.05	486	443	724	7.21	98.5	785 [b)]	766 [b)]	1030	792 [b)]
Sotalol	1	582	637	507	549	1,550	524 [b)]	523 [b)]	211	525 [b)]
Sulfadiazine	0.8	1,060	0.725	560	19.6	928	504 [b)]	503 [b)]	18	504 [b)]
Sulfamethoxazole	0.2	276	3.65e-04	851	2,250	1,290	648	203	255	730 [b)]
Telmisartan	0.5	1,990	49.6	806	2,520	7470	885 [b)]	881 [b)]	53.7	886 [b)]
Testosterone	0.1	43.1	56.1	68.1	5.3	3.25	67.5 [b)]	66.4	31.2	67.9 [b)]
Tetracycline	0.6	2,260	309	6,700	12.6	2.25	5,560 [b)]	5,540 [b)]	3,160	5,570 [b)]
Tramadol	0.1	634	705	618	461	578	803	790	2,660	808 [b)]
Trimethoprim	0.5	1,580	183	549	1,050	608	602 [b)]	600 [b)]	801	603 [b)]
Valsartan	0.8	12,600	2,090	16,000	2,580	3,770	13,400 [b)]	13,400 [b)]	395	13,400 [b)]

API	Excr[a)]	PEC_{inf} [ng/L]								
		FI	SE	DE	LV	EE	PL	LT	DK	RU
Warfarin	0.01	14.4	7.65	0.227	13.8	14.2	5.8 [b)]	5.55 [b)]	15.9	5.9 [b)]
Venlafaxine	0.05	385	384	340	46.5	129	415	405	604	419 [b)]

a) Excretion rate used in the calculation.
b) No national sales data available. Average value used.

Annex 6 – Calculated concentrations in effluent wastewater

API	RR[a)]	PEC_{eff} [ng/L]								
		FI	SE	DE	LV	EE	PL	LT	DK	RU
Allopurinol	0.998	2.63	2.43	9.14	2.13	3.76	8.1 [b)]	8.01 [b)]	3.38	8.14 [b)]
Atenolol	0.758	291	1,130	192	55.9	97.2	87.6 [b)]	19 [b)]	325	232 [b)]
Bezafibrate	0.589	56.6	124	391	351	345	351	349	345	351 [b)]
Bisoprolol	0.184	1,120	238	858	610	51.1	770 [b)]	767 [b)]	68.8	772 [b)]
Carbamazepine	0.120	345	346	434	803 [b)]	764 [b)]	799 [b)]	221 [b)]	310 [b)]	594 [b)]
Citalopram (Escitalopram)	0.240	298	365	207	13.2	26.7	247 [b)]	244 [b)]	381	248 [b)]
Clarithromycin	0.291	161	258	567	991	1,320	985 [b)]	287 [b)]	347	650 [b)]
Diclofenac	0.0640	4,910	3,080	3,570	11,000	12,500	2,320 [b)]	2,840 [b)]	1,740	1,510 [b)]
Dipyridamole	0.888	25.9	6.21	0.688	0.0107	0.00189	8.42	8.06	36.8	8.57
Doxycycline [c)]	0.888	85.2	44.9	52.9 [b)]	84 [b)]	1150	67.8 [b)]	67.5 [b)]	24.3 [b)]	67.9 [b)]
Eprosartan	0.958	135	5.83	66.2	0.889	1.26	62.4 [b)]	62.2 [b)]	61.8	62.4 [b)]
Erythromycin	0.549	7.9	49.7	189	23.6	1.22	162	1.01	67.5	163 [b)]
Fluconazole	0.362	216	181	50.5	116	112	88.9 [b)]	88.7 [b)]	330	89 [b)]
Gabapentin	0.778	6,290	6,260	4,170	4,550	2,500	4,750	4,740	9,160	4,760 [b)]
Gemfibrozil	0.836	2.87	17.2	0	6.47	5.91	6.5 [b)]	6.36 [b)]	63.9	6.55 [b)]
Hydrochloro-thiazide	0.354	4,590	677	7,890	1,630	2,410	6,680	6,670	3,550	6,690
Ibuprofen	0.950	360	190	154	466	429	10.2 [b)]	87 [b)]	414	217 [b)]
Irbesartan	0.301	152	86.3	237	17.3	0	230 [b)]	224 [b)]	32.1	232 [b)]
Ketoprofen	0.673	7.38	19.3	0.61 [b)]	12.6 [b)]	42	7.55 [b)]	7.23 [b)]	0.0743 [b)]	7.68 [b)]
Levetiracetam	0.952	784	536	966	85.2	133	882 [b)]	879 [b)]	619	883 [b)]
Losartan	-0.105	974	661	182	157	190	479 [b)]	466 [b)]	2180 [b)]	484 [b)]
Mesalazine	0.976	1,290	1,150	483	86.2	212	616 [b)]	615	1,130	617 [b)]
Metformin	0.998	1,030	435	732	556	643	659 [b)]	359 [b)]	597	693 [b)]
Metoprolol	-2.22	2,470 [b)]	3,900	8,220	3,700 [b)]	6,170 [b)]	431 [b)]	3,170 [b)]	5,970 [b)]	6,230 [b)]

API	RR[a)]	PEC_{eff} [ng/L]								
		FI	SE	DE	LV	EE	PL	LT	DK	RU
Naproxen	0.954	615	954	91.8 [b)]	173 [b)]	632	348 [b)]	60.1 [b)]	181 [b)]	248 [b)]
Nebivolol	0.989	0.0353	1.02e-05	0.181	0.484	0.597 [b)]	0.177 [b)]	0.172 [b)]	0.0225	0.178 [b)]
Norethisterone	0.976	0.0697	0.0381	0.0415 [b)]	0.0225	0.0126	0.0484 [b)]	0.0472 [b)]	0.0237	0.0489 [b)]
Ofloxacin	0.865	4.5	0.00298	13.3	30.8	6.3	11.2 [b)]	11.2 [b)]	0.00673	11.2 [b)]
Olanzapine	0.913	2.73	9.69	0.807 [b)]	0.851	1.08	2.25 [b)]	2.21 [b)]	1.85	2.27 [b)]
Paracetamol	0.987	347	511	5.79	127	208	191 [b)]	15.8 [b)]	1,080	194 [b)]
Progesterone	0.830	3.96	2.34	6.82	16.2 [b)]	4.87 [b)]	7.05 [b)]	6.88 [b)]	3.32	7.12 [b)]
Quetiapine	0.831	141	75.9	70.7	64.3	82.4	91.5 [b)]	89.3 [b)]	113	92.3 [b)]
Sertraline	0.913	3.84	14.2	5.31	1.42	4.17	10.8	10.4	22.6	11 [b)]
Simvastatin	0.975	12.1 [b)]	11	18	0.179	2.44	19.5 [b)]	19 [b)]	25.5	19.6 [b)]
Sotalol	-0.0640	619	678	540	584	1,650 [b)]	558 [b)]	557 [b)]	225	559 [b)]
Sulfamethoxazole	0.955	12.5	1.65e-05	38.4	102	58.2	29.3 [b)]	9.17 [b)]	11.5	33 [b)]
Telmisartan	0.620	756	18.9	306	958	2,840	337 [b)]	335 [b)]	20.4	337 [b)]
Testosterone	0.855	6.27	8.16	9.9 [b)]	0.771	0.473	9.81 [b)]	9.66 [b)]	4.53 [b)]	9.87 [b)]
Tetracycline [c)]	0.888	253	34.6	750	1.41	0.251	622 [b)]	620 [b)]	353	623 [b)]
Tramadol	0.0310	614	683	599	447	560	778 [b)]	766 [b)]	2,580	783 [b)]
Trimethoprim	0.313	1,090	126	377	719	417	414	412	551	415 [b)]
Valsartan	0.708	3,680	613	4670	754	1,100	3,920	3,910	115	3,930 [b)]
Venlafaxine	0.198	309	308	273	37.3	103 [b)]	333 [b)]	325 [b)]	485	336 [b)]

a) Removal rate used in the calculations.
b) No sales data available. Average value used.
c) The sum concentration of tetracycline and doxycycline was measured in the project CWPharma (Ek Henning et al. 2020). The WWTP-removal rate based on this data was used in estimating the effluent concentration.

Annex 7 –Univariate sensitivity analysis

Univariate sensitivity analysis

A univariate sensitivity analysis was carried out to estimate the sensitivity of the calculation results to changes in individual parameters. This analysis was carried out by making incremental changes to the values of 24 variables identified to affect the result. Changes in the total load to the Baltic Sea, mean concentration at river mouth locations and mean concentrations at coastal areas were selected as the end-points, for which results were compared between test-parameters.

To carry out the sensitivity analysis, a calculation loop was created, where each variable was assigned either the default value, or a variable-specific test-value. Each variable was tested using 11 different values. The sensitivity analysis was carried out for a generic dummy-substance. The country-specific sales of this dummy substance were taken as the average of the eight substances presented in Table 2 of this report. The parameters and the range of values used in the sensitivity analysis are presented in Table A7.1

Table A7.1. Test-variables in the univariate sensitivity analysis

Variable		Min	Default	Max	Unit
A	Parameter describing temperature effect on degradation (α in Eq. (9))	0.045	0.09	0.18	-
$DT50_{bio}$	Half-life for biodegradation	10	100	1,000	d
$DT50_{photo}$	Half-life for photodegradation	20	200	2,000	d
Excr	Excreted fraction (E in Eg. (1))	0.01	0.5	1	-
F_{photo}	Fraction of water where photolysis occurs in inland waters	0.0015	0.015	0.15	-
Flow-mod	Modifier for river flow volume	0.5	1	2	-
h1	Depth of the surface layer in coastal waters	0.05	0,5	1	m
h2	Depth of the middle layer in surface waters	1	2,5	5	m
k_{sedpoc}	Sedimentation rate	10	20	30	g/m^2
Koc	Distribution coefficient (adsorption)	150	1500	15,000	L/kg
PT	Fraction of unused medicines delivered to proper treatment, varies with country	0.05	See Table 3	1	-
rho_w	Density of marine water	901.8	1 002	1,102.2	kg/L
RR	Removed fraction at WWTP	0.01	0.5	1	-
Sales	Modifier for national sales	0.1	1	10	-

Variable		Min	Default	Max	Unit
SNC	The fraction of domestic wastewaters that is treated, varies with country	0.05	See Table 3	1	-
T	Average temperature in inland waters	4.1	8.3	16.5	°C
$T_{divline}$	Division line above which T=7 °C, and below T=9 °C	2 945 500	4 300 000	5 172 500	-
T_{ref}	Reference temperature for biodegradation	12.5	25	50	°C
$Coast_{divline1}$	Northern division line for coastal waters	3 700 500	4 300 000	5 172 500	-
$Coast_{divline2}$	Southern division line for coastal waters	2 945 500	3 700 000	4 200 500	-
Unused	Fraction of medicines left unused	0.05	0.5	1	-
V_flow	River flow speed	0.015	0.15	1.5	m/s
Waste2Sewer	Fraction of unused medicines flushed to the sewer network	0,01	0,5	1	-
Z	Radiation decreasing from surface layer to the next (1/z) in the coastal areas	1	4	10	-

Variables with linear impact on results

There were nine variables which had a linear impact on the value of at least one of the selected end-points. Three of these parameters (Excr, Sales, Waste2Sewer) resulted in a parallel impact on all of the end-points. The impact of variables Excr and Sales are presented in Figure A7.1. On the other hand, changes in SNC, PT, Unused and F_{photo} resulted in opposite impacts on all the end-points. Additionally, h1 had an opposite impact on the plateau concentration in coastal waters (AA_conc). The impacts of RR and SNC are presented in Figure A7.2.

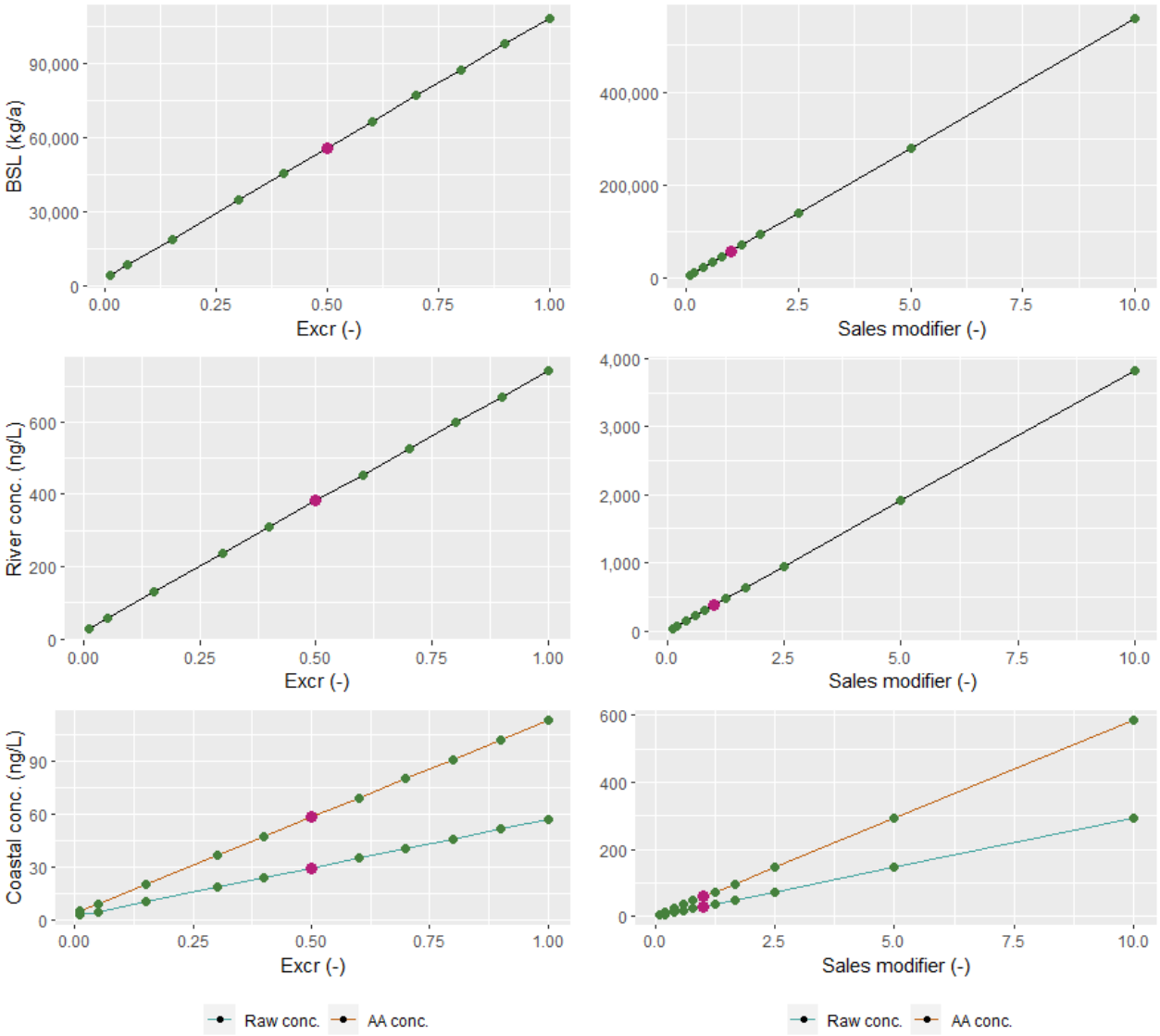

Figure A7.1. The impacts of API-specific excretion rate and sales on the load to the Baltic Sea (BSL), mean concentration at river mouths, and mean concentrations at coastal areas. The red point presents the default value.

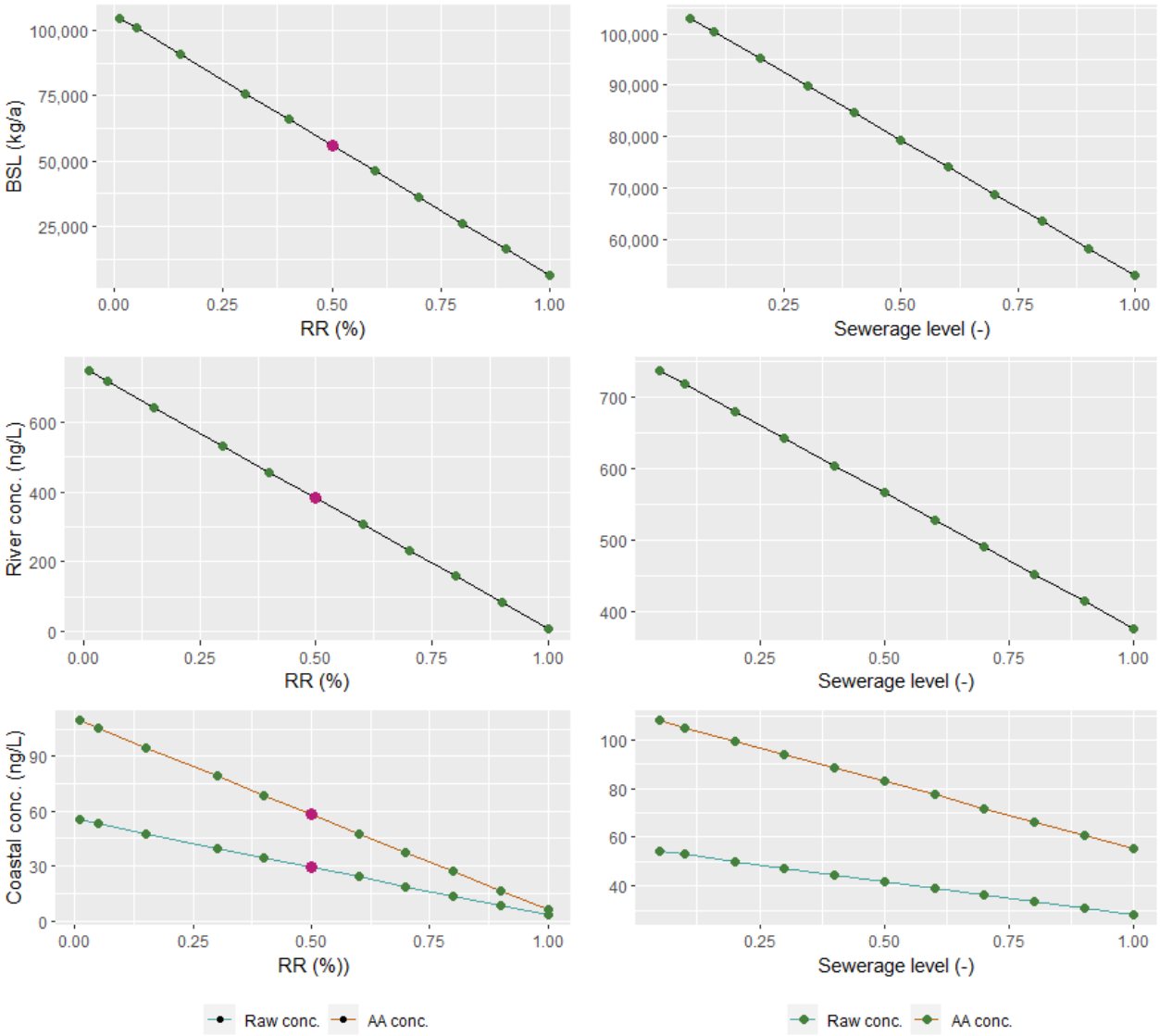

Figure A7.2. The impacts of removal rate at WWTP and sewer network coverage on the load to the Baltic Sea (BSL), mean concentration at river mouths, and mean concentrations at coastal areas. The red point presents the default value.

The variables with the greatest impacts on the outcomes were Excr, RR, Sales and SNC. Each variable with a linear impact on the outcomes is presented with the slope of the change in Table A7.2.

Table A7.2. Variables with a linear impact on the outcome.

Variable	Slope			
	BSL	R-mouth conc.	Coastal AA conc.	Coastal raw conc.
Excr	110,000	720	110	55
RR	-100,000	-750	-100	-53
Sales	56,000	380	58	29
SNC	-53,000	-380	-55	-28
Unused	-14,000	-120	-13	-6.5
Waste2Sewer	6,600	43	3.6	7.2
F_photo	-4,900	-2.6	-5.2	-2.7
PT	-4,100	-30	-4.4	-2.2
h1	0	0	-0.88	0

Variables with a nonlinear impact on results

The majority of the variables had a nonlinear impact on the calculation outcomes. The fraction of medicines that gets flushed into the sewer network, i.e. does not go through metabolic processes, was the variable with the highest nonlinear impact on the load of the dummy substance to the Baltic Sea. On the other hand, there were some parameters, to which the calculation method was especially sensitive, when the parameter approached the extreme values in the tested range. For instance, the impact of flow speed increased with decreasing values. A similar impact would be seen if degradation half-lives were to be decreased. The impacts of these variables are presented in figures Figure A7.4 and Figure A7.3. The peculiar impact $T_{divline}$ and $Coast_{divline}$ had on the results is explained by the distribution of population and consequent emissions on both the northern and southern sides of those division lines.

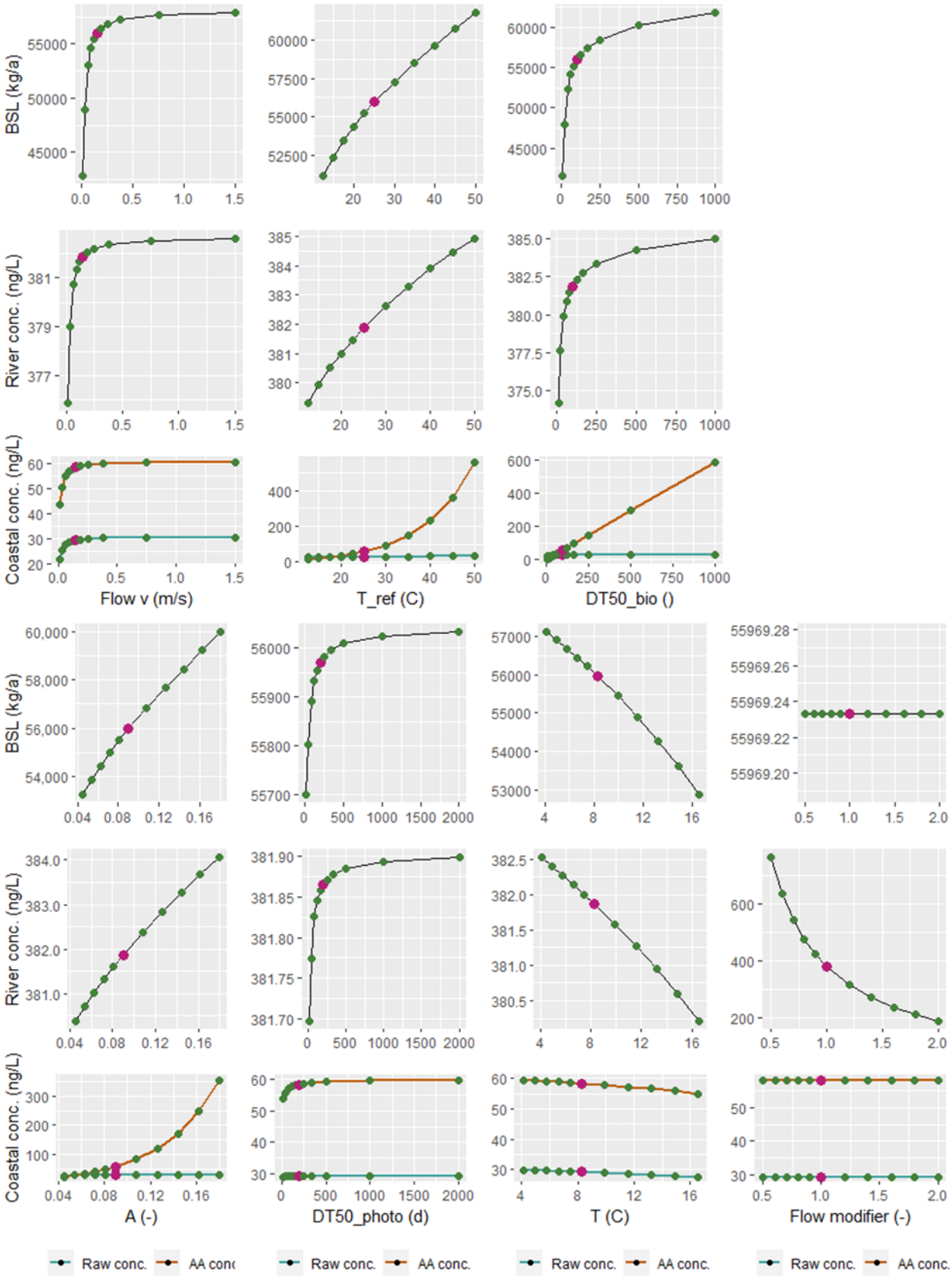

Figure A7.3. The impacts of different variables on the calculation outcomes.

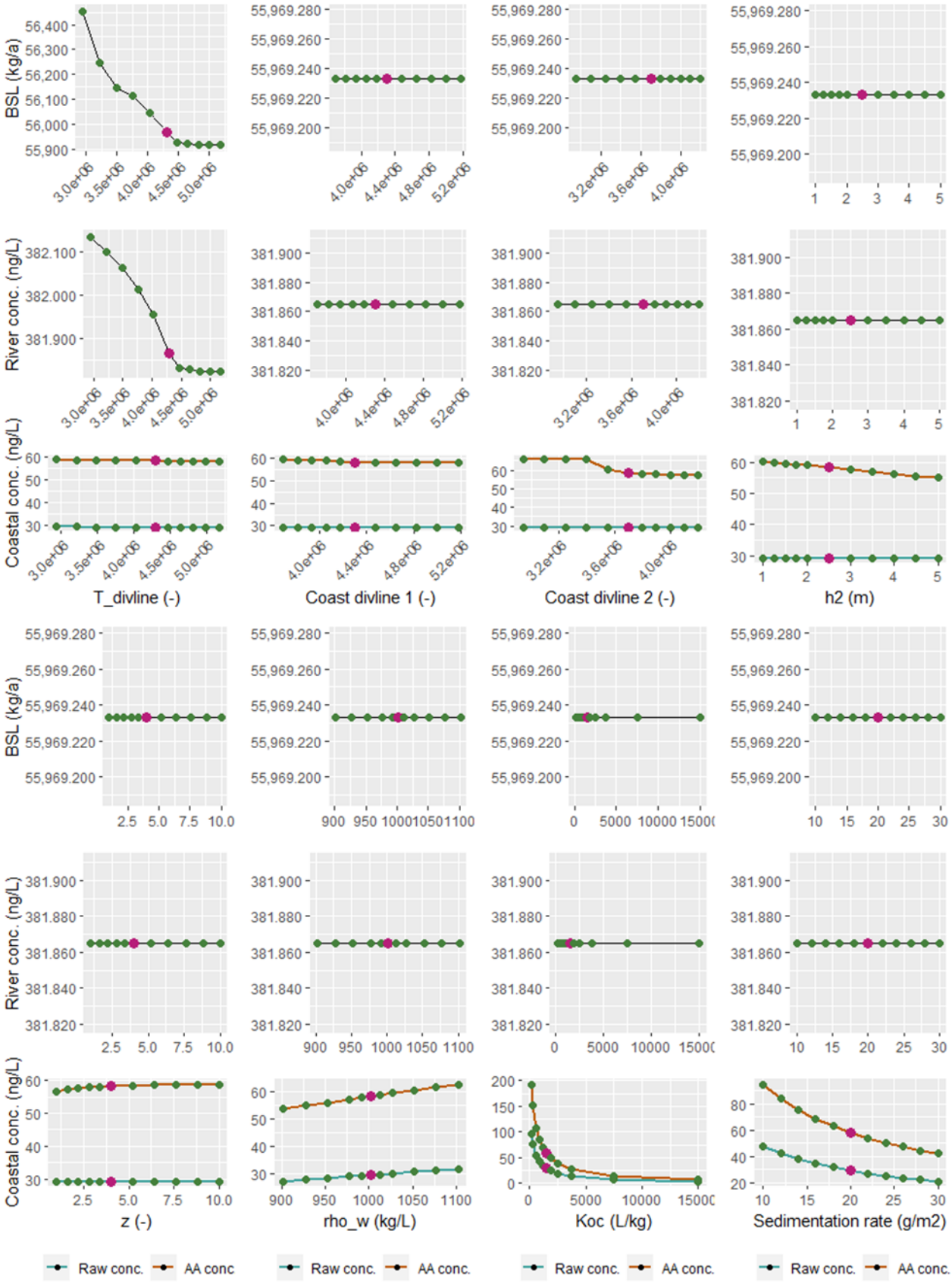

Figure A7.4. The impacts of different variables on the calculation outcomes.